Epigenetic Regulation of Chronological and Replicative Longevity in *Saccharomyces cerevisiae*

Jonathan Ayling
Linacre College
Trinity 2012

Thesis submitted in partial fulfilment of the requirements for the degree of Doctor of Philosophy in Biochemistry at the University of Oxford

Approximate word count: 49,172 words

EPIGENETIC REGULATION OF CHRONOLOGICAL AND REPLICATIVE LONGEVITY IN *SACCHAROMYCES CEREVISIAE*

A thesis submitted to the University of Oxford for the degree of

Doctor of Philosophy

Abstract

Ageing and senescence remain among the most intriguing questions in biology. *Saccharomyces cerevisiae* has become well established as a fertile model system for the investigation of ageing. Remarkable conservation has been found to exist between interventions extending lifespan in higher animals and yeast – genetic, chemical, and nutritional – suggesting a network of common regulatory pathways controlling large-scale shifts in gene expression involved in senescence. While it has been proposed that epigenetic regulation controls these shifts, evidence remains incomplete. To address this question, novel longevity mutants were isolated in *S. cerevisiae* using a purpose-designed high-precision screen based on ageing culture outgrowth. A novel long-lived mutant in uncharacterised gene *YDR026C* was discovered and found to participate in a pathway distinct from TOR signalling, but share epistasis with the histone deacetylase *SIR2*, a well established regulator of replicative longevity and rDNA maintenance. Through equilibrium density centrifugal separation of culture subpopulations, *sir2Δ* and *ydr026cΔ* cultures were found to demonstrate reduced and improved maintenance of post-diauxic quiescence respectively, previously shown to underlie chronological survival in strains including *snf1Δ*. Development of a quantified TUNEL-based assay for genome fragmentation indicated early apoptotic-like behaviour in the *sir2Δ* strain. Microdissection experiments and sectored-colony assays of strains containing an rDNA-embedded *ADE2* reporter determined that *ydr026cΔ* cells also exhibit extended replicative lifespan, and reduced recombination at the rDNA spacer region hotspot, abrogated in *sir2Δ* strains. *SIR2* is well established to repress RNA polymerase II-derived transcripts in the rDNA spacer region, including IGS1-R. Northern analysis determined Ydr026c also silences transcription in the spacer, possibly through preventing termination of the main rRNA transcript, interfering with IGS1-R expression. By transformation with a vector overexpressing IGS1-R, partial reconstitution of the *sir2Δ* phenotype was observed, including rDNA hyperrecombination, shortened replicative longevity, and higher-order chromatin structure restoration. These data suggests a model whereby non-coding rDNA spacer transcripts epigenetically determine rDNA maintenance through recombination, leading to physiological phenotypes of replicative and chronological ageing.

Acknowledgements

Foremost I would like to acknowledge the superb support, advice, and scientific guidance of my supervisor, Prof. Jane Mellor, throughout the course of my D.Phil. I must also give thanks for the wonderful input and encouragement of members of the Mellor lab in countless formal and informal discussions – particularly Michael Youdell, David Clynes, Ana Barros, Françoise Howe, Tania Nguyen, Struan Murray, Simon Haenni, and Harry Fischl. Without the diligence and skill of our stellar lab technician, Anitha Nair, it is doubtful whether much of this work would have been possible. Several talented undergraduate students have also contributed to the ageing work in the Mellor lab: particularly Prateek Choudry and Kate Rockcliffe. Gene expression and bud count data in figure 21b-d was produced by Prateek Choudry. I would also like to thank David Sinclair for the gift of the W303AR5 strain and Robbie Loewith for plasmid pJU841.

Finally I would like to thank my family, friends and flatmates for their priceless support through the experimental and writing phases of the project. A very special thank you to Caroline, for helping me keep a sense of perspective through the four year adventure that this project has been.

Jonathan Ayling
Linacre College

Submitted for the degree of
Doctor of Philosophy
Trinity Term, 2012

Table of Contents

1 Introduction

1.1 The biological problem of ageing

Ageing is simultaneously one of the most familiar everyday biological processes and arguably the most poorly understood – both in the specific underlying mechanisms driving the ageing process and the function, if any, senescence plays in nature. Diseases associated with the ageing of humans: cancer, cardiovascular disease, and neurodegenerative disease; increasingly dominate healthcare expenditure in the developed world (WHO, 2007) and intense study has been applied to specific intervention in these disorders. However, individual treatment of each disease as they arise in an ageing individual is not optimal. If a basic ageing process does exist – and if this can be modified through safe practical intervention – then multiple diseases of senescence may be targetable through the underlying course of senescence. To many this represents the ultimate goal of the science of biogerontology (Olshansky et al., 2004).

Many unanswered questions stand as barriers to any possibility of realisation of this goal. The basic physical or biological drivers of ageing are still unknown. It may be that senescence represents an inevitable physical deterioration that cannot be reversed, or that the individual diseases associated with mammalian ageing are unconnected. It is unclear what role ageing plays in natural world, and to what degree senescence has been specifically selected for. Over more than one hundred years, attempts to resolve these basic questions underlying the science of ageing have lead to the development of numerous competing, and often mutually exclusive, theories of ageing (Medvedev, 1990). While the reality of loss of physiological function as we grow older may seem inevitable to the

human observer, this is not the case in a variety of diverse organisms that appear not to age at all, and much recent evidence suggests that the course of ageing can be dramatically retarded. Much debate also surrounds the specific mechanisms through which physiological deterioration occurs in ageing animals: genetic or epigenetic dysfunction (Bandyopadhyay and Medrano, 2003; Kenyon, 2010), genomic instability (Busuttil et al., 2004), metabolic or mitochondrial dysfunction (Shigenaga et al., 1994), reactive oxygen species (ROS) generation (Schoneich, 1999), protein oxidation (Stadtman and Berlett, 1997) and defective autophagy or proteolysis (Grune et al., 2004) are possible culprits, amongst many others. Because of the lack of a clear framework model for ageing research and the complexity of conducting basic research in humans, numerous model systems have been proposed and successfully used to study elements of the ageing process. These range from cultured mammalian cells (Hayflick, 1974); to microorganisms (Lynch, 2005), *Caenorhabditis elegans* (Johnson and Lithgow, 1992), *Drosophila melanogaster* (Arking, 1988) to rodents (Myers, 1978) and primates (Peters et al., 1998). The budding yeast *Saccharomyces cerevisiae* is well established as a powerful and practical system for genetic dissection of basic biological processes. Surprisingly, perhaps, in the last 15 years *S. cerevisiae* has shown great value as a model organism for the study of ageing (Kaeberlein, 2010).

1.2 A common ageing process

Most animals in domestication away from the rigours of nature – for example humans – do not live forever. Physiological degeneration occurs with age, and appears to culminate with the greatly increased likelihood of various diseases of ageing. Mortality increases stepwise in the same way (Brody and Schneider, 1986). These diseases are disparate in terms of

pathophysiology, and it is not immediately obvious that they occur as the result of a common ageing process and not as the individual degeneration of particular tissues, for example the heart muscle. The rate of mortality in ageing humans and animals is highly predictable and has been studied for several centuries as an important part of actuarial science. Benjamin Gompertz defined a function accurately describing population remaining alive over time in protected ageing animals by assuming an age-dependent exponential increase in mortality combined with an age-independent mortality component: the Gompertz-Makeham law of mortality (Gompertz, 1825). This predicts a characteristic sigmoidal curve showing rapid increase of mortality at a threshold age, followed by a long tail of fortunate long-lived individuals (**Figure 1**). It is perhaps unsurprising that the incidence of cancer, major cardiovascular disease, and neurodegenerative disease follow the same kinetics in humans (Brody and Schneider, 1986; Driver et al., 2008). Detailed analysis of the contributing variables coincident with diagnosis of these diseases firmly place them within the category of *age-dependent* – that is, chronological age is the best predictor of disease occurrence. Age is the biggest risk factor for cancer (Sasieni et al., 2011), cardiovascular disease (Lloyd-Jones et al., 1999), neurodegenerative disease (Lindsay et al., 2002) and osteoporosis (Ross, 1996) beyond any other variable of genetics or environment. Natural variations in longevity, presumably caused by genetics or environment, correlate with incidence of these diseases. This is true both for long-lived individuals (Andersen et al., 2012) and populations ageing at different rates in the developed world, for example on the coastline and interior of Croatia (Masanovic et al., 2009). This applies for all the diseases of ageing, suggesting an ability to alter the underlying ageing process. Due to the obvious practical restrictions of studying this phenomenon in humans, much of this data is only correlative and retrospective.

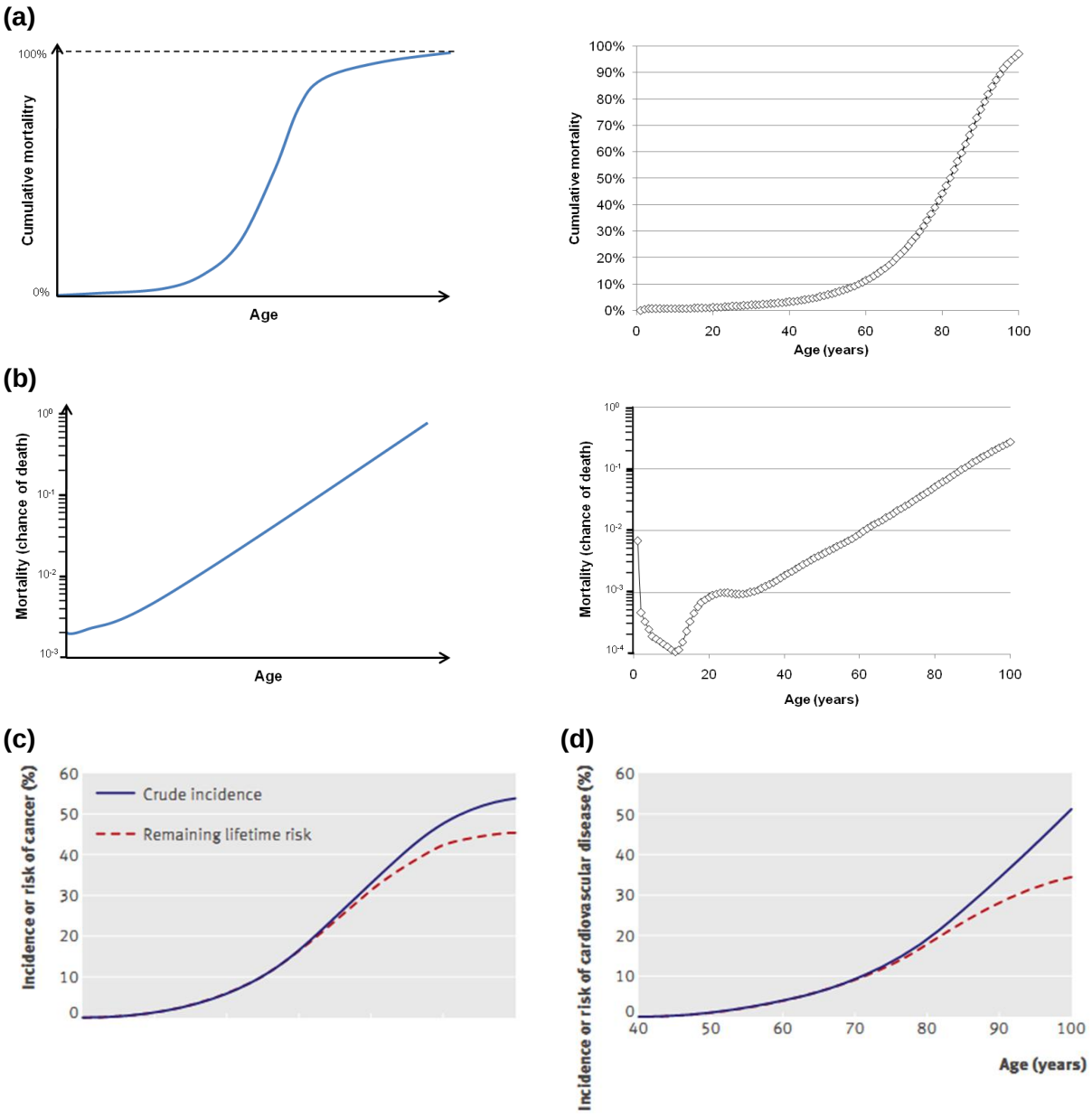

Figure 1. Characteristic sigmoid mortality and morbidity curves produced over the process of ageing can be modelled by the Gompertz-Makeham law. This postulates both age-dependent and (minor) age-independent contributors to mortality – defined as the proportion of the population succumbing to death or disease over a particular time interval. **(a)** Mortality associated with age. The left hand panel shows an idealised plot of cumulative mortality over time by the Gompertz-Makeham law of mortality. The right hand plot shows real human mortality data for age-specific death rates for the population of the USA in 2003 (CDC, 2006). **(b)** Obedience to the Gompertz-Makeham model can be vividly shown by plotting log(mortality) vs. time. With an exponentially rising age-dependent mortality contribution, this should generate a straight line with a gradient equal to that age-dependent variable (idealised plot, left panel). Transforming the 2003 CDC data in this way (right panel) gives a very good straight line agreement for most ages. Non-linear regions of the plot indicate the now minor impact of extrinsic mortality upon human lifespan in the developed world: infant mortality (ages 0-1) and risky adolescent behaviour (ages 17-20). The incidence of both **(c)** cancer and **(d)** cardiovascular disease follow highly similar sigmasoid curves correlating highly with age. Indeed, ageing is the major risk factor for both these age-related diseases. Figures (c) and (d) adapted from (Driver et al., 2008).

The discovery, almost 90 years ago, of a simple and dramatic anti-ageing intervention in rodents: *dietary* or *caloric restriction* (CR); made prospective experiments possible in a number of models (McCay et al., 1935). Rats allowed only 60-70% of their *ad libitum* food intake were found to exhibit not only greatly enhanced longevity, but also show retardation of all the indices of age-related physiological deterioration normally observed (Masoro, 1988). This included cancer incidence, age-related kidney disease, and neurological measures (Saxton and Kimball, 1941; Weindruch and Walford, 1982; Ingram et al., 1987). The caloric restriction phenomenon has since been found to be a robust anti-ageing intervention in many of the models tested: yeast, worms, flies and mice show dramatic improvements in lifespan and healthspan (Heilbronn and Ravussin, 2003). However, translation of the caloric restriction effect to primates, which are presumed to give the best indication of whether a similar phenomenon could be operating in humans, has given conflicting results. One initial large study, and one smaller, showed that long-term caloric restriction experiments performed on rhesus monkeys gives significant enhancement to physiological function and survival at advanced age (Bodkin et al., 2003; Colman et al., 2009). However, a more recent attempt to replicate these results indicated that while calorie restricted rhesus monkeys showed reduced age-related illnesses, no direct change in survival was observed (Mattison et al., 2012). There is even some evidence of effective calorie restriction in humans, although the efficacy of this as an intervention is controversial (Shanley and Kirkwood, 2006; Speakman and Hambly, 2007). Ageing biomarkers in calorie-restricted humans appear to indicate a reduction in the predicted risk of athleroschlerosis and diabetes: low levels of inflammatory factors such as TNF-α and c-reactive protein correspond with similar effects in calorie restricted rodents. (Holloszy and Fontana, 2007). Retrospective studies of caloric restriction of children up to the limit of malnutrition during the Hunger Winter famine in the Netherlands during the second World War have shown that, contrary to this period of low nutrient availability being detrimental

to health later in life, protection from colorectal cancer results even many years later (Hughes et al., 2009). Caloric restriction seems to be modifying some common routine of ageing, contrary to the specific treatments for age-related diseases which have no beneficial effect on future healthspan. On the side of genetics, the rate of ageing in humans has a clear heritable component and this determines the rate of incidence of seemingly physiologically unrelated ageing associated diseases (Cournil and Kirkwood, 2001). This evidence is strongly suggestive of a common, underlying pathway of ageing responsible for the ageing-related diseases observed in the humans and model organisms.

1.3 Why do we age?

This evidence for a common pattern of ageing diseases is now rarely disputed. However, whether treatments can be designed to interfere with the process of a program of ageing – without disastrous unintended consequences – is less clear. In order to answer this question, the underlying process of ageing: physical inevitability, or regulatory pathway refined by natural selection, must be understood. To this end, numerous theories of why ageing occurs have been proposed. There has been an explosion of these in the last few decades: in an attempt to systematically catalogue these theories, Medvedev counted over 300 competing and often mutually exclusive theories of ageing (Medvedev, 1990). Why ageing should occur at all is a puzzle. In principle, given unlimited energy and nutrient resources (effectively the case for humans in the modern developed world and model organisms in the laboratory), tissues and cells should be capable of continual repair and maintenance. Why does the somatic tissue of a mouse degenerate leading to death after a few years, when human tissue performing almost identical metabolic and developmental processes lasts for scores? As Williams put it over 50 years ago: *"It is remarkable that*

after a seemingly miraculous feat of morphogenesis a complex metazoan should be unable to perform the much simpler task of merely maintaining what is already formed." (Williams, 1957). To further emphasize this paradox, there appear to be a limited group of diverse animals that do not age at all by any of the commonly used measures: such as the red sea urchin, ocean quahog, and naked mole rat (Vaupel et al., 2004; Finch, 2009; Kim et al., 2011; Ridgway and Richardson, 2011). This phenomenon is known as *negligible senescence*.

In biology, answers to teleological ("why") questions such as these fall into two categories (**Figure 2**). Firstly, biological phenomena can occur because of the restrictions of the laws of chemistry and physics. It is thermodynamically impossible, for example, to favourably convert CO_2 and water to carbohydrate without the input of energy. Alternatively, the phenomena may occur as a result of the optimisation of natural selection. The fixation of CO_2 to carbohydrate in sunlight does not occur spontaneously, but natural selection has furnished the green plant with a complex refined system to catalyse just that reaction for the benefit of its survival. Attempts to answer the question: "why do we age?" – has therefore developed around two classes of explanation: physical necessity and biology expediency.

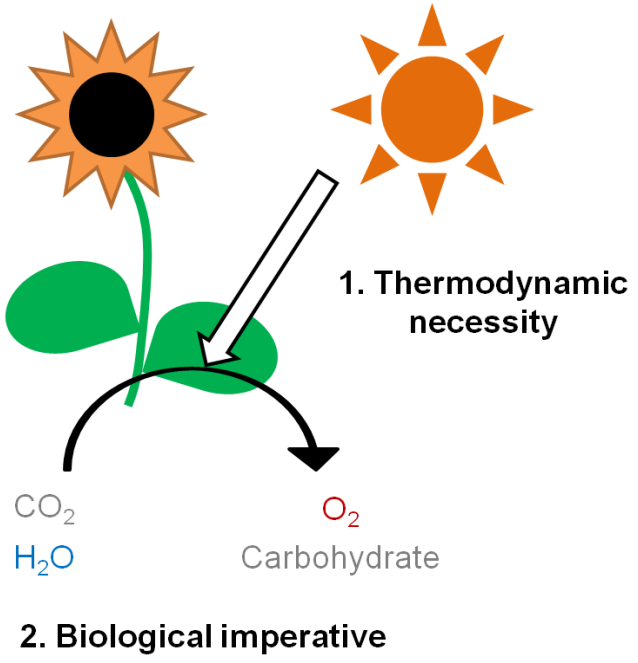

Figure 2. Teleological explanations in biology. The phenomenon of ageing is one of the few "unsolved problems" of biology (Medawar, 1952). When we want to know "why?" something happens in a living system, two epistemologically satisfying, non-mutually exclusive explanations are possible. Phenomena can occur because of **(1)** the *necessity* of the laws of physics and chemistry, or **(2)** because of *biological imperative* developed by natural selection. An example is the photosynthesising plant above. The question "why does a plant photosynthesise like this?" has two answers. Condensation of CO_2 with water to form carbohydrate is thermodynamically highly unfavourable and will not occur spontaneously. The laws of physics are immutable, and photosynthesis cannot occur without the input of energy from, in this case, sunlight **(1)**. The second answer is that natural selection has furnished the plant with a complex optimised system to allow photosynthetic fixation of CO_2 – because it is hugely beneficial to the plant's survival in its ecological niche **(2)**. Applying this simple example to the complex question: "why do we age?" – illuminates the theories of ageing that have developed in the last hundred years. Does ageing occur because of physical necessity? Or is it biologically useful? Or both?

1.4 Original theories of ageing: programmed senescence

The oldest theories of ageing focussed on simple teleological explanations of ageing. On the side of biological expediency, Weismann postulated that *"worn out individuals are not only valueless to the species, but they are even harmful, for they take the place of those which are sound"* (Weismann, 1889). This is the theory of programmed senescence (**Figure 3a**). The *rate of living* hypothesis is almost as venerable and argues on the side of

physical inevitability: animals have a roughly fixed amount of metabolic activity available to them, and this either wears out the somatic tissue or leads to accumulated damage that eventually kills the animal (Pearl, 1928). A corollary of this is that organisms with slow metabolism, or those that do not reproduce, should be longest lived (**Figure 3b**).

Theoretical and empirical problems exist with both of these theories of ageing. Because ageing seems to be a normal part of the life history of an animal, it is tempting to conceptualise it as a programmed process selected for as beneficial to the species. But, as pointed out by Kirkwood, this rationale is circular: ageing is responsible for removing "worn out" members of a species, but this wearing out is itself only contingent upon ageing occurring in the first place. Given that the rates of senescence are greatly variant between species, this theory does not explain why the selection of physical degeneration with age would be advantageous (Kirkwood, 2005). Empirical ecological evidence argues against a programme of ageing. For most animals the inherent risks of the natural world (starvation, predation, disease etc.) are responsible for the vast majority of deaths. It is very rare for an animal in the wild to ever reach old age, let alone die from age-related diseases. As an example, only 10% of mice survive beyond one year in the wild – while age-related diseases in mice in domestic context are not observed until 2-3 years have elapsed (Phelan and Austad, 1989; Berry and Bronson, 1992). This is very evident from the enormous increase in the life expectancy of humans over the last few hundred years: the common age-associated diseases which have recently become such a large medical and economic problem only become major causes of death once average life expectancy exceeds 50 years old (Driver et al., 2008). It was pointed out by Medawar that because very few animals ever reach old age in the wild, and even fewer reproduce at that age, the selective pressure applied to ageing animals should have little force on evolution of the whole population (Medawar, 1952). There is therefore little selective driving force for the emergence of a concerted programme of ageing; even before considering the problem of "cheating"

individuals in this altruistic scheme. Where rare examples of unusual life histories do exist in the animal world that appear to indicate a programme of ageing the situation is not clear cut. Pacific salmon are well known to decay and die rapidly after spawning. It has frequently been assumed that this is an altruistic programme of ageing and the main cause of mortality in these fish (Morbey et al., 2005). However, recent observations of pacific salmon populations indicate that mortality rates are extremely high both before *and* after reproduction: 99% of individuals are killed by natural stresses before spawning, with only 0.2% being killed directly afterwards (very few adults need to reproduce to perpetuate the species) (Funk et al., 2005). From this perspective, it is reproduction in the pacific salmon that is unusually timed, not ageing.

1.5 Original theories of ageing: damage accumulation

Theories of ageing based upon physical limitation are harder to dismiss. Caloric restriction appears to support the rate of living hypothesis, and there are numerous candidates for the types of physical damage that might accumulate: damage to genomic or mitochondrial DNA, damage to membrane components, protein oxidation and denaturation and aggregation of proteins, and pathological accumulation of damaged material. But direct evidence for this damage has not been forthcoming (de Magalhaes, 2005), and there are serious theoretical objections as well. Animals such as some species of rockfish, red sea urchin, and giant tortoise exhibit *negligible senescence*: they do not appear to show any physiological degeneration over time and do not lose reproductive capacity (Finch and Austad, 2001; Ebert and Southon, 2003). A single genus of rockfish contains both short-lived and negligibly senescent members: calico rockfish have an average lifespan of 12 years compared to 205 years for rougheye rockfish (Cailliet et al., 2001). Giant tortoises have such longevity that the lives of those in captivity are generally only ended by violent accident. Moreover, there is no correlation between metabolic activity and slow ageing (Economos, 1981). Animals that have experienced a change in ecological niche without major change in metabolism over evolutionary time can have dramatically extended lifespan – development of eusociality in ants extended lifespan by around one hundred fold (Keller and Genoud, 1997). Most problematically, to prevent the degeneration of the species it is clear that this damage must not be propagated to progeny animals through the germline. Germline cells are metabolically active, and if damage can be cleared in this context, why not from somatic cells? It is clear that neither a programmed (selected-for) nor necessitated (physical) mechanism is alone sufficient to explain the phenomenon of ageing.

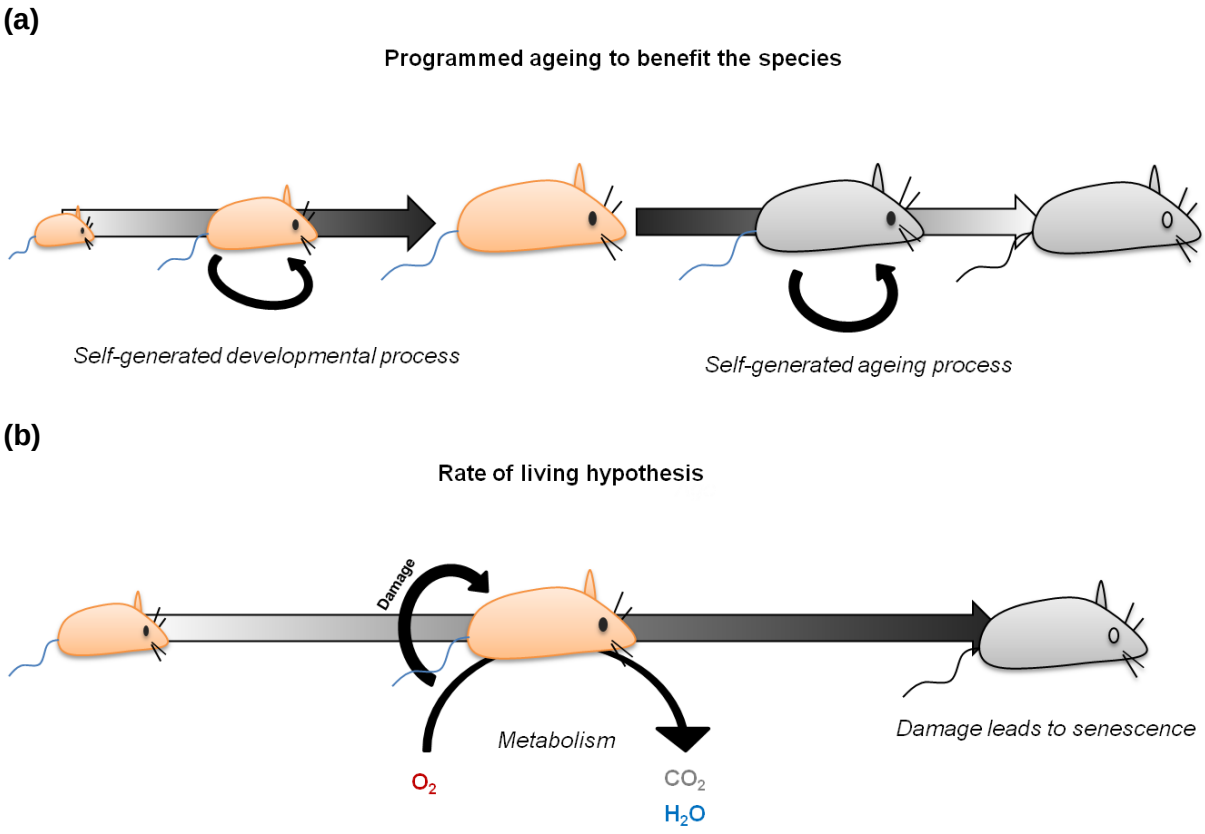

Figure 3. Original theories of ageing. **(a)** Programmed ageing is an example of a purely biological imperative explanation for the phenomenon of ageing. It is encapsulated as "*worn out individuals are not only valueless to the species, but they are even harmful, for they take the place of those which are sound*" (Weismann, 1889). A specific, active, *ad hoc* regulatory mechanism kills old animals for the altruistic benefit of the species. **(b)** The *rate of living* hypothesis is an explanation of senescence purely on the grounds of physical necessity. Vital metabolism inescapably produces damage, which accumulates and leads to ageing and mortality. A corollary of this is that faster metabolism should lead to shorter lifespan.

1.6 Evolved senescence

The evolutionary theory of ageing has developed from a synthesis of the two ideas and become widely accepted (Kirkwood and Austad, 2000). The hypothesis of Medewar – that in the absence of managing selective pressure at old age, physiological processes become dysregulated leading to ageing – has become empirically well supported. Artificial breeding of fruit flies and nematode worms at advanced age leads to selection of long-lived animals, as predicted (Rose and Charlesworth, 1980; Luckinbill et al., 1984; Walker et al., 2000). In the wild, the hazardousness of ecological niche correlates with rapidity of ageing and evolution of protective mechanisms (e.g. wings) corresponds with increased longevity (Shattuck and Williams, 2010). Evolutionary development of eusociality in ants is associated with a 100-fold increase in lifespan; island populations of opossums protected from predation are dramatically longer-lived (in neutral environment) than mainland animals; and the rate of age-related mortality correlates negatively with presenescent mortality in the wild in birds (Austad, 1993; Keller and Genoud, 1997; Ricklefs, 1998). Williams' concept of *antagonistic pleiotropy* – the selection of alleles which yield desirable traits in young animals and undesirable in old – is often incorporated into this (Kirkwood, 2005). The mechanism of physiological degeneration with age is usually postulated to be damage accumulation.

Modern theories of ageing attempt to explain the mechanism linking the two theories. A modern theory of ageing must explain :

1. How a handful of disparate animals are negligibly senescent
2. How damage is not inherited in the germline
3. How calorie restriction appears to dramatically extend lifespan
4. The wide individual variation in longevity between genetically identical individuals

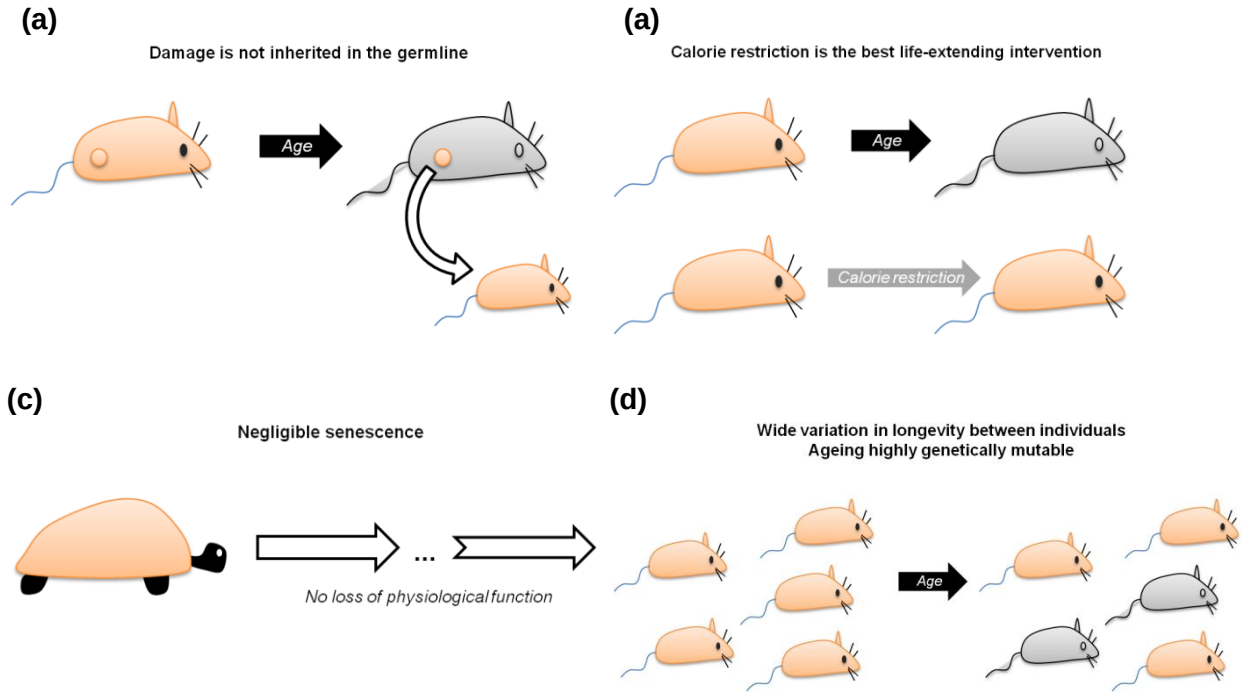

Figure 4. Four problems to be addressed by any successful theory of ageing. **(a)** Damage to cellular components such as mitochondria and the germline often correlates with ageing. If damage accumulation is the cause of ageing, how does the germline escape this phenomenon? Accumulation of damage in the germline would lead to degeneration of the species. **(b)** Calorie restriction remains the most effective life-extending interventions in myriad model systems. Any theory of ageing needs to explain this effect. **(c)** Certain organisms appear to exhibit *negligible senescence* and might not to age at all. Physiological function and reproductive capacity even *increase* with age, rather than falling. **(d)** Ageing is (currently) both an inevitable, and highly mutable, process. A collection of genetically identical individuals will age at greatly different rates, and lifespan can be greatly extended or reduced by many well studied mutants, drugs, and environmental interventions.

The *disposable soma* theory of Kirkwood attempts to reconcile these facts (Kirkwood, 1977). Kirkwood postulates that damage, caused as an inevitable by-product of metabolism, accumulates in all cells. Eventually this damage becomes problematic and the tissue experiences ageing. The damage can be repaired, but only with the investment of energy and nutrients. Because cells of the soma only need to last as long as the animal is likely to reproduce, little energy is invested into repair. Integrity of germline cells is critical for the perpetuation of the species, so here much energy is expended to prevent damage. The soma is maintained only as long as the average lifespan of the animal in the wild,

which is invariably considerably shorter than the encroachment of old age – hence it is *disposable*. Variations in the relative partitioning of resources to the maintenance of germline and soma in different animals – according to how long the soma is functionally important in the wild – explains variations in lifespan of metabolically similar animals and the negligible senescence of virtually indestructible animals such as the giant tortoise. Antagonistic pleiotropy is postulated to play an important role in this partition in somatic cells. Specific mechanisms of damage are theoretically open-ended, but oxidative DNA damage by ROS is generally considered the prime suspect (Wei, 1998; Sanz et al., 2006).

1.7 Pseudoprogrammed ageing

While *disposable soma* is perhaps the predominant modern theory of ageing, it is not without its controversies (Blagosklonny, 2007a). *Drosophila* which are prevented from reproducing are significantly longer-lived (Sgro and Partridge, 1999) : if the partition of resources in the germline and soma have been set over evolutionary time in accordance to how long the soma is likely to withstand extrinsic mortality, it is unclear how this mechanisms could have developed to alter this partition due to lack of reproduction. More seriously, if it is lack of resources that allows damage to accumulate, why would calorie restriction – up to the point of starvation – be such an effective anti-ageing intervention? Kirkwood has argued that in lean times animal metabolism shifts to partition more resources to somatic cell maintenance, but this appears to invoke a program of ageing which the theory categorically disagrees (Kirkwood and Shanley, 2005). Disposable soma theory can explain the plasticity of longevity between individuals and following genetic and drug interventions through modified resource partition. However, no intervention can extend lifespan in an animal much beyond that of calorie restriction. So while the partition

mechanism is plastic, there must also be some robust mechanism causing ageing even with unlimited resources. More generally for damage theories of ageing, attempts to directly demonstrate accumulation of damage in ageing tissues have led to ambiguous results. Several age-related diseases, such as cancer, are clearly damage-dependent (Loeb et al., 2003). However, it is difficult to show that DNA damage is a causative agent of ageing in mammals; rates of mutation are insufficient to lead to senescence; excessive generation of ROS in mice can both reduce and extend longevity; and antioxidants have had little success in extending lifespan in clinical trials (Balaban et al., 2005; Howes, 2006; Pinton et al., 2007; Vermulst et al., 2007; Lapointe et al., 2009). This picture is complicated by the operation of hormesis in response to potentially damaging agents such as reactive oxygen species: it has been suggested that extended longevity in mice overproducing ROS is due to improved stress response (Lapointe et al., 2009). While it is commonly accepted that ageing cannot be programmed, Blagosklonny has suggested an alternative, which is a *quasi-programme* of ageing: continuation of a useful program of early life (Blagosklonny, 2007b). While this programme plays a vital, stringently selected-for role in development, its continuation into old age when selective pressure is weak allows it to drive physiological degeneration (a form of antagonistic pleiotropy). Because it has no purpose in later life, it does not contradict Medawar's well-supported evolutionary theory; but neither is it driven by inevitable physical damage. Because it is required for development, the pathway is lethal if removed and yet genetically plastic. Inhibition of TOR signalling after development can extend lifespan and healthspan in mice (Harrison et al., 2009). It is postulated that TOR signalling forms an integral part of this quasi-programme: TOR mutants have been showed to exhibit extended lifespan in a diverse range of models, reconstituting the effects of calorie restriction (Evans et al., 2011).

These ageing theories make a number of predictions. Disposable soma theory predicts that calorie restriction will have limited effect on humans (as we have already optimised our

lifespan – small benefit seen would be ascribed to restriction of a sub-optimal diet, eg reduction of intake of saturated fats); and that, due to the primacy of accumulated damage, anti-ageing therapies will be difficult or impossible. The emergence of microbial models of ageing – particularly *Saccharomyces cerevisiae* – has provided a simplified system to test these theories as well as potential anti-ageing interventions.

(a)

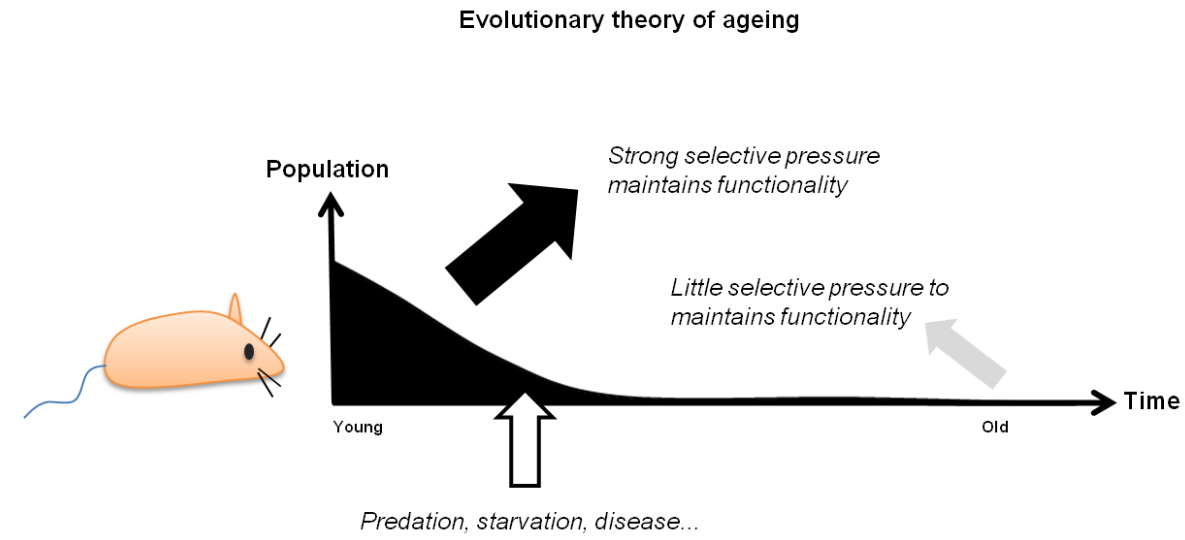
Evolutionary theory of ageing
Population
Strong selective pressure maintains functionality
Little selective pressure to maintains functionality
Time
Young
Old
Predation, starvation, disease...

(b)

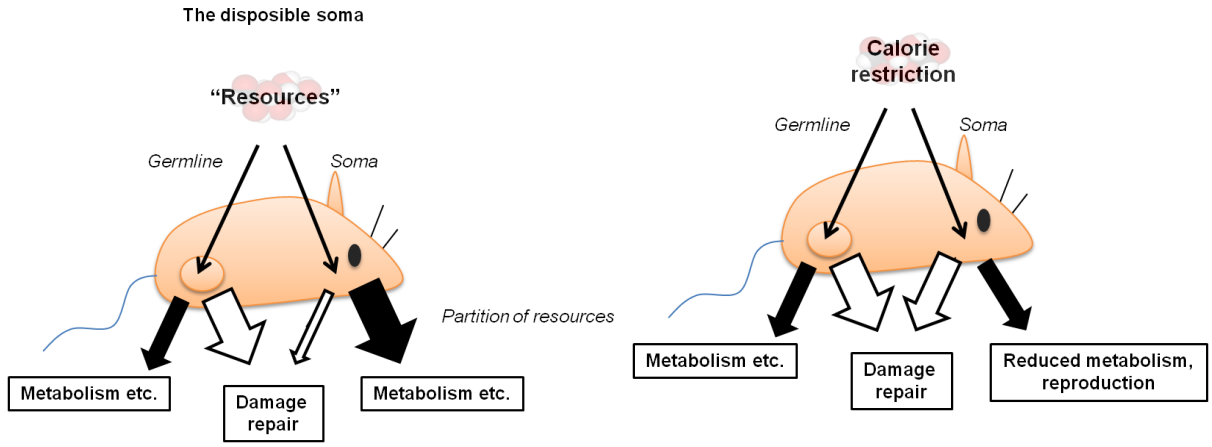
The disposible soma
"Resources"
Germline
Soma
Partition of resources
Metabolism etc.
Damage repair
Metabolism etc.
Calorie restriction
Germline
Soma
Metabolism etc.
Damage repair
Reduced metabolism, reproduction

(c)

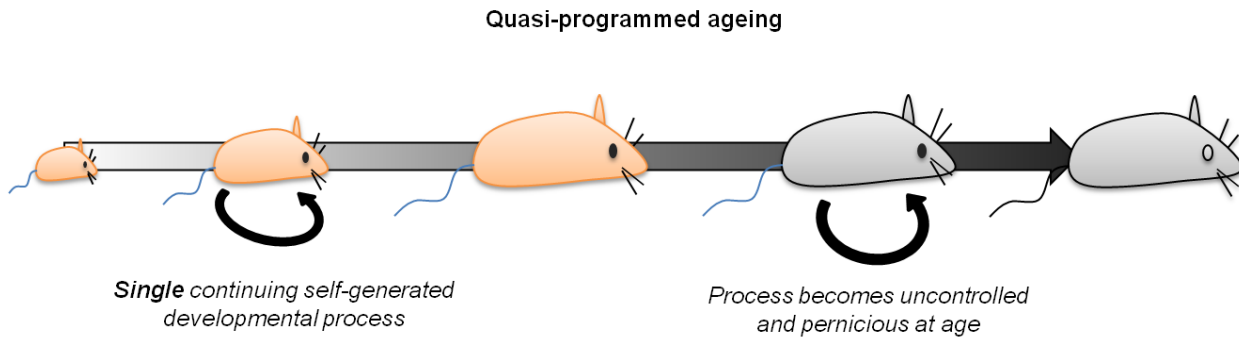
Quasi-programmed ageing
Single continuing self-generated developmental process
Process becomes uncontrolled and pernicious at age

Figure 5. Modern theories of ageing **(a)** Medawar's evolutionary theory of ageing is now supported by numerous independent lines of investigation (Kirkwood and Austad, 2000). This relies upon the observation that, because of the extreme rigours of undomesticated life (starvation, predation, disease, cold, etc.) very few animals in the wild ever reach old-age. Even fewer have a chance to reproduce at this age, and natural selection becomes effectively blind to their fate. Because so few are alive at advanced age, little selective pressure is applied to the species as a whole to maintain vital physiological processes in old animals – a natural selection "shadow" prevents the selective pressure that reins in the destructive nature of random regulatory drift. Random physiological degeneration then causes ageing and senescence. However, the mechanisms underlying the ageing process are not strictly specified, and modern theories have attempted to include these while addressing the problems shown in Figure 4. **(b)** Kirkwood's theory of *disposable soma* is the most widely supported of these (Kirkwood, 1977). This postulates that the physiological decay over ageing is caused by continuous accumulation of damage to cell components. Because damage is clearly not perpetuated through the germline (Figure 4a), and germline cells are not metabolically dissimilar from somatic cells, a mechanism must exist to repair the damage in somatic cells. This repair requires *resources*, presumably energy and nutrients. Less resources are partitioned into the maintenance of the soma than the germline: it is *disposable*, a carrier for the precious germline. The lack of repair in the soma occurs because no selective pressure exists to keep it maintained: this is therefore a development of the evolutionary theory of ageing, and does not require an *ad hoc* program of senescence. Calorie restriction (right) is hypothesised to modify somatic resource partition to preserve the soma for later reproduction. **(c)** The disposable soma theory has considerable difficulty explaining the pervasive phenomenon of calorie restriction induced lifespan extension (Figure 4b). Usually invoked is adaptive behaviour that will only impact animals getting to very old ages which they are never likely to reach in the wild – a program of ageing. Blagosklonny's theory of *quasi-programmed ageing* attempts to address this paradox (Blagosklonny, 2007b). This postulates that ageing is not caused by damage accumulation at all (although damage may occur as a downstream consequence of physiological failure during senescence) – but by the derangement of developmental processes that are beneficial in the early life of the animal. Ageing is not programmed, but the consequence of the de-regulated running on of an earlier program: a *quasi-program*. Because of this conversion of function, this theory broadly falls under the umbrella of *antagonistic pleiotropy*.

1.8 Microbial ageing

Saccharomyces cerevisiae exhibit two forms of senescent viability loss. That budding yeast cells have limited replicative capacity has been known for over 60 years (Mortimer and Johnston, 1959). If a fresh virgin mother cell is placed on rich medium, and any daughter cells produced removed by microdissection, only a finite number of daughters can be produced before the cell loses replicative viability. More recently, a second mode of ageing has been discovered: that undividing yeast cells have a finite chronological longevity and viability is lost over time without cell division (MacLean et al., 2001). Post-mitotic cultures are prepared by allowing growth of logarithmic cultures to the point of carbon source exhaustion: at this point growth becomes very slow (or stops) and cells enter a state of quiescence, slowly losing viability over time (**Figure 6**). Although growth is show, considerable reserves of non-fermentable carbon sources (largely acetic acid and ethanol) remain in the medium, and so yeast in this state are not considered to be calorie restricted.

The ageing – replicative and chronological – observed in *Saccharomyces cerevisiae* has several factors in common with senescence in higher organisms. Loss of viability is initially slow, rapidly rising over time or generation to give the signature sigmasoid profile – following the Gompertz-Makeham law of survival and suggesting an age-dependent increase in mortality characteristic of ageing (Laun et al., 2007). Many common interventions, including calorie restriction and disruption of TOR signalling, can extend both modes of longevity in yeast (Longo et al., 2012). And not inconsequentially, loss of viability over replicative or chronological age appears to be directly opposed to ecological microbial optimisation for rapid culture growth (Querol et al., 2003), suggesting an un-selected for and unprogrammed developmental side-effect characteristic of age.

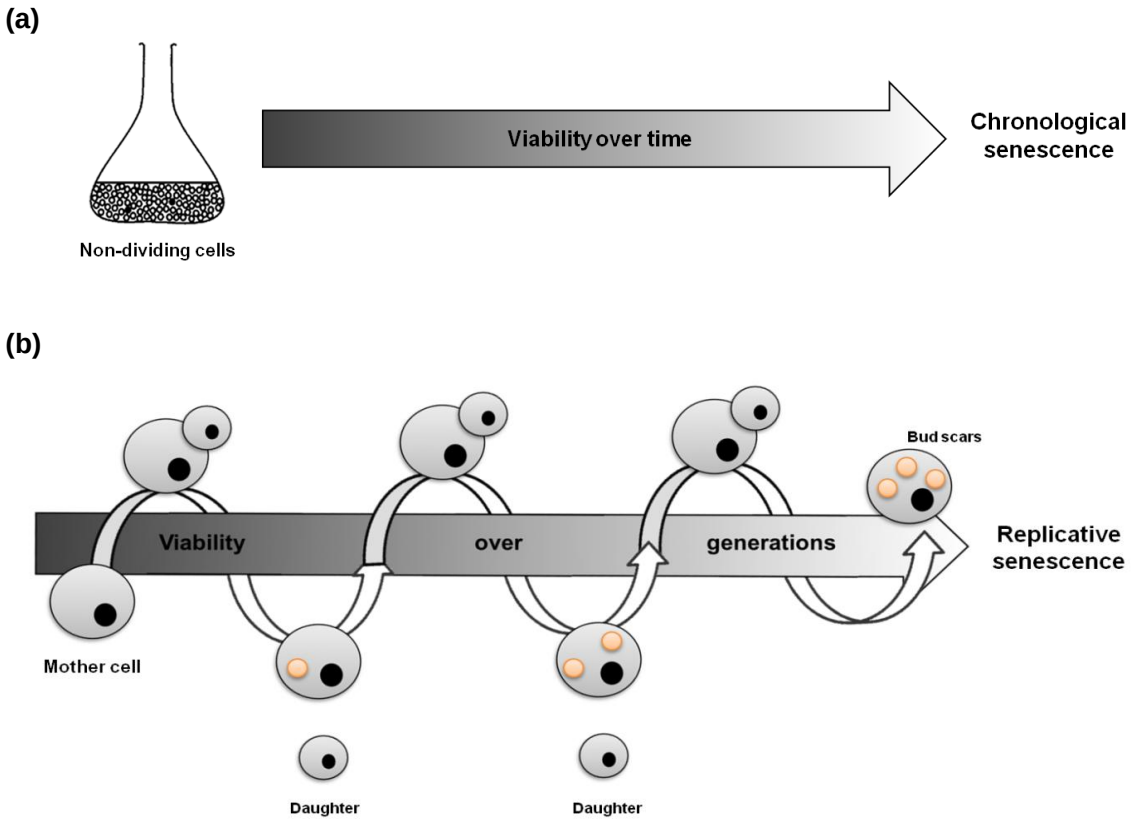

Figure 6. *Saccharomyces cerevisiae* experience two modes of ageing: chronological and replicative senescence. **(a)** Chronological ageing is the increase in mortality and loss of physiological function associated with senescence over time. A post-mitotic non-dividing culture of *S. cerevisiae* will gradually lose viability over time, usually measured as the ability to re-initiate growth upon medium replenishment. **(b)** Replicative ageing is the increase in mortality and physiological dysfunction associated with cell division. A single virgin yeast mother cell can divide 10-50 times before succumbing to replicative senescence and becoming incapable of producing further daughters. Until very late in the replicative ageing timecourse new daughters are fully viable.

That unicellular organisms experience ageing is counter-intuitive: budding yeast appears to be highly optimised for unrestrained rapid expansion to crowd out other organisms when resources are abundant, and ageing seems paradoxical in this context. Based on the theories of ageing above, several theoretical alternatives for yeast ageing are possible.

Firstly, since yeast do not have a differentiated soma and germline, it may seem unclear how the disposable soma theory would operate in yeast ageing. However, cell division in *S.*

cerevisiae is highly asymmetric, and this asymmetry may be sufficient to define the budding mother as somatic, while the new daughter continues perpetuation of the colony and constitutes the germline (Kirkwood and Austad, 2000; Henderson and Gottschling, 2008). The mother cell must then be subject to some physical degradation over time: indeed, there is evidence that chronologically old mothers are less replicatively viable (Ashrafi et al., 1999) and old mothers eventually produce defective daughters (Jazwinski et al., 1989). Because the mother cell is less valuable to survival of the lineage, fewer resources are partitioned to repair damage and senescence occurs. From the perspective of quasi-programmed ageing, the developmental processes that lead to maturation and budding of a mother cell can continue as an uncontrolled malignant quasi-program, eventually leading to senescence. However, symetrically dividing *Schizosaccharomyces pombe* cells have also been shown to possess limited replicative and chronological lifespan; this has been suggested to indicate the lack of culture asymmetry leads to culture mortality (Barker and Walmsley, 1999; Chen and Runge, 2009).

Alternatively, discrete differentiation may exist within a yeast population. Because in a haploid culture all the cells are clonally identical, altruistic group selection is likely to be strong (Severin et al., 2008). Antagonistic pleiotropy, mediated by the disposable soma or quasi-programmed mechanisms, can then favour senescence of one population to enhance the survival of another. The recent discovery of just such differentiation in ageing yeast cultures has bolstered this view of yeast senescence (Allen et al., 2006). Stochastic differences in culture microenvironment are likely to underlie development of this culture heterogeneity.

1.9 Microbial models of senescence

Initially, considerable resistance existed to the suggestion of using a single-celled eukaryote as a model of mammalian ageing (Gershon and Gershon, 2000). Apart from the obvious physiological, metabolic, and evolutionary divergence between yeasts and humans, it was unclear whether the phenomenon observed in the case of *S. cerevisiae* represented true ageing as familiar in multicellular eukaryotes, and so there is some doubt as to whether observations made in this model would be translatable to higher organisms. The discovery of a large number of interventions (nutritional, genetic, and chemical) which can modify the rate of senescence in both yeast and more complex ageing models (nematodes, fruit flies, mice and primates), and the demonstration that these interventions operate through perturbation of homologous regulatory mechanisms has established yeast replicative senescence as part of a conserved longevity system. The first of these, and still the strongest intervention, is calorie restriction (CR). First observed in rodents over 100 years ago, calorie restriction has since been shown to extend lifespan in most of the model organisms so far tested (Heilbronn and Ravussin, 2003). CR has a strong effect on yeast replicative and chronological lifespan (Lin et al., 2000); as does disruption of the TOR signalling pathway, which is implicated in models ranging from worms, flies and mice in regulation of longevity (Kaeberlein et al., 2005b). Rapamycin, a drug which strongly inhibits TOR signalling, has been shown to increase lifespan of mice (Harrison et al., 2009), worms (Robida-Stubbs et al., 2012) and flies (Bjedov et al., 2010), and can also extend the replicative lifespan of yeast (Ha and Huh, 2011). Screens in yeast identified the sirtuin lysine deacetylase Sir2, responsible for RNA polymerase II transcription repression at the rDNA, silent mating locus and telomeres as part of the RENT complex and Sir2/Sir4 (Blander and Guarente, 2004), as an important driver of replicative longevity (Kaeberlein et al., 1999). Sirtuin proteins, and an activating drug resveratrol, has since been shown to have a role in longevity of worms, flies (Wood et al., 2004) and even mice (Kawahara et al., 2009): resveratrol has been found to specifically activate mammalian Sirt1, Sirt5 and

Sirt3 isoforms (Gertz et al., 2012), but to also have inhibitory effects on *C. elegans SIR-2.1*, a homologue of Sirt1 (Markus and Morris, 2008). Original studies suggested sirtuins were required for the life-extending effect of caloric restriction in both *C. elegans* and *Drosophila* and that caloric restriction functioned through activation of the sirtuin pathway (Rogina and Helfand, 2004; Wang and Tissenbaum, 2006); however reanalysis of mutant strains used in both these models suggests that co-segregating genetic background factors were responsible for this effect and calorie restriction-mediated life-extension can occur in fly and worm strains lacking sirtuins (Burnett et al., 2011). However, sirtuins still appear to play a role in the ageing of higher animals: overexpression of sirtuin SIRT6 in male mice has been found to lead to a robust extension of lifespan (Kanfi et al., 2012). Replicative longevity in *S. cerevisiae* has hence been adopted as a simple and adaptable model of senescence for rapid screening of genetic, drug and nutritional interventions.

Evidence has also accumulated demonstrating the correspondance of specific molecular mechanisms associated with ageing in *S. cerevisiae* in higher organisms. Replicative senescence in yeast is strongly associated with genomic stability. *S. cerevisiae* do not suffer from telomere attrition, possessing several mechanisms for regeneration of telomeres, but do experience high levels of instability at the rDNA locus (Defossez et al., 1998). Genomic instability has long been associated with replicative crisis in cultured mammalian cells, and has more recently been demonstrated associated with ageing in mice and fruit flies and other models including human lymphocytes (Counter et al., 1992; Vijg and Dolle, 2002; Li and Vijg, 2012). Failure of a quiescent state leading to apoptosis and necrosis is characteristic of senescent behaviour in mammalian cells. Uncontrolled re-entry to the cell cycle is one of the defining characteristics of tumours and undesirable apoptosis and necrosis underlie many ageing pathologies such as neurodegeneration and cardiovascular disease (MacLellan and Schneider, 1997; Yuan and Yankner, 2000). Perhaps surprisingly, quiescent culture subpopulations have recently been described in ageing yeast; failure of

this quiescence mechanism is correlated with senescence and loss of viability (Gray et al., 2004). *S. cerevisiae* do not contain conventional caspases and for many years it was thought that budding yeast lack an apoptotic pathway (Kang et al., 1999). The discovery of apoptosis-like modes of cell death in yeast (fragmentation of genomic DNA, release of cytochrome c from mitochondria, inversion of phosphatidylserine in plasma membrane) has revealed that in some scenarios, apoptosis and necrosis is responsible for viability loss in senescent yeast cells (Herker et al., 2004). Similarly, accumulation of damaged protein through dysfunctional proteolysis is often postulated to be an upstream cause of senescence in some ageing post-mitotic mammalian systems (Cuervo et al., 2005). Protein oxidation and recycling of cell components through autophagy has been discovered to play an important role in the determination of yeast lifespan (Reverter-Branchat et al., 2004).

1.10 Epigentics of longevity

As a simple genetic model system, *S. cerevisiae* is uniquely useful in investigating the role of epigenetic regulation of physiological processes by modifications to chromatin context. Senescence involves genome-wide and long-term shifts in the pattern of transcription and gene regulation (Zhang et al., 2003) and it is hypothesised that such large-scale control of a complex physiological response can occur through epigenetic modification of chromatin (Bandyopadhyay and Medrano, 2003; Mellor, 2010).

Epigenetic regulation has been demonstrated to play a role in transcriptional control of physiological processes including response to amino acid starvation, cell cycle progression, ribosomal protein expression, and meiosis in yeast. Gcn4 is a transcriptional regulator of genes including *PHO8* responding to amino acid starvation and is dependent upon the histone acetyltransferase and remodelling complexes SWI/SNF, SAGA/SLIK and Mediator (Gregory et al., 1999). This has been shown to lead to H3 hyperacetylation *in vitro* (Vignali et al., 2000) and at the *HIS3*, *PHO8, PHO5* and *GAL1* promoters *in vivo* (Krebs et al., 2000). The histone acetyltransferase Esa1 in NuA4 which acetylates residues on histone H4 has been found to be essential for progression through mitosis and cytokinesis (Clarke et al., 1999). Esa1 can stimulate transcription *in vitro* in an acetyl-coenzyme A dependent fashion (Ikeda et al., 1999) and is specifically recruited to and regulates ribosomal protein-encoding genes *in vivo* (Reid et al., 2000). Repression of meiotic genes has been shown to be dependent upon recruitment of the ATP-dependent chromatin remodelling factor Isw2 by regulator Ume6 (Goldmark et al., 2000) through nucleosome repositioning. Ume6 also recruits histone deacetylase Rpd3, suggesting a role for histone modification in this process (Kadosh and Struhl, 1998).

In mammals, epigenetic regulation has been associated strongly with coordination of phases of development, X chromosome inactivation, as well as tissue specialisation, stress response, and cancer development (Reik et al., 2001; Jones and Baylin, 2002; Lau et al., 2004; Gheorghe et al., 2010; Chaumeil et al., 2011).

However, study of epigenetic contribution to longevity is a relatively new field and not as well established, despite the early proposal of such a relationship (Macieira-Coelho, 1980). Global loss of DNA CpG methylation correlates with crisis and senescence in cultured cells (Wilson and Jones, 1983), with age in mice (Wilson et al., 1987) and human leukocytes (Fuke et al., 2004), and is specific to the rDNA locus in rats (Oakes et al., 2003). Conversely, immortal cell lines contain steady levels of CpG methylation (Young and Smith, 2001). Whether a causal mechanism exists between depleted DNA methylation and senescence remains to be demonstrated. It is hypothesised that repressive regulatory genes are desilenced through CpG island demethylation during ageing: inhibiting DNA methylation in human fibroblasts leads to activation of $p21^{waf\text{-}1}$ (Young and Smith, 2001), and CpG methylation loss is associated with genomic instability in tumours (Lengauer, 2003). Similarly, hypermethylation of tumour suppressor gene promoters during ageing has been implicated in tumour development (Fraga and Esteller, 2007). Mutation of the RecQ helicase WRN has been demonstrated in the human progeroid disorder Werner syndrome. Hypermethylation of the WRN promoter has been found to occur in human tumour cells, and it is hypothesised that WRN acts as an ageing-related tumour suppressor in humans (Agrelo et al., 2006).

Evidence for specific histone modifications is sparser. Fibroblasts deficient in the histone acetyltransferase p300 show slow proliferation and rapid senescence, and overexpression of dominant-negative p300 leads to early senescence (Yao et al., 1998; Bandyopadhyay et al., 2002). Histone deacetylase (HDAC) inhibitors and overexpression of HDAC mutants leads to lifespan extension in flies (Kang et al., 2002; Rogina et al., 2002). However,

treatment with HDAC inhibitors have been observed to lead to early senescence in human fibroblasts (Ogryzko et al., 1996), raising questions about the specificity of the hyperacetylation promoted by these drugs. Nevertheless, p300/CBP activity levels have been shown to decline in the tissues of ageing mice (Li et al., 2002).

Studies in yeast have brought to attention the role of the sirtuin lysine acetyltransferase protein family in senescence. Sir2 in yeast is responsible for deacetylation of histones H3 and H4 and strains lacking this protein are dramatically short lived (Fabrizio et al., 2005); in animals sirtuin downregulation correlates with ageing (Sommer et al., 2006) and sirtuin-activating drugs can increase the longevity of mice (Baur et al., 2006). It has been hypothesised that under caloric restriction and diminished glycolytic and mitochondrial metabolism, demand for the sirtuin substrate NAD^+ is reduced, increasing the activity of sirtuin HDACs and providing a direct link between metabolic mediators of longevity and chromatin (Guarente, 2000).

Scattered evidence also exists for the role of other chromatin modifying activities in ageing. Senescent fibroblasts accumulate H3K9 methylation-dependent heterochromatin foci (Narita et al., 2003), and it has been suggested that lower levels of H3K27me3 associate with *in vitro* senescence (Bracken et al., 2007). Human swi/snf protein BRG1 has been shown to induce senescent morphology in cultured cells, and related Brm1 protein accumulates in the livers of ageing mice (Shanahan et al., 1999; Iakova et al., 2003). Roles for DNA methylation and histone acetylation, methylation and remodelling in senescence induction are potentially a consequence of the high degree of cross-talk between different modes of chromatin modification (Vaissiere et al., 2008). Yeast represent a powerful model for the dissection of potential epigenetic modulations underlying the physiology of the ageing process.

1.11 Physiology and non-coding RNAs

The development of high-resolution cDNA tiling arrays has allowed the analysis of transcript production in both senses over the entire yeast genome. This technique and cDNA sequencing has revealed that both the yeast and mammalian genomes are extensively transcribed in both directions over much of its length (Katayama et al., 2005; Kapranov et al., 2007; Perocchi et al., 2007). This suggests that transcription of the genome is not limited to functional genes but is in fact remarkably pervasive (Xu et al., 2009). In yeast, direct measurement of transcriptional activity by NET-Seq (nascent elongating transcript sequencing) have verified these results, and as most transcripts are 5' capped and polyadenylated RNA polymerase II appears to be responsible for the transcripts (Churchman and Weissman, 2011).

One of the first clear-cut functions for non-coding RNAs to be found was RNA interference (RNAi), elucidated by Fire and Mello in *C. elegans* (Fire et al., 1998). In organisms that contain the RNAi machinery (ie. including mammals, *C. elegans*, *D. melanogaster*), non-coding RNAs may be processed to produced micro-RNAs (miRNAs), or converted to siRNAs from double-stranded RNA, which can suppress gene expression post-transcriptionally through the action of RISC (Hammond et al., 2000) or at the level of transcriptional silencing as mediated by RITS (Verdel et al., 2004). Roles for small non-coding RNAs in this way have been identified in mammals, flies, worms, plants, and fission yeast (Gesellchen and Boutros, 2004; Esquela-Kerscher and Slack, 2006; Jones-Rhoades et al., 2006; Colmenares et al., 2007; Kato and Slack, 2008). However, cDNA sequencing indicates that even in higher eukaryotes, a large proportion of transcription products neither contain coding open reading frames or are processed to miRNAs: these are termed *long non-coding RNAs* (lncRNAs), generally defined as fulfilling the above criteria and having a length greater than 200 residues (Wang and Chang, 2011).

The biological roles of these lncRNAs in higher eukaryotes are still poorly defined; the best understood long non-coding RNA is Xist, responsible for establishing X-inactivation in sex chromosome dosage compensation in mammals (Heard, 2004) Xist is a long (17 Kb) RNA product of the X-inactivation locus (Penny et al., 1996). Cloning of the Xist sequence demonstrated that, despite being spliced and polyadenylated, it contains no open reading frames and does not exit the nucleus (Brockdorff et al., 1992), and hence represented a functional long non-coding RNA in mammals. Xist RNA has since been found to progressively coat the expressing chromosome, leading to a cascade of chromatin state changes which convert the initially labile state of silencing to robust X-inactivation (Heard, 2004). Expression of Xist is sufficient to cause inactivation of chromosomes *in vivo* on the expressing chromosome, and hence Xist-mediated X-linked inactivation occurs in *cis* (Penny et al., 1996).

In mammalian cells, various long non-coding RNAs have recently been identified, operating both in *cis*- and *trans*- (Wang and Chang, 2011) by various mechanisms. In *cis*, long non-coding RNAs may operate through the modification of local chromatin state leading to activation or repression of nearby genes; for example the Air RNA which is transcribed from the second intron of the *Igf2-r* gene, accumulates at the promoter, and leads to recruitment of histone methyltransferase G9a and polycomb complex to effect gene silencing (Nagano et al., 2008); through titration away and sequestration of regulatory factors, as in the minor promoter transcript of the *DHFR* locus which inhibits recruitment of pre-initiation complex by sequestering TFIIB at the promoter itself (Martianov et al., 2007); or as scaffolds for the assembly of regulatory factors, as in the case of *HOTAIR*, a *HOXC* expressed transcript, which recruits both the polycomb component PRC2 and a demethylation complex containing LSD1, CoREST and REST which antagonizes gene activation (Tsai et al., 2010). In *trans*, some long non-coding RNAs have been shown to work to recruit regulatory factors to specific sites in the genome. The long non-coding

transcript *Jpx* is required for Xist activation and induction of X-linked inactivation. Post-transcriptional depletion of *Jpx* transcript using RNAi is sufficient to block X-inactivation, and *Jpx* supplied in *trans* can rescue knockouts of the gene (Tian et al., 2010). Similarly, the transcription-silencing long non-coding transcript LincRNA-p21 affects gene silencing at multiple loci across the genome, and ectopic overexpression of the transcript can lead to apoptosis induction through a series of changes in gene expression (Huarte et al., 2010).

It is now well established that the genome of *Saccharomyces cerevisiae* is pervasively transcribed and that the expression of many of these non-coding transcripts is modulated by environmental conditions (Xu et al., 2009). Because *S. cerevisiae* does not contain an operating RNAi pathway (Nakayashiki et al., 2006) and is highly genetically tractable, this organism has become a key model for the dissection of the function of non-RNAi mediated non-coding RNAs. Non-coding transcripts in yeast have been classified according to whether they are stable in wild-type cells (SUTs), stable only in strains lacking the nuclear exonuclease Rrp6 (CUTs), or stable only in strains lacking the cytosolic exonuclease XrnI (XUTs) (Wyers et al., 2005; David et al., 2006; van Dijk et al., 2011). Many transcripts run in antisense direction to a protein-encoding pre-mRNA, possibly mediated by transcription-promoting activity of the terminator regions (Venters and Pugh, 2009). Non-coding RNA polymerase II-derived transcripts are present even in the extensive rDNA array on chromosome XII. In the spacer region between the main RNA polymerase I transcript of adjacent rDNA repeats numerous small transcripts have been identified (Li et al., 2006).

In known examples of regulation of gene expression by yeast non-coding RNAs, generally the mechanism of action is operation in *cis*, with some evidence for local chromatin modification by the transcription machinery producing the non-coding RNA.

A non-coding transcript produced upstream of the *SER3* gene appears to repress it under rich medium conditions. The mechanism appears to function in *cis* through Spt2-dependent

deposition of nucleosomes, occluding activator binding sites (Martens et al., 2004; Pruneski et al., 2011; Thebault et al., 2011). *IME4* is repressed in haploid cells through an antisense non-coding RNA designated *RME2*; this is repressed in diploids through a1-α2 complex. The mechanism is unknown but is suggested to work in *cis* (Hongay et al., 2006; Gelfand et al., 2011). Another example of regulation by non-coding RNA in *cis* is the repression of the zinc-dependent alcohol dehydrogenase genes *ADH1* and *ADH3* by the zinc-starvation induced non-coding RNA *ZRR1* (Bird et al., 2006).

One of the most well understood mechanisms of repression through transcription of non-coding RNA in *cis* is regulation of the *GAL* cluster (*GAL7-GAL10-GAL1*) by a long non-coding antisense RNA originating in the coding region of *GAL10* and running across *GAL1*. (Houseley et al., 2008). The non-coding RNA originates from a relatively well-defined promoter proximal to binding sites of the Reb1 transcription factor; disruption of the Reb1 consensus binding site prevents production of the antisense RNA. When the locus is not induced, Reb1 binding occurs and the resultant non-coding transcript leads to deposition of K36 trimethylation in *cis*, in turn repressing expression of *GAL1* and *GAL10* through recruitment of the histone deacetylase Rpd3 (Houseley et al., 2008).

However, examples of trans-acting non-coding RNA action have also been demonstrated. Expression and transposition of the Ty1 retrotransposon has been shown to be regulated by a non-coding antisense transcript, *TY1*. In strains null for the cytosolic RNA decay exonuclease Xrn1, steady state ncRNA accumulation could be demonstrated and enhanced repression of the Ty1 retrotransposon. Moreover, ectopic overexpression of the *TY1* antisense from a galactose-induced construct could itself repress expression of the retrotransposon gene (Berretta et al., 2008).

The *PHO84* antisense RNA has a better understood mechanism in *trans*. By stabilisation of the antisense transcript in strains mutant for the nuclear exosome component Rrp6 it was

shown that this non-coding RNA can repress the coding transcript through recruitment of histone deacetylase Hda1 to the promoter (Camblong et al., 2007). Interestingly, in addition to this mechanism the transcript was also shown to repress *PHO84* in *trans* through an Hda1-independent mechanism The presence of an additional copy of *PHO84* on a plasmid or integrated into the genome produces sufficient additional antisense to repress sense transcription from the native copy of the gene (Camblong et al., 2009). The existence of separately mediated pathways emphasizes the biological relevance of the *trans*-acting mechanism.

The non-coding transcripts detected in the rDNA spacer region are repressed by the lysine deacetylase sirtuin Sir2; functionally, their appearance correlates with the rDNA maintenance phenotypes observed in the *sir2Δ* mutant, namely enhanced recombinational hotspot activity and genomic instability; increased rDNA copy number count; and loss of silencing (Gottlieb and Esposito, 1989; Smith and Boeke, 1997; Oakes et al., 1999). The role of these spacer transcripts in these phenotypes is unknown. RNA polymerase II activity in the spacer region has been demonstrated to be inverse to that of RNA polymerase I activity on the main rDNA transcript (Cioci et al., 2003). Interestingly, under specific conditions the entire rDNA array can be transcribed by RNA polymerase II, producing viable rRNA (Vu et al., 1999).

Little research has been performed on any physiological role non-coding RNAs may play in the epigenetic regulation of the ageing process. Interestingly, *PHO84* expression has been found to be repressed in aged cells; this is suggested to be linked to the reduction in Rrp6 expression and the concomitant enhancement of the *PHO84* antisense non-coding transcript (Camblong et al., 2009). Epigenetic regulation, perhaps through non-coding RNAs, may represent an efficient way to coordinate the changes in gene expression occurring over the ageing process. If conserved mechanisms of physical degeneration: such as genomic stability, quiescence failure, or dysfunctional apoptosis and necrosis are

regulated in this way, then intervention in non-coding RNA function may represent a simple and viable anti-ageing therapy.

2 Aims

The aim of this thesis is to identify novel genes regulating chronological and replicative ageing in *Saccharomyces cerevisiae*, the disruption of which leads to longevity extension. The focus will be on gene products which mediate this effect through epigenetic means, and which appear to demonstrate a common regulatory mechanism between the two domains of ageing. Initially, a screen will be developed to allow identification of yeast chronological longevity mutants, and replicative longevity measured by microdissection. The mechanism of enhanced longevity will then be investigated in light of the role of quiescent culture subfractions in this process; followed by analysis of the chromatin and transcriptional activity of the loci at which the gene products are predicted to function. Finally, an experiment to recapitulate the mutant ageing phenotype by overexpression of a non-coding RNA will be described.

3 Materials and methods

3.1 Strains

Strains in this study were derived from the BY4741, BY4742 and W303 backgrounds unless otherwise noted (Table 1). The W303R (W303 *ade2-1 RDN1::ADE2 RAD5*) strain containing a single copy of the ADE2 marker embedded within the rDNA array was a gift from David Sinclair (Harvard Medical School). Deletion strains were constructed as previously described (Longtine et al., 1998). Strains containing plasmids pYES2 and pJU841 were transformed as previously described (Maniatis et al., 1982).

Strain	Parent	Genotype	Origin
BY4741		*MATa*; *his3Δ*; *leu2Δ*; *met15Δ*; *ura3Δ*	EUROSCARF
BY4742		*MATα*; *his3Δ*; *leu2Δ*; *lys2Δ*; *ura3Δ*	EUROSCARF
FY168		*MATa*; *his3 4-917Δ*; *lys2Δ*; *leu2Δ*	Open Biosystems
W303R		*MATa*; *leu2-3*,112 *trp1-1*; *can1-100; ura3-1; his3-11,15*; *ade2-1*; *RDN1::ADE2*; *RAD5*	D. Sinclair
sch9Δ	BY4741	*sch9Δ::KanMX*	EUROSCARF
spt7Δ	BY4741	*spt7Δ::KanMX*	EUROSCARF
spt8Δ	BY4741	*spt8Δ::KanMX*	EUROSCARF
gcn5Δ	BY4741	*gcn5Δ::KanMX*	EUROSCARF
spt7-217	FY168	*spt7–217::KanMX*	EUROSCARF
ydr026cΔ	BY4741	*ydr026cΔ::KanMX*	EUROSCARF
sir2Δ	BY4741	*sir2Δ::KanMX*	EUROSCARF
snf1Δ	BY4742	*snf1Δ::KanMX*	EUROSCARF
acs1Δ	BY4741	*acs1Δ::KanMX*	EUROSCARF
ach1Δ	BY4741	*ach1Δ::KanMX*	EUROSCARF
fob1Δ	BY4741	*fob1Δ::KanMX*	EUROSCARF

Strain	Parent	Genotype	Origin
sir2Δ ydr026cΔ	BY4741	*sir2Δ::HIS3*; *ydr026cΔ::KanMX*	This study
tor1Δ	BY4741	*tor1Δ::KanMX*	EUROSCARF
rim15Δ	BY4741	*rim15Δ::KanMX*	EUROSCARF
tor1Δ ydr026cΔ	BY4741	*tor1Δ::HIS3*; *ydr026cΔ::KanMX*	This study
WT *SCH9*	BY4741	*BY4741 pRS416*	This study
sir2Δ SCH9	BY4741 *sir2Δ*	*sir2Δ pRS416*	This study
WT *SCH9* (OE)	BY4741	*BY4741 pJU841*	This study
sir2Δ SCH9 (OE)	BY4741 *sir2Δ*	*sir2Δ pJU841*	This study
W303R *sir2Δ*	W303R	*sir2Δ::TRP1*	D. Sinclair
W303R *ydr026cΔ*	W303R	*ydr026cΔ::KanMX*	This study
W303R *fob1Δ*	W303R	*fob1Δ::HPH*	D. Sinclair
W303R *sir2Δ ydr026cΔ*	W303R	*sir2Δ::TRP1*; *ydr026cΔ::KanMX*	This study
W303R *fob1Δ ydr026cΔ*	W303R	*fob1Δ::URA3*; *ydr026cΔ::KanMX*	This study
W303R *fob1Δ sir2Δ*	W303R	*fob1Δ::HPH*; *sir2Δ::KanMX*	This study
W303R *ade2Δ*	W303R	W303R *ade2Δ::HIS3*; *RDN1::ADE2*	This study
W303R *ade2Δ sir2Δ*	W303R *ade2Δ*	*sir2Δ::TRP1*	This study
W303R *ade2Δ ydr026cΔ*	W303R *ade2Δ*	*ydr026cΔ::KanMX*	This study
W303R *ade2Δ sir2Δ ydr026cΔ*	W303R *ade2Δ*	*sir2Δ::TRP1*; *ydr026cΔ::KanMX*	This study
W303R EV	W303R	*pYES2*	This study

Strain	Parent	Genotype	Origin
W303R FBR(F)	W303R	*pYES2::FBR(F)*	This study
W303R FBR(R)	W303R	*pYES2::FBR(R)*	This study
W303R *ydr026cΔ* EV	W303R	*ydr026cΔ::KanMX*; *pYES2*	This study
W303R *ydr026cΔ* FBR(F)	W303R	*ydr026cΔ::KanMX*; *pYES2::FBR(F)*	This study
W303R *ydr026cΔ* FBR(R)	W303R	*ydr026cΔ::KanMX*; *pYES2::FBR(R)*	This study
W303R *sir2Δ* EV	W303R	*sir2Δ::TRP1 pYES2*	This study
W303R *sir2Δ* FBR(F)	W303R	*sir2Δ::TRP1*; *pYES2::FBR(F)*	This study
W303R *sir2Δ* FBR(R)	W303R	*sir2Δ::TRP1*; *pYES2::FBR(R)*	This study
W303R *fob1Δ* EV	W303R	*fob1Δ::HPH*; *pYES2*	This study
W303R *fob1Δ* FBR(F)	W303R	*fob1Δ::HPH*; *pYES2::FBR(F)*	This study
W303R *fob1Δ* FBR(R)	W303R	*fob1Δ::HPH*; *pYES2::FBR(R)*	This study
W303R *sir2Δ* *ydr026cΔ* EV	W303R	*sir2Δ::TRP1*; *ydr026cΔ::KanMX*; *pYES2*	This study
W303R *sir2Δ* *ydr026cΔ* FBR(F)	W303R	*sir2Δ::TRP1*; *ydr026cΔ::KanMX*; *pYES2::FBR(F)*	This study
W303R *sir2Δ* *ydr026cΔ* FBR(R)	W303R	*sir2Δ::TRP1*; *ydr026cΔ::KanMX*; *pYES2::FBR(R)*	This study
BY EV	BY4741	*pYES2*	This study
BY FBR(F)	BY4741	*pYES2::FBR(F)*	This study
BY FBR(R)	BY4741	*pYES2::FBR(R)*	This study
BY *ydr026cΔ* EV	BY4741	*ydr026cΔ::KanMX*; *pYES2*	This study
BY *ydr026cΔ* FBR(F)	BY4741	*ydr026cΔ::KanMX*; *pYES2::FBR(F)*	This study
BY *ydr026cΔ* FBR(R)	BY4741	*ydr026cΔ::KanMX*; *pYES2::FBR(R)*	This study

Strain	Parent	Genotype	Origin
BY *sir2Δ* EV	BY4741	*sir2Δ::KanMX*; *pYES2*	This study
BY *sir2Δ* FBR(F)	BY4741	*sir2Δ::KanMX*; *pYES2::FBR(F)*	This study
BY *sir2Δ* FBR(R)	BY4741	*sir2Δ::KanMX*; *pYES2::FBR(R)*	This study

Table 1. List of strains used in this study.

3.2 Plasmids

Plasmids pJU841 was a gift from Robbie Loewith (University of Geneva). Plasmids pYES2::FBR(F) and pYES2::FBR(R) were constructed from plasmid pYES2 in this study. A region corresponding to the non-coding transcript *IGS1-R* was amplified by PCR from genomic DNA (FBR). pYES2 was cut with *HindIII*, blunt ends generated with Klenow, and dephosphorylated with calf intestinal phosphatase. The FBR fragment was ligated to the blunt ends in both orientations to generate pYES2::FBR(F) and pYES2::FBR(R).

Plasmid	Origin
pRS416	Robbie Loewith
pJU841 *SCH9*^{T723D,S726D,T737E,S758E,S765E}	Robbie Loewith
pYES2	Invitrogen
pYES2::FBR(F)	This study
pYES2::FBR(R)	This study

Table 2. List of plasmids used in this study.

3.3 Primers

DNA primers used throughout this study were obtained from Eurofins. Primer sequences are listed in Table 3.

Primer	Sequence (5' – 3')	Method	Section used
YDR026C-KO(F)	tatctattgggtctgtatatgtttgg gaaagtaacccttc-cggatccccggg ttaattaa	Gene knockout	3.1
YDR026C-KO(F)	gccgtttcttgtctgcgtcaagaaga aagataaaggtaga-gaattcgagct cgtttaaac	Gene knockout	3.1
SIR2-KO(F)	tattaatttggcacttttaaattatt aaattgccttctac-cggatccccggg ttaattaa	Gene knockout	3.1
SIR2-KO(R)	ccagctttaatgtgccgatgagggaa aaatggtttgaatg-gaattcgagct cgtttaaac	Gene knockout	3.1
FOB1-KO(F)	ttaacgattgtgtgagtgtgaatttg tgctgaggataaca-gaattcgagct cgtttaaac	Gene knockout	3.1
FOB1-KO(R)	acctatggtgactcctcctttcattc tatcctacatatta-gaattcgagct cgtttaaac	Gene knockout	3.1
U4(F)	atccttatgcacgggaaa	RT-PCR	4.7
U4(R)	aacacaatctcggacgaatc	RT-PCR	4.7
ACS1(F)	gcgcatggtcaacaaagctc	RT-PCR	4.7
ACS1(R)	ccatgcacacccgttgattc	RT-PCR	4.7
ATG1(F)	ccgaggttactgagggccac	RT-PCR	4.7
ATG1(R)	ggctcttgataatgcattag	RT-PCR	4.7
SIP18(F)	gggaaagaacgccaaatcct	RT-PCR	5.2
SIP18(R)	gccagcgttcatctttgttc	RT-PCR	5.2
MLH2(F)	atcctgcatgcacaaaacaa	RT-PCR	5.2
MLH2(R)	aggcttgcaaaagactggaa	RT-PCR	5.2
CAR(F)	ccacctaccgaccaactttc	Northern probe template	7.2
CAR(R)	gaggtgttatgggtggagga	Northern probe template	7.2
FBR(F)	tccccactgttcactgttca	Northern probe template	7.2
FBR(R)	agggctttcacaaagcttcc	Northern probe template	7.2
ETS(F)	catgtttttacccggatcat	Northern probe template	7.2
ETS(R)	ctaagtgggtactggcaggag	Northern probe template	7.2
ADE2(F)	aaggcctcacaactctggac	Northern probe template	7.2

ADE2(R)	gtgaaattctttggcattgg	Northern probe template	7.2
25S3'(F)	catgtttttacccggatcat	ChIP	7.3
25S3'(R)	ctaagtgggtactggcaggag	ChIP	7.3
25S mid(F)	ccggaatcttaaccggattc	ChIP	7.3
25S mid(R)	agttggacgtgggttagtcg	ChIP	7.3
5.8S(F)	gaaatgacgctcaaacaggc	ChIP	7.3
5.8S(R)	aaactttcaacaacggatc	ChIP	7.3
18S mid(F)	ggcccaaagttcaactacga	ChIP	7.3
18S mid(R)	acaattggagggcaagtctg	ChIP	7.3
18S 5'(F)	tcgccgagaaaaacttcaat	ChIP	7.3
18S 5'(R)	ttccgtattttccgcttcc	ChIP	7.3
NTS1-2(F)	cattatgctcattgggttgc	ChIP	7.3
NTS1-2(R)	agggaaatggagggaagaga	ChIP	7.3
T (outer nest)	gcatattgctgtgtgttccatagta	3C	7.4
T (inner nest)	cactctatgcgtttctatatggttg	3C	7.4
25S (outer nest)	attgcgtcaacatcactttctgac	3C	7.4
25S (inner nest)	ttgtccgtaccagttctaagttgat	3C	7.4
5.8S (outer nest)	ggtaaaacctaaaacgaccgtactt	3C	7.4
5.8S (inner nest)	agaaggaaatgacgctcaaacag	3C	7.4
18S (outer nest)	gccctgtatcgttatttattgtcac	3C	7.4
18S (inner nest)	cactatcctaccatcgaaagttga	3C	7.4
P (outer nest)	taacctgtcaccttgaaactacctc	3C	7.4
P (inner nest)	actttcatgttctgtttcgacctac	3C	7.4
HMS2(F)	ccagttcaccaaagtcatcct	3C control	7.4
HMS2(R)	aagctggcgttaatttccct	3C control	7.4
FBR(F)	tcttcccagtagcctcatcc	Cloning	8.1
FBR(R)	tttgcgtggggataaatcatttg	Cloning	8.1

Table 3. List of primers used in this study.

3.4 PCR conditions

PCR was performed under various conditions for different procotols described in this study (Table 4).

Protocol	Polymerase	Initial	Denaturation	Annealing	Extension	Final
General PCR	Phusion	$98^{O}C$ 5 mins	$98^{O}C$ 10s	$55\text{-}60^{O}C$ 30s	$72^{O}C$ 20-60s	$72^{O}C$ 5 mins
qPCR	Sensimix	$94^{O}C$ 5 mins	$94^{O}C$ 30s	$55\text{-}61^{O}C$ 30s	$72^{O}C$ 30s	$72^{O}C$ 5 mins
3C	Phusion (Mg^{2+} depleted mix)	$98^{O}C$ 5 mins	$98^{O}C$ 10s	$59^{O}C$ nest 1 $60^{O}C$ nest 1 30s	$72^{O}C$ 20s	$72^{O}C$ 5 mins

Table 4. PCR conditions

3.5 Media

Rich medium (YP) was composed of 1% Difco yeast extract (BD) and 1% bactopeptone (BD). Minimal medium (CS) was composed of yeast nitrogen base with ammonium sulphate (BD) and complete supplement mixture as per the manufacturer's instructions. Media was supplemented with 2% glucose or galactose as appropriate. For the development of red pigment in *ade2* strains, adenine depleted minimal medium without uracil was required. This was prepared with only 20 mg/ml adenine to promote induction of the adenine synthesis pathway.

3.6 Yeast culture

From solid growth media, cell cultures were inoculated into 3-5ml liquid rich medium with 2% glucose overnight. These pre-cultures were used to inoculate appropriate volumes of medium to a cell density measured at OD_{600} = 0.2. Cultures were incubated at $30^{O}C$ with rotation at 200rpm unless otherwise noted. For logarithmic growth phase cells, growth was allowed to continue until a medium turbidity of OD_{600} = 0.5-0.8 was obtained. For post-

diauxic cultures, growth was allowed to continue for 36 hours or more as specified before cells were harvested. For chronological ageing experiments, pre-cultures were used to inoculate 3-5ml CS medium supplemented with 1% glucose and these grown overnight. The CS pre-cultures were then diluted 100-fold into 10ml CS medium with 1% glucose in 50ml flasks and incubated at 30^{O}C shaking at 100rpm. For study of culture subfractionation, 100ml rich medium culture in 500ml flasks was inoculated at OD_{600} = 0.2 and incubated at 30^{O}C with shaking at 100rpm.

3.7 Cloning

Vectors constructed as above cloned into shuttle vectors were transformed at 42^{O}C into competent DH5α *E. coli* and plated onto selective LB-ampicillin medium using the standard protocol (Maniatis et al., 1982). Transformants were cultured at 37^{O}C in LB-ampicillin, and plasmid purified using a plasmid miniprep kit (QIAgen). Clones were screened by PCR, restriction enzyme digestion, and sequencing to ensure correct inserts were incorporated.

3.8 Transformation of *Saccharomyces cerevisiae*

Transformation of yeast plasmids and for homologous recombination was performed according to the standard lithium acetate protocol (Ito et al., 1983). Cells were grown to logarithmic phase in rich medium, harvested, washed with sterile water, and resuspended in 0.1M lithium acetate in TE. Following 1hr or more incubation at 4^{O}C, competent cells were transformed with 700 μl 40% PEG in a solution of 0.1M lithium acetate in TE, 10 μl calf thymus DNA (Sigma), and 10 μl of PCR product to be transformed. Cells were incubated at 30^{O}C for 30 minutes, before heat shock at 42^{O}C for 20 minutes with 40 μl DMSO (Sigma) added. Following heat shock, cells were pelleted gently (5000g, 1 min), washed in

sterile water, and incubated in rich medium with 2% glucose for 6 hours to recover. Cells were then harvested, washed, and plated on appropriate selective media. Colonies were screened for transformants after 3 days incubation at 30^{O}C by PCR analysis of genomic DNA purified from several colonies.

3.9 Extraction of genomic DNA from *Saccharomyces cerevisiae*

Cells were harvested from 5-10ml of stationary phase rich medium culture and resuspended in 200 µl DNA extraction buffer (2% Triton X-100, 1% SDS, 100 mM NaCl, 100 mM Tris-HCl pH 8.0, 1mM EDTA pH 8.0) with 200 µl acid-washed glass beads and 200 µl 25:24:1 v/v phenol:chloroform:isoamyl alcohol. The mixture was vortexed vigorously for 20 minutes, and the organic and aqueous phases then separated by centrifugation at 13krpm for 15 minutes. 500 µl DNA precipitation solution (6:1 v/v ethanol to 7.5M ammonium acetate) was added to the aqueous phase to precipitate genomic DNA. The DNA pellet was washed with 70% ethanol and resuspended in 100 µl 10mM Tris pH 8.0. DNA recovery was measured by nanodrop spectrometry at 260 nm.

3.10 Colony formation over chronological ageing

Chronological longevity was initially measured by serial dilution drop plates and colony-forming unit (CFU) ability of ageing cultures. Ageing culture aliquots were removed at agepoints, and 5 serial ten-fold dilutions performed in 100 µl sterile water for each sample. 7 µl of each dilution series were then dropped onto rich medium plates and incubated at 30^{O}C for 2 days to allow colonies to develop. To assay CFU viability, cell densities of agepoint aliquots was measured by haemocytometer counting, and aliquots diluted appropriately (10^{5}-10^{4} fold) in sterile water to achieve 100-300 cells in 100 µl solution.

100 μl of this cell suspension was then plated on 3 to 5 rich medium plates, which were incubated for 2-3 days at 30^{O}C to allow viable cultures to develop. Relative viability was then determined by the average count of developing colonies compared to the calculated number of cells deposited on each plate.

3.11 Chronological ageing by outgrowth

30 μl aliquots were removed from ageing cultures and diluted in 120 μl rich medium with 2% glucose carbon source in 100-well high throughput plates. Three (*mechanical*) replicates of each biological replicate were inoculated to increase precision. The plates were incubated in a Bioscreen C machine (Oy Growth Curves Ab Ltd) at 30^{O}C with continuous shaking and measurement of culture turbidity at OD600 every 20 minutes for 24 hours. Outgrowth curve turbidity data was automatically recorded by the measurement software. Outgrowth curves were then analysed in Excel and MATLAB using the software and model developed in this study, described in section 4.3. Initial viability values as well as culture growth rates (doubling times) were calculated. Mechanical replicate averages were used to determine average initial viability for each biological replicate, with anomalous mechanical replicates (caused by e.g. infection) automatically discarded. Biological replicate data was used to plot viability curves over the ageing timecourse, calculate median chronological lifespans, and perform statistics (Student's t-test).

3.12 RNA extraction from *Saccharomyces cerevisiae*

Logarithmic or post-diauxic growth phase cultures were prepared and harvested by centrifugation at 5,000 g for 5 mins. Whole RNA was extracted from yeast using the hot phenol method: cells were resuspended in 400 μl TES (10 mM Tris-HCl pH 7.5, 5 mM EDTA pH 8.0, 1% SDS) and the same volume of acidified phenol:chloroform (pH 4.5) was

added. The mixture was incubated at 65°C for 20 minutes with periodic strong vortexing. The organic and aqueous phases were separated by centrifugation at 13 krpm for 15 minutes, and the aqueous phase transferred to 600 µl ethanol. 30 µl 4M sodium acetate stock was then added to precipitate RNA. RNA was pelleted by centrifugation and resuspended in RNAse free water. RNA yields were determined by nanodrop spectrometry at 260nm.

3.13 Northern blotting

10 µg RNA was separated on 1.2% FA (20 mM MOPS, 5 mM Sodium Acetate, 1mM EDTA, pH 7) agarose gels containing 1.1% formaldehyde at 3.5 V/cm for 2 hours before overnight transfer to neutral nylon membranes (Magna) by wet blotting overnight using 20X SSC as transfer buffer as previously described (Maniatis et al., 1982). RNAs were fixed to the membranes by baking at 80°C for 2 hours and blocked at 65°C in PerfectHyb (Sigma) hybridisation buffer for 2 hours. Radiolabelled strand-specific probes were added and allowed to hybridise to the membranes at 65°C overnight. Non-specifically bound probe was removed by a series of 20 minute washes at 65°C: twice in 1X SSC/0.1% SDS, once in 0.2X SSC/0.1% SDS, once in 0.1X SSC/0.1% SDS, and twice in 0.05X SSC/0.1% SDS. Membranes were exposed to Kodak X-ray photographic film for between 24 hours and 7 days to obtain suitable exposures. Loading levels of RNA were monitored by abundance of 18S and 26S rRNA in each lane by ethidium bromide staining.

3.14 Southern blotting

DNA samples to be analysed were separated on appropriate TAE- or TBE-agarose gels with or without ethidium bromide staining. For large DNA species > 5 kb, depurination was performed by soaking gels in 125 mM HCl solution for 15 minutes. DNA was

denatured *in situ* by soaking gels in denaturation buffer (0.5M NaOH, 1M NaCl) for 15 minutes with gentle agitation; the gel was then neutralised by an equivalent soak in neutralisation buffer (1M Tris pH 7, 3M NaCl) for 20 minutes. DNA was transferred to neutral nylon membrane (Magna) overnight by wet blotting using 20X SSC as transfer buffer, and fixed to the membrane by baking at 80^{O}C for 2 hours. Membranes were blocked by incubation with PerfectHyb buffer (Sigma) for 2 hours at 65^{O}C prior to addition of radiolabelled probe, allowed to hybridise to the membrane at 65^{O}C overnight. Non-specifically bound probe was removed by a series of 30 minute washes: once in 2X SSC/0.1% SDS at 60^{O}C, and then twice in 1X SSC/0.1% SDS at 65^{O}C. Membranes were exposed to photographic film for between 24 hours and 7 days to obtain suitable exposures and signals quantified using an Fuji FLA-3000 phosphorimaging system (Fujifilm).

3.15 Generation of radiolabelled strand-specific probes

Radiolabelled strand specific probes were synthesised by an asymmetric PCR reaction in the presence of α-^{32}P-dCTP. A template for the reaction corresponding to the entire region constituting the probe was generated by PCR using Phusion DNA polymerase (Thermo) upon *S. cerevisiae* genomic DNA template and purified using PCR cleanup kit (QIAgen). Labelled primer extension reactions were performed using Taq DNA polymerase (Sigma) and one primer cognate to the sense of the probe to be produced in the presence of 0.925 MBq α-^{32}P-dCTP per reaction. Radiolabelled product was then purified away from unincorporated radiolabel using a Sephadex G-50 column.

3.16 Generation of non-strand specific probes

Non-strand specific probes (for Southern blots) were generated by the random priming method. DNA corresponding to the probe desired was purified as a plasmid or generated by

PCR as above. Random 9-mer primers were hybridised to the template following denaturation at 100^{O}C for 5 minutes and rapid cooling. Primers were extended in the presence of 0.74 MBq of α-^{32}P-dCTP per reaction using Exo(-)-Klenow (Invitrogen) at 37^{O}C for 15 minutes. Radiolabelled products were purified away from unincorporated label on Sephadex G-50 columns. The probe was then denatured at 95^{O}C for 5 minutes in the presence of an excess of calf thymus DNA (Sigma).

3.17 Reverse transcription

cDNA was produced from cellular RNA by reverse transcription. 1000 ng purified RNA was treated with DNase I (Sigma) in supplied buffer in the presence of RNase inhibitor RNase OUT for 1 hr at 37^{O}C. 250 ng DNA-free RNA was then reverse transcribed at 50^{O}C using QIAgen Superscript III in supplied buffers with RNase OUT. To determine background levels of contaminating genomic DNA, negative controls were performed in the absence of reverse transcriptase. Material input was controlled for by normalisation to levels of U4 snRNA abundance.

3.18 Quantitative PCR (qPCR)

Quantitative PCR was performed using a QIAgen Rotor-gene 6000 real-time PCR machine. Samples were mixed with reaction buffer, SYBR-green labelled deoxynucleotides (Sensimix) and appropriate 20-bp primers to produce an assayed PCR product 100-300 bp long using a Corbett robotics pipetting robot. Amplification data was normalised to previously prepared genomic DNA standards and quantified using Rotor-gene software.

3.19 Isolation of ageing culture subpopulations

Dense (quiescent) and less-dense (non-quiescent) cell culture subfractions were isolated from bulk ageing cultures by density equilibrium centrifugation of harvested cells over self-forming Percoll (Sigma) density gradients. 45 ml Percoll mixture (9:1 Percoll to 1.5 M NaCl solution) was added to 50 ml Corex centrifuge tubes, sealed, and centrifuged at 13.8 krpm in a JA-17 rotor (Beckmann centrifuge) to generate a density gradient. $2x10^9$ cells were harvested, washed and resuspended in 1ml 150 mM Tris pH 7.5, and applied to the columns. Equilibrium density centrifugation was performed at 1500 rpm for 60 minutes in a Jouan CR3 centrifuge. Columns were photographed using an Konica Minolta Dimage A1 camera, and cell subfractions recovered using a 1000 μl pipette from within the gradient. Cell morphology of subfractions was investigated and recorded using an Zeiss Axioskop microscope and Axiovision 4.5 software.

3.20 Terminal deoxynucleotidyl transferase dUTP nick end labelling (TUNEL) assay

$1x10^9$ cells were washed and fixed in 3.7% formaldehyde solution in 1X PBS pH 8.0 for 10 minutes. Cells were washed in 1X PBS pH 8.0, and then resuspended in 1 ml 70% ethanol at room temperature for 1 hour. After washing in PBS, 100 μl cell suspension was taken as a positive control and treated with 8 μl DNase I (Roche) in DNase I reaction buffer at 37^OC for 1 hour. TUNEL reaction was performed using a TUNEL assay kit (Roche) on 100 μl cell suspension, with samples incubated with enzyme and fluorescein-dUTP substrate or without enzyme or substrate as negative controls. Reaction mixture was incubated for 3 hours at 37^OC away from light. Cells were then washed in PBS, and resuspended in 1 ml 1X PBS pH 8.0. Fluorescein incorporation was measured by flow cytometry on a BD FACScan using the FL1 filter and a laser voltage of 789V without gating. Fluorescence

intensity was measured in 40,000 cells from each sample, data being collected on a linear and logarithmic scale. Cytometry profiles were statistically compared using the Kolmogorov-Smirnov non-parametric test for independence of distribution.

3.21 Replicative lifespan

Replicative lifespans were measured by micromanipulator dissection of buds from n>25 plated individual virgin mother cells on rich medium plates. Cells were streaked on rich plates and allowed to grow for 2 days at 30^{O}C. A micromanipulator (Singer) was then used to isolate individual cells, which were plated in a pool. Buds produced by these cells were therefore known to be virgin mothers, and these were moved to defined grid positions on the plate. While incubating at 30^{O}C, plates were inspected every 90-120 minutes to check for new daughters. Daughters were removed by micromanipulation and tallied; virgin mothers that never produced any daughters were deemed unviable and excluded from the experiment. After the initial division, mothers which failed to produce any daughter cells for more than three contiguous inspections were deemed replicatively senescent and censored. Censor data was used to construct replicative viability curves, which were then compared using the non-parametric log-rank test for mortality.

3.22 Purification of replicatively aged cells

Amino groups of cell walls of $1x10^{8}$ inoculating cells were labelled with biotin by incubation with reactive NHS-LC-biotin (Sigma) in 1X PBS pH 8.0 for 30 minutes at 4^{O}C. Cells were washed in sterile 1X PBS pH 8.0 and used to inoculate 1 l cultures in rich medium (2% glucose) in 3 l flasks. Cultures were incubated at 30^{O}C with shaking at 180rpm for sufficient time for the required doubling times to elapse. Cultures were then harvested, washed in 1X PBS pH 8, and 100 μl iron-streptavidin beads (Sigma) added. The

mixture was incubated at 4^{O}C for 10 minutes prior to the beads and associated biotinylated cells being recovered by magnetic sorting. Magnetic beads were washed in 1X PBS, before DNA was isolated from the recovered cells by phenol:chloroform extraction.

3.23 Extrachromosomal ribosomal circles (ERCs)

Genomic and ERC DNA was extracted from recovered cells by a gentle protocol using yeast lytic enzyme (MP Biomedicals) to digest cell walls. Following removal of cell walls, cells were lysed in low osmolarity solution (0.1 M MES, 1 mM EDTA, 0.5 mM MgCl2, pH 6.4) and DNA extracted using phenol:chloroform. An equal volume of phenol:chloroform:isoamyl alcohol 25:24:1 was added to the lysed cells, shaken lightly to mix, and phases separated by centrifugation at 13krpm in a desktop centrifuge. The aqueous phase was transferred to 1ml ethanol, and 25 μl 5M NaCl added to precipitate DNA. DNA pellets were recovered by centrifugation at 13 krpm for 20 minutes and resuspended in 50 μl 10 mM Tris pH 8.0. Yields were measured by nanodrop spectrometry at 260nm. ERCs and genomic DNA were separated on 0.8% 1X TAE-agarose gels at 4^{O}C running at 1V/cm for 36 hours without ethidium bromide. DNA was Southern blotted onto neutral nylon membrane and hybridised to this membrane by baking at 80^{O}C for 4 hours. Membranes were hybridised with a probe generated by random priming of plasmid pYRIG12, containing one rDNA repeat copy, in the presence of 0.74 MBq α-^{32}P-dCTP using Exo(-) Klenow (Random Priming Kit, Roche), and washed as standard for Southern blots. Membranes were exposed to x-ray film for 1-2 days to obtain suitable exposures for comparison.

3.24 rDNA recombination assay

Logarithmic phase cultures of appropriate strains in the W303R background were prepared and diluted 10^3-10^4 fold in sterile water. 50-200 μl cell suspension was spread onto rich medium or low adenine CS-ura plates to distribute 100-300 cells per plate. Plates were incubated at 30^OC for 2-4 days to allow colony growth, followed by incubation at 4^OC to promote accumulation of red pigment formed as an intermediate of adenine biosynthesis.. Half-sectored colonies on all plates were counted, and total colonies excluding pre-reverted (red) colonies estimated by counting. Comparisons were performed using Student's t test.

3.25 Chromatin immunoprecipitation (ChIP)

Chromatin immunoprecipitation was performed according to the method previously described by Morillon *et al* (Morillon et al., 2003). 50 ml logarithmic phase cultures in rich medium were harvested and cells crosslinked in 1% formaldehyde (Fisher) in 1X PBS pH 8.0 for 30 minutes at room temperature. Excess formaldehyde was quenched by addition of 2.5 ml 2.5M glycine and cells washed twice in cold 1X PBS. Cells were then resuspended in 500 μl FA buffer (0.1% SDS, 1% Triton X-100, 10 mM HEPES pH 8.0, 0.1% sodium deoxycholate, 150 mM NaCl, 1 mM AEBSF, 0.8 μg/ml Pepstatin A, 0.6 μg/ml leupeptin, 0.1 μl/ml Z-Leu-Leu-Leu-Al). Cells were lysed by vigorous grinding with glass beads in two 1 minute bursts using a MagNa lyser (Roche) at 4^OC. Fixed chromatin was fragmented by sonication using a Bioruptor (Comso Bio) for 30 minutes at 4^OC (1 minute high power pulses, 20 second intervals) to a fragment size of less than 500bp. Immunoprecipitation was performed by incubation of a one in ten dilution of sonicated chromatin with anti-H3 antibody (AbCam) at 4^OC with rotation overnight. Purification of immunoprecipitated complex was carried out by adding 40 μl 50% slurry of protein-A sepharose beads (CL-4B Amersham) in FA buffer blocked with 10μg sonicated salmon sperm DNA and rotating at

room temperature for 90 minutes. Beads were washed of unprecipitated material using TSE-150/500 buffers (1% Triton X-100, 0.1% SDS, 2 mM EDTA, 20 mM Tris-HCl pH 8.0, 150/500 mM NaCl), LiCl wash buffer (250 mM LiCl, 1% NP-40, 1% sodium deoxycholate, 1mM EDTA, 10 mM Tris-HCl pH 8.0) and TE. Elution was performed using 500 µl elution buffer (1% SDS, 0.1 M $NaHCO_3$) at 65^OC for 30 minutes. Crosslinking was reversed by incubation at 65^OC overnight after adding NaCl to 70 mM final concentration. Residual protein and RNA was digested using Proteinase K and RNase A prior to DNA purification using QIAquick PCR purification columns (QIAgen). Recovered DNA was quantified using qPCR as described above. Control samples were prepared without addition of antibody (immunoprecipitation control) and containing total input chromatin (input controls). Immunoprecipitation signal was calculated as

$$S = \frac{IP - NO}{TOT}$$

where S is calculated signal, IP is quantified sample immunoprecipitation, and NO and TOT are quantified immunoprecipitation and total controls respectively. NO controls were prepared as experiment but without addition of antibody, while total controls contained DNA purified before immunoprecipitation. Average signals were calculated from three quantified mechanical qPCR repeats.

3.26 Chromosome conformation capture (3C)

An assay was developed for sensitive and reproducible chromosome conformation capture over the rDNA locus of *Saccharomyces cerevisiae* (fully described in section 7.4). 50ml logarithmic phase culture was harvested and crosslinked in 1% formaldehyde 1X PBS pH 8.0 for 10 minutes at room temperature. Excess formaldehyde was quenched by addition of 2.5 ml 2.5 M glycine, and cells washed in cold MG/K buffer (35 mM K_2HPO_4, 65 mM

KH_2PO_4, 5 mM $MgCl_2$ pH 6.5). Cell walls were removed by digestion using 50 U yeast lytic enzyme (MP Biomedicals) in spheroplasting buffer (MG/K buffer with 25 mM DTT, 1.2 M sorbitol) at 30^{O}C for 30-60 minutes. Spheroplasts were washed with MES wash buffer (0.1 M MES pH 6.4, 1 mM EDTA, 0.5 mM $MgCl_2$, 1.2 M sorbitol) prior to resuspension in 1 ml MES lysis buffer (0.1 M MES pH 6.4, 1 mM EDTA, 0.5 mM $MgCl_2$) and incubation on ice for 15 minutes to lyse spheroplasts. Discontinuous sucrose gradients were prepared in 35 ml Corex centrifuge tubes using a 5 ml cushion of 1.8 M sucrose solution with 10 ml 1.1 M sucrose solution in MES lysis buffer. Lysed mixture was applied to the column and nuclei purified by equilibrium centrifugation at 10 krpm for 10 minutes in a JA-17 rotor (Beckmann J2-21 centrifuge) at 4^{O}C. Upper and lower pellets were removed from the tubes by water wash and the nuclear pellet at the interface resuspended in 1 ml CSK buffer (100 mM NaCl, 300 mM sucrose, 10 mM PIPES, 3 mM MgCl2, 1 mM EGTA). 100 µl nuclear preparation was taken and resuspended in 100 µl NEBuffer 4 (50 mM potassium acetate, 20 mM Tris-acetate, 10 mM magnesium acetate, 1 mM DTT pH 7.9). 10 µl 1% SDS was added and the mixture incubated at 37^{O}C for 10 minutes to lyse nuclei; 11 µl 10% Triton X-100 was then added to sequester excess SDS. 10 µl (50 U) restriction enzyme *BfaI* (NEB) was added and the reaction incubated at 37^{O}C overnight with periodic shaking. The enzyme was heat inactivated at 65^{O}C for 10 minutes, and the solution diluted with 1170 µl pure water. Ligation was carried out with 30 µl (1200 U) T4 DNA ligase (NEB) at 16^{O}C for 4 hours, with periodic shaking, in fresh manufacturer-supplied ligase buffer (NEB). Chromatin was then decrosslinked at 65^{O}C overnight after the addition of 100 µl 5 M NaCl and 20 µl 20 mg/ml Proteinase K (Sigma). DNA was purified by phenol:chloroform extraction and precipitation in 70% ethanol with sodium chloride and glycogen. DNA pellets were washed with 70% ethanol and resuspended in 50 µl 10 mM Tris pH 8.0, prior to treatment with RNase A to remove any contaminating RNAs. Analytic PCR reactions to detect 3C re-ligation products were

performed with nested primers using Phusion DNA polymerase (Finnzyme) in supplied buffer with reduced Mg^{2+} concentration through addition of 7 μl 2.5 mM dNTP solution per 50 μl reaction. PCR reactions were performed for 25 and 18 cycles for each nest. Aliquots were removed in the 14^{th}, 16^{th} and 18^{th} cycles of the second nest for analysis. PCR products were separated on 1% TBE-agarose gels stained with ethidium bromide and Southern blotted without depurination as described above. Membranes were probed using a radiolabelled probe generated by random priming of a region homologous to the terminator 3C primer, and hence all *bona fide* 3C re-ligation products. Membranes were exposed to photographic film for 3-12 hours, and 3C signals quantified using a Fujifilm phosphorimaging system. Random ligation controls were prepared by digestion of 20 μg purified wild-type genomic DNA with 50 U *BfaI* at 37^{o}C for 4 hours. Following heat inactivation of the enzyme, fragments were religated using 2000 U T4 DNA ligase in supplied buffer (NEB) at 16^{O}C for 4 hours. DNA was purified by phenol extraction and PCR reactions/Southern blotting analysis performed as above. Loading control analysis was performed by qPCR with unnested convergent primers homologous to an uncut region of the *HMS2* locus.

4 Chronological longevity

4.1 Introduction

In most tissues of multicellular organisms, senescence is manifested by the decline in function of post-mitotic cells over time. The physiology of the most pressing age-related human diseases: neurodegeneration, ageing of the circulatory system, connective tissue deterioration and tumour formation; is largely that of deranged regulation of long-surviving cells (Wallace, 2005). Because of the practical difficulties of study of ageing in higher organisms and the utility of easy genetic manipulation, there have long been attempts to establish microbiological models of senescence (Mortimer and Johnston, 1959) that can be used to investigate some of the basic underlying questions of why ageing occurs; to dissect the specific mechanisms through which cells succumb to senescence and how that senescence manifests physiologically; and to rapidly screen homolog mutations and novel compounds with the hope of drug discovery or design. While *Saccharomyces cerevisiae* represents a highly genetically tractable model organism, traditional attention to ageing in this model has been focussed upon *replicative longevity*: failure of replicative viability after limited production of daughter cells (Bitterman et al., 2003). The finite replicative longevity of *Saccharomyces cerevisiae* has been noted for over 60 years (Barton, 1950) and the observation that mutants of genes homologous to those shown to extend lifespan in multicellular organisms and, in particular, calorie restriction, can lengthen reproductive capacity in yeast has made this the primary model system in this organism (Kaeberlein et al., 2007). However, budding yeast also undergo senescence in a post-mitotic sense, a mode of ageing arguably closer to that observed in neurodegeneration, heart disease, or

connective tissue degeneration (Muller et al., 1980). This is *chronological longevity*, and is measured as the survival of post-mitotic cells over elapsed time (Fabrizio and Longo, 2003). Survival in this context is measured as the capacity to regrow upon nutrients again becoming available: this generally correlates with metabolic viability (Allen et al., 2006; Alvers et al., 2009a). Chronological lifespan, too, is readily mutable by genetic, nutrient and drug interventions (**Figure 7**). In particular, mutants of the TOR signalling pathway, long characterised as important in nutrient signalling and lifespan extension in worms (Vellai et al., 2003), flies (Kapahi et al., 2004) and mice (Sharp and Bartke, 2005) show extended chronological lifespan in yeast (Powers et al., 2006); as does calorie restriction (Smith et al., 2007), still the most robust anti-ageing intervention across a large range of species (Masoro, 2005). Hence, in more recent years, chronological ageing of yeast has attracted attention as a more analogous microbiological model of the ageing processes of post-mitotic tissues of higher organisms (MacLean et al., 2001; Chen et al., 2005).

Chronological senescence in single-celled organisms such as yeast faces the same theoretical problems discussed in section 1.8. It is in principle possible, given unlimited nutrient reserves, to continually repair cellular machinery over time and maintain its function. While it is likely that cells accumulate damage in critical components such as genomic DNA (Wilson et al., 2008), telomeres (Harley and Villeponteau, 1995), the mitochondrial genome or electron transport chain (Shigenaga et al., 1994), or oxidised proteins (Sohal, 2002) over time, for perpetuation of the species to be possible, a damage-free version of these components must be passed to future generations via the germline. In multicellular organisms, the *disposable soma* theory of ageing hypothesises that repair processes are sufficiently enhanced in the germline to prevent the transmission of these damaged components (the soma is not as lucky and becomes subject to senescence) (Kirkwood, 1977). But in single-celled organisms the traditional view is of a lack of somatic differentiation: the entire culture represents the germline. Given that the

(starvation) conditions under which yeast chronologically age is a very common experience for the fungus in the natural environment (Lewis and Gattie, 1991), loss of viability over time would seem to represent a paradoxical reduction in fitness of individual cells and be selected against. Indeed, survival in this state is likely to be an important test of fitness for the culture as a whole.

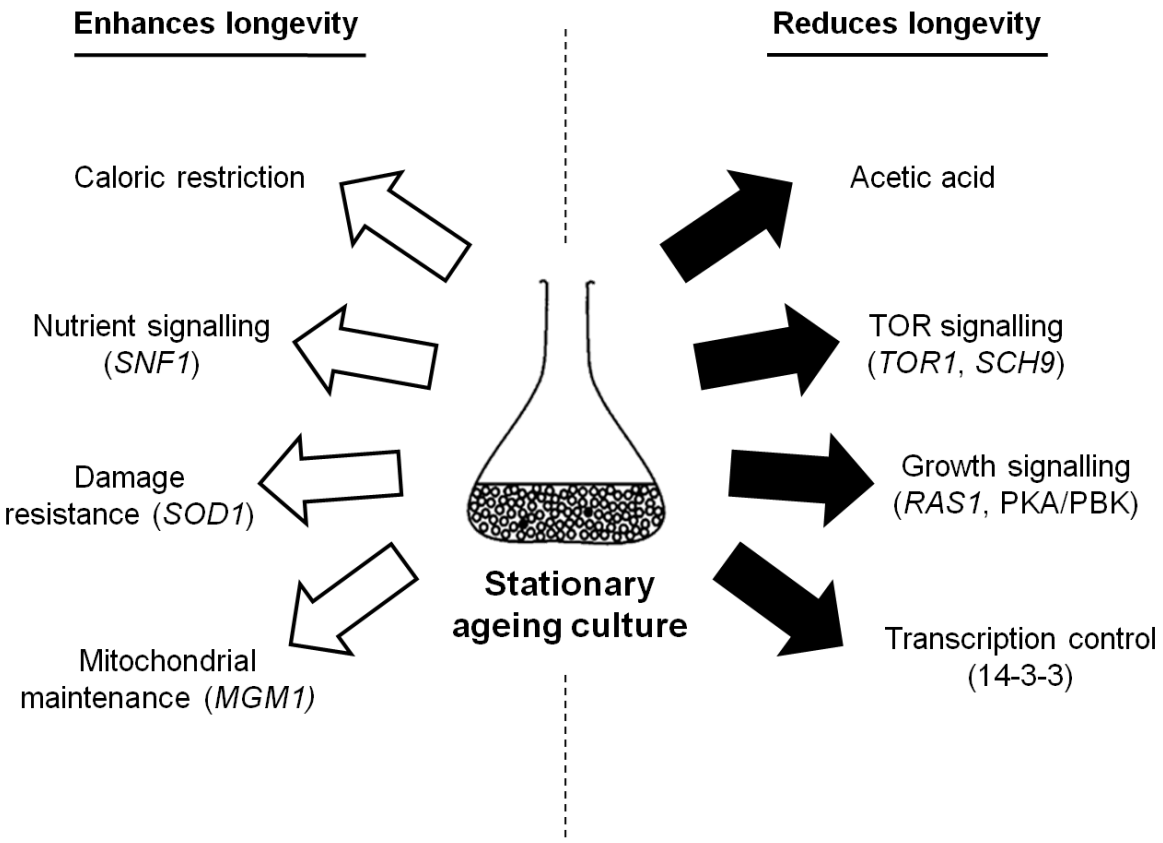

Figure 7. Documented environmental and genetic interventions extending and reducing chronological longevity in *Saccharomyces cerevisiae*. A wide range of such interventions have been discovered over the last 15 years. Caloric restriction, in common with many other models of ageing, greatly extends chronological longevity in this system. This effect has been discovered to be at least partially mediated by accumulation of acetic acid in the extracellular medium. Disruption of numerous signal transduction pathways has been found to both accelerate and disrupt chronological ageing, including TOR signalling, ras-mediated signalling, protein kinase A and B, and AMP-dependent kinase signalling. Mitochondrial maintenance and protection against radical-mediated damage also appears to play an important role in chronological longevity. Finally, some evidence exists for regulation of pro-ageing genes by chromatin modifying enzymes such as *BMH1* (14-3-3).

Given this paradox, it is worth examining the assumptions underlying this model to determine whether a major discrepancy exists between loss of viability over time in stationary yeast cultures and senescence in multicellular organisms.

Is the chronological loss of viability observed in yeast cultures an inevitable consequence of the conditions of stationary cultures? It is possible that these conditions are sufficiently damaging that all cells in the culture lose viability at a similar rate, and no physiological mechanism of rescue exists – ageing in this form represents a physical inevitability. Conversely, repair mechanisms which antagonise senescence triggered by damage accumulation may be operating at full capacity. Several lines of evidence argue against this model. Firstly, numerous interventions can greatly modify the chronological lifespan of yeast. Genetic interventions, which make a strain less fit in logarithmic growth phase, can extend median survival in the post-diauxic phase by 3-fold or longer (e.g. deletion of *SCH9*) (Fabrizio et al., 2001). The mutability of the ageing process suggests that the functions leading to damage accumulation – if this does underlie senescence – are controlled by normal regulatory pathways. Secondly, the most striking intervention extending chronological lifespan is calorie restriction. The disposable soma theory posits that repair mechanisms become limited by energy availability: this would make enhanced survival in the presence of less nutrient availability counter-intuitive (Blagosklonny, 2007a).

Lastly, if accumulated damage prevents production of new daughters upon re-availability of nutrients, then it might be expected that this damage would persist in the newly replicating culture, and outgrowths derived from aged cultures would be less fit than unaged outgrowths. This does not appear to be the case – extremely aged yeast cultures can give rise to stably fit strain lineages upon regrowth. *Saccharomyces cerevisiae* recovered from shipwrecked bottles has demonstrated that yeast can survive in excess of two hundred years in a stable quiescent state prior to viable regrowth (Prokesch, 1991). It is possible that

reprovision of nutrients allows a burst of repair to accumulated damage: in this case, it is the partitioning of repair resources that determines longevity, as in disposible soma.

This suggests a resolution to the paradox. Cytokenesis in *S. cerevisiae* is highly asymmetrical – and this asymmetry provides a basis for the differentiation of a culture into more than one homogeneous cell type. If damage – or the propensity to acquire damage over chronological ageing – is partitioned to only the mother cell, then the resulting population of mothers and daughters can be considered heterogeneous (Piper et al., 2002). If the fitness of this entire heterogeneous culture is considered, then, an altruistic programme of ageing that improves the long-term survival of the culture as a whole would resolve this paradox. If this model is correct, then stationary phase cultures of *Saccharomyces cerevisiae* may represent a closer model to the senescence of heterogeneous multicellular organisms than previously supposed. The conservation of numerous regulatory pathways that impact chronological ageing both in yeast and higher organisms bolsters this model (Kaeberlein et al., 2007).

One major point of divergence in the yeast model and chronological senescence in, for example, mammalian cells, is the metabolic shift experienced by post-mitotic yeast. Logarithmically growing yeast cells liberate energy extremely quickly exclusively from glycolysis of fermentable carbon sources to yield ethanol (Pfeiffer et al., 2001). In post-diauxic and stationary culture, metabolism is almost completely aerobic, with oxidation of this ethanol to acetic acid and finally complete catabolism to CO_2. Aerobic metabolism is inhibited by the presence of high concentrations of glucose used as standard laboratory conditions for rapid growth, but occurs to a considerable degree once medium glucose concentrations fall below 0.1%, for example in continuous culture systems (Verduyn et al., 1990; Entian and Barnett, 1992). Under these conditions, self-establishing cycles of oxidative and reductive metabolism have been observed within maintained cultures (Reinke and Gatfield, 2006). Conditions where fermentable carbon sources are relatively

scarce are more representative of the niche to which *Saccharomyces* have evolved to fit in undomesticated contexts – primarily oak leaves and soil (Replansky et al., 2008) – and therefore study of physiological response and viability maintenance in yeast under these conditions should be biologically meaningful. In general, caloric restriction strikingly enhances the chronological lifespan of ageing yeast: it is usually effected through resuspension of post-diauxic ageing cultures in sterile water to remove all residual nutrients. Experiments (**Figure 8**) have demonstrated that removal of acetic acid arising from fermentation and oxidation of glucose, alone is sufficient to completely reconstitute the calorie restriction phenomenon (Burtner and Kaeberlein, 2009). This only occurs when the pH is sufficiently low to maintain the acetic acid in conjugate acid form: a simple buffer can also extend lifespan. This discovery has been a source of controversy over the prominence of acetic acid which is a minor metabolite but does not accumulate to high levels within mammalian tissues, in the chronological ageing process in yeast (Skutches et al., 1979). If acetic acid is specifically and directly responsible for loss of viability in stationary culture – through uncoupling of the inner mitochondrial membrane potential gradient, for instance (Piper et al., 2001) – then this may undercut the validity of yeast as a model for this system. Several lines of evidence however suggest that downstream metabolism of acetic acid, as the primary carbon source for post-diauxic yeast, acts indirectly to drive ageing. Firstly, other weak acids such as propionic acid (or simply low pH in itself) fails to exhibit similar pro-ageing effect. This suggests that direct physical perturbation of cellular machinery, such as gradient uncoupling, is not responsible. Secondly, chronological lifespan extending interventions such as increase in osmolarity or deletion of *SCH9* have no effect upon acetic acid accumulation in the medium, but rather appear metabolically resistant to the abundance of acetic acid (Burtner and Kaeberlein, 2009). Finally, calorie (or acetic acid) availability is not responsible for the entirety of the yeast chronological ageing phenomenon. Numerous long-lived mutants remain longer-

lived than wild-type under calorie restricted conditions, and calorie restricted wild-type cultures still undergo relatively rapid loss in viability (Fabrizio and Longo, 2003).

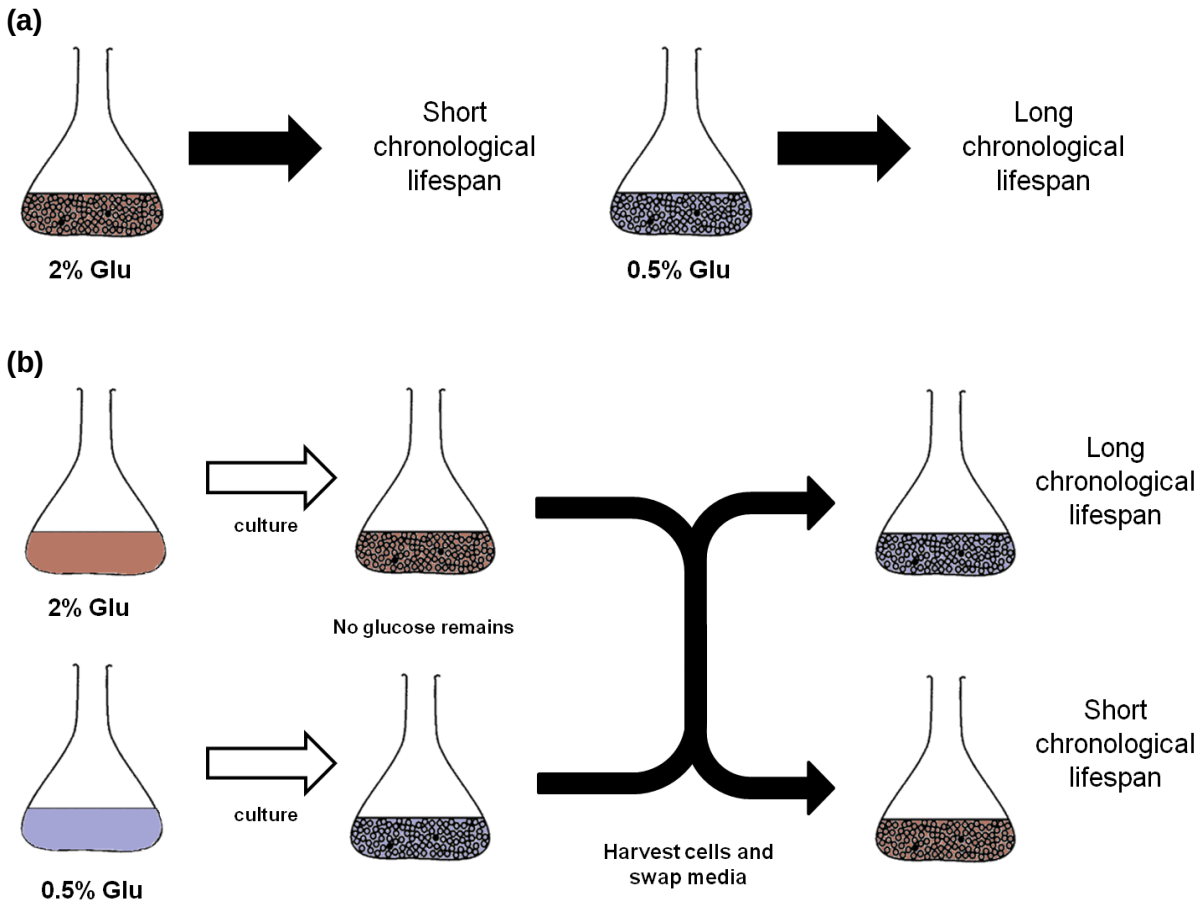

Figure 8. Previous experiments by Burtner and Kaeberlein showing a cell-extrinsic medium component (acetic acid) is sufficient to reconstitute the caloric restriction effect on chronological longevity in yeast. **(a)** Cells inoculated into minimal medium supplemented with 2% glucose as carbon source exhibit markedly reduced lifespan compared to those inoculated into medium with 0.5% glucose and so subject to moderate calorie restriction. The medium glucose-dependent factor determining longevity must either modulate ageing by modifying a persistent state of the culture cells over the ageing timecourse (*cell intrinsic*) or through a persistent component of the medium (*cell extrinsic*). **(b)** To distinguish between these two possibilities, an experiment was performed whereby cultures inoculated into high and low glucose media were harvested and resuspended in cell-free media of the other culture. Mass spectrometry indicated absence of glucose in the medium at this culture stage. The medium was necessary and sufficient to reconstitute the calorie restriction effect in the initially high glucose culture, verifying the cell extrinsic model. The medium factor was later demonstrated to be acetic acid (Burtner and Kaeberlein, 2009).

Chronological longevity has traditionally been studied in yeast through measurement of colony-forming unit (CFU) capacity of ageing post-diauxic cultures. Mutants discovered with modified (generally extended) chronological lifespan using this technique include: metabolic mutants such as those defective for respiration; damage resistance and repair mutants such as superoxide dismutase; mutants for genes involved in mitochondrion maintenance; mutants of the TOR, AMP-dependent kinase, protein kinase A and B, and ras-mediated signalling pathways; and chromatin maintenance mutants such as 14-3-3 that transduce signals to gene expression (Fabrizio et al., 2003; Longo, 2003; Bonawitz et al., 2007; Lorenz et al., 2009; Wang et al., 2009; Scheckhuber et al., 2011). Previous work in the Mellor group discovered a chronological ageing phenotype for mutants of the SAGA/SLIK lysine/histone acetyltransferase complex. Dysregulation of metabolic gene expression over the post-diauxic shift including those controlling glycolysis, oxidative phosphorylation and the TCA cycle, the retrograde response and glyoxylate cycle, and autophagy correlate with extended chronological lifespan phenotypes in a constitutively active C-terminal truncation mutant of *SPT7* (*spt7-217*) and reduced longevity in *spt7Δ* and *spt8Δ* mutant strains.

To extend this work and carry out a small-scale screen of available mutants for chronological ageing phenotypes, a more robust and efficient assay based upon outgrowth of ageing culture was developed. A novel uncharacterised mutant, *ydr026cΔ*, was found to have reliably enhanced chronological lifespan, and genetic analysis was applied to dissect the pathway in which this mutant may act.

4.2 Chronological lifespan: initial screen

Chronological longevity of *S. cerevisiae* cultures has traditionally been measured by retention of colony forming unit capacity in stationary phase cultures maintained under carefully controlled conditions of temperature, aeration, and nutrient content over time. CFU capacity has been measured by serial dilution on drop plates (Smith et al., 2007) or spreading a number of cells, counted by haemocytometer, on multiple plates (Fabrizio et al., 2001). The former approach has the drawbacks of relative insensitivity (generally only order of magnitude changes are easily resolved), poor statistical power, and difficulty in normalising to initial (unaged) differences in plating viability. However, it does allow easy comparison of different ageing strains. The latter gives more statistical power but is labour intensive and requires considerable optimisation of culture dilutions to yield useful data. These properties of the traditional methods for measuring variations in CLS mean that screening for CLS mutants is best performed with the drop-plate technique to detect significantly strong CLS phenotypes, with the CFU-counting technique used to verify and quantify individual phenotypes.

To this end, in developing a screen to identify chromatin-maintenance mutants with ageing phenotypes we identified a number of such mutants using the drop plate technique. Aerated stationary phase cultures were kept in CS medium on a 1% glucose carbon source at 30^{O}C. Drop plates were prepared from aliquots of these cultures. **Figure 10a** shows a typical timecourse for WT strain *BY4741* demonstrating loss of colony forming capacity over chronological ageing. Strongly detectable effects are only visible after considerable lengths of time, consistent with the relative insensitivity of the technique and reported values (Smith et al., 2007). From this screen several strains were identified as having detectable and reproducible CLS phenotypes. Strains lacking the AMP kinase/S6 kinase homologue *SCH9*, a component of the TOR signalling pathway (Longo, 2003), have previously been

identified as having dramatically extended chronological lifespans: this was again identified in this screen (**Figure 10b**). Previous work in the Mellor group has identified the SAGA/SLIK lysine acetyltransferase complex components as downstream targets of TOR signalling to the nucleus mediated by Sch9. Mutants deficient in SAGA/SLIK signalling were found to be strongly and robustly short lived in the chronological screen. Mutants lacking the Spt7 structural components of the complex experience loss of complex integrity and recruitment of SAGA-required component Spt8 (Wu and Winston, 2002); such *spt7Δ* strains were short lived in this screen (**Figure 10c**). Strains null for the acetyltransferase catalytic subunit *GCN5* had similarly curtailed lifespans (**Figure 10d**). Conversely, this screen identified a C-terminal truncation mutants of *SPT7* (*spt7-217*) as exhibiting extended CLS compared to WT (**Figure 10e**), while N-terminal and null mutants demonstrated shortened CLS. This strain constitutively expresses a truncated form of Spt7 normally produced by processing in the native SAGA complex to produce SLIK, which has been shown to be activated by the retrograde response following the diauxic shift (Jazwinski, 2005).

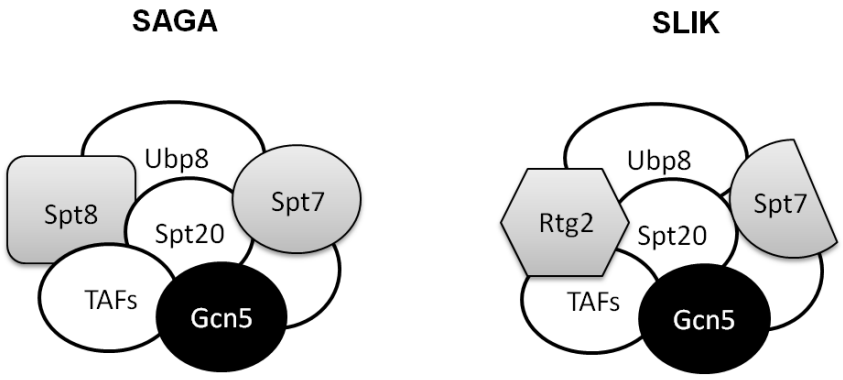

Figure 9. SAGA and SLIK gene complexes, important epigenetic regulators of gene expression in *S. cerevisiae*. Strains containing attenuated complexes lacking the catalytic subunit Gcn5 or structural components Spt7/Spt8 were found to have short chronological longevity, while strains constitutively overexpressing active the SLIK form of the complex (containing C-terminally truncated Spt7) were found to have extended lifespan.

This preliminary work also identified the largely uncharacterised mutant *ydr026cΔ* as demonstrating an extended chronological lifespan (**Figure 10f**). Ydr026c is a poorly-characterised putative myb-like DNA binding protein with homology to Reb1 in yeast and mammalian RNA polymerase I transcription termination factor (TTF-1). *In vitro* and *in vivo* evidence suggests Ydr026c colocalises with Fob1 and Sir2 in the nucleolus and may bind in the spacer region between rDNA repeats (Mohanty and Bastia, 2004; Ha et al., 2012). *fob1Δ* and *sir2Δ* strains have strong inverse replicative ageing phenotypes, and modified chronological ageing has been reported for *sir2Δ* mutants. Ydr026c may therefore represent a novel mediator of chronological ageing.

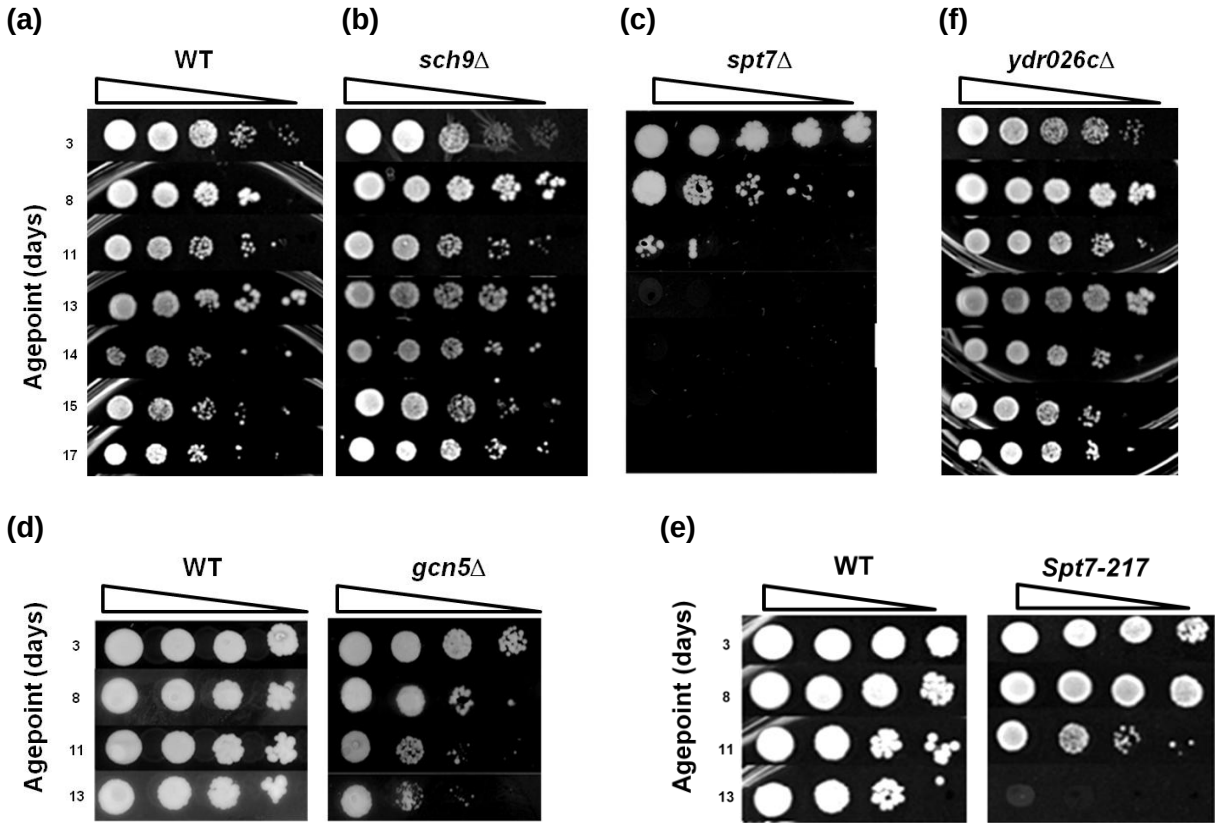

Figure 10. Serial dilution drop plates to determine falling viability over the course of chronological ageing. Stationary phase cultures were maintained in CS medium at 30^{O}C under standardised conditions. Aliquots were removed at agepoints, serially diluted, and spotted onto rich medium plates. **(a)** Typical viability timecourse for wild-type (BY4741 background) culture over chronological ageing. **(b)** TOR signalling mutants such as *sch9Δ* are well established as having extended chronological longevity in yeast, as reproduced in this viability timecourse. **(c)** and **(d)** mutants containing deletions of SAGA/SLIK complex regulatory subunit Spt7 and catalytic subunit Gcn5 was found to greatly shorten chronological lifespan. **(e)** A mutant expressing a C-terminal truncated form of Spt7 (Spt7-217) produces a constitutively SLIK-form complex, and gives higher median viability at day 8, before catastrophic loss of viability. **(f)** The largely uncharacterised mutant *ydr026cΔ* was found to demonstrate enhanced viability over chronological age.

To genetically dissect the pathways underlying the ageing phenotypes in the TOR mutants, SAGA/SLIK mutants, and *ydr026cΔ* strains, ageing cultures were subjected to the more rigorous colony-counting assay to verify the phenotypes observed. The effects observed in the previous screen were largely upheld, although the calculated median lifespans were considerably shorter than those estimated in the drop-plate experiments, probably due to the greater insensitivity of that method over early timepoints.

This assay replicated the extended chronological lifespan phenotype of the *spt7-217* truncation mutant (**Figure 11a**) and the reduced longevity of the *spt7Δ* null mutant with quantitatively significant differences observed. The previously reported short-lived nutrient sensing mutant *snf1Δ* was also found to be short-lived by this assay (**Figure 11b**).

The colony-counting assay verified the extended lifespan phenotype observed in the *ydr026cΔ* mutant strain. Interestingly, assay of a strain lacking the lysine/histone deacetylase Sir2, which has been shown to interact with Ydr026c *in vivo* (Ha et al., 2012), demonstrated a shortened chronological lifespan (**Figure 11c**).

A prediction of the hypothesis that idiosyncratic chronological ageing in yeast is not caused by direct action of the accumulation of acetic acid in the stationary phase medium is that metabolism of this acetic acid is responsible for its pro-ageing effect. To test this hypothesis, chronological lifespans of strains null mutant for *ACS1* and *ACH1*, responsible for synthesis of acetyl-CoA from acetic acid in the cytosol and mitochondrion respectively, were measured by viable colony counting (**Figure 11d**). Markedly extended longevity was observed in both of these mutants strains, suggesting that inhibiting the metabolism of acetic acid can have a protective effect even when it is present in the medium.

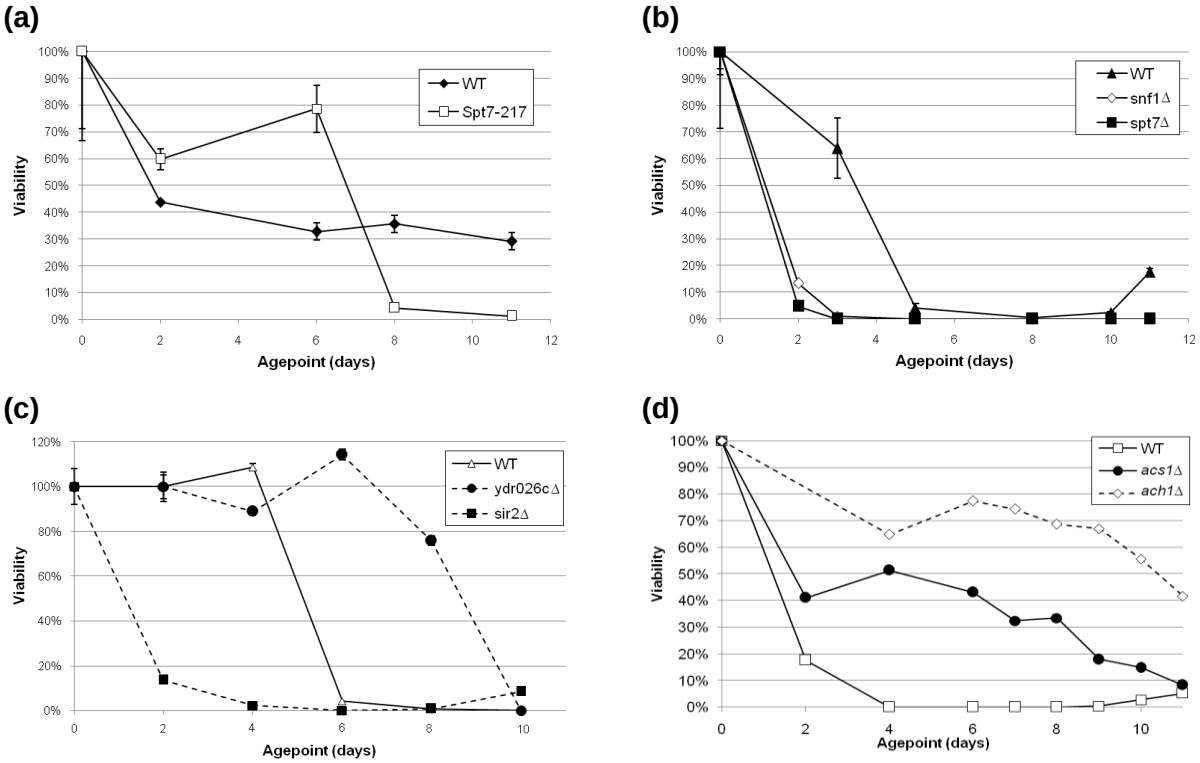

Figure 11. Colony-forming unit capacity of chronologically ageing cultures. Aliquots were taken from ageing stationary cultures, diluted, and plated onto rich medium to determine CFU capacity. Data is normalised to individual culture densities and expressed as a proportion of the initial viability. Error bars are SEM for n=3 replicates. Considerable variation in absolute wild-type longevity is observed, indicative of the great sensitivity of ageing cultures to conditions of oxygenation etc. **(a)** Viability curves for wild-type culture and a strain expressing C-terminal truncated Spt7, verifying a longer chronological lifespan (followed by rapid loss of viability) in this mutant. **(b)** Viability curves for wild-type culture and null mutants for the SAGA complex component Spt7 and AMPK signalling component Snf1. Both demonstrate strongly curtailed chronological longevity. **(c)** Viability curves for null mutants for the rDNA maintenance gene *SIR2* and uncharacterised mutant *ydr026cΔ* demonstrating shortened and lengthened CLS respectively. **(d)** Viability curves for the acetic acid metabolism mutants *acs1Δ* and *ach1Δ* demonstrate an enhanced chronological lifespan in these strains with reduced acetic acid metabolic capacity.

4.3 Higher precision measurements of chronological longevity

In the course of these experiments it became clear that both methods are considerably limited for measurement of chronological ageing of large numbers of strains or experimental repeats. In order to aid future experiments and to improve the statistical power of comparisons with WT ageing cultures, an alternative methodology for measuring CLS was designed. Previous work (Murakami et al., 2008) has suggested that the rate of outgrowth of aliquots of ageing culture can be used as a measure of the remaining viability of that culture. Small amounts of culture are removed and inoculated into rich medium. This is incubated under standard conditions, and the turbidity of the suspension periodically measured to determine the growth phase of the cells. Extrapolation of this growth curve can yield an estimate of the initial number of growing cells, and hence the current viability of the bulk ageing culture. The basic protocol for outgrowth analysis is shown in **Figure 12a**.

Taking this previous work as a basis, a new methodology was designed to measure CLS in a high-throughput fashion.

Firstly, a practical means of obtaining the many outgrowth curves of many ageing cultures was required. A Bioscreen C 30^{O}C incubated shaking microplate reader was used to incubate outgrowth cultures in 100-well plates transparent to light at 600nm. Over the course of 24 hours this apparatus would allow culture growth while taking turbidity timepoints of the growing cultures and recording growth-curve data. The ageing experimental cultures themselves were found to be highly sensitive to levels of aeration, and so for small-scale experiments 100ml flasks were used under standard rotary shaking at 100 rpm.

(a)

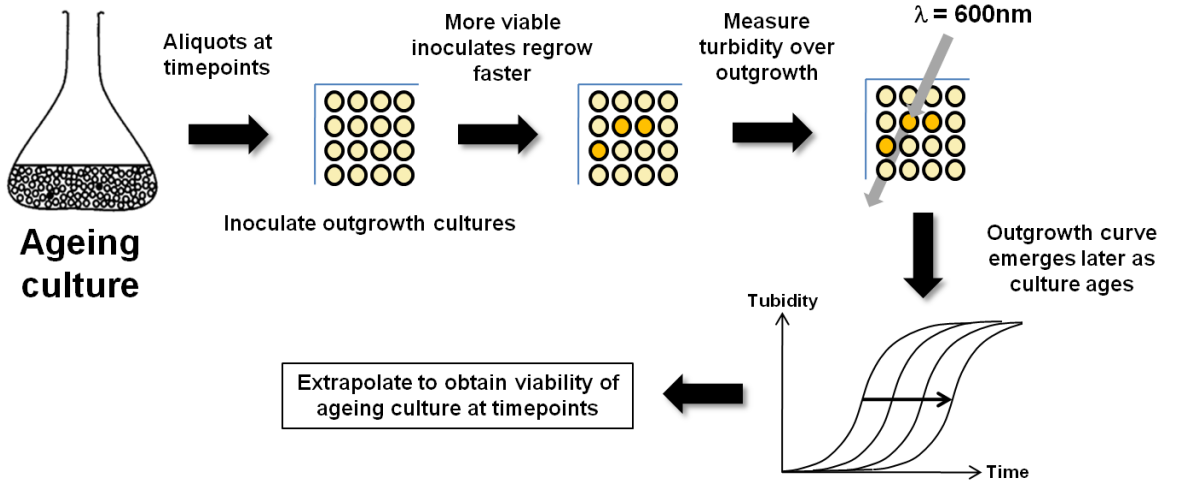

(b)

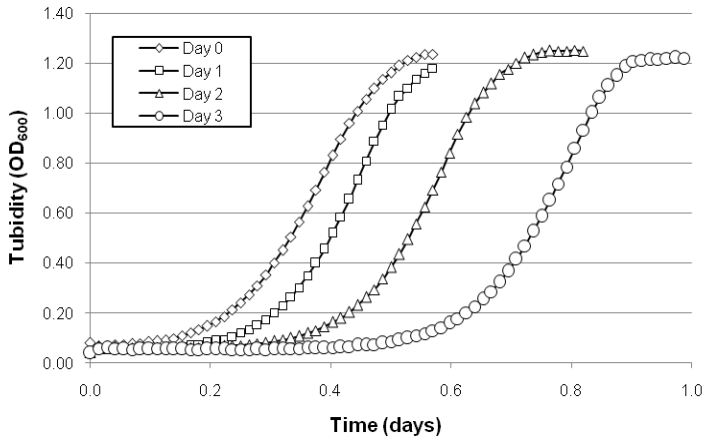

(c)

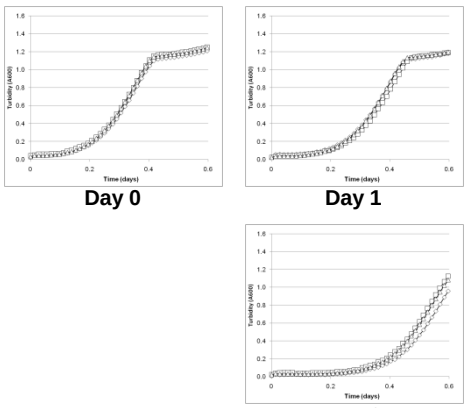

(d)

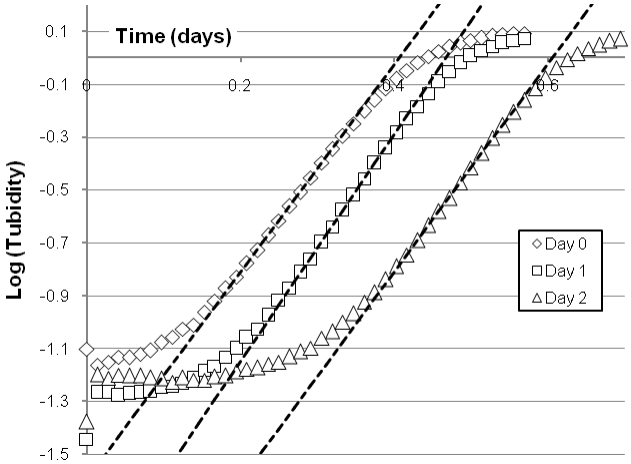

(e)

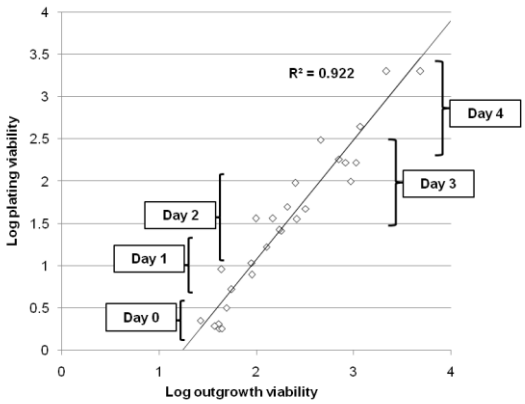

Age (days)	Doubling time (mins)	Initial viability (OD_{600})
0	109 ± 1.1	0.024 ± 0.0010
1	104 ± 2.7	0.011 ± 0.0010
2	113 ± 2.5	0.005 ± 0.0006

Figure 12. (a) Basic methodology for measuring ageing culture viability by outgrowth. A continuously maintained ageing culture has aliquots removed at timepoints. These are used to inoculate fresh rich medium and incubated at 30^{O}C for ~24 hours to allow outgrowth. Growth is monitored as increasing turbidity of the medium. Older culture aliquots contain progressively reduced payloads of viable cells, leading to retardation of outgrowth curve emergence through the ageing experiment. Extrapolation of the outgrowth data gives an estimate of aliquot viability. **(b)** Typical outgrowth curves for the first 3 days of a wild-type chronological ageing experiment. 5 μl aliquots of ageing culture were inoculated into 145 μl rich medium in a 100-well plate, and incubated at 30^{O}C with 100rpm shaking in the Bioscreen C. Turbidity was monitored every 20 minutes for 24 hours by absorbance at 600nm. Each outgrowth curve consists of three phases: a lag phase after inoculation, followed by a phase of logarithmic growth. Once $OD_{600} > 1.0$, exponential growth slows as the diauxic shift is approached. A clear retardation of outgrowth emergence is given as the parent culture ages. **(c)** Biological replicates of ageing cultures with measured outgrowth over chronological age. Very good agreement can be observed between biological replicates, with small amounts of divergence introduced later in the ageing timecourse. **(d)** Semi-logarithmic plots of the outgrowth curves shown in (b), with a regression line indicating the region of logarithmic growth. It can be observed that very well-behaved log-phase growth is observed between $\log(OD_{600})$ of -1.0 to -0.3 (OD_{600} = 0.1 to 0.9) at all the agepoints measured. Based on the model of outgrowth kinetics discussed, each growth rate can be determined from the gradient of the regression line through the logarithmic region and the initial viability determined from the Y-axis intercept. These values are tabulated below with associated standard errors. Over the ageing timecourse modest but significant variations in doubling time are observed, but a five-fold reduction in initial viability is responsible for the majority of outgrowth curve retardation. **(e)** Comparison of initial viability values from a series of chronological ageing experiments with a variety of strains (wild-type, *ydr026cΔ*, *sir2Δ ydr026cΔ*, *fob1Δ ydr026cΔ* & *tor1Δ ydr026cΔ*) measured by both the colony-forming plating assay or outgrowth analysis. Good agreement is given between the two techniques, with the results correlating to a highly significant degree (R^2 = 0.922, $p < 0.001$). Lack of systematic disparity between viability values measured by the two techniques suggests variations in inoculation lag time do not greatly influence viabilities estimated by outgrowth extrapolation.

Secondly, a robust model for interpreting outgrowth curve data as chronological viability was required. Previous work has made a number of assumptions when interpreting outgrowth data which may introduce unaccounted for imprecision or inaccuracies in the estimation of chronological viability. To correct for this a model was constructed to take account of all the available data generated by outgrowth curves in analysis. The model assumes that:

1. Cultures maintaining viability will produce logarithmic outgrowth curves
2. Time of emergence of outgrowth curves is dependent upon –
    a. Intrinsic rate of outgrowth
    b. Initial viability of inoculated cells
3. An initial lag phase exists before logarithmic growth dynamics are observed which is not significantly variable in terms of growth rate over the course of CLS for each strain

Given these premises, it would be expected that an inoculated aliquot of initial viability v_o (in arbitrary units) with a doubling time of g (mins) and initial growth lag phase λ (doubling times) would exhibit growth dynamics:

$$OD_{600} = v_0 \cdot 2^{t/g\ -\ \lambda}$$

at time t where OD_{600} is recorded turbidity. Hence,

$$\ln\left(OD_{600}\right) \ = \ \ln(v_0) \ + \ \left(\frac{t}{g} - \lambda\right) \ \ln 2$$

and

$$\ln\left(OD_{600}\right) \ = \ \ln(v_0) \ + \ \frac{t}{g}\ln 2 \ - \ \lambda \ln 2$$

letting constant $k = \lambda \cdot \ln 2$,

$$\ln\left(OD_{600}\right) \;=\; \ln(v_0) \;+\; \frac{t}{g}\ln 2 \;-\; k$$

The initial viability v_0 can be estimated by extrapolation to t = 0

$$\ln\left(OD_{600}\right) = \ln\left(v_0\right) - k$$

and therefore $v_0 = OD_{600} \cdot e^k$

If k is constant, this gives the initial viability of the culture at ageing timepoints scaled to a factor constant throughout the experiment (premise 3). A semi-log plot of turbidity over time will therefore allow linear regression to obtain the initial viability as well as the doubling time at each viability timepoint.

This model is improved over those previously used for outgrowth analysis in two main areas. Most seriously, earlier models have assumed that outgrowth doubling rates of ageing cultures remain equal over the course of the experiment (usually several weeks) (Murakami and Kaeberlein, 2009). Preliminary experiments suggested that considerable slowing in the growth rate of cultures tended to occur as ageing progressed, implying that if left unaccounted this assumption would produce accelerated ageing data (**Figure 13**).

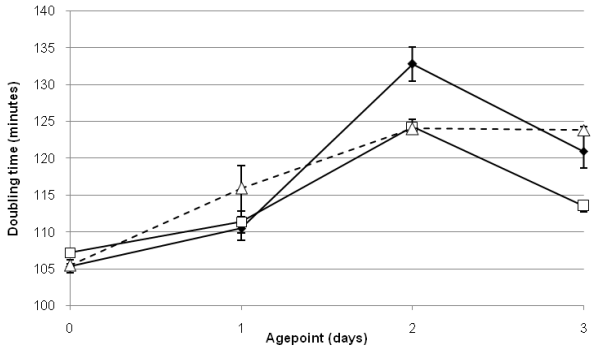

Figure 13. Doubling times of three wild-type cultures markedly increase over chronological ageing. Error bars are SEM.

Secondly, this approach allows data from the whole outgrowth curve to be used in the estimation of the extrapolated initial viability, compared to thresholded models such as that of Murakami *et al.* which are reliant on the mean of two readings are hence potentially greatly perturbed by imprecision associated with those readings (Murakami et al., 2008). Linear extrapolation gives much greater statistical power allowing more reliable comparisons of CLS. Individual turbidity readings produced by the screening apparatus (Bioscreen C) can occasionally be strongly anomalous: in a model where two critical measurements determine the viability measurement the effect of this is emphasized, while using whole-curve linear extrapolation, such outliers are easy to automatically detect and exclude without compromising the analysis. Additionally, thresholding methods require specification of an arbitrary turbidity value which is assumed to be within log-phase growth: linear regression allows observation and verification that log phase growth is occurring and so avoids this assumption.

It is important that the premises of this new model are empirically valid. Preliminary experiments demonstrated that for a variety of strains over the course of chronological ageing, assumptions (i) and (ii) were very robust. Exponential growth dynamics are seen between 3 and 12 hours after inoculation following a slow lag phase and preceding slowing of growth when turbidity exceeds ~1.5 (**Figure 12b**). Semi-log plots of these outgrowth curves indicate a highly linear relationship between t and ln (A_{600}) in this region, validating log-phase growth (**Figure 12c-d**). This was observed not only with fresh cells but also over an exhaustive ageing timecourse – even at very low viabilities outgrowth cultures eventually exhibit exponential growth dynamics. The emergence of the outgrowth curves can be seen to shift to later timepoints as cultures age. From the semi-log plots, doubling times and extrapolated initial viabilities can be measured for sample ageing cultures (**Figure 12d**). These indicate that this slower outgrowth is not exclusively the product of slowing doubling rate, but is largely also determined by falling initial viability (assumption

ii). However, doubling rate does significantly change over the course of chronological ageing in these strains.

Premise (iii) is more difficult to measure directly, as it is difficult to separate the contribution of changing lag phase and reduced inoculate viability to delayed outgrowth curves. Plate-spreading and CFU-counting of ageing cultures measures viability of seeded cells without any contribution from growth kinetics such as inoculation lag. By performing a series of chronological ageing experiments on a collection of long-lived and short-lived strains previously identified, and performing both outgrowth curve analysis with Bioscreen C data and CFU-counting at each timepoint, the degree to which the two techniques for measuring CLS agreed could be determined. Chronological ageing experiments were performed with WT, *ydr026cΔ*, *ydr026cΔ sir2Δ*, *ydr026cΔ tor1Δ*, and *ydr026cΔ fob1Δ* strains, having a range of CLS longevity phenotypes, over the course of six days. Aliquots removed at each daypoint were either subjected to outgrowth and analysis as described above, or directly plated, and absolute regrowth viability determined by both methods. Any systematic error on the part of outgrowth analysis was hypothesised to be caused by changing lag times in the inoculated outgrowths. **Figure 12e** shows this comparison: good agreement is generally observed between viabilities measured by the two techniques over the whole range of viabilities observed ($R^2 = 0.922$, $p < 0.001$). Viability curves constructed from the two approaches are also highly similar for the same strains, as are estimated median viabilities.

This approach simplifies measurement of viability data from ageing cultures - in high-throughput mode (2 x 100-well plates in each Bioscreen C, inoculation by pipetting robot) large numbers of biological repeats can be processed simultaneously to give high statistical power. The large amounts of turbidity data generated by the protocol however requires systematic analysis. The workflow for this analysis, originally accomplished manually, is shown in (**Figure 14a**).

The data must be normalised, filtered for anomalous results, subjected to linear regression and the resultant initial viabilities collated and statistically analysed. The final result is a series of viability readings falling over time as the culture ages: from these, median viability can be estimated with associated statistical comparisons. To reduce inefficiency and propensity for error in performing this manually, software was written embedded in Microsoft Excel Spreadsheets and as a MATLAB interface to automate the whole process. This software was used for all subsequent analyses of outgrowth data and has been used to analyse data from a high-throughput CLS screen performed by a spin-out company from the laboratory. The software takes raw turbidity data recorded by the Bioscreen C as input and is supplied with the parameters of the experiment (**Figure 14b**) – strain names, number of biological and mechanical (outgrowth) replicates, the turbidity range in which to search for logarithmic growth, as well as parameters to identify anomalous readings.

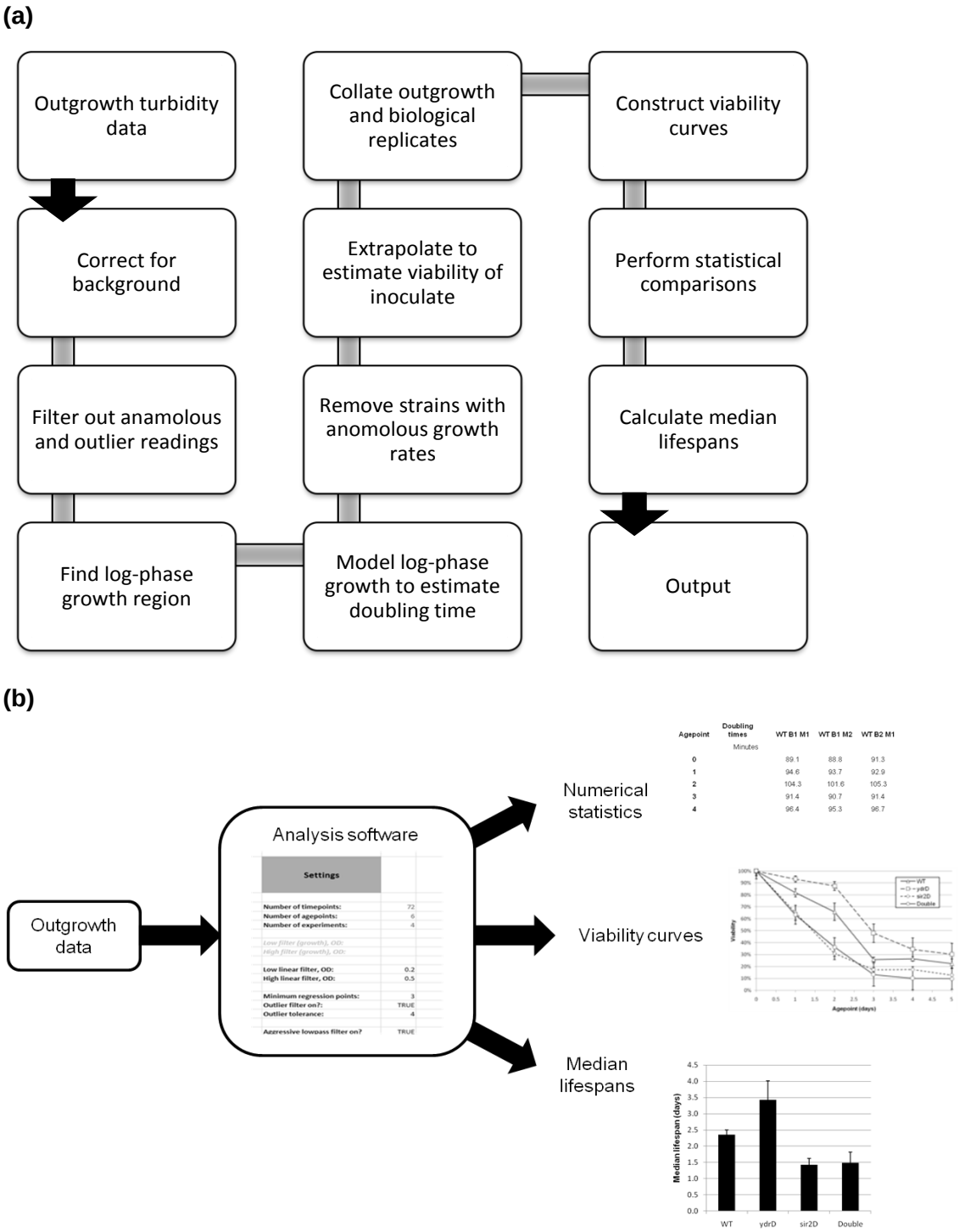

Figure 14. (a) Workflow for analysis of outgrowth data generated by the Bioscreen C. Raw data must be corrected for medium turbidity; filtered for anomalous readings; converted to semi-log form; the (linear) region of log-phase growth found; the doubling time calculated using linear regression; anomalous doubling times excluded; the initial viability estimated; mechanical and biological replicates combined and statistics calculated; viability curves constructed; and median chronological lifespans estimated; and statistics performed on that data.**(b)** Viability analyser software was written in Excel and MATLAB to automate the analysis workflow above. The user inputs experimental settings and raw Bioscreen C output, and the software can automatically return statistical results, viability curves and median lifespan data.

Several types of outlier filter are automatically applied to the data: Individual readings are excluded from analysis if they are grossly different from readings directly before and after. This is the most common type of anomalous reading obtained.

1. Logarithmic portions of curves are excluded if they occur isolated from the main logarithmic region to exclude short runs of anomalous readings.
2. Outgrowth curves are eliminated if greater than a defined number of anomalous readings are found.
3. Outgrowth curves are eliminated if the kinetics of growth falls outside defined limits: too fast (< 60 mins) generally indicates bacterial infection, too slow (>200 mins) improper inoculation.

Automatic outlier exclusion in this fashion minimises user error or bias in dealing with anomalous readings. The software produces a series of outputs both to aid optimising running experiments and perform final analysis of ageing data:

1. Outgrowth curves and log-linear plots can be made for user-specified combinations of strains, agepoints, and biological and mechanical replicates. This is useful to observing the course of running experiments and identifying defective cultures (e.g. infection).
2. Doubling time data is available for all outgrowth curves tested.
3. Extrapolated viability data is available for each strain at each agepoint, both for individual biological replicates and averaged (with statistical information) across the experiment. This intuitively shows the course of ageing for each experiment and can help identify biological replicates behaving unusually.
4. Viability curves are interpolated to provide an estimate of median lifespan for each strain, with associated statistical comparisons. This data is outputted in chart format.

Chronological ageing data is typically expressed as viability curves, with comparisons being performed between median (50%) lifespan of different strains, as this measure tends to express the biggest phenotypic differences. Maximal lifespans become difficult to measure as only a small proportion of the culture remains viable, and so are strongly affected by imprecision in estimation of viability rates, and it is unusual to compare strains in this way in the *S. cerevisiae* literature. Statistical comparisons are performed at individual agepoints based on error measured for biological and mechanical replicates and combined, as well as at the interpolated median lifespan.

While intra-experimental consitency of longevity curves was good, indicating acceptable precision of the outgrowth ageing assay, surprising variability remained between wild-type strains in separate experiments. Initially, much variability was found to be caused by relatively small differences in culture volume and agitation rate, but when these are eliminated inter-experiment comparability is still low. In some cases this can be ascribed to different wild-type backgrounds (eg. **Figure 17**), but in others inter-experimental variability remains even with the same wild-type background (eg. **Figure 15a/b**). Because of this, median lifespans relative to the intra-experiment wild-type have been used for inter-experiment comparison.

4.4 Chronological lifespan phenotypes in putative rDNA maintenance mutants

Preliminary data had demonstrated a chronological ageing phenotype associated with a number of null mutants of proteins implicated in regulation of the rDNA array, including the uncharacterised protein Ydr026c (**Figure 11c**). Because regulation of replicative longevity also appeared to be modified in these mutants, larger scale chronological ageing

experiments were performed with outgrowth analysis to provide more reliable data on CLS phenotypes exhibited by these mutants.

Initial experiments were performed to validate the extended lifespan of *ydr026cΔ.* Four further experiments, comprising three biological repeats each, were performed and loss of viability over time estimated using culture outgrowth analysis. Moderate, consistent extension of lifespan is measured in the *ydr026cΔ* compared to the WT strains (**Figure 15a**).

sir2Δ strains are well characterised in their short replicative lifespan phenotype. However, the literature on the chronological lifespan of *sir2Δ* is mixed with respect to the magnitude and tendency of the phenotype. Previous reports have suggested a shortened chronological lifespan in the majority of backgrounds, with an increased maximal and 10% lifespan in the BY4741 background and a reduced median lifespan (Fabrizio et al., 2005). To resolve these inconsistencies, we performed a measurement of chronological lifespan using our outgrowth system (**Figure 15a**). Consistently shortened median CLS was observed in the *sir2Δ* mutant, significantly reduced from WT. To test whether the *sir2Δ* CLS phenotype was epistatic to the *ydr026cΔ* CLS phenotype, the double mutant *ydr026cΔ sir2Δ* was included in this experiment. A short CLS is observed, not significantly different from the single *sir2Δ* mutant, suggesting a similar epistatic relationship. These phenotypes remained consistent through two experimental replicates of 9 cultures each.

Another rDNA maintenance mutant which has a strong replicative lifespan effect is deletion of the replication fork blocking protein Fob1. *fob1Δ* mutants are the archetypal replicatively long-lived strain, their longevity thought to be determined by the greatly reduced recombinogenicity of the rDNA spacer regions in the null mutant. However, outgrowth experiments performed with ageing *fob1Δ* strains suggested little difference in chronological lifespan from wild-type (**Figure 15b**).

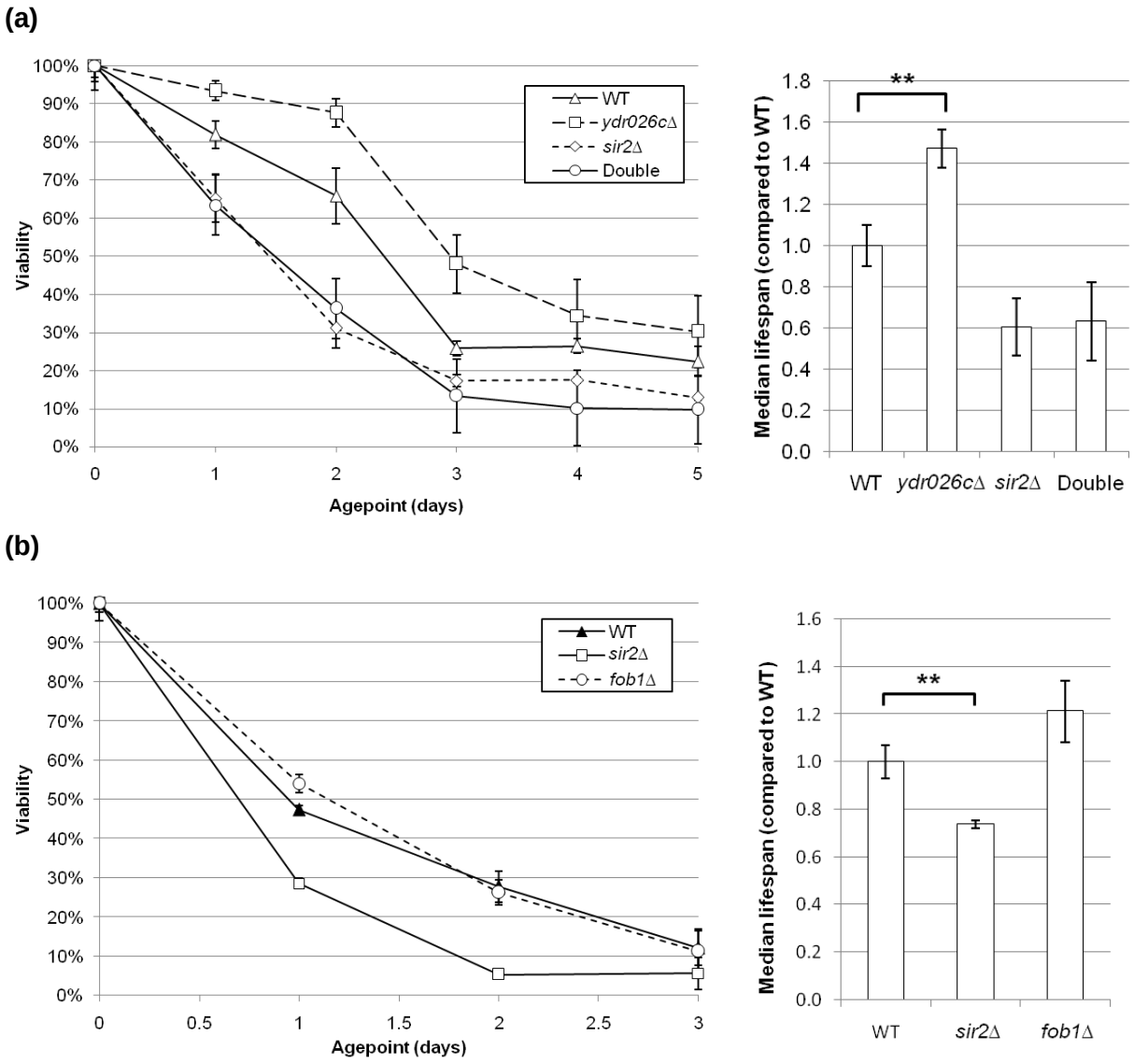

Figure 15. Viability curves and median lifespan data as determined by outgrowth analysis of chronological ageing stationary phase cultures for wild-type cells and null mutant strains for selected rDNA maintenance mutants. Data is for three simultaneous biological replicates, and each collection of experiments was replicated n=4 times. Error bars are SEM. **(a)** Data for wild-type, *ydr026cΔ*, *sir2Δ* and *ydr026cΔ sir2Δ* (double) mutants. **(b)** Data for wild-type, *fob1Δ* and *sir2Δ* mutants.

4.5 Chronological lifespans of TOR pathway and SAGA/SLIK mutants

Disruption of TOR pathway signalling is associated with increased chronological longevity in a number of experimental models (Blagosklonny, 2008). Previous work and plating experiments suggested an extended chronological lifespan of the *tor1Δ* mutant and *sch9Δ*, which is thought to play an important role in signal transduction in the TOR pathway in *S. cerevisiae*. Outgrowth experiments (**Figure 16a**) verified that both of these strains have chronological lifespans greatly extended beyond that of wild-type, as previously reported. In particular, the *sch9Δ* has a median lifespan close to three-fold that of wild-type, generally the longest CLS observed in these experiments. A strain lacking *RIM15*, a kinase implicated in downstream TOR signalling, is also long-lived under these conditions.

Conversely, it was hypothesised that overexpression of a hyperactive mutant of the kinase Sch9 would give a shortened chronological lifespan. Ageing stationary cultures were set up using a wild-type strain containing plasmid pJU841 overexpressing the constitutively active Sch9 mutant *SCH9*^{T723DS726DT737ES758ES765E} (Urban et al., 2007), or an empty vector, in defined medium lacking uracil to ensure the plasmid was not lost. Outgrowth analysis of these ageing cultures (**Figure 16b**) indicated a significantly reduced chronological lifespan in the strain expressing hyperactive Sch9 compared to control. It should also be noted that the reduced nutrient content of the ageing medium appeared to extend the chronological lifespans of all strains in this experiment.

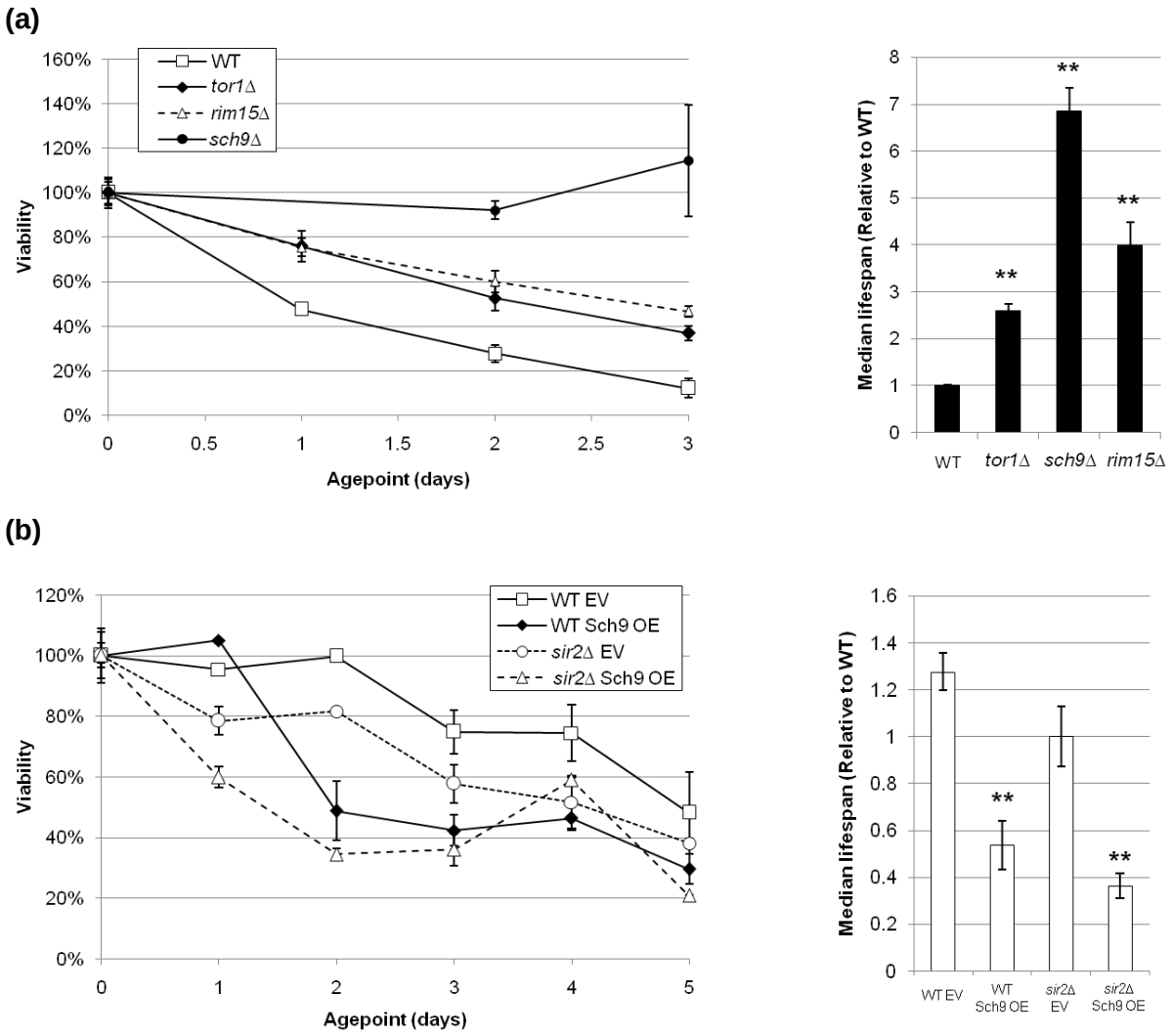

n = 9 replicates. ** p < 0.05 compared to wild-type

Figure 16. Viability curves and median lifespan data as determined by outgrowth analysis of chronological ageing stationary phase cultures for wild-type cells and strains with modified TOR signalling. Data are for three simultaneous biological replicates (error bars are SEM), and each collection of experiments was replicated n=3 times. **(a)** Data for wild-type, *tor1Δ*, *rim15Δ* and *sch9Δ* null mutants. All these mutants with disrupted TOR signalling demonstrate significantly enhanced chronological lifespan above wild-type, with the strongest effect (as previously reported) in the *sch9Δ* strain. **(b)** Data for wild-type and *sir2Δ* strains containing an empty vector or construct pJU841 overexpressing a constitutively hyperactive mutant allele of Sch9 (Sch9 OE). Conversely, constitutive stimulation of the TOR pathway leads to significantly reduced chronological lifespan compared to wild-type. Furthermore, the already short-lived *sir2Δ* strain is has its chronological lifespan further reduced when the strain contains the Sch9 overexpression construct. Ageing and outgrowth experiments were performed in CS medium without uracil for plasmid maintenance.

Mutants of the SAGA/SLIK histone acetyltransferase complex were also implicated in the previous screen to have a CLS phenotype. Previous work in the lab has identified this complex as part of the downstream signal transduction of the TOR pathway to chromatin, as demonstrated by its response to rapamycin treatment (unpublished work). Null mutants for several components of the complex: scaffolding proteins Spt7 and Spt8, retrograde response protein Rtg2, and the lysine acetyltransferase catalytic subunit Gcn5 – exhibited shortened CLS in preliminary plating experiments (**Figure 10**). Measurement of chronological lifespan by outgrowth analysis verified this short lifespan in the *spt7Δ*, *spt8Δ* and *gcn5Δ* strains. Conversely, a C-terminal truncation mutant of Spt7 (*Spt7-217*) thought to produce a constitutively active form of the SLIK complex was previously shown to have an extended chronological lifespan. Outgrowth experiments performed with this strain validated this result (**Figure 17a**).

To test whether a genetic relationship existed between the chronological ageing phenotypes observed in the TOR signalling mutants and the rDNA maintenance mutants, double mutants were produced and ageing cultures subject to outgrowth viability analysis. Strains with null mutant *TOR1* are found to demonstrate significantly elevated chronological lifespan. However, when *tor1Δ* mutants are combined with the already long-lived *ydr026cΔ* mutants, a considerable additive effect in lengthening of chronological lifespan is observed suggesting a lack of epistasis between these two pathways (**Figure 17b**).

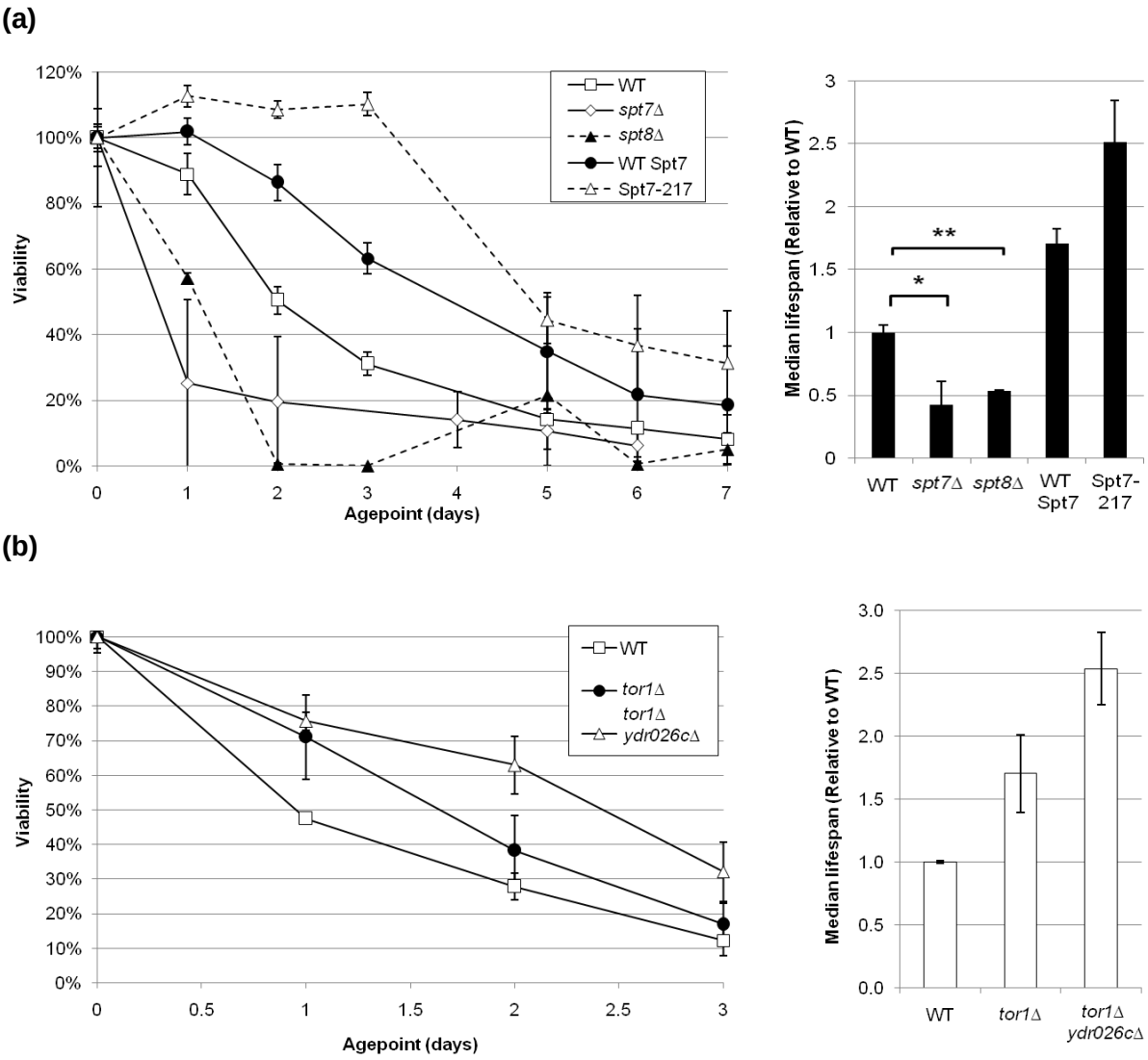

n = 3 replicates. ** p < 0.05, * p < 0.01 compared to WT.

Figure 17. Viability curves and median lifespan data as determined by outgrowth analysis of chronological ageing stationary phase cultures. Data is for three simultaneous biological replicates (error bars are SEM). **(a)** Chronological viability curves for null and truncation mutants of subunits of the SAGA/SLIK complex: null mutants *spt7Δ* and *spt8Δ*, and a strain solely expressing a C-terminal truncation mutant of SPT7 under the endogenous promoter, Spt7-217 which constitutively drives production of the SLIK form of the complex. Disruption of SAGA/SLIK function in the null mutants gives dramatically shortened chronological lifespan compared to wild-type. Conversely, the constitutively active SPT7 mutant demonstrates significantly elevated chronological lifespan compared to wild-type. **(b)** Outgrowth viability curves demonstrating a synthetic effect upon chronological longevity of disruption of TOR signalling and the rDNA maintenance mutant *ydr026cΔ*. *tor1Δ* exhibits extended median lifespan as above, but a double mutant *tor1Δ ydr026cΔ* demonstrates significant enhancement of chronological longevity beyond this effect.

To further investigate this genetic relationship, plasmid pJU841 overexpressing the constitutively hyperactive Sch9 mutant was transformed into strains containing deletions of *SIR2*. The *sir2Δ* Sch9DE strain exhibits even shorter chronological lifespan than either mutant alone, again suggesting an additive effect and genetically separate pathways regulating chronological lifespan (**Figure 16b**).

4.6 Medium composition

Previous work has suggested that medium nutrient composition plays a critical role in mediating chronological lifespan. The lifespan-extending effect of caloric restriction has been shown in yeast cultures to be caused by the lack of formation and accumulation of the metabolic intermediate acetic acid in the medium. Removal, or neutralisation, of this acetic acid is sufficient to reconstitute the effects of calorie restriction. This effect was easily reproduced monitoring viability by outgrowth analysis, both by water washing and buffering of the medium at pH 7 to maintain secreted acetic acid in its acetate form, which is not described as having pro-ageing effects (**Figure 18a-b**).

It is controversial whether accumulation of acetic acid in the ageing medium contributes to its pro-ageing effect directly (through, for example, diffusion into and acidification of the cytosol or mitochondrial matrix) or through downstream metabolic consequences. It is utilised metabolically by conversion to acetyl-coenzyme A by the acetyl-coA synthetase isoforms Acs1 and Acs2 as well as Ach1. To investigate this question, strains were prepared null for *ACS1* and *ACH1*. The lifespans of all of these strains are moderately increased compared to wild-type cultures under the same conditions, suggesting an active metabolic process is responsible for the effect that acetic acid has on chronological ageing (**Figure 18c**).

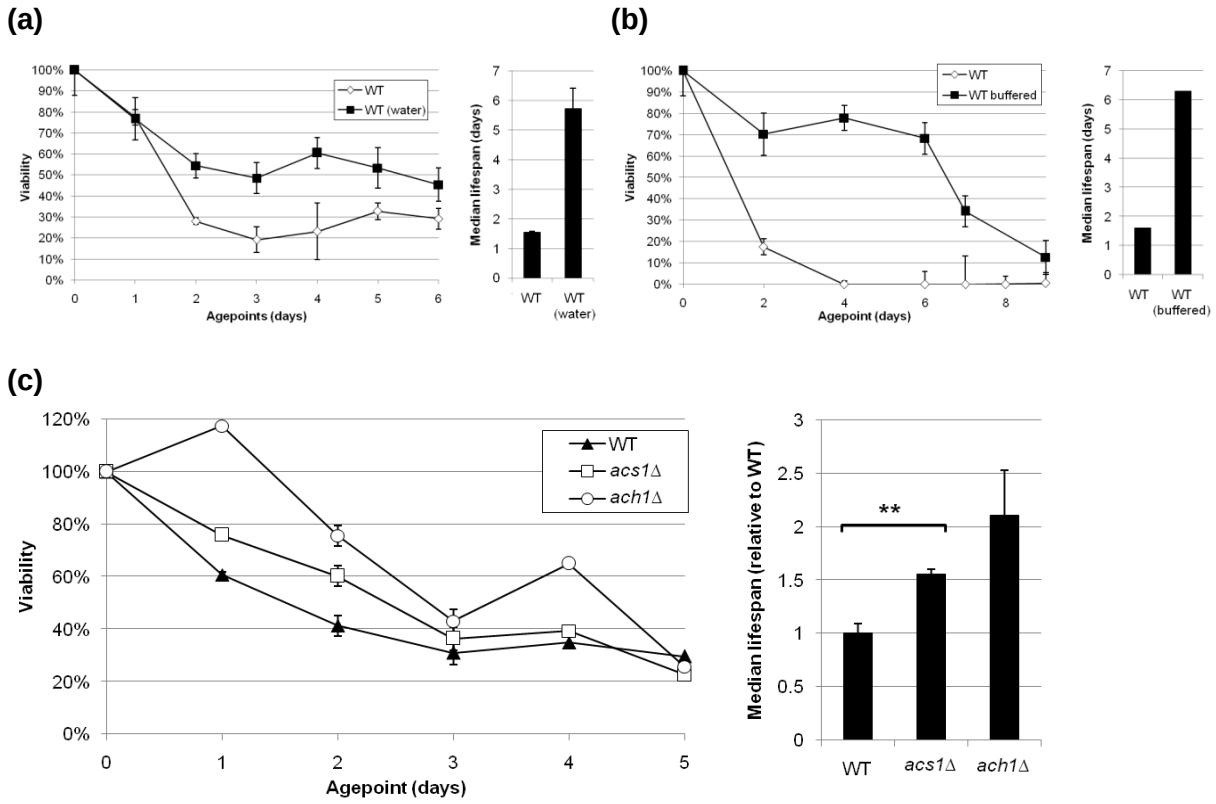

n = 3 replicates. ** p < 0.05 compared to WT.

Figure 18. Viability curves and median lifespan data as determined by outgrowth analysis of chronological ageing stationary phase cultures. Data is for three simultaneous biological replicates (error bars are SEM). **(a)** Calorie restriction by removal of residual post-diauxic carbon sources. One culture of a wild-type strain was inoculated and allowed to proceed through the diauxic shift. Upon reaching stationary phase cell density ($2x10^8$ cells/ml) the culture was split, and one half harvested, washed and resuspended in sterile water. The other continued in the original medium. As has previously been reported (Fabrizio et al., 2005), the washed culture demonstrated markedly enhanced chronological longevity. **(b)** An effect of similar magnitude could be observed if, instead of replacement of the medium, a phosphate buffer was added following the diauxic shift to maintain the medium close to pH 6. Neutral pH alone has previously been shown not to be responsible for the calorie restriction effect; rather, the neutral pH maintains acetic acid in its acetate conjugate form and prevents reuptake. **(c)** Outgrowth experiments verifying the extension in chronological longevity previously measured for the acetic acid metabolism mutants *acs1Δ* and *ach1Δ* in the colony viability assay. Significant lifespan extension is given in both strains.

This raises two possibilities for the mechanism of chronological lifespan extension in these two genetic classes of mutants: these mutants are metabolically modified and accumulate reduced amounts of medium acetic acid, or are resistant to the acetic acid accumulated in the medium. To investigate this, a further series of experiments were performed. Cultures were inoculated into 1% glucose CS medium under standard conditions as usual, but after the 36 hours required to reach stationary phase cell densities, cells were washed twice in 30^0C sterile water, and resuspended in the same volume of water for the remainder of the experiment.

When the TOR pathway signalling mutant *tor1Δ* is cultured in the absense of nutrients (calorie restricted conditions), the observed chronological lifespan remains extended relative to the wild-type, although not to the extent observed in unwashed cells (**Figure 19a**). This suggests that some proportion of TOR signalling inhibits chronological longevity through an acetic acid-independent mechanism. In contrast to acetic acid containing medium, when the mutants *ydr026cΔ* and the double mutant *ydr026cΔ tor1Δ* are cultured in the absense of nutrients, no enhancement of median chronological lifespan is observed above that of wild-type and *tor1Δ* strains respectively (**Figure 19b**). This suggests an acetic acid-dependent mechanism operating in the *ydr026cΔ* strain to extend chronological lifespan, again distinct from the TOR pathway. Interestingly, when *sir2Δ* and *sir2Δ ydr026cΔ* strains are subject to ageing without acetic acid, a reduced chronological lifespan is again observed, suggesting another acetic acid-independent pathway distinct from the TOR pathway which takes epistatic precedence over that regulated by Ydr026c (**Figure 19b**).

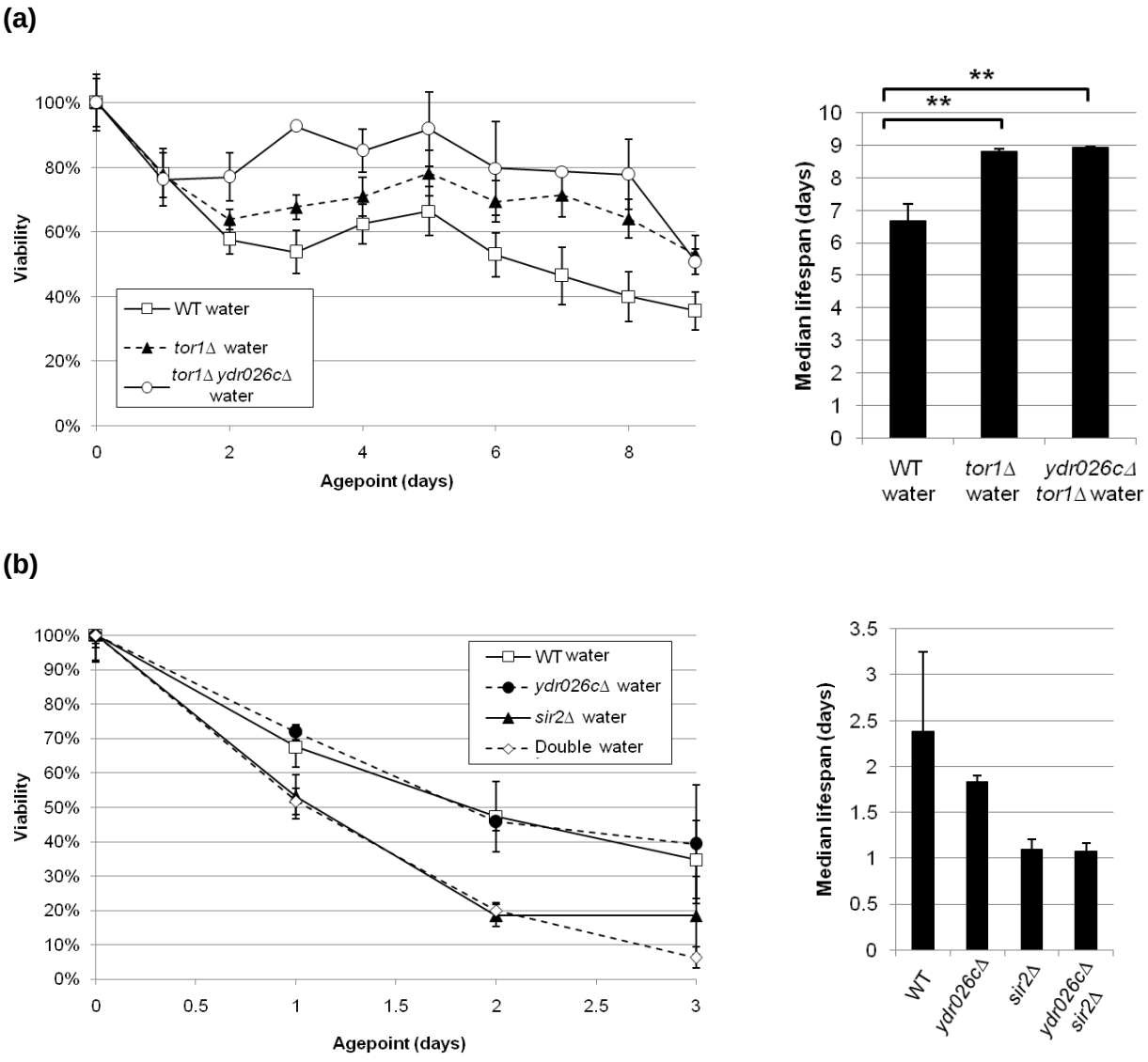

Figure 19. Viability curves and median lifespan data as determined by outgrowth analysis of chronological ageing stationary phase cultures subject to resuspension in water after growth through the diauxic shift. Data is for three simultaneous biological replicates (error bars are SEM). **(a)** Chronological viability curves for wild-type, the *tor1Δ* mutant and the *tor1Δ ydr026cΔ* double mutant when cells are resuspended in water after growth to stationary phase. The *tor1Δ* mutant remains long-lived compared to wild-type, which is itself has considerably extended chronological lifespan compared to standard medium conditions. However, the additional extension usually observed in the *tor1Δ ydr026cΔ* double mutant is weak and not significant under these conditions, and no significant increase in median lifespan is measured. **(b)** Chronological viability curves for wild-type and rDNA maintenance null mutants *ydr026cΔ*, *sir2Δ* and double mutant *sir2Δ ydr026cΔ* (*double*) resuspended in water after growth to stationary phase. The *ydr026cΔ* mutant is consistently long-lived under standard conditions but when medium is removed gives a profile not significantly different from wild-type. In contrast, the short-lived *sir2Δ* and *sir2Δ ydr026cΔ* strains maintain their short lifespan relative to wild-type when under calorie restriction.

4.7 Metabolic gene expression in chronological lifespan mutants

Entrance to the stationary phase experienced during chronological ageing in *S. cerevisiae* is associated with a suite of metabolic changes associated with the diauxic shift that occurs between fermentative and aerobic metabolism. During log phase growth, carbohydrate carbon sources are rapidly anaerobically fermented to ethanol, which in turn is quickly oxidised to acetic acid. After 16-24 hours of continuous growth, a 2% carbon source medium will be depleted and metabolism becomes reliant upon oxidative phosphorylation (Brauer et al., 2005). Much of this diauxic shift is mediated by changes in metabolic gene expression. Fermentative genes such as glycolytic enzymes *HXK1* and *ENO2* are expressed during log phase growth, while oxidative genes such as *CIT1* and *CIT2* (citric acid cycle), *ATP17* (oxidative phosphorylation), *ACS1* (acetic acid uptake) and *ATG1* (autophagy marker) are expressed after the diauxic shift (Brauer et al., 2005; Galdieri et al., 2010).

Because of the importance of this shift in the entry to stationary phase and the role acetic acid plays in modulating chronological lifespan, the expression levels of these genes was measured in cells before and after diauxic shift in a number of strains exhibiting chronological lifespan phenotypes. cDNAs produced by randomly primed reverse transcription of bulk RNA extracted from log phase or stationary phase cells were subjected to qPCR with primers specific to metabolically important genes. In WT cells, distinction of pre- and post-diauxic gene expression patterns was extremely clear (**Figure 20**). When gene expression in mutants of the SAGA/SLIK complex were compared, significant differences were observed in the ratios of log phase and stationary phase metabolic gene expression (**Figure 20a-b**).

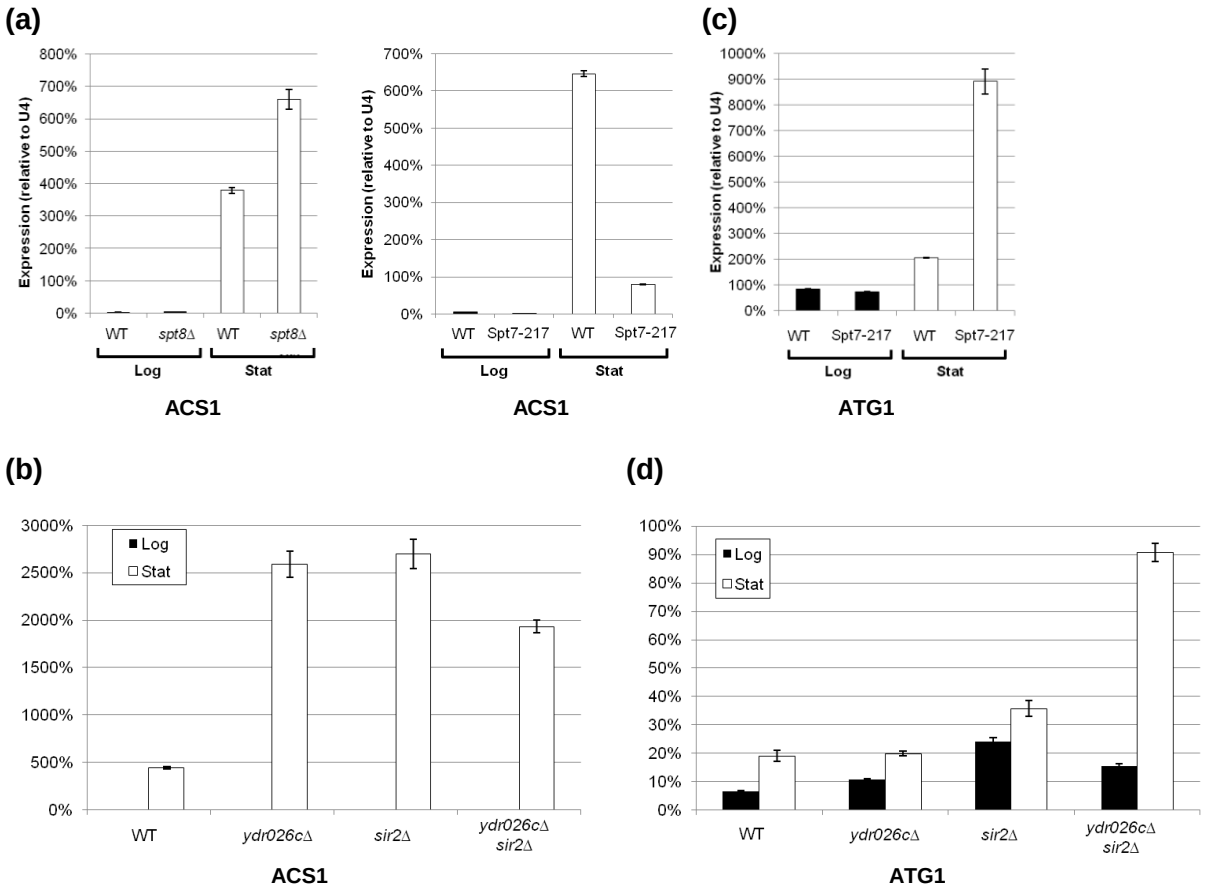

Figure 20. Gene expression profiles for two genes activated during the post-diauxic shift, *ACS1* (acetate metabolism) and *ATG1* (autophagy regulation) in logarithmic phase (log) and stationary phase (stat). Transcript levels were measured in total cDNA by qPCR and data is normalised to input by expression of U4. **(a)** *ACS1* is strongly expressed following the diauxic shift. Enhanced levels of *ACS1* expression are observed in the short-lived SAGA/SLIK mutant *spt8Δ*, while significantly reduced levels are detected in the long lived Spt7 truncation mutant Spt7-217, compared to wild-type. As an *acsΔ* strain is long-lived, it is hypothesised that underexpression of *ACS1* allows reduced acetic acid metabolic utilisation and promotes longevity. **(b)** However, the pattern of *ACS1* expression levels in the rDNA maintenance mutants does not correlate with their chronological longevity phenotypes: *ACS1* expression appears elevated in all the mutants tested. **(c)** *ATG1* expression rises around 2-fold following the diauxic shift. A very strong induction of *ATG1* is consistently found in the long-lived truncation mutant *Spt7-217*. **(d)** However, in the rDNA maintenance mutants, the highest levels of *ATG1* expression following the diauxic shift were observed in the *sir2Δ* and *sir2Δ ydr026cΔ* short-lived mutants.

In the short-lived *spt8Δ* strain, higher levels of post-diauxic gene expression (*ACS1*) were observed; conversely, in the long lived constitutive truncation mutant *Spt7-217*, lower levels of *ACS1* expression were observed (**Figure 20**). Interestingly, this strain also exhibited a significant increase in expression of the autophagy regulatory gene *ATG1* following the diauxic shift. *atg1Δ* mutants have been shown to be short-lived, and there is evidence that effective autophagy is a key component of chronological longevity (Eisenberg et al., 2009). This suggests a correlation between suppression of post-diauxic metabolic activity and increased chronological longevity in these strains.

This raises the question of whether this relationship is maintained in the rDNA maintenance mutants exhibiting modified chronological longevity phenotypes. Pre- and post-diauxic levels of *ACS1* and *ATG1* gene expression were measured in the *ydr026cΔ* long-lived mutant, the *sir2Δ* short-lived mutant, and the short lived double mutant *ydr026cΔ sir2Δ* as above (**Figure 20c-d**). No consistent pattern was observed in a selection of log phase and stationary phase expressed genes (*ACS1, ATG1, HXK1, ATP17, ENO2*), suggesting that, in agreement with the separate genetic epistasis discussed above, an alternative mechanism is responsible for the chronological longevity phenotypes in these strains.

4.8 Discussion

Despite post-mitotic senescence arguably representing a microbial model of ageing closer to the most problematic effects in mammals, genetic interventions modifying chronological longevity in *S. cerevisiae* are a relatively recent discovery compared to the intense study directed at replicative longevity. Apart from caloric restriction, many of the interventions

discovered so far are disparate and many areas of regulation remain poorly understood, particularly at the level of chromatin regulation.

In order to investigate epigenetic mutants with potential chronological ageing phenotypes, a series of preliminary experiments were performed using conventional methods for determining chronological longevity. Novel and opposite longevity phenotypes were observed in the SAGA/SLIK mutants *spt7Δ* and *spt7-217* (**Figure 16**). A strain null mutant for the largely uncharacterised *YDR026C* which encodes a putative nucleolar DNA-binding protein was found to have a long-lived phenotype (**Figure 15**) – a tantalising result, as rDNA maintenance proteins have a prominent role in control of replicative longevity (Hoopes et al., 2002).

It was quickly determined that the deficiencies of these techniques make robust quantitative, statistical comparison of viability data over time difficult. To validate the phenotypes observed in the preliminary experiments rigorously, the ageing culture outgrowth protocol (Murakami and Kaeberlein, 2009) was adapted for efficient biological reproducibility. Through a number of refinements to the analysis algorithm an outgrowth analysis protocol was designed that correlated very strongly with other techniques for determining fall of culture viability over chronological age, and produced robust, reproducible and comparable chronological ageing data.

Using this protocol, previously observed lifespan phenotypes in SAGA/SLIK mutants, TOR signalling mutants, and *ydr026cΔ* could be reproduced. Strains mutant for the histone deacetylase *SIR2* which is necessary for the majority of replicative lifespan-extending interventions, and with which Ydr026c interacts *in vivo* (Ha et al., 2012), were additionally found to exhibit a dramatically reduced chronological lifespan. An ambiguous phenotype has previously been reported for *sir2Δ* strains, with attention focussed on an increased maximal lifespan in some backgrounds rather than the reduced median lifespan (Fabrizio et

al., 2005). In our system, *sir2Δ* strains were found to have invariably shortened maximal and median chronological lifespans. Moreover, this short-lived phenotype was found to be epistatic to the lifespan extension observed in *ydr026cΔ* mutants, suggesting a concerted genetic pathway controlling chronological lifespan. As previously reported, the *fob1Δ* strain which plays a critical role in replicative longevity did not have a chronological ageing phenotype (**Figure 15**) (Smith et al., 2007).

Assay of strains disrupted for TOR signalling *tor1Δ*, *sch9Δ*, and *rim15Δ* reproduces an extended chronological lifespan. Epistasis experiments on strains containing mutations of both the TOR pathway and *YDR026C* or *SIR2* demonstrated additive effects on the chronological longevity phenotypes, suggesting genetic independence of these two longevity regulatory pathways. Similarly, while caloric restriction (by resuspension of stationary cultures in water) greatly extended the longevity of both wild-type and *tor1Δ* mutant cultures, no such effect was observed in the *ydr026cΔ* strains, emphasising the discrete nature of these two pathways. Additionally, overexpression of a constitutively hyperactive Sch9 mutant was capable of reducing chronological longevity in both wild-type and *sir2Δ* strains, suggesting an additive effect in reducing chronological lifespan.

Further experiments tested the hypothesis that while lack of accumulation of acetic acid in the extracellular medium is sufficient to reconstitute the effects of caloric restriction, it is the downstream oxidative metabolism of this post-diauxic carbon source that causes the pro-ageing effects, rather than direct physical assault on cellular components. Mutants were constructed lacking Acs1 and Ach1, responsible for the majority of the utilisation of acetic acid (through synthesis of acetyl-CoA) in the cytosol and mitochondrion respectively. *asc1Δ* and *ach1Δ* were found to exhibit extended chronological longevity, suggesting that metabolism of accumulated acetic acid is required to counter the longevity effect of caloric restriction.

Ydr026c is a poorly characterised protein and little is known about its physiological function. Polypeptide motif analysis indicates that it contains a myb-like DNA binding region near its C-terminus. We have found that DNA homology comparison within *Saccharomyces cerevisiae* and more generally indicates that *YDR026C* is a close paralog of the nutrient-dependent transcriptional regulator *REB1*, and a homolog of the mammalian RNA polymerase I transcription termination factor TTF-1 (**Figure 21**). Genome-wide ChIP-on-chip experiments have determined that the consensus binding site for the Ydr026c protein is well defined as *TTACCCGG* (Harbison et al., 2004). Inverted repeats of this consensus site flank the yeast rDNA cassette, appearing just before the promoter and terminator of the main RNA polymerase I-derived 35S transcript. Mammalian TTF-1 binds in a similar position in the mammalian rDNA array where it drives termination of the RNA-polymerase I transcript (Sander and Grummt, 1997; Langst et al., 1998); it has also been suggested that TTF-1 mediates higher-order chromatin structure formation in the mammalian nucleolus (Németh et al., 2008). Yeast two-hybrid and coimmunoprecipitation experiments have demonstrated that Ydr026c can colocalise with other nucleolar proteins including Sir2 and Fob1 (Mohanty and Bastia, 2004). More recently, *in vivo* ChIP studies have demonstrated that Ydr026c can be detected binding to the rDNA spacer region near the predicted binding site at the 35S transcript terminator, and suggested that this binding is dependent upon the fork-blocking protein Fob1. It has also been suggested that strains lacking Ydr026c experience loss of silencing in the rDNA spacer region (Ha et al., 2012). No chronological ageing phenotype in *ydr026cΔ* strains has yet been reported.

Previous work in the Mellor group (David Clynes, personal communication) has suggested that the chronological longevity phenotypes observed in mutants of the chromatin modifying complex SAGA/SLIK have correlated with failure to activate a suite of metabolic genes associated with the diauxic shift. To determine whether a similar correlation could be observed for the putative rDNA maintenance mutants *ydr026cΔ* and

sir2Δ, gene expression of several of these post-diauxic genes (*ACS1*, *ATG1*, *HXK1*, *ATP17*, *ENO2*) were measured by qPCR of total cellular cDNA. No consistent pattern emerged correlating with the chronological ageing phenotypes, strongly suggesting that this is not the underlying mechanism of ageing intervention in these mutants.

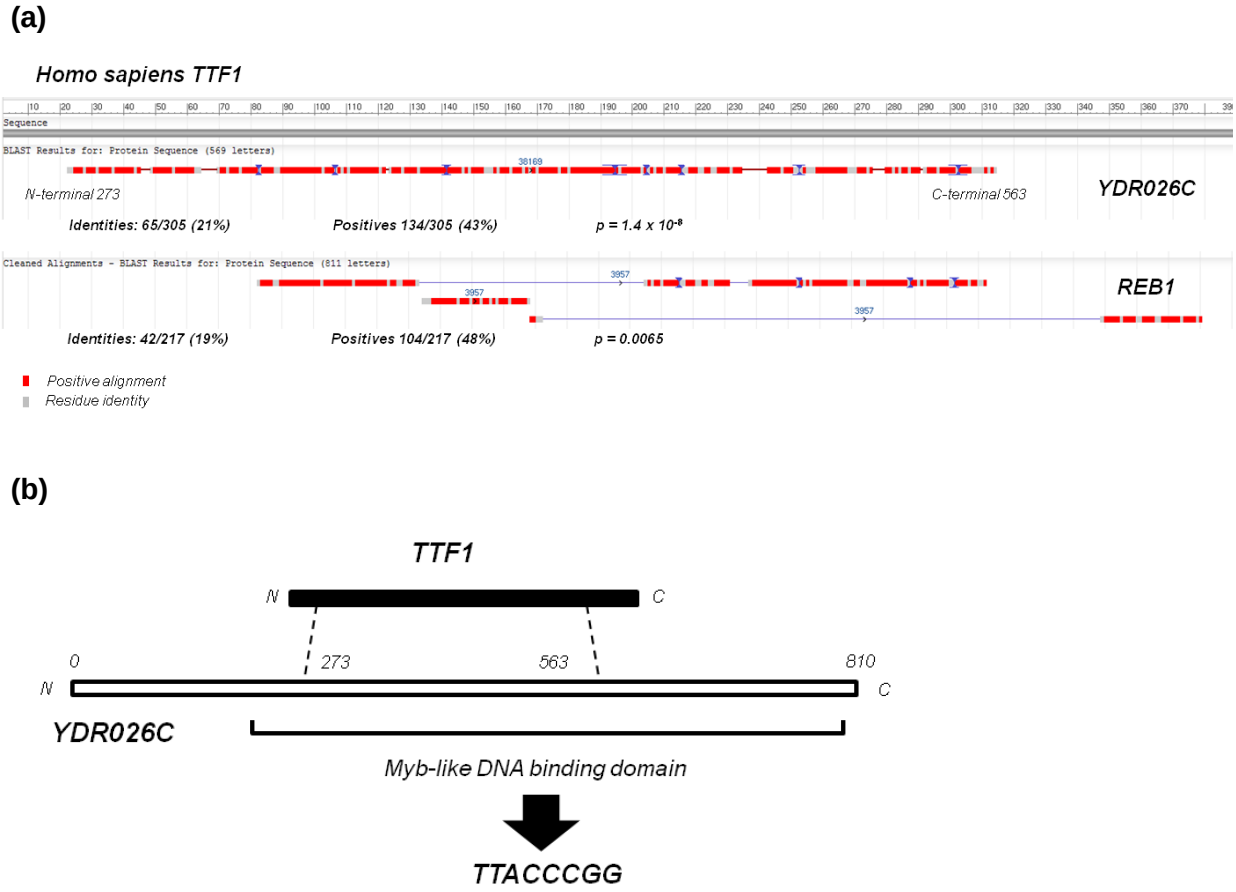

Figure 21. (a) Alignment of protein sequences representing best yeast matches of *Homo sapiens* TTF1 transcript varient 2. Significant *S. cerevisiae* translated ORF sequences aligning with TTF1 are the poorly characterised protein *YDR026C*, and the DNA-binding transcription factor *REB1* ($p = 1.4x10^{-8}$ and 0.0065 respectively). Best alignment is given over the C-terminal domains of each protein, containing the putative and demonstrated DNA binding domain respectiely. Alignment performed using NCBI blast.**(b)** Schematic of alignment of TTF1 with YDR026C. Good alignment is given over the first part of the C-terminal myb-like DNA binding domain, while the extreme C-terminal and the N-terminal domain of unknown function does not align. Genome-wide ChIP experiments have demonstrated this domain has a binding consensus of TTACCCGG.

5 Quiescence

5.1 Introduction

Chronological longevity in *Saccharomyces cerevisiae*, as defined in (Longo et al., 1996) and measured in the outgrowth assay developed and described in the previous chapter, is the maintenance of culture viability over time in a post-diauxic ageing culture. The prevailing conditions during this culture phase are therefore fundamental to an understanding of the chronological ageing phenotypes discussed in the previous chapter.

When inoculated into rich or minimal medium containing typical carbon source concentrations (1-2%), budding yeast follow a characteristic and stereotypical growth profile (**Figure 22**). Immediately following inoculation a brief lag phase is observed, where little cell division and culture growth occurs, usually for 0.5-2 hours. During this period, cells adapt to the new culture conditions through induction of genes appropriate for the metabolism of the newly available nutrients: specifically those for the glycolytic pathway, fermentation to ethanol and acetic acid, the pentose phosphate pathway, amino acid synthesis, and synthesis of carbohydrate storage forms – primarily glycogen (Lillie and Pringle, 1980; Ronne, 1995; Livas et al., 2011). Operation of glycolysis and fermentation leads to accumulation of cytosolic ATP. Immediately after the lag phase, growth begins in earnest, and exponential growth dynamics are generally observed as each generation of daughters completes the cell cycle in a comparable period of time (the *doubling time*) (Slator, 1913).

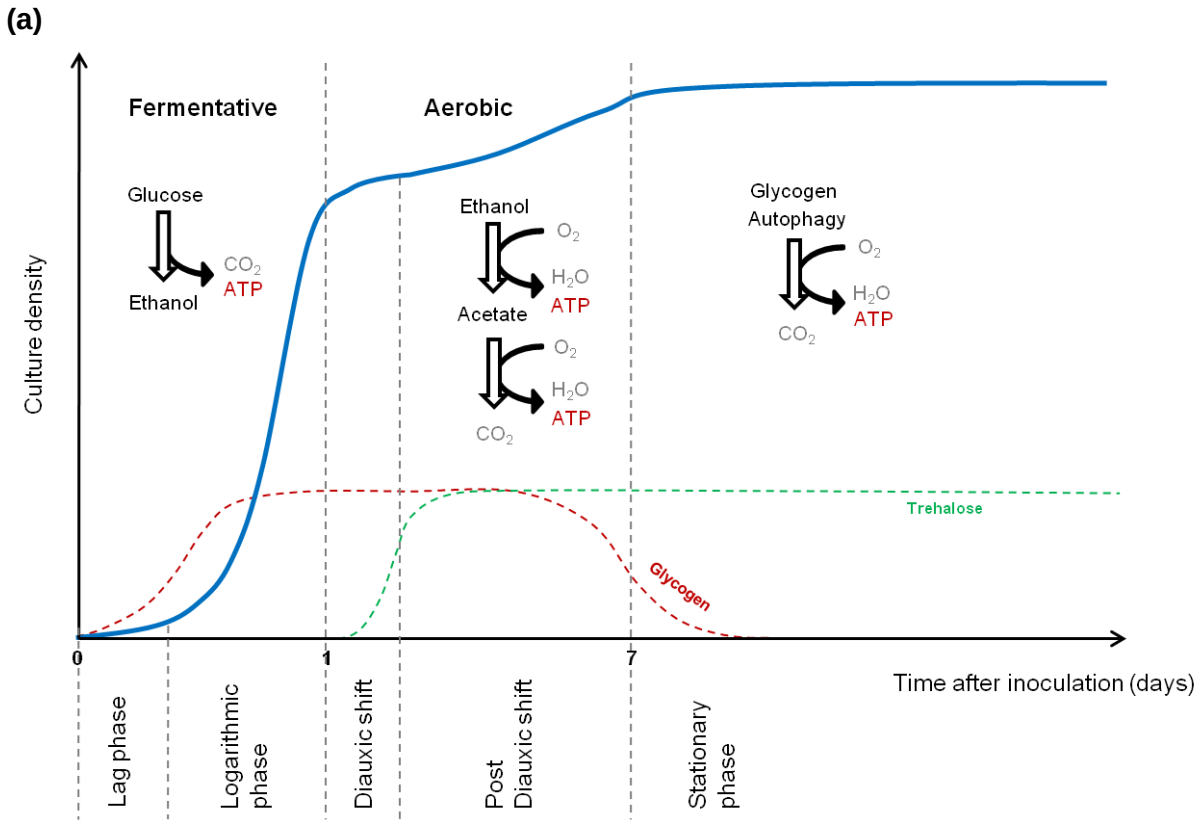

Figure 22. Typical growth phases of *Saccharomyces cerevisiae* following inoculation at low cell density (blue line). **(a)** Following a brief lag phase during which cells acclimatise to new medium conditions through synthesis of appropriate catabolic enzymes, growth begins in earnest fuelled by rapid fermentation leading to exponential culture expansion (logarithmic phase). This continues until all fermentable carbon sources, such as glucose, are exhausted (after ~24 hours). Following a major metabolic readjustment (the "diauxic shift"), growth continues slowly for 7 days or more fuelled by aerobic oxidation of ethanol and acetate secreted into the medium. When these are exhausted growth stops entirely, and true *stationary phase* is encountered. Cells survive here at basal metabolic rate by oxidation of amino acids recovered in autophagy and stored glycogen, which is accumulated from logarithmic phase (red line). Storage carbohydrate trehalose is accumulated from the diauxic shift (green line), and in quiescent cells is not utilized until growth needs to be resumed.

Energy for growth, as ATP, is provided almost exclusively by fermentative catabolism of glucose and equivalent carbon sources to generate ethanol (Verduyn et al., 1990; Entian and Barnett, 1992). In non-petite laboratory yeast backgrounds (i.e. those with normal mitochondrial function), ethanol is quickly oxidised in an oxidative phosphorylation-dependent process to acetic acid, which is secreted and accumulates in the medium (Postma et al., 1989). Growth will continue in this fashion until a limiting factor – typically nutrient

availability – prevents unrestricted biomass accumulation (preliminary experiments performed in our lab investigating supplementation of post-diauxic cultures with additional carbon and nitrogen sources have found virtually unrestricted growth will occur, to cell densities 5 to 10-fold that of unsupplemented stationary cultures and beyond – data not shown). In rich medium, fermentable carbon source exhaustion generally limits logarithmic growth. To continue metabolism after this point, cells must undergo a suite of metabolic changes to allow them to adapt to respiration of non-fermentable carbon sources and oxidative metabolism. This is termed the *diauxic shift*, and involves the induction of numerous genes (DeRisi et al., 1997) controlling the citric acid cycle, oxidative phosphorylation (Hardwick et al., 1999), oxygen radical and stress response (Werner-Washburne et al., 1993), and the glyoxylate pathway (Haurie et al., 2001); as well as the repression of glycolysis and the slowing of the cell cycle (Werner-Washburne et al., 1993). Growth slows markedly following this phase (the *post-diauxic shift*), with low, linear rates of culture density growth observed. Energy is then provided by oxidative metabolism in the mitochondrion of fermentation products residual in the medium (Dickinson and Schweizer, 1999) – first ethanol then largely acetic acid – as well as glycogen stored during logarithmic growth (Lillie and Pringle, 1980) and amino acids released by autophagy and proteolysis (Kamada et al., 2004). The storage carbohydrate trehalose is, however, accumulated during this phase (Lillie and Pringle, 1980). After several weeks in the post-diauxic shift phase (or if aged in water as in calorie restriction experiments) the non-fermentable carbon sources are depleted, and growth ceases entirely – the true *stationary phase*.

Because of the very low rates of growth during the post-diauxic culture phase during which chronological longevity is measured (it is sometimes erroneously referred to as *stationary phase*) – the traditional view of cell physiology and hence chronological ageing in these cultures is that of cellular quiescence. Quiescence is usually characterised by the shift of a

suite of metabolic and genetic activities leading to the exit from the cell cycle, minimisation of protein synthesis, and modified and lowered levels of transcription (Gray et al., 2004). Quiescence is commonly invoked in microorganisms such as *Saccharomyces cerevisiae* by limiting nutrient conditions (carbon source, nitrogen source, or micronutrients such as phosphate) (Thevelein et al., 2000) and in multicellular organisms by differentiation in response to intercellular signalling, nutrient and growth factor deprivation (Blomen and Boonstra, 2007). Starvation is probably the most common stress for a single-celled eukaryote such as budding yeast (Lewis and Gattie, 1991) while maintenance of stable and functional post-mitotic cell state in critical for longevity and prevention of cancer development in multicellular eukaryotes (Dasgupta et al., 2006). A conserved regulatory signalling network controlling cell cycle exit in single-celled eukaryotes and multicellular organisms (including, for example, TOR signalling) suggests a common genetic mechanism exists in inducing this state (Valcourt et al., 2012). Because of the greatly diminished availability of carbon, nitrogen, and energy sources following the post-diauxic shift, successful development of quiescence might be hypothesised to be a key determinant of chronological longevity in ageing yeast. Upon carbon source depletion, yeast cells have been shown to exit the cell cycle and enter a stationary development phase G_0 (Radonjic et al., 2005; Allen et al., 2006). Stationary cells exist in a resting state that preserves their viability during harsh nutrient conditions and allows them to survive longer (Allen et al., 2006) and retain their ability to resume growth once nutrients once again become available.

Upon passage through diauxic shift, it was initially thought that quiescence was triggered in a step-wise fashion when proliferating cells detected the depletion of fermentative carbon source – with daughter cells produced during this phase differentiating into quiescent cells (Gray et al., 2004). However, recent work has demonstrated that substantial non-quiescent subpopulations exist within post-diauxic phase ageing cultures (Allen et al.,

2006) and it has been proposed that this differentiation occurs during the logarithmic and diauxic shift phases of growth (**Figure 23**). The non-quiescent cell subpopulation continues to produce non-quiescent daughter cells, which are unprepared for the nutrient restriction that follows the diauxic shift and so have limited viability. The quiescent cell subpopulation produced daughters which enter a stable quiescent state and remain viable throughout the post-diauxic and stationary phases (Davidson et al., 2011). The non-quiescent mother cells are thought to more rapidly lose their quiescence characteristics and succumb to the same fate as the non-quiescent subpopulation, leading to depletion of culture viability. In contrast, quiescent cells maintain a minimal metabolism through oxidation of non-fermentable acetic acid and stored lipids, only slowly depleting stored glycogen and accumulating levels of stored trehalose (Gray et al., 2004). Trehelose has been shown to be necessary for effective exit of quiescence when nutrients become more abundant and resumption of logarithmic growth (Shi et al.); hence the quiescent subfraction appears to be optimised for survivability during periods of starvation and foundation of a new culture when conditions have improved. Loss of non-quiescent cells spares remaining medium nutrients for the more viable subfraction, and dead cell lysis releases additional nutrients into the medium (Herker et al., 2004; Rockenfeller and Madeo, 2008). Depletion of the less viable non-quiescent subpopulation of cells differentiated during logarithmic growth may therefore represent a cooperative survival strategy for the culture as a whole (Davidson et al., 2011).

Quiescent budding yeast cells share a number of characteristics common to quiescent eukaryotic cells: exit from the cell cycle, diminished protein, ribosome and mRNA synthesis, and reduced emphasis on glycolytic metabolism (Valcourt et al., 2012). Quiescent yeast cells arrest growth as unbudded daughter cells that are larger and denser than non-quiescent cells (Allen et al., 2006), and demonstrate a 90-fold reduction in protein synthesis (Boucherie, 1985) and 10-fold reduction in mRNA synthesis (Choder, 1991).

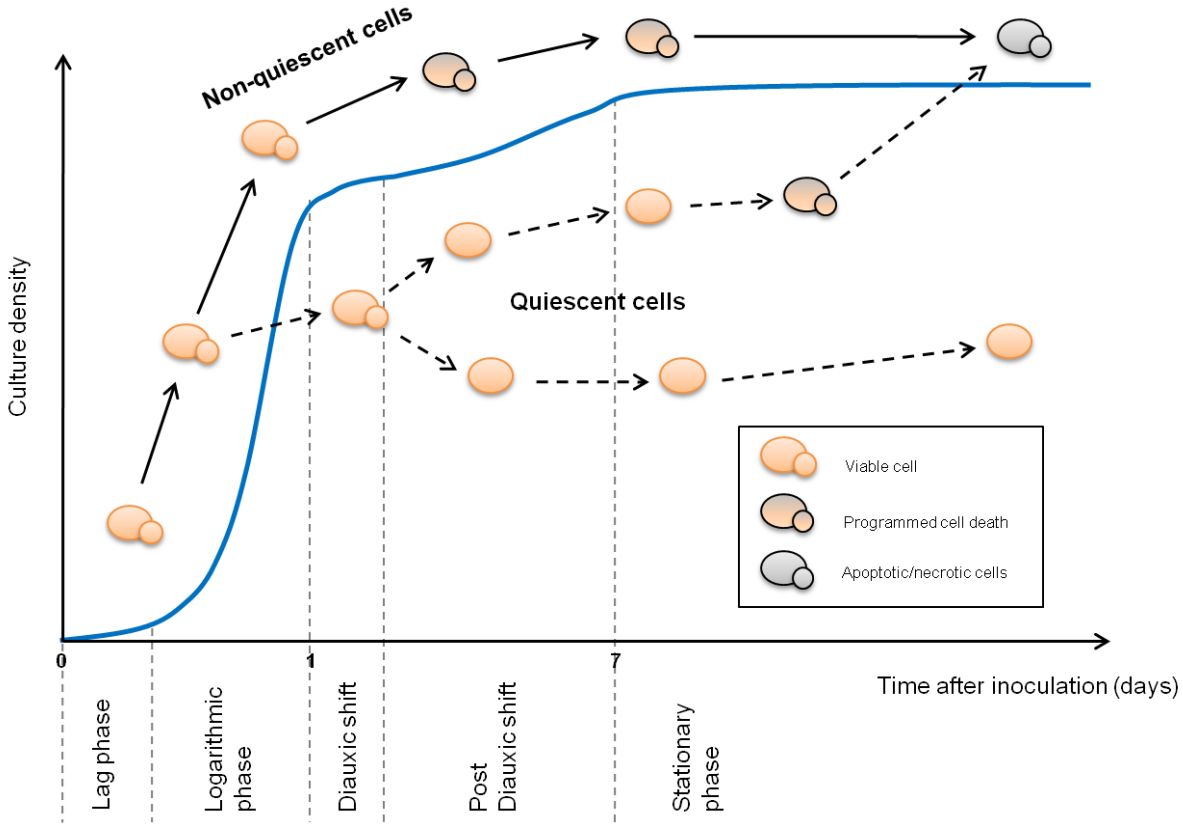

Figure 23. Differentiation of post-diauxic ageing *Saccharomyces cerevisiae* cells into quiescent and non-quiescent subpopulations. Following the diauxic shift, as well as low-nutrient adapted unbudded quiescent cells, there also exists within the culture a subpopulation of low density, unadapted, budding non-quiescent cells. Differentiation into these two physiological modes, rather than occurring progressively with the first new generation exposed to low nutrient concentrations, has been shown to occur during the diauxic shift and as early as the logarithmic phase. The non-quiescent mother cells continue to bud and produce non-quiescent daughters, while the quiescent mothers slowly produce stably quiescent daughters. The non-quiescent population rapidly loses viability due to induction of apoptosis and necrosis pathways caused by inadequate aerobic metabolism; the quiescent mother cells eventually lose their quiescent programming, leading to a re-emergence of the non-quiescent population and their apoptosis.

They exhibit greatly enhanced tolerance to extremes of temperature and osmolarity, and are chronologically longer lived (Gasch et al., 2000; Allen et al., 2006). Upon replenishment of nutrient availability, quiescent yeast cells will synchronously re-enter the cell cycle (Allen et al., 2006). High-throughput gene expression analysis of quiescent and

non-quiescent subfractions of post-diauxic cultures has demonstrated enhanced expression of genes regulating aerobic respiration, acetic acid and ethanol metabolism, trehalose synthesis, and stress response genes (Radonjic et al., 2005), identifying as strongly expressed markers the genes *SIP18* and *MLH2* for quiescent and non-quiescent subfractions respectively.

Saccharomyces cerevisiae, while lacking Bcl-2 components (Bax etc.) of the apoptotic regulatory pathway of higher organisms (Greenwood and Ludovico, 2010), can undergo cell death characteristic of both apoptosis and necrosis (Rockenfeller and Madeo, 2008). Apoptotic yeast cells exhibit numerous markers associated with apoptosis in other systems, including transition of phosphatidylserine to the outer leaflet of the plasma membrane (Madeo et al., 1997), release of cytochrome c and AIF from the mitochondrion (Ludovico et al., 2002; Wissing et al., 2004), depolarisation of the mitochondrial membrane (Pozniakovsky et al., 2005), chromatin condensation and genomic DNA fragmentation (Madeo et al., 1997). Yeast possess a protein with *metacaspase* activity, Yca1, stimulated in this state (Madeo et al., 2002) and yeast apoptotic regulators such as *CDC48* which can induce apoptosis in mammalian cells (Shirogane et al., 1999). Chronologically aged yeast succumb to apoptosis and *yca1Δ* mutants show longer chronological longevity, but reduced fitness (Fabrizio and Longo, 2003; Herker et al., 2004). Acetic acid, absence of which is sufficient to reconstitute the calorie restriction effect in chronological ageing, has been shown to specifically induce apoptotic cell death (Ludovico et al., 2001; Burtner and Kaeberlein, 2009). Fragmentation of the genome, as assayed by fluorescent deoxynucleotide end-labelling (TUNEL assay), has been used as a marker of apoptosis versus necrosis in mammalian and yeast systems (Carmona-Gutierrez et al., 2010).

Necrosis – lytic cell death unassociated with the characteristic markers of apoptosis – also occurs in chronologically and replicatively ageing yeast (Eisenberg et al., 2009). It has been argued that necrosis constitutes the default cell death upon metabolic failure: mutants

with disrupted apoptosis, such as defective endonuclease G, exhibit reduced apoptosis but eventual elevated necrotic death (Buttner et al., 2006). However, tight regulation of necrosis has also been described suggesting an active role in programmed cell death (Zong and Thompson, 2006).

Because induction of the quiescent state during the diauxic shift involves responding to relatively rapid changes in nutrient levels, mutants deficient in the signalling network communicating perceived nutrient depletion may be hypothesised to demonstrate defective entry to quiescence and curtailed chronological lifespan. The implication that continued metabolism (availability of aerobic carbon sources such as acetic acid, activation of oxidative phosphorylation or generation of reactive oxygen species) lowers chronological lifespan, whilst suppressed metabolic activity (by, for example, caloric restriction) increases chronological lifespan underlines the importance of limited metabolism after the diauxic shift. The ability of different strains to produce a stable and persistent quiescent fraction has previously been correlated with their survival in stationary phase during chronological ageing (Li et al., 2009; Madia et al., 2009). It was therefore hypothesised that the ability, or failure, to produce this long-lasting quiescent fraction was responsible for a significant number of observed chronological lifespan mutants.

One such short-lived mutant has been previously identified as *snf1Δ*. Snf1 is a serine/threonine protein kinase that is homologous to mammalian AMP-dependent kinase (AMPK) (Hardie et al., 1998) and has been identified as a key regulatory protein in the glucose repression signalling network (Smets et al.; Mayordomo et al., 2002). Loss of function of Snf1 leads to the inability to activate expression of genes normally subject to glucose repression, including those required for the diauxic shift, oxidative metabolism, and maintenance of a stable quiescent state (Gray et al., 2004).

A series of experiments were performed to investigate production of quiescent and non-quiescent culture subpopulations over chronological ageing in post-diauxic cultures in the *snf1Δ* mutant, to determine whether its shortened longevity correlated with deficiencies in entry to quiescence. Density equilibrium centrifugation of heterogeneous post-diauxic phase cultures on density gradients such as Percoll yields two highly discrete subfractions consisting of quiescent and non-quiescent cells. This assay was then applied to the putative rDNA maintenance mutants *sir2Δ* and *ydr026cΔ* with uncharacterised chronological ageing phenotypes, to determine whether a similar model of quiescence regulation could explain the phenotypes observed.

5.2 Subpopulation differentiation in ageing wild-type and *snf1Δ* cultures

In the absence of an alternative physiological mechanism for the chronological longevity phenotypes observed in the putative rDNA maintenance mutants discussed in chapter 4, capacity for development of a quiescent subpopulation was investigated as a possible underlying cause. A culture subpopulation separation assay was applied to ageing cells of the short lived strain *snf1Δ* which has previously been shown to have a pronounced subpopulation distribution phenotype. Strains were inoculated into rich medium and stationary cultures developed, with aliquots removed at specific agepoints.

Chronological longevities were found to be considerably extended when ageing cultures were kept in rich medium, probably as a result of the superior buffering effects of the medium preventing accumulation of the conjugate acid form of acetic acid (considerably less acidification of the medium was observed over time compared to SC medium). Logarithmically growing wild-type cultures after 3 hours were found to produce only non-quiescent, non-dense subfractions as expected. Following the post-diauxic shift (24 hours), however, the entirety of the culture becomes represented by the quiescent denser band. Over time, as the culture ages, the non-quiescent upper fraction re-emerges, correlating with loss of viability of the culture (**Figure 24a**). Purification of the two subfractions allowed individual analysis of the quiescent and non-quiescent cells. Microscopic examination of these revealed that the log-phase and re-emerging upper fraction consisted of small, highly budded cells, while the lower fraction consists of much larger, dense, phase bright cells with thick cell walls and very large vacuoles. Quantification of bud occurrence in purified subfractions verified this trend (**Figure 24b**).

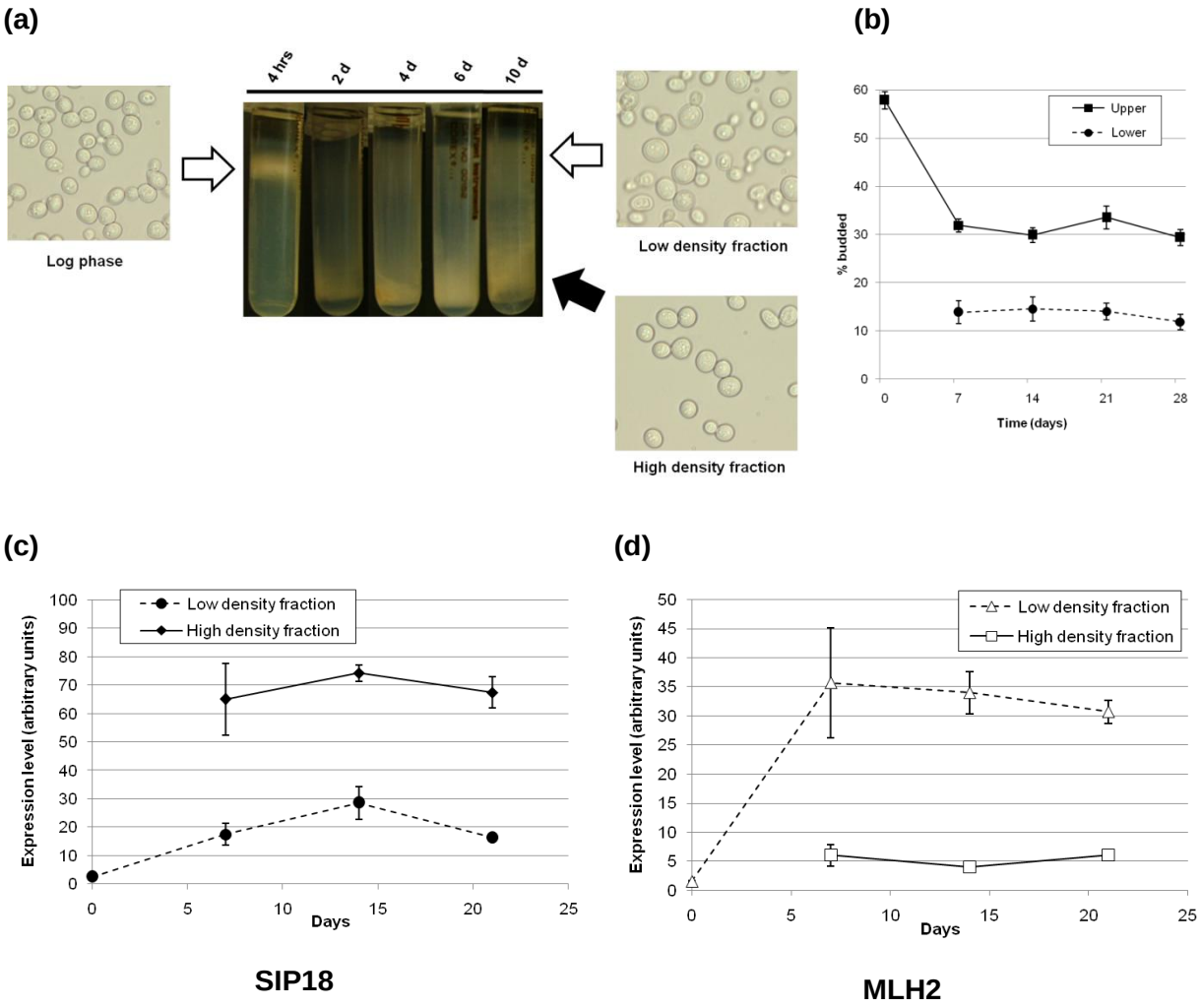

Figure 24. Emergence of two distinct cell culture subpopulations over chronological ageing. **(a)** Chronological ageing series of a wild-type culture inoculated into rich medium and growing through the diauxic shift to stationary phase densities. Aliquots were removed at agepoints, the cells washed, and cells separated according to density by density equilibrium centrifugation over a self-forming gradient of Percoll. Logarithmic phase cultures (4 hrs) contain cells of uniformly low density and form a band near the top of the gradient; these cells are relatively small and highly budded. Following the diauxic shift (2 days) the entirety of the culture consists of much denser cells forming a single band near the bottom of the tube; these cells are much larger, have large vacuoles, thick cell walls, and are largely unbudded. These cells have previously been identified as *Quiescent*. After ~4 days a distinct low-density band begins to appear alongside the dense cells. These are relatively smaller, and are considerably more highly budded. The emergence of this *Non-Quiescent* subfraction is hypothesised to indicate failing chronological viability. **(b)** Quantification of proportion of budded cells appearing in each culture subfraction, determined by microscopy on fractions purified from 4 day old wild-type stationary culture on Percoll gradients. **(c)** Expression levels of the quiescence marker gene *SIP18* and **(d)** non-quiescence marker gene *MLH2* determined by qPCR on cDNA generated using RNA extracted from culture subfraction of an ageing wild-type culture. Low levels of *SIP18* are expressed in logarithmic phase cells (day 0) and in the low density fraction, suggesting this subpopulation has not entered quiescence. Significantly higher expression levels are measured in the high density subfraction. The pattern is reversed in the case of MLH2 expression, with low levels of expression maintained in the denser fraction. Data for **(c)** and **(d)** produced by Prateek Choudry.

Transcript analysis by qPCR of reverse transcribed message demonstrated that the marker genes *SIP18* and *MLH2*, specific for the quiescent and non-quiescent subpopulations respectively, were greatly enriched in the appropriate purified subfractions. Expression levels of *SIP18* in whole culture was also found to be much higher following the diauxic shift and the first few days of chronological ageing (**Figure 24c-d**).

Pre- and post-diauxic culture of the short-lived *snf1Δ* mutant was prepared and the density subfractions of the culture population analysed. *snf1Δ* cultures were observed to exhibit a strikingly different pattern of culture differentiation: throughout the course of the experiment the entire culture consists of low density cells identified with the non-quiescent fraction. No detectable high-density fraction could be isolated. These cells were found to exhibit morphological characteristic distinctive of the non-quiescent fraction and to demonstrate relatively low levels of expression of the *SIP18* quiescence marker (**Figure 25**).

5.3 Genomic fragmentation in ageing cultures

To further investigate whether the ability of cultures to form quiescent and non-quiescent subpopulations following the post-diauxic shift could influence chronological lifespan, a genomic fragmentation assay was developed to allow for detection of apoptosis-like behaviour in individual culture subfractions. Such behaviour has been associated with the non-quiescent fraction at advanced stages of chronological ageing and is hypothesised to represent failure in the viability of that subpopulation of cells. The TUNEL assay relies upon diffusion of terminal deoxynucleotidyl-transferase and fluorescein-labelled nucleotides into permeabilised cells. Free DNA ends, such as generated by fragmentation of genomic DNA, are substrates for the enzyme, and become fluorescently labelled.

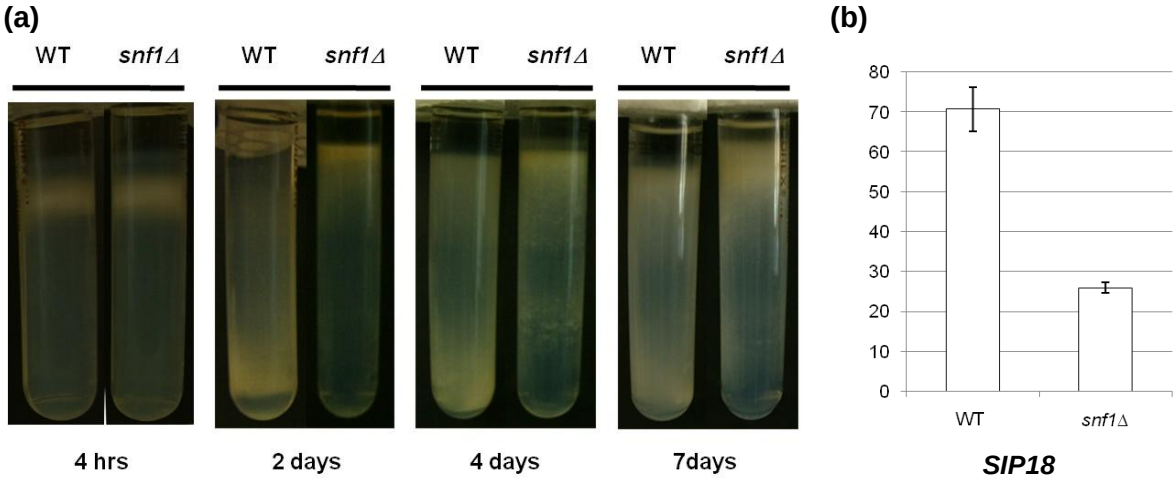

Figure 25. The chronologically short-lived nutrient signalling null mutant *snf1Δ* exhibits a strong and unusual culture differentiation phenotype. **(a)** Cell density subfractions of ageing wild-type and *snf1Δ* cultures separated on Percoll gradients. During logarithmic growth, both strains contain only cells of low density. Cells in the wild-type culture quickly become highly dense following the diauxic shift, and then slowly develop a low density fraction over time. Cells of the *snf1Δ* culture, in contrast, never develop a high density quiescent subfraction. **(b)** *SIP18* expression levels measured in day 4 ageing wild-type and *snf1Δ* cultures by qPCR of reverse transcribed message and normalised to percentage of U4 signal. Markedly reduced expression levels of the quiescent marker gene *SIP18* are seen in the *snf1Δ* strain, suggesting that this culture does not enter quiescence normally. Error bars are SEM of n=3 biological repeats.

Fluorescent response can then be detected in each cell using flow cytometry apparatus. Cell samples were taken from whole cultures, quiescent, or non-quiescent culture subfractions and fixed in formaldehyde. Cells were permeabilised with ethanol, and treated with Triton X-100 and sodium citrate. Cells were alternatively treated with fluorescent substrate; fluorescent substrate and TdT enzyme; DNase I to generate free DNA ends followed by substrate and enzyme; or untreated. Following the TUNEL reaction, cells were washed, resuspended and analysed by flow cytometry (**Figure 26a**).

Wild-type stationary phase cells were subjected to this assay. A strong and significant increase in the fluorescence profile recorded was observed in the case of the DNase I treated cells, above the untreated cells and those with no enzyme in the reaction.

Intermediate signal was observed in the cells untreated with DNase I (**Figure 26b**). This suggests that this protocol is specific and sensitive enough to detect DNA fragmentation in cells extracted from culture subpopulations.

Whole culture samples were taken from ageing wild-type and *snf1Δ* cultures at an intermediate agepoint (7 days) and subjected to the TUNEL assay. Wild-type cells produced a range of recorded fluorescence values similar to the negative control, demonstrating little free DNA end generation. *snf1Δ* cells, in contrast, produced a strong and significantly higher median fluorescence, exceeding that recorded for the DNase I positive control (**Figure 27a**). This suggests that *snf1Δ* cells at this agepoint experience considerable fragmentation of their genomic DNA compared to the wild-type, and that this may be responsible for the correlate loss of viability of this strain at comparatively early agepoints.

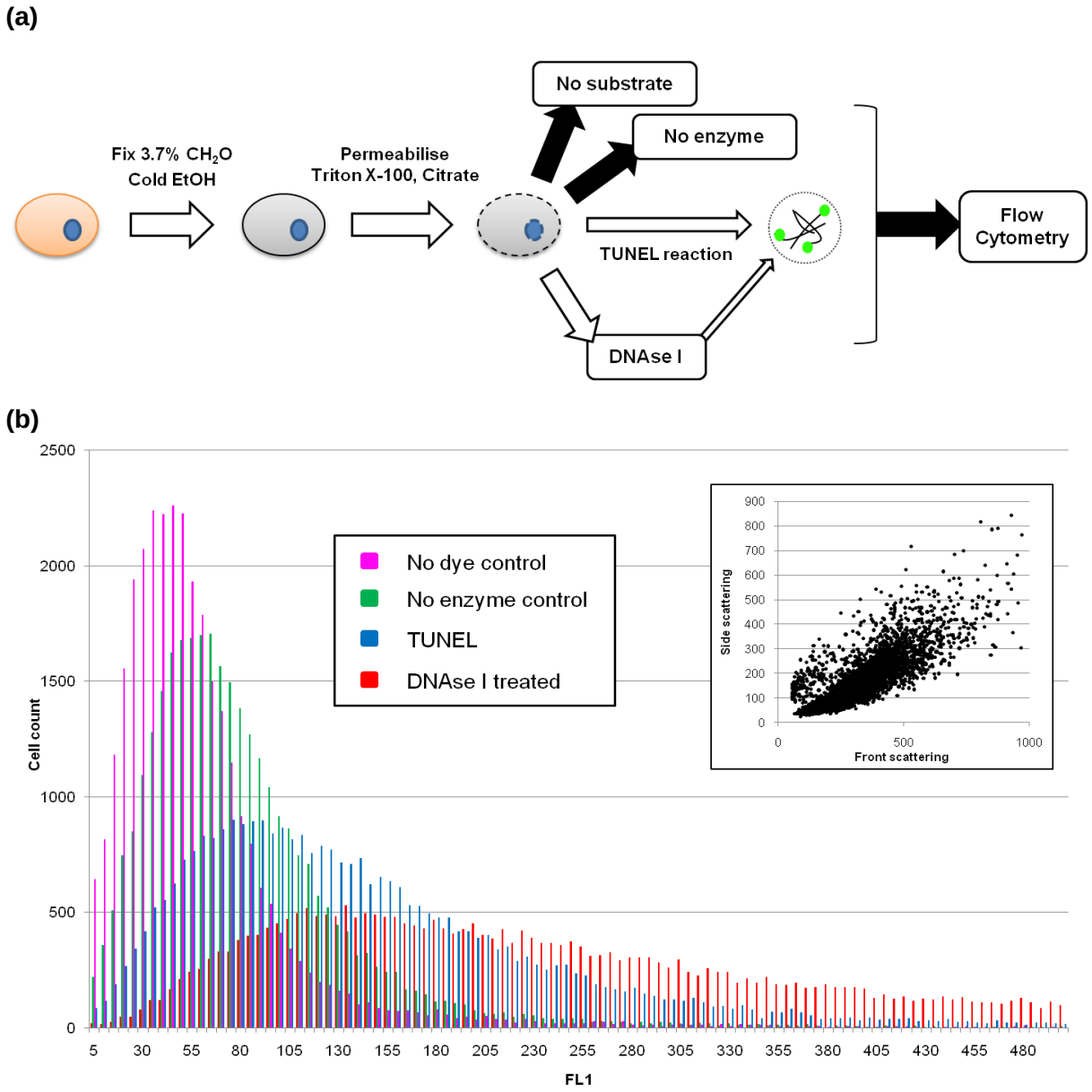

Figure 26. Assaying apoptosis-like genome fragmentation in ageing yeast subpopulations. The terminal deoxynucleotidyl-transferase dUTP nick end-labelling (TUNEL) assay was adapted for use in *S. cerevisiae*. **(a)** Harvested 4-day old cells were fixed in formaldehyde and cold ethanol, and permeabilised with Triton X-100 and sodium citrate. TUNEL reaction mixture (terminal transferase enzyme and fluoresceine-labelled dUTP substrate) was added to aliquots of permeabilised cells, either complete or without enzyme or substrate, and incubated for 4hrs at 37^{O}C. A further aliquot of permeabilised cells was treated with DNase I at 37^{O}C for 1 hr to fragment the nuclear genome, before being subject to the TUNEL reaction. Treated cells were washed, resuspended, and fluorescein incorporation measured by flow cytometry on a BD FACScan machine. **(b)** Linear fluorescence histogram indicating fluorescein-dUTP incorporated into cells in the TUNEL assay by flow cytometry of 40000 cells. Controls without dye or enzyme as well as cells subject to genomic fragmentation by DNase I treatment are indicated. The peak is strongly skewed to the right in cells treated with DNase I compared to the controls lacking enzyme or dye, indicating detectably greater incorporation. Wild-type cells subject to the reaction (TUNEL) give a peak intermediate between the positive and negative controls, suggesting measurable amounts of DNA fragmentation occur under these conditions.

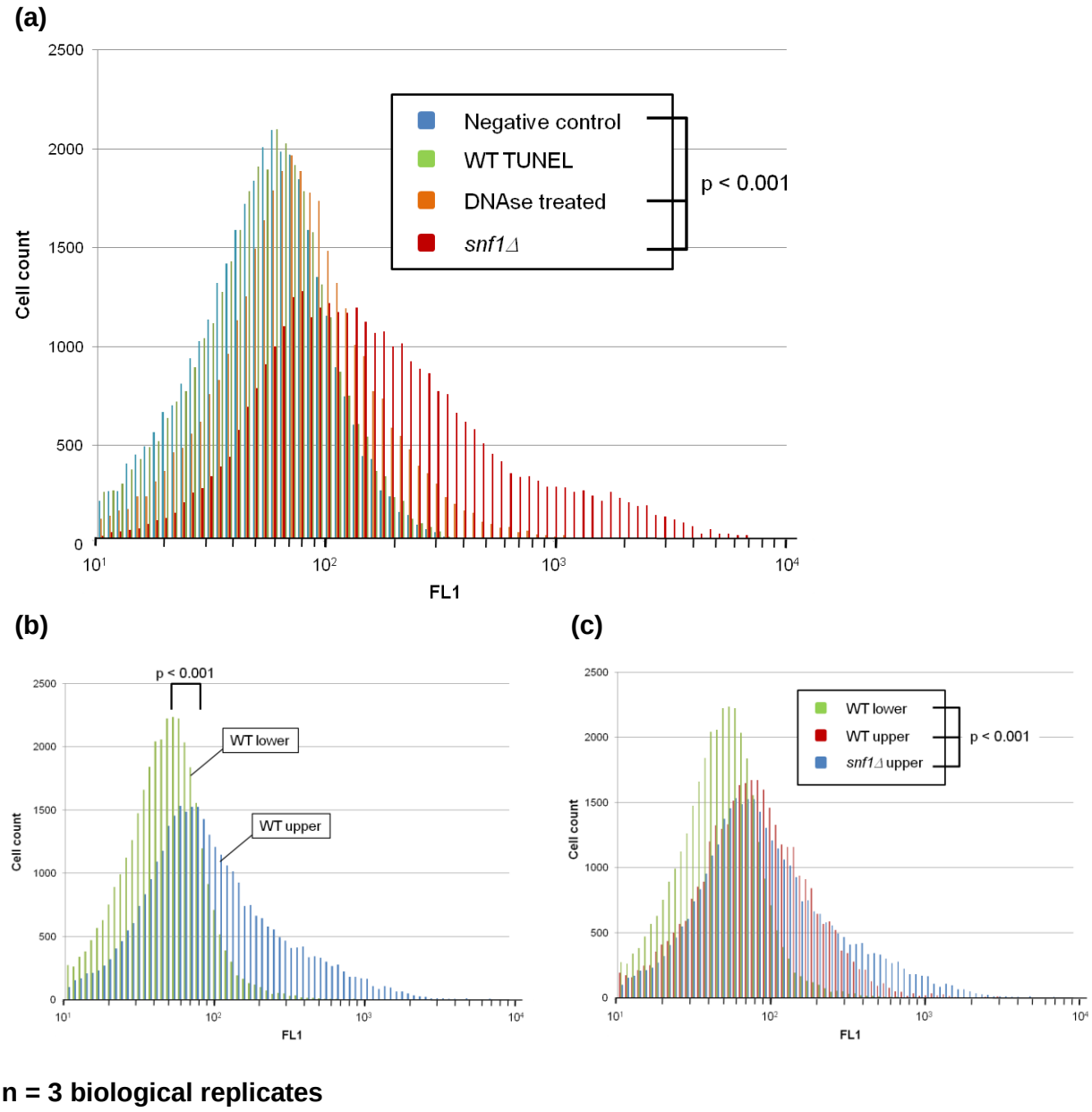

Figure 27. Histograms of logarithmic fluorescein-dUTP incorporation in TUNEL treated 7-day old wild-type and *snf1Δ* cells measured by flow cytometry. All experiments were replicated, n=3. **(a)** Ageing wild-type and *snf1Δ* whole culture cells, with negative (no terminal deoxynucleotidyl transferase) and positive (DNase I treated) controls. Wild-type cells at this age-point demonstrate fluorescence levels comparable to the negative control and not significantly different. In marked contrast *snf1Δ* cells exhibit extremely strong fluorescence incorporation, exceeding even that of the DNase I treated control. This suggests extensive genomic fragmentation in the *snf1Δ* cells at this agepoint. **(b)** Cells purified from the lower (dense) and upper (less dense) culture subpopulations of a wild-type culture. A single moded peak is given in each case, with a strong and significant shift to the right for the low density subfraction cells. This indicates the two subpopulations of ageing wild-type culture at moderate agepoints can also be distinguished by DNA fragmentation levels. **(c)** Cells purified from the upper (less dense) subfractions of *snf1Δ* cells. This subpopulation records a fluorescence incorporation similar to that of the low density wild-type subpopulation, suggesting that the strong incorporation observed in the *snf1Δ* whole culture is due to the predomination of this non-quiescent subpopulation.

To investigate whether apoptosis-like genomic fragmentation was associated with the quiescent or non-quiescent subfraction of the ageing cultures, these subpopulations were purified from percoll gradients as above for both the wild-type and *snf1Δ* strains and harvested cells washed and subject to the TUNEL reaction and flow cytometric analysis. At day 7, only a low density (non-quiescent) subfraction could be extracted from the *snf1Δ* culture, while both high and low density fractions could be isolated from the wild-type culture, with the quiescent fraction predominating. The quiescent subfraction of the wild-type culture gave a low range of fluorescent values similar to both experiments performed with whole-culture samples and the negative control, as may be expected as this subfraction forms the bulk of the population. The non-quiescent subfraction, however, produced a range of fluorescent values not significantly lower than that recorded for the DNase I positive control and the *snf1Δ* whole-culture (**Figure 27b**). This highly responsive subfraction represents only a small proportion of the total culture and so is difficult to detect in experiments performed with heterogeneous whole culture. This result suggests that the non-quiescent subpopulation of the wild-type culture at intermediate chronological age has undergone considerable genomic fragmentation. It is hypothesised that this represents apoptosis-like events occurring in this subpopulation leading to the loss of viability over the course of chronological ageing in these cells. Re-emergence of this subpopulation at advanced chronological age is therefore expected to be linked to higher genomic instability and loss of viability. As would be expected, the isolated non-quiescent fraction of the *snf1Δ* culture exhibited fluorescence signal as high as the bulk culture, which it effectively constitutes (**Figure 27c**).

5.4 Quiescence in putative rDNA maintenance mutants *sir2Δ* and *ydr026cΔ*

Following the development of this assay for culture subpopulation differentiation and genomic fragmentation over chronological lifespan, the system was applied to the putative rDNA maintenance mutants *ydr026cΔ* and *sir2Δ* found to exhibit chronological ageing phenotypes. Rich medium cultures of wild-type, *ydr026cΔ*, *sir2Δ* and double mutant *ydr026cΔ sir2Δ* cells were inoculated and culture subpopulation emergence over the ageing timecourse monitored by percoll gradient equilibrium centrifugation (**Figure 28a**). All four strains showed exclusively low-density non-quiescent subfractions during exponential phase growth (4 hours) and all demonstrated complete transition to high-density quiescent subfraction following the diauxic shift. This suggests that the short lived strains *sir2Δ* and *ydr026cΔ sir2Δ* do not entirely fail to produce a quiescent fraction in the same way as *snf1Δ*. However, relatively early in the timecourse (day 4) both of these strains show re-emergence of the non-quiescent low-density subfraction when the wild-type and *ydr026cΔ* mutant shows very low levels of this subpopulation. By day 6 this non-quiescent subfraction exists in roughly equal ratio to the dense, quiescent subfraction. Only much later in the timecourse do the wild-type and *ydr026cΔ* strains show significant re-emergence of the non-quiescent subpopulation. At day 18, the wild-type culture has accumulated a considerable non-quiescent subfraction, while the long-lived *ydr026cΔ* strain lags partially behind (**Figure 28b**).

Samples were purified from the quiescent and non-quiescent fractions for each of these strains throughout the ageing timecourse and the morphology of the cells comprising these fractions recorded. As before, logarithmically growing wild-type cells were found to be small and highly budded. Following the diauxic shift, the quiescent fraction of the wild-type culture consisted of larger, unbudded, thick walled cells of high density; the non-

quiescent fraction consisted of smaller, highly budded cells. Over the course of chronological ageing, cells of the quiescent fraction were found to slowly increase in size, wall thickness and vacuole volume while remaining stably unbudded until late in the timecourse. Cells of the non-quiescent fraction remained small and highly budded, and after day 6 began to show some evidence of degradation of cell walls and release of vacuole contents. Late in the timecourse, cells of the quiescent fraction were found to re-exhibit budding, correlating with the re-emergence of the non-quiescent fraction in the wild-type strain (**Figure 29a-b**).

Cells isolated from the subfractions of the ageing *sir2Δ* and *ydr026cΔ sir2Δ* cultures demonstrated markedly different morphology from the wild-type. Logarithmically growing cells were small and highly budded, as expected. However, cells extracted from the dense subpopulation following the diauxic shift were found to be relatively small and also highly budded. Over the course of chronological ageing, cells of the denser fraction became larger and acquired larger vacuoles (but not to the same extent as wild-type cells of equivalent fraction), but remained highly budded. Cells of the abundant non-dense fraction were also found to have an highly unusual morphology. From early in the timecourse these cells were found to exhibit features characteristic of pseudohyphal growth, becoming very large and generating long cylindrical extensions. These properties persisted throughout the ageing timecourse (**Figure 29a-b**).

The long-lived *ydr026cΔ* strain was also found to demonstrate cell morphologies differing from that observed in ageing wild-type cells. Early in the timecourse the appearance of *ydr026cΔ* cells is similar to that of wild-type. However, at extended agepoints, when quiescence in the wild-type dense subfraction begins to fail and budded cells re-emerge, equivalent cells from the *ydr026cΔ* culture remain large, thick walled and unbudded. Additionally, as the low-density upper fraction does begin to emerge in the *ydr026cΔ*

culture at extended agepoints, cells of that fraction are less budded than that of wild-type, and generally resemble quiescent cells to a greater degree: they are much larger and less budded than wild-type, despite their low density (**Figure 29a-b**).

Quantification of the proportion of cells exhibiting budding confirmed this trend (**Figure 28c**). Following the diauxic shift, the non-quiescent subfraction of the wild-type culture maintained ~50% budded cells, while proportion of budded cells in the quiescent subfraction fell to less than 10%. At day 18 buds reappear in the dense subfraction, correlating with loss of quiescence in this subpopulation. The *ydr026cΔ* strain demonstrates significantly reduced proportion budding both in the quiescent and nonquiescent culture subfractions. The proportion budded also remains low in the dense subfraction until markedly later in the timecourse (day 28), suggesting delayed loss of quiescence in this strain. *sir2Δ* and *sir2Δ ydr026cΔ* strains show the opposite trend, with highly budded cells being abundant (>50%) in the quiescent population throughout the timecourse, suggesting a failure of entry to quiescence.

RNA was isolated from the purified ageing culture subfractions, and qPCR was performed on whole cell cDNA to assay expression levels of the quiescence marker gene *SIP18*. *SIP18* expression levels remained low in exponentially growing cells and immediately following the diauxic shift in heterogeneous whole cultures. At agepoints following this, high levels of *SIP18* expression were measured in wild-type and *ydr026cΔ* quiescent fractions, with considerably lower levels assayed in non-quiescent subfractions. Significantly lower levels of *SIP18* expression were recorded in the dense subfractions of the *sir2Δ* and *ydr026cΔ sir2Δ* mutants from day 4 onwards, suggesting incomplete entry to the quiescent state was achieved in these two strains (**Figure 28c**).

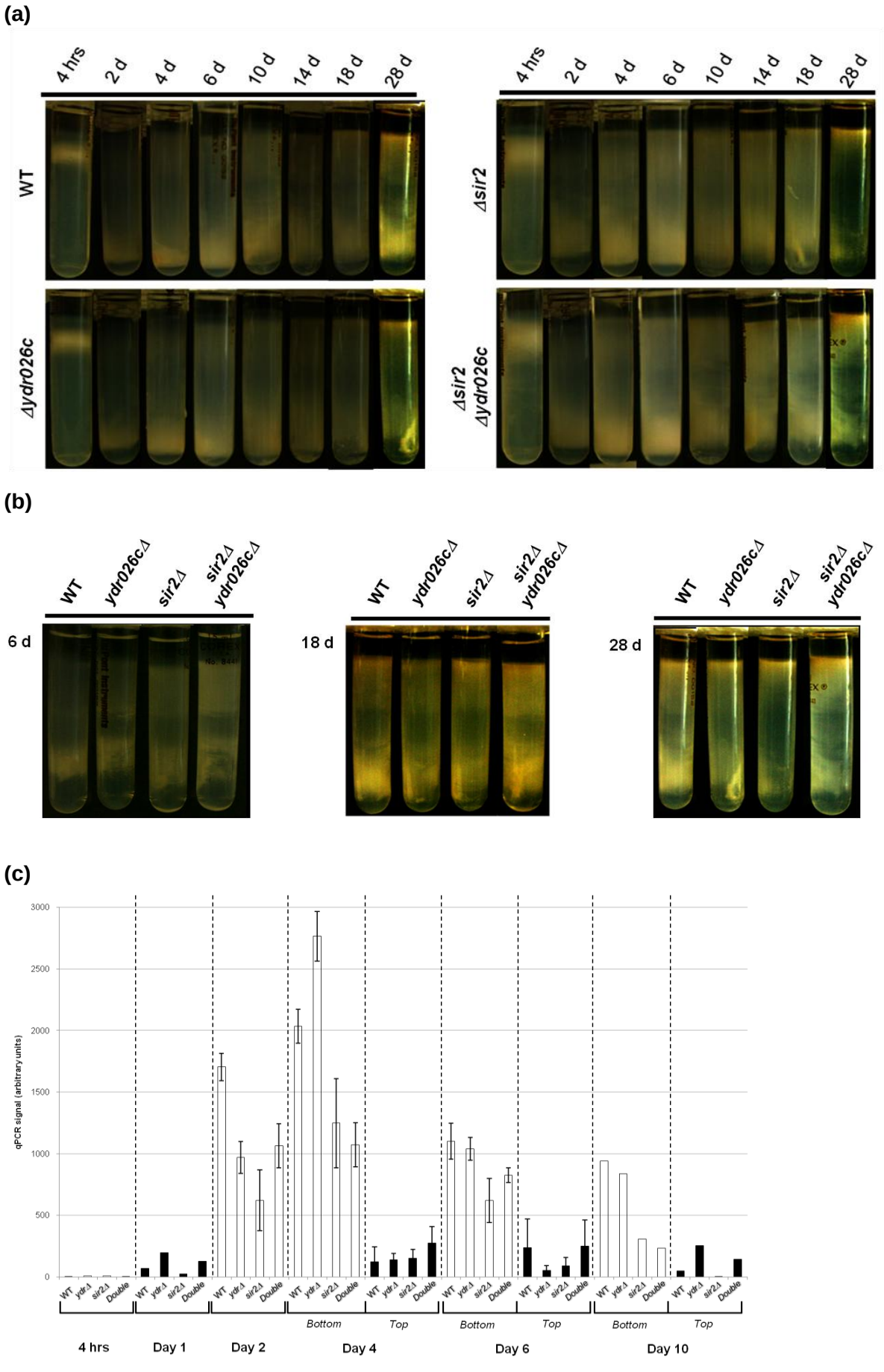
(a)
4 hrs
2 d
4 d
6 d
10 d
14 d
18 d
28 d
WT
Δydr026c
Δsir2
Δsir2 Δydr026c
(b)
WT
ydr026cΔ
sir2Δ
sir2Δ ydr026cΔ
6 d
18 d
28 d
(c)
qPCR signal (arbitrary units)
3000
2500
2000
1500
1000
500
0
WT
ydr.Δ
sir2.Δ
Double
Bottom
Top
4 hrs
Day 1
Day 2
Day 4
Day 6
Day 10

Figure 28.

Figure 28. (a) and **(b)** Culture differentiation in putative rDNA maintenance mutants. Cultures of wild-type, *ydr026cΔ*, *sir2Δ* and *sir2Δ ydr026cΔ* strains were inoculated into 250 ml rich medium and allowed to grow through the diauxic shift. At each daypoint, aliquots of cells were removed, washed, and centrifuged to density equilibrium over a percoll gradient. **(c)** Quiescence marker *SIP18* expression in respective culture subfractions. RNA was isolated from culture fractions separated on the gradients above. cDNA was prepared by reverse transcription, and transcript abundances of quiescence marker *SIP18* were determined by qPCR normalised to extracted yield of U4 cDNA. *SIP18* expression levels can be observed to rise markedly following induction of quiescence, and to be greater in the lower (quiescent) subfraction compared to the upper (non-quiescent). Levels of *SIP18* expression are also somewhat repressed in *sir2Δ* and *sir2Δ ydr026cΔ* strains, correlating with impaired maintenance of quiescent fraction in those strains.

Figure 29. Cell morphologies in **(a)** high and **(b)** low density subfractions of ageing cultures. Cells extracted from the gradients in **Figure 28Error! Reference source not found.** were investigated microscopically. Unusual morphology is rapidly visible in the *sir2Δ* and *sir2Δ ydr026cΔ* strains, correlating with impaired maintenance of the quiescent fraction in those strains. Somewhat enhanced maintenance of the unbudded quiescence phenotype is visible in the *ydr026cΔ* strain. This is borne out by **(c)** Quantification of budded cell abundance in culture subfractions over the ageing timecourse (Q = quiescent, NQ = nonquiescent).

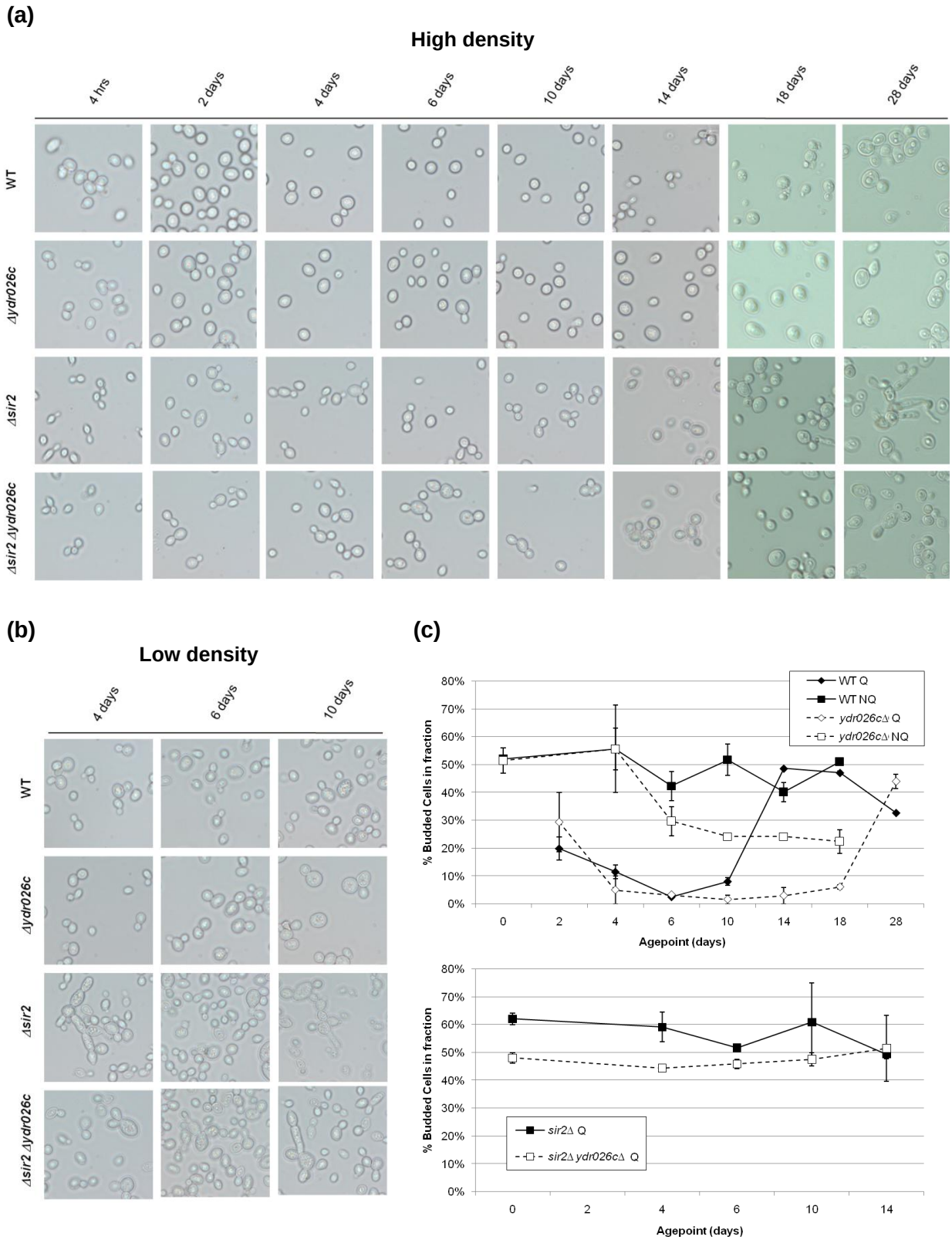

Data gathered from 3 independent replicates

Figure 29.

5.5 Genomic fragmentation in ageing *sir2Δ* and *ydr026cΔ* cultures

To investigate whether the changes in non-quiescent culture fraction re-emergence and cell morphology were associated with apoptotic-like behaviour as in the *snf1Δ* short-lived mutant, samples isolated from the quiescent and non-quiescent subpopulations of the ageing cultures of wild-type, *sir2Δ* and *ydr026cΔ sir2Δ* were subject to DNA fragmentation assay by TUNEL reaction and flow cytometry. Cells taken from wild-type and *sir2Δ* whole-cultures at intermediate agepoint (day 6) were analysed for fluorescein incorporation.

Wild-type cells showed a single peak with a comparatively small amount of recorded fluorescence. *sir2Δ* cells demonstrated a bi-modal distribution, suggesting the presence of two discrete incorporating fractions within the population. The peak corresponding with greater TUNEL activity showed significantly stronger fluorescein incorporation than the wild-type peak, as well as than the low-activity peak from the same culture. Cells taken from whole-cultures of the double mutant *ydr026cΔ sir2Δ* which has the same differentiation phenotype as the *sir2Δ* mutant were found to exhibit a similar bi-modal distribution of fluorescence (**Figure 30a**).

To determine whether the fractions identified as exhibiting different levels of DNA fragmentation corresponded to quiescent and non-quiescent culture subpopulations, cells from these subpopulations were isolated as before and subjected to TUNEL assay. Cells from the non-quiescent fraction of the wild-type culture at day 6 were found to exhibit higher levels of incorporation than whole culture, as expected (**Figure 30b**). Cells from the non-quiescent fraction of the *sir2Δ* and *ydr026cΔ* mutants were assayed as having significantly higher levels of incorporation, suggesting enhanced levels of genomic fragmentation in this subpopulation. However, cells from the quiescent fraction of these

strains exhibited the same bi-model distribution of fluorescein incorporation observed in the bulk culture (**Figure 30c**). The higher fluorescence peak is again significantly higher compared to the incorporation distribution in the wild-type quiescent fraction, and is comparable to levels observed in the non-quiescent fractions. This suggests that considerable genomic fragmentation and apoptotic-like behaviour is occurring in the denser subfractions of the *sir2Δ* and *ydr026cΔ sir2Δ* strains over chronological ageing, concomitant with the failure of this fraction to enter a stable quiescent state as demonstrated by continued budding behaviour and lower expression of *SIP18*.

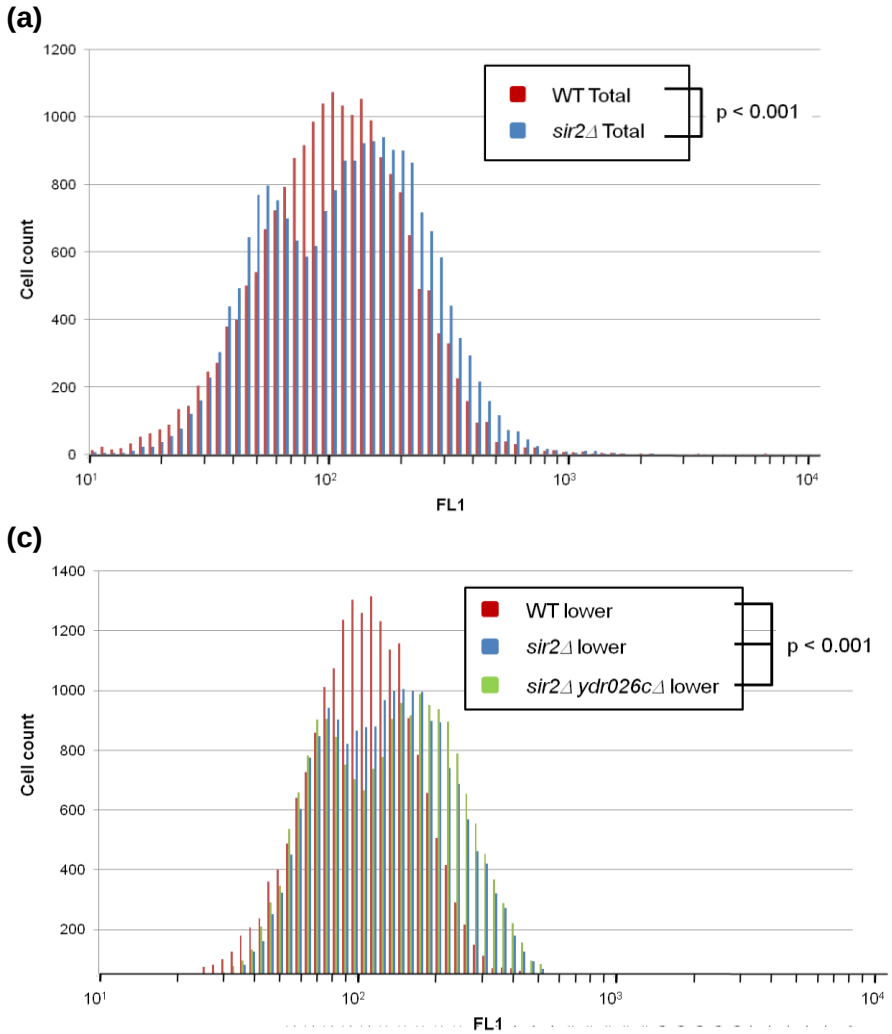

Strain subfraction	Mode FL1 (AU)
WT Upper	138.9
WT Lower	108.6
sir2Δ Upper	209.6
ydr026cΔ sir2Δ Upper	177.8
sir2Δ Lower (1)	78.1
sir2Δ Lower (2)	150.9
ydr026cΔ sir2Δ Lower (1)	75.0
ydr026cΔ sir2Δ Lower (2)	185.3

Figure 30. FACS analysis of TUNEL incorporation in 6 day old cultures of wild-type, *sir2Δ*, and *sir2Δ ydr026cΔ* mutant strains. **(a)** The *sir2Δ* strain shows exhibits a bimodal peak of fluorescein incorporation compared to wild-type. **(b)** The wild-type upper and subfraction has elevated TUNEL activity, but not the degree observed in the *sir2Δ* and *sir2Δ ydr026cΔ*. **(c)** The *sir2Δ* and *sir2Δ ydr026cΔ* lower fractions also contain a bimodal distribution, suggesting significant apoptotic activity in this usually quiescent subfraction.

5.6 Discussion

The capacity for entry and stable maintenance of a quiescent culture subpopulation has been hypothesised to underlie extended chronological lifespan in several long-lived yeast mutants (Allen et al., 2006). To investigate whether novel chronological ageing phenotypes associated with putative rDNA maintenance mutants *sir2Δ* and *ydr026cΔ* correlated with development of quiescenc7uhyghe culture subfraction, a series of assays were developed to allow the separation, purification and analysis of quiescent and non-quiescent cells from ageing cultures in rich medium. Quiescent cells purified from post-diauxic wild-type culture exhibited high density, low index of budding, large size, thickened cell walls and greatly elevated expression of quiescence marker *SIP18*. Conversely, non-quiescent cells were of low density, highly budded, and expressed the *MLH2* marker associated with non-quiescence. The *snf1Δ* mutant, previously described as being deficient in aerobic metabolism of non-fermentable substrates and failure to enter quiescence, was used to validate the capacity of the assay to isolate non-quiescent cells. The non-quiescent subpopulation of ageing yeast cultures has been shown to undergo a programme of cell death exhibiting many of the characteristics of apoptosis. An assay to measure genomic fragmentation by fluorescent end-labelling (TUNEL) was adapted for use in *S. cerevisiae* and robust quantification of this variable developed using flow cytometry. Non-quiescent subfractions of all the strains measured demonstrated markedly higher genomic fragmentation than quiescent fractions. The short lived strains *snf1Δ, sir2Δ,* and *sir2Δ ydr026cΔ* additionally demonstrated high levels of genome fragmentation in whole ageing culture and denser cell subfractions (for *sir2Δ* and *sir2Δ ydr026cΔ*).

In most regards, the Percoll equilibrium centrifugation assay developed for isolation of differentiated culture subpopulations corresponds to that described in the literature (Allen

et al., 2006). Cells isolated from dense and less-dense subfractions conform in morphology to those observed in previous studies. Marker gene expression demonstrates at least 20-fold purification of the respective subfractions away from bulk culture, and the strong phenotype of the *snf1Δ* strain recapitulates what has previously been described in this mutant: effective lack of entry to quiescence and inability to survive in post-diauxic culture (Hardie et al., 1998; De Virgilio, 2012). This evidence supports the validity of the separation technique.

Some discrepancies are present between these observations and the earlier literature describing isolation of culture density subfractions. In two wild-type backgrounds we observe almost complete transition of cultured cells from low-density during the logarithmic phase to high density following the diauxic shift at 24 hours. Allen *et al* record a somewhat slowed emergence of the denser subpopulation with a residual low density subfraction persisting throughout this process (Allen et al., 2006). In accord with our observations, this non-quiescent subfraction becomes more abundant after 4 days after inoculation. This discrepancy is likely to be due to environmental culture conditions: small changes in culture aeration (caused by, for example, different flask capacities) have been found to have a large influence on chronological longevity and so are likely to modify the dynamics of quiescence transition over the diauxic shift. More recent studies (Davidson et al., 2011) have demonstrated transition to quiescent subfraction on timescales close to those observed here (24 hours) suggesting the same process is being observed.

The yeast protein kinase B and AMP-dependent protein kinase homolog Snf1 has long been recognised as a negative regulator of glucose repression (Young et al., 2003). The *snf1Δ* mutant was one of the first identified as exhibiting defective adaptation of metabolism for aerobic respiration over the diauxic shift (Hardie et al., 1998), greatly shortened chronological lifespan, and elevated generation of longevity-reducing superoxide anions over chronological ageing (Weinberger et al., 2010). It has been hypothesised that

this leads to failure in differentiation to the quiescent state (De Virgilio, 2012). We have reproduced the strong chronological longevity phenotype in this strain, and the strong phenotype of the *snf1Δ* strain is ideal for further validation of the quiescent cell isolation and genomic fragmentation assays. Complete failure to enter quiescence does indeed appear to be demonstrated by the *snf1Δ* mutant. No dense subfraction could be recovered at any agepoint; the less-dense subfraction exhibits all the morphological characteristics of non-quiescent cells, including high degrees of budding; and quiescence marker *SIP18* expression is markedly reduced (**Error! Reference source not found.**). This appears to upport the hypothesis of failed differentiation.

A corollary to this model is the hypothesis that failure to enter to quiescence is followed by a programme of cell death leading (primarily) to apoptosis (Herker et al., 2004; Rockenfeller and Madeo, 2008). Apoptosis in *Saccharomyces cerevisiae* has previously been assayed by phosphatidylserine presence in the outer leaflet of the cell membrane, loss of mitochondrial membrane potential, and genomic fragmentation (Carmona-Gutierrez et al., 2010). By correlation with the other markers, fluorescent end-labelling of fragmented genomic DNA ends, as established in mammalian cells through the TUNEL assay has been used as a reliable identifier of apoptosis versus necrosis (Wissing et al., 2004; Buttner et al., 2006). TUNEL staining is specific to single-stranded over double-stranded breaks, which distinguish necrotic over apoptotic death in mammalian cells (Ribeiro et al., 2006). Previous studies of apoptosis in yeast have measured TUNEL staining by fluorescence microscopy which can be difficult to quantify and compare samples over a linear range. Much of the published material showing microscopy of TUNEL stained cells also indicates staining throughout the cell and not confined to the nucleus e.g. (Khan et al., 2005), suggesting a relatively late stage of genomic fragmentation (with genomic fragments leaking into cytoplasm) was being measured. To enhance the precision of this assay, flow cytometry was used to measure fluorescein-dUTP incorporation following TUNEL

treatment. This protocol has previously been used to measured genomic fragmentation in yeast in other physiological contexts (Carré and Guilloton, 1997). The model of Davidson (Davidson et al., 2011) suggests that non-quiescent cells, emerging from the diauxic shift, will suffer from metabolic insufficiency and activate a program of cell death through the post-diauxic phase. We demonstrated reproducibly greater fluorescein incorporation in less-dense, non-quiescent culture subfractions compared to the denser quiescent subfractions of wild-type cultures in mid post-diauxic growth phase, further supporting activated apoptosis in this subpopulation. Moreover, the *snf1Δ* mutant demonstrated even more greatly enhanced TUNEL incorporation, strongly suggesting activation of programmed cell death in this strain as a mechanism for its greatly reduced chronological lifespan.

Unlike the *snf1Δ* mutant, selected mutants of the TOR pathway, and SAGA/SLIK regulatory complex previously studied in our group, the chronological longevity phenotypes associated with putative rDNA maintenance mutants *sir2Δ*, *ydr026cΔ* and *sir2Δ ydr026cΔ* appear not to correlate with dysregulation of post-diauxic metabolic gene expression (section 4.7). Protein synthesis is massively (~300-fold) suppressed in quiescent cells (Boucherie, 1985) through a combination of modification of eIF2α, reduced ribosomal protein synthesis, and reduction in synthesis of mature processed rRNA (De Virgilio, 2012). Repression of ribosomal protein synthesis, reduction in the recruitment of RNA polymerase I to the 35S rDNA, induction of 35S transcription, expression of pre-rRNA processing factors, and regulation of ribosome assembly have been implicated in the suppression of ribosome biogenesis and share partial regulation by TOR signalling pathway kinase Sch9 (Claypool et al., 2004; Berger et al., 2007; Liko et al., 2007; Vanrobays et al., 2008; Singh and Tyers, 2009), mutant strains of which exhibit one of the longest observed chronological longevities (Fabrizio et al., 2001) and an unusual subpopulation phenotype whereby no quiescent subfraction is formed (unpublished work,

Mellor lab). Sir2 has long been implicated in silencing of RNA polymerase II transcription at the rDNA locus (Li et al., 2006), and Ydr026c has been shown to also regulate silencing over the spacer regions to which it putatively binds (Ha et al., 2012). A natural hypothesis is therefore whether dysregulation of rDNA expression causes failure of entry to quiescence in the *sir2Δ* and *sir2Δ ydr026cΔ* mutant strains and leads to curtailed chronological longevity. Conversely, it might be supposed that *ydr026cΔ* strains exhibit enhanced rDNA silencing, giving a more stable quiescent subpopulation and increasing longevity.

Of these mutant strains, all three produce a single, dense subfraction upon traversing the diauxic shift. However, while wild-type culture requires 6-10 days for the non-quiescent subpopulation to strongly emerge, the short lived *sir2Δ* and *sir2Δ ydr026cΔ* mutants yield this subfraction only 4 days after inoculation. Morphological inspection of the cells also suggests a failure of quiescence maintenance in this subfraction: while the cells remain dense, presumably due to trehalose accumulation, they remain highly budded. Metabolic stress is also quickly and readily apparent in the non-quiescent subpopulation of these two strains: cells exhibit morphology characteristic of pseudohyphal growth early following the post-diauxic shift, suggesting an insufficiency of nutrients, particularly nitrogen (Lengeler et al., 2000) to provide for protein synthesis. The *SIP18* marker of quiescence is also markedly less expressed in these strains. The high levels of TUNEL dye incorporation in these two strains, as well as the bimodal profile of fluorescence end-labelling in the quiescent fraction, suggests that programmed cell death occurs as early as 6 days following inoculation in both the strains and also occurs in the denser subpopulation, and that this may underlie the short chronological lifespan previously observed. The increase in density of cells entering the post-diauxic growth phase is thought to be due to the accumulation of stored nutrients, particularly trehalose (glycogen appears not to contribute to as great a degree) (Allen et al., 2006). This suggests that, while maintaining normal levels of

trehalose storage, the denser subfraction of the *sir2Δ* and *sir2Δ ydr026cΔ* mutant strains fail to properly enter quiescence and activate pathways of programmed cell death leading to early apoptosis. Metabolic failure in this case could be caused by nitrogenous nutrients becoming limiting for protein synthesis, if ribosome construction is not downregulated. This could also explain the pseudohyphal type failure observed in the non-quiescent fraction (and which is eventually observed in the denser fraction as well). The converse phenomenon has been observed in the *sch9Δ* mutant in previous experiments carried out by our group: this strain produced only a low-density subpopulation following the diauxic shift, but has a reduced rate of apoptosis (Madia et al., 2009) and has a very long chronological lifespan. This suggests that a failure to achieve high density through carbohydrate storage is not a barrier to stationary phase survival: and that reduced metabolism requirements during this phase (as in caloric restriction) promotes chronological longevity.

The *ydr026cΔ* mutant, in contrast, has a long chronological lifespan. This strain appears to have somewhat enhanced quiescence maintenance: the emergence of the non-quiescent subfraction occurs strongly at day 18 post-inoculation in the wild-type strain, but not until day 28 when *YDR026C* is deleted. This difference is more striking in the maintenance of quiescent cell morphology in the *ydr026cΔ* mutant. Large, thick walled, large vacuoled, unbudded cells are maintained in the quiescent fraction of the *ydr026cΔ* mutant for 28 days post-inoculation, when the wild-type strain experiences a general failure of quiescence at 14 days, with budding re-emerging and many smaller daughter cells evident. Moreover, the non-quiescent fraction of *ydr026cΔ* appears to demonstrate enhanced survival in post-diauxic culture above wild-type: the cells are larger, significantly less budded, and despite their depletion of dense stored carbohydrates appear to remain at least partially quiescent. If *ydr026cΔ* mutants exhibit enhanced suppression of ribosome biogenesis following the

diauxic shift, then even in the event of depletion of stored trehalose then quiescence will be maintained by reduced protein synthesis.

As for the chronological longevity phenotype, *sir2Δ* shows epistasis over *ydr026cΔ* in quiescence maintenance. Generally this suggests that both mutations operate in the same regulatory pathways. Because of the time-dependent nature of the chronological ageing and culture phenotypes, however, it is possible that disruption of Sir2 function causes an early failure in chronological ageing, masking later events that would demonstrate a *ydr026cΔ* phenotype. While it is challenging to separate these two interpretations, the quiescence differentiation data for *sir2Δ* and *sir2Δ ydr026cΔ* mutants suggests a common pathway. The continued transition of culture subpopulations in the *sir2Δ* mutant from day 10-28 suggests (a proportion of) the initially denser fraction cells remain metabolically viable and are depleting their dense stored carbohydrates. The existence of viable cells at this agepoint should make influence of the *ydr026cΔ* phenotype detectable, whether in the persistence of denser subfraction or the morphology of quiescent and non-quiescent cells – neither of these appears to be the case. Hence, competing influences over regulation of the rDNA is hypothesised to be the underlying mechanism in both mutants.

These data further support a novel role for the *SIR2* and *YDR026C* genes in the regulation of chronological longevity, and due to the respective established and putative roles at the rDNA of the two gene products (Gottlieb and Esposito, 1989; Ha et al., 2012), suggest dysregulation of the rDNA may represent a new mechanism controlling chronological senescence in this system through establishment of the stable quiescent state observed as cells pass through the diauxic shift. The *sir2Δ* mutant exhibits a marked phenotype of failure to maintain quiescence and loss of its culture subfraction, leading to re-entry to the cell cycle and genomic fragmentation, suggesting apoptotic or necrotic cell death relatively early in the ageing timecourse. Some evidence exists for enhanced maintenance of

quiescence in the *ydr026cΔ* mutant at the end of the timecourse; and *ydr026cΔ* cells maintain non-budded quiescent morphology for longer than the wild-type controls, suggesting quiescence maintenance also has a role in the long-lived phenotype observed in this strain.

6 Replicative longevity

6.1 Introduction

Replicative lifespan – the median number of daughters a dividing mother cell can produce before failure of reproductive viability (Bitterman et al., 2003) – has traditionally been the dominant way in which *Saccharomyces cerevisiae* have been used as a model of ageing and senescence. The observation that each yeast mother cell can produce only a finite number of offspring is over 60 years old (Barton, 1950). Soon after these observations the Gompertz-type kinetics of yeast replicative viability loss (Gompertz, 1825) – producing a characteristic sigmasoid mortality curve – was suggested to represent a form of senescence and ageing analogous to that in higher organisms. The limit of replicative capacity did not seem to be limited by the surface of the mother cell available for budding: temporarily blocking the cell cycle to increase cell size has no effect upon replicative longevity (Kennedy et al., 1994). Extending this analogy was the observation of similar replicative limit (*Hayflick limit*) experienced by many lines of untransformed mammalian cells in culture (Hayflick and Moorhead, 1961; Kuilman et al., 2010). The ability of tumour-derived mammalian cultured cells to transgress this replicative senescence barrier was seen as a demonstration of the organismal opposition of cancer formation and ageing – where senescence is a mechanism to suppress transformation (Campisi, 1997). While many of the specific ageing-associated diseases in humans appear to occur primarily in post-mitotic tissue (e.g. neurodegeneration), loss of replicative potential, particularly of stem cells, may underlie more general degradation in physiological function with ageing, for example in wound healing (Campisi, 2000).

The acceptance of a microbial model of mammalian senescence (see section 1.9) and the adoption of yeast replicative ageing as a highly tractable system for genetic investigation into the underlying mechanisms of ageing has led to the discovery of numerous interventions sharing considerable commonality with other models of senescence (**Figure 31**).

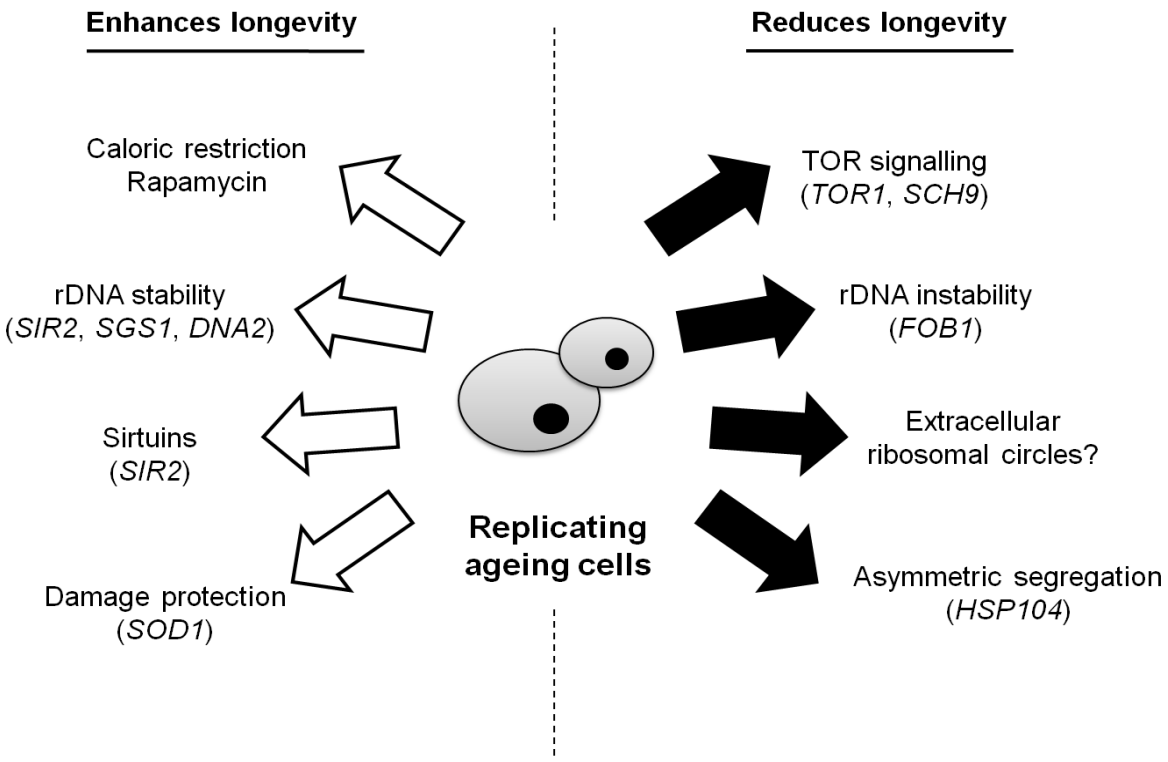

Figure 31. Documented environmental and genetic interventions extending and reducing replicative longevity in *Saccharomyces cerevisiae*. Replicative lifespan has been studied in yeast for over 50 years, during which a diverse range of modifying interventions have been discovered. The discovery that, as in most other models of senescence, calorie restriction greatly enhances replicative longevity in yeast established *S. cerevisiae* as a model system exhibiting commonly conserved senescence mechanisms. Simulating calorie restriction by TOR pathway disruption or administration of TOR-inhibiting drugs similarly enhances replicative longevity. Genomic instability, manifested by hyperrecombinogenicity at the rDNA locus, is also associated with replicative ageing and the calorie restriction effect. Factors promoting rDNA stability (*SIR2, SGS1, DNA2*) enhance replicative longevity, while those promoting recombination have the converse effect (*FOB1*). Extrachromosomal ribosomal circles (ERCs) are associated with rDNA instability, but may not represent a causal factor in replicative senescence. SIR2 modulates both genomic stability at the rDNA and other processes such as asymmetric segregation. Oxidative damage by ROS and segregation of oxidised proteins, also plays a role in the senescence process (Reverter-Branchat et al., 2004).

Following the later discovery of chronological ageing in non-replicating yeast cells (chapter 4) it was found that many of these interventions were common to the two modes of ageing, suggesting common underlying pathways of senescence regulation. Moreover, many of these interventions also readily modulate longevity in other models of senescence. Caloric restriction, the best established universal life-extending intervention, has a strong extending effect upon replicative longevity; as does disruption of TOR signalling in mutants lacking the *SCH9* and *TOR1* genes, or by treatment with the TOR-signalling inhibiting macrolide rapamycin (Lin et al., 2000; Kaeberlein et al., 2005b; Ha and Huh, 2011). Strong replicative ageing phenotypes have been found associated with strains mutant for rDNA maintenance genes *SIR2* and *FOB1*. Sir2 is a sirtuin lysine/histone deacetylase associated with silencing of RNA polymerase II-mediated transcription from several loci including the rDNA (Blander and Guarente, 2004). Sirtuin proteins and resveratrol have since been shown to have a role in longevity of worms, flies and mice, although the extent to which sirtuins mediate lifespan extension by calorie restriction is controversial (see section 1.9) (Wood et al., 2004). The maintenance of asymmetric cell division appears to be critical for replicative ageing to progress: asymmetric segregation of oxidatively damaged proteins has been shown to correlate with replicative senescence, and disruption of division asymmetry by deletion of *HSP104* can ameliorate replicative senescence in *sir2Δ* strains (Erjavec et al., 2007). Mutation of *SIR2* in *S. cerevisiae* leads to instability at the rDNA locus: high levels of recombination and repeat length variation (Gottlieb and Esposito, 1989; Kobayashi et al., 2004). Aged yeast cells experience general hyper-recombination, as measured by loss of heterozygosity (McMurray and Gottschling, 2003), and genomic instability is associated with ageing in higher organisms (Morley, 1998). Several mutants disrupting rDNA maintenance have strong replicative longevity phenotypes in yeast: longest lived is the *fob1Δ* strain, which has greatly enhanced genomic stability at the rDNA (Defossez et al., 1998). Several other rDNA maintenance genes

including *SGS1*, *UTH4*, *PUF4*, *DNA2* and *SRS2* have been implicated in regulation of replicative lifespan in yeast (Kennedy et al., 1997; Sinclair et al., 1997; McVey et al., 2001; Weitao et al., 2003). *SGS1* is the yeast homolog of the human RecQ DNA helicase WRN, mutation of which has a well established role in the human progeria Werner syndrome (Moser et al., 1999). Werner syndrome patients experience high levels of recombination-mediated genomic instability, which is suggested to underlie the progeroid condition (Cox and Faragher, 2007).

Despite the existence of these common anti-ageing interventions, replicative ageing in yeast still raises theoretical questions associated with ageing in a single-celled organism. The traditional view of replicative senescence in multicellular organisms is of suppression of tumour formation: by providing an additional barrier to replicative expansion, transformation becomes less likely. In this view, limited replicative potential in a single-celled organism is paradoxical – in direct opposition to this, if the nutrients are available (as they are in the conditions typically used to measure yeast replicative ageing) yeast seem to be finely optimised for as rapid growth as metabolically possible, presumably to crowd out other microorganisms invading their food source (Querol et al., 2003). However, this simple theory of programmed senescence in mammals as a barrier to cancer is challenged both theoretically and empirically. Modern theories of ageing (see section 1.6) dispute the existence of programmed senescence. Often cited as the best example of directed senescence, tumour suppressor p53 signalling is an important downstream mediator of replicative crisis in cultured mammalian cells (Artandi and Attardi, 2005). Original experiments demonstrated high level overexpression of p53 in mice reduces tumour incidence while increasing physiological senescence (Tyner et al., 2002) as predicted by the antagonistic hypothesis. However, physiologically the system does not appear to be so clear cut. Enhanced levels of p53 expression under physiological control in mice have been shown in more recent studies to reduce tumour incidence without additional senescence

(Garcia-Cao et al., 2002; Mendrysa et al., 2006) or even to result in mice with both extended healthy longevity and reduced tumour incidence (Matheu et al., 2007). In this system, therefore, expression of p53 has not been optimised by selection as a program of ageing – tumour suppressor behaviour is not antagonistic to longevity (Giaimo and d'Adda di Fagagna, 2012). Only under highly optimal nutrient conditions are yeast likely to reach the replicative lifespans obtainable in the laboratory – and therefore other mechanisms such as damage accumulation (Kirkwood and Austad, 2000) and pseudoprogrammed ageing (Blagosklonny, 2007a) have therefore been proposed to underlie yeast replicative senescence. If age-dependent derangement of a conserved regulatory mechanism is responsible for the decline in replicative viability, then this bolsters replicative senescence in *S. cerevisiae* as a model of ageing in general.

Despite the commonalities between replicative senescence in yeast and ageing in higher organisms, there does exist an ageing-related phenomenon that has been argued to be an idiosyncratic cause of ageing in yeast (Sinclair and Guarente, 1997). *Saccharomyces cerevisiae* contains an rDNA array of 100-200 copies of a 9.1 kb repeat. Each repeat contains a replication origin (ARS), the 35S and 5S rRNA templates, as well as a non-transcribed spacer region (**Figure 32a**). Replication proceeds bidirectionally from the ARS in the spacer region, but is arrested in one direction by the fork-blocking protein Fob1 (Kobayashi and Horiuchi, 1996). Such fork arrest creates a recombinogenic hot-spot which plays an important role in rDNA copy number maintenance and repair and also in the stability of the rDNA array (Kobayashi et al., 1998). Intercopy recombination between rDNA copies can lead to excision of one or more repeats. These are known as *extrachromosomal ribosomal circles*, or ERCs. As plasmids containing an ARS sequence but lacking a centromere, they experience asymmetric segregation upon cell division, and accumulate in mother cells (**Figure 32b**). Because of this, ERC accumulation has long been observed to correlate with replicative age (Sinclair and Guarente, 1997).

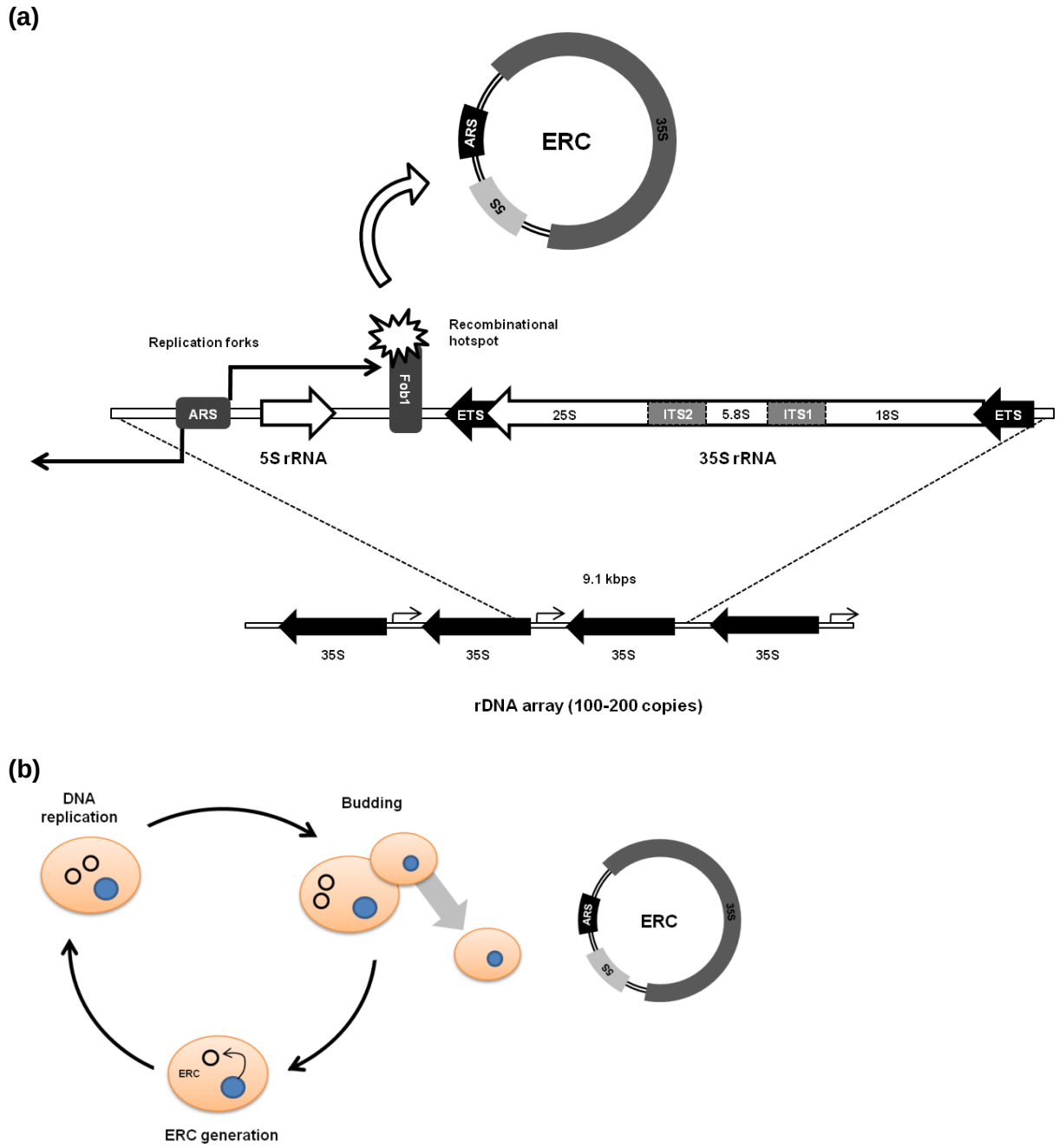

Figure 32. Replication fork blocking in the rDNA spacer region. **(a)** Each of the 100-200 copies of the chromosome XII 9.1 kb rDNA repeat contains an origin of replication (ARS) in the spacer region upstream of the main 35S RNA-polymerase I promoter. Replication initiates bidirectionally but is arrested by the fork-blocking protein Fob1 which *in vitro* and *in vivo* experiments (Mohanty and Bastia, 2004) show binds to a region just downstream of the termination site of the neighbouring 35S transcript. High frequency of stalled replication forks at this locus (the *recombination hotspot*) leads to recruitment of the repair machinery (*DNA2*) and stimulates recombination between homologous regions. Recombination between neighbouring repeats on the same chromosome can lead to excision of circles containing one or more 9.1 kb rDNA repeats. **(b)** These circles – *extrachromosomal ribosomal circles* (ERCs) – contain a replication origin but no centromere, and so are duplicated during S-phase replication but segregate asymmetrically to the mother cell upon cytokenesis. Because of this, ERCs accumulate exponentially in

mother cells over replicative ageing and it is often suggested that they contribute to replicative senescence.

Moreover, in many of the strains that modify rDNA stability and replicative age, such as *sir2Δ* and *fob1Δ*, correlate changes in ERC accumulation are observed (Kaeberlein et al., 1999). Because of this, the earliest proposed mechanisms for yeast replicative ageing was based on ERC accumulation (Defossez et al., 1998).

Because ERCs replicate upon every cell cycle revolution, but accumulate in the mother cell, they might appear to represent a biological clock that could produce replicative senescence after a predetermined number of cell divisions. ERCs would then represent an ageing factor that would eventually become toxic to the mother cells. One hypothesised mechanism for this toxicity was the sequestration of the Sir2 protein required for rDNA stability: titration of this away from the genomic rDNA repeats would lead to further genomic instability (Smith et al., 1998). Original experiments with ectopic introduction of ERCs appeared to artificially accelerate replicative ageing (Sinclair and Guarente, 1997).

However, while ERC production correlates with genomic instability at the rDNA and replicative age of mother cells in most strains, it is unclear whether this correlation represents a causative mechanism of replicative senescence. Arguing against this is more recent discovery of several different classes of mutants that exhibit modified replicative longevity without disruptions in ERC production, such as protein synthesis mutants (Heeren et al., 2009) and mutations in the *SGS1* Werner-like helicase (Heo et al., 1999). More recently, mutants which disrupt genomic stability over the rDNA and shorten replicative lifespan without accumulation of ERCs have been discovered (Hoopes et al., 2002; Merker and Klein, 2002). Age-associated genomic instability does not always correlate with ERC formation, and indeed an opposite correlation has been reported (McMurray and Gottschling, 2003; Ganley et al., 2009). Recent studies suggest that

genomic instability, accentuated at the rDNA, is the cause of both replicative senescence and the production of ERCs, which are usually diagnostic of this instability. By modifying the efficiency of the ARS replication origins in a 2-rDNA copy containing strain, mutants could be produced that accumulate widely variant numbers of ERCs (dependent upon rDNA ARS for replication) but largely similar rDNA instability. In these mutants replicative lifespans uncorrelated with ERC accumulation were measured (Ganley et al., 2009).

The ERCs used in the ectopic accumulation experiments, unlike natural ERCs, did not contain a replication origin and it has since been found that general accumulation of these types of plasmid shorten replicative lifespan (Laun et al., 2007). *fob1Δ* mutants have virtually undetectable ERC levels, but finitely extended replicative lifespans (Defossez et al., 1999). This suggests that ERCs, while a marker of rDNA instability and replicative ageing in most strains, are a symptom rather than a cause of the chromosomal instability that underlies replicative ageing in yeast. Moreover, *S. cerevisiae* also contain other self-replicating DNA circles resulting from genomic instability and derived from the telomeres (Horowitz and Haber, 1985); and mammalian cells have been found to contain extrachromosomal self-replicating minicircles from the rDNA (Cohen et al., 2010). Hence, while the accumulation of ERCs may be idiosyncratic to ageing yeast mother cells, the similar response of the conserved underlying senescence mechanism to common interventions suggests that yeast replicative longevity remains a useful model of senescence in higher organisms.

While the physiological conditions of yeast undergoing replicative and chronological ageing are quite distinct, there appears to exist considerable overlap between the mechanisms modulating longevity in both domains. Lifespan – and healthspan – in animals is probably determined by a combination of both types of senescence: chronological for post-mitotic, long-lived tissues such as neurones; replicative for regenerating tissues (e.g.

stem cells and fibroblasts) (Kuilman et al., 2010). If senescence is not the result of inevitable accumulation of physical damage then the common selective pressure driving regulatory biological pathways are likely to impact both modes of ageing in similar ways. *Saccharomyces cerevisiae* have the unique advantage of allowing the isolated study of each mode of ageing independently under conditions physiologically normal for the model organism. Interplay between the two forms of ageing in yeast as a model is shown by many anti-ageing interventions. Calorie restriction is a potent intervention in both forms of senescence, and simulation of this through disruption of TOR signalling extends both replicative and chronological lifespan (Kaeberlein et al., 2007); while inhibiting the pathway through the drug rapamycin has been shown to have similar effects (Kamada et al., 2004; Ha and Huh, 2011). While *FOB1* deletion only has an effect upon replicative longevity, *sir2Δ* strains are well characterised in producing reduced replicative longevity while conflicting results have been reported upon chronological senescence (Fabrizio et al., 2005). Additionally, mutations affecting autophagy and apoptosis have been found to play a role in both modes of ageing (Alvers et al., 2009b; Morselli et al., 2009). Moreover, ageing in one domain can influence the other: virgin cells which have accrued chronological age in stationary phase have dramatically reduced replicative longevity (Ashrafi et al., 1999). In a *pseudoprogrammed* model of ageing – where both replicative and chronological senescence occurs as a result of normally healthy pathways becoming dysfunctional, such observations become explicable: common regulators of growth and development become, effectively, regulators of longevity.

6.2 Replicative ageing phenotypes in putative rDNA maintenance mutants

Replicative lifespans are defined in *S. cerevisiae* as the number of daughter cells an individual viable mother cell can produce before succumbing to replicative senescence and ceasing to bud. Although a number of morphological changes accompany replicative ageing such as an increase in cell size and thickening of the cell wall, traditionally the most accurate method for measurement of replicative longevity of different strains is microdissection removal of the buds from mother cells growing on rich medium plates using a micromanipulator. Individual plating of >25 mother cells and recording the generation when replicative senescence is reached yields a viability curve, typically giving a median replicative lifespan (RLS) of around 20 generations for wild-type strains. Statistical comparisons can be made between such viability curves using the log-rank test, which is well established for non-parametric comparison of discrete censored data (Bland and Altman, 2004), and can establish strains as possessing enhanced or shortened replicative lifespans.

rDNA maintenance mutants have long been associated with an array of strong replicative longevity phenotypes. The *fob1Δ* mutant is well established as a paradigm of replicative life extension, while the *sir2Δ* mutant is well recognised as being strongly short-lived (Defossez et al., 1999; Kaeberlein et al., 1999). Because of the hypothesised role of *YDR026C* in rDNA maintenance (Ha et al., 2012) and the consistent enhancement in chronological lifespan of the null *ydr026cΔ* mutant, as well as the epistasis with *sir2Δ* in these experiments (**Figure 15**), a series of experiments were carried out to investigate whether a replicative ageing phenotype was also associated with the *ydr026cΔ* mutant.

(a)

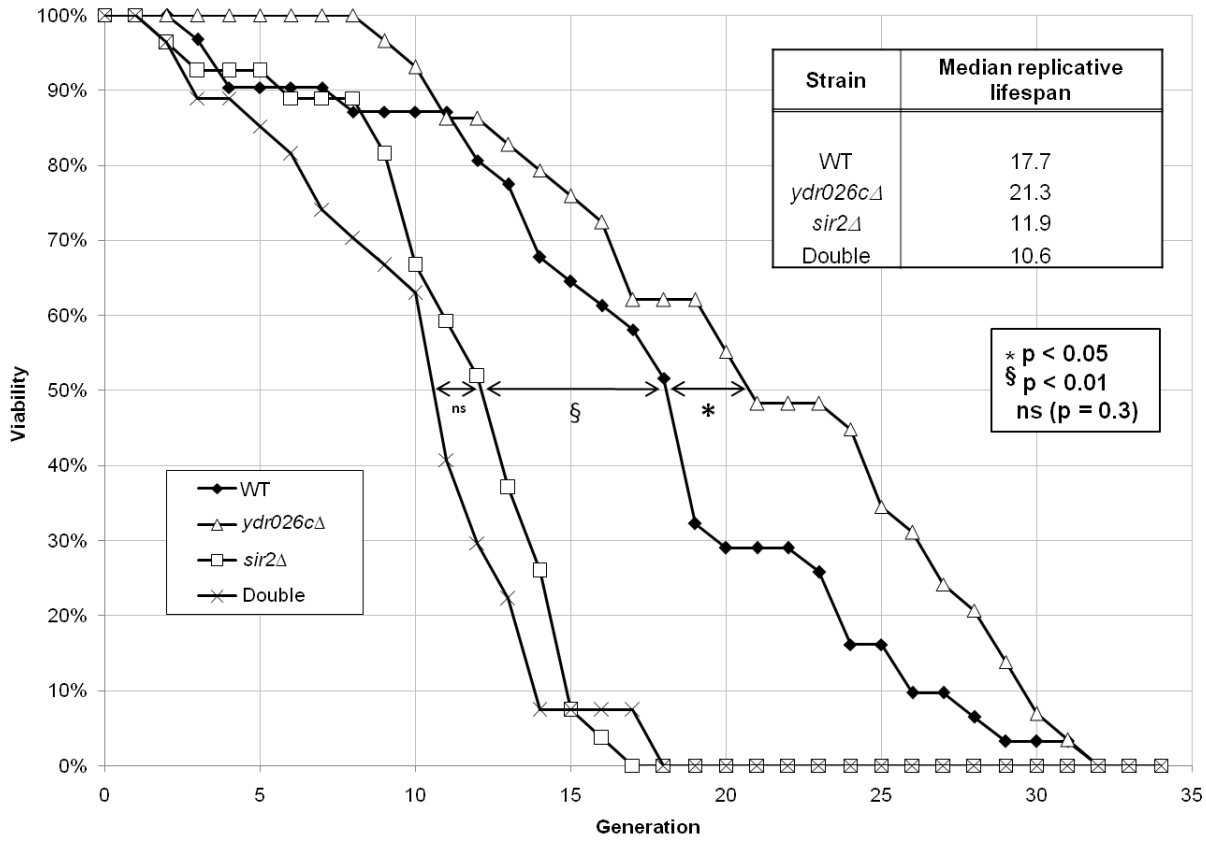

Figure 33. Replicative lifespans of wild-type, *ydr026cΔ, sir2Δ* and *sir2Δ ydr026cΔ* strains measured by microdissection. **(a)** n > 27 individual virgin mother cells of each strain were plated onto rich medium using a micromanipulator. Cells were inspected every 90 minutes and new daughters removed by microdissection. Cells which had failed to produce any daughters for three contiguous inspections were deemed to have succumbed to replicative senescence and were censored. *ydr026cΔ* cells were found to have a moderate and significant ($p < 0.05$) increase in replicative lifespan compared to wild-type (21.3 generations over 17.7 generations). As previously reported, *sir2Δ* cells demonstrated a marked and significant reduction in replicative lifespan compared to wild-type (11.9 generations, $p < 0.01$). The double mutant *sir2Δ ydr026cΔ* was found to have a short replicative lifespan comparable to the *sir2Δ* mutant (10.6 generations, not significantly different). Statistical comparisons were made using the log-rank test for mortality; median replicative lifespans were calculated by using linear interpolation of mean-smoothed viability curve data at 50% replicative viability.

Replicative lifespan was measured by microdissection of wild-type, *ydr026cΔ*, replicatively short-lived strain *sir2Δ,* and the double null mutant *ydr026cΔ sir2Δ* cells on rich media plates. Daughters produced were recorded and cells censored once no daughters had been produced for the usual time taken to allow two generations (270 mins). Viability curves and median replicative lifespans were calculated (**Figure 33**). The *sir2Δ* mutant, as previously reported (Kaeberlein et al., 1999), was found to be strongly and significantly short-lived compared to wild-type with a median replicative lifespan of 11.9 generations below the wild-type of 17.7 generations (significant to $p<0.01$). However, the *ydr026cΔ* mutant was found to be moderately and consistently longer-lived with respect to wild-type: median replicative lifespan was 21.3 generations (significant over WT to $p<0.05$). The double null mutant *ydr026cΔ sir2Δ* demonstrated a viability loss similar to the *sir2Δ* single mutant strain, with a median lifespan of 10.6 generations, not significantly different from that measured for *sir2Δ* ($p = 0.3$). Hence, the *ydr026cΔ* mutant was found to be replicatively as well as chronologically long-lived. The epistasis with *sir2Δ* also remained the same, with mutants lacking *SIR2* being short lived in both domains of ageing.

6.3 rDNA recombinogenicity

One of the major correlates of replicative lifespan is stability and maintenance of the rDNA array (McMurray and Gottschling, 2004). The repeated array of 100-200 9.1 kb rDNA repeats on chromosome XII is highly recombinogenic, with a large proportion of recombination activity dependent upon replication fork blocking by Fob1 near the replication origin in the rDNA spacer regions. Recombination between neighbouring repeats at this locus can lead to excision of rDNA repeats as exogenous circles – these extrachromosomal rDNA circles (ERCs) correlate with replicative age, and have been

hypothesised to be one contributing cause of replicative senescence in *S. cerevisiae* (Defossez et al., 1998), although other replicative lifespan mutants have been identified where replicative senescence is either independent of ERC formation or where ERC formation is a marker of rDNA degeneration rather than the underlying driver of senescence (Merker and Klein, 2002; Ganley et al., 2009). The *sir2Δ* mutant experiences strong transcription desilencing in the rDNA cassette and spacer regions, and this correlates with greatly enhanced rates of recombination between rDNA repeats (Gottlieb and Esposito, 1989).

Recombination rates at the rDNA hotspot locus in yeast can be assayed by the rate of loss of a marker cassette integrated into one rDNA copy in the array. The *ADE2* gene is a convenient marker for this purpose, as on medium containing appropriate amounts of adenine, ADE^+ cells produce white colonies, while ADE^- cells accumulate the purine biosynthesis intermediate phosphoribosylaminoimidazole which polymerises and leads to intensely red-coloured colonies. Loss of the *ADE2* marker, reversion to the ADE^- phenotype, and appearance of red colonies, is therefore indicative of the frequency of hotspot recombination occurring at the rDNA locus. In order to produce accurate estimates of the rate of recombination for each cell division, rather than the frequency of reversion events, it is necessary to measure the occurrence of reversion events for only the initial cell division upon the seeding of each new colony. When a recombination event occurs (**Figure 34**) that leads to removal of the marked rDNA repeat from one chromatid, one of the daughters does not receive the *ADE2* marker. If the daughters remained undisturbed on the plate, the equally split geometry of the colony is maintained, and assuming equal rates of growth a heterogeneous mature colony is given, half-sectored with ADE^+ (white) and ADE^- (red) cells (**Figure 35a-b**). Conversely, if reversion occurs later in the growth of the colony, then quarter (second division), eighth (third division), sixteenth (fourth division) etc. sectored colonies can be generated, as in **Figure 35c**. In practice, the ADE^- portion of

colonies often exhibit slightly reduced fitness in colony growth due to reduced purine availability and therefore appear slightly smaller. By recording only the reversions resulting in half-colony formation and excluding from analysis pre-reverted (fully red) or smaller sectored colonies, the rate of these recombination events per cell division can be accurately measured.

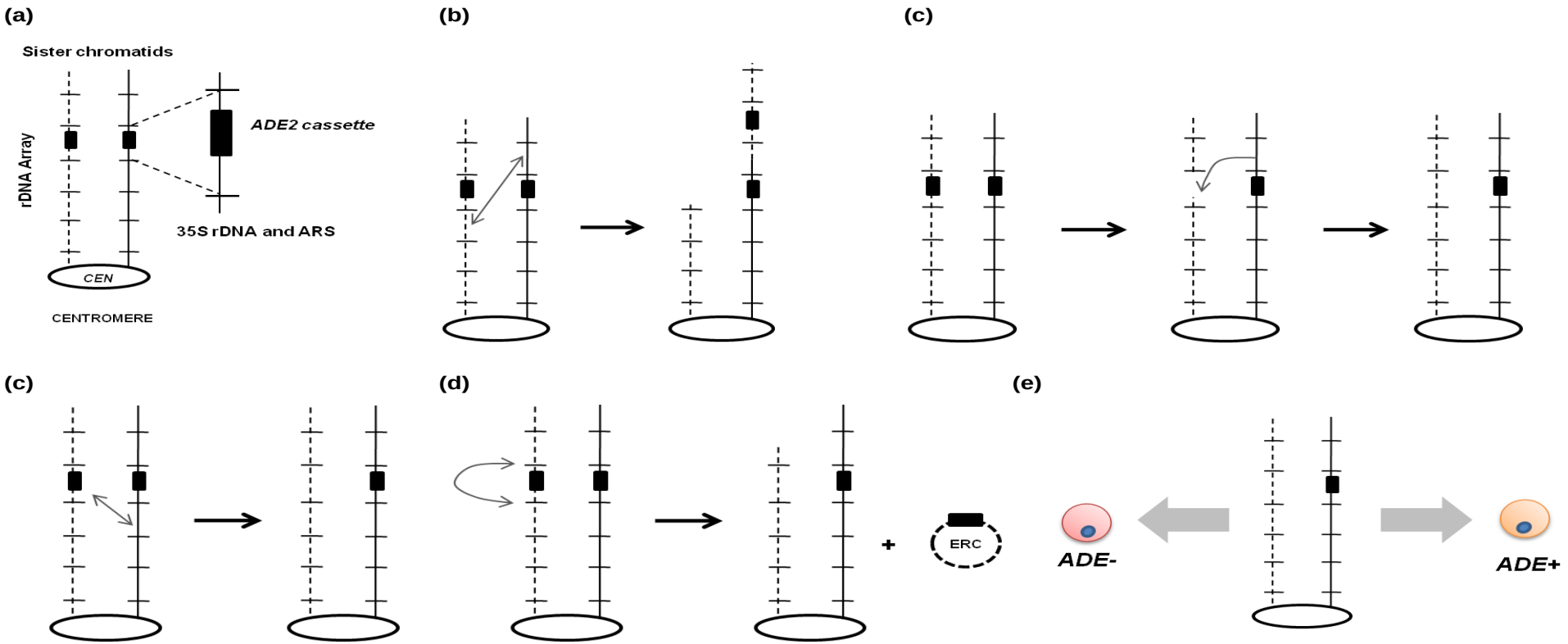

Figure 34. Modes of homologous recombination resulting in loss of the rDNA-embedded *ADE2* allele from one daughter cell **(a)** Sister chromatids of chromosome XII containing the rDNA array and one copy of an embedded *ADE2* cassette. **(b)** Unequal sister-chromatid exchange. This occurs reciprocally between two sister chromatids and results in one daughter containing two copies of the *ADE2* marker and the other none. **(c)** Single strand invasion of a non-marker containing repeat from either chromatid into the marker containing repeat leads to marker loss upon resynthesis of the repeat. **(d)** Gene conversion occurs non-reciprocally and results in loss of the marker from one chromatid. **(e)** Circle (ERC) formation occurs when neighbouring repeats recombine. The ERC will be retained in the mother: if the chromosomal marker is also then the daughter will lack the marker. **(f)** Segregation of sister chromatids to daughter cells leads to reversion to ADE$^-$ in one daughter.

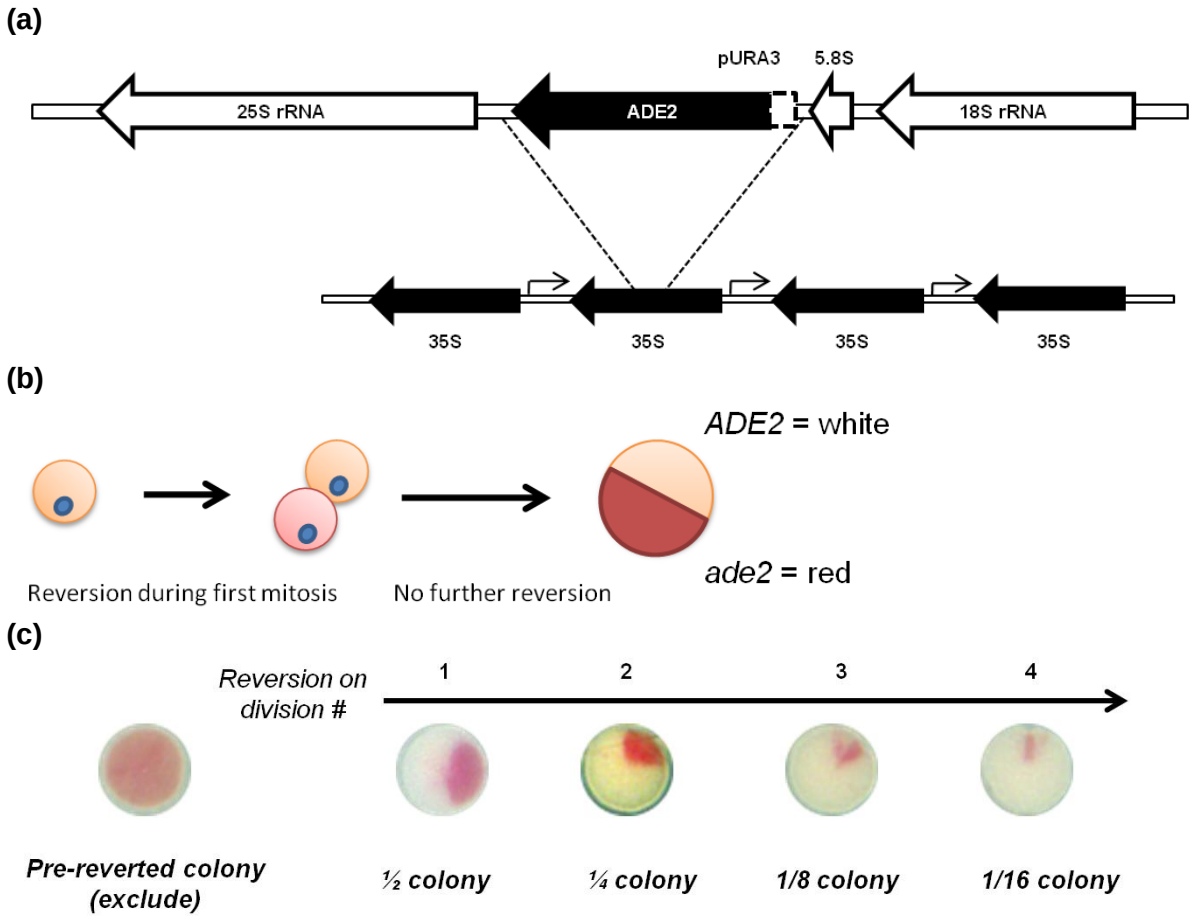

Figure 35. Assaying unequal recombination rates at the *S. cerevisiae* rDNA locus. **(a)** Recombination at a locus is most easily measured by loss of a marker cassette integrated near the region. The *ADE2* marker is convenient for this purpose in yeast, as *ade2* cells accumulate a red-pigmented intermediate of purine biosynthesis that is easily observed in plated colonies. Strain W303R consists of a *RAD5* W303 strain containing a single integrated *ADE2* marker in one rDNA repeat. The strain was constructed by integrating plasmid pDS40, containing an *S. cerevisiae ADE2* cassette following a *URA3* promoter, into W3031-A, followed by repair of the *rad5* locus by homologous recombination. The marker is integrated in the centre of one rDNA repeat following 5.8S template, in the same sense as the main rRNA transcript. **(b)** If marker loss occurs through recombination in the first cell division after cells are plated, then one daughter inherits a functional *ADE2* allele while the other becomes *ade2*. Because *S. cerevisiae* cells are largely immobile on agar plates, these daughter cells lead to growth of heterogeneous colonies half of which are *ade2* and accumulate red pigment, while the other are *ADE2* and appear white. **(c)** Precise geometric proportions of the red sector in mature colonies indicates when the recombination reversion event occurred. Half, quarter, eighth and sixteenth-sectored colonies are produced upon reversion on the first, second, third or fourth division respectively. Completely red colonies are also commonly observed in quickly recombining strains: these reverted before plating, and are excluded from any analysis. Slightly reduced fitness of the *ade2* half of the colony often lead to slightly reduced size in mature half-sectored colonies.

(a)

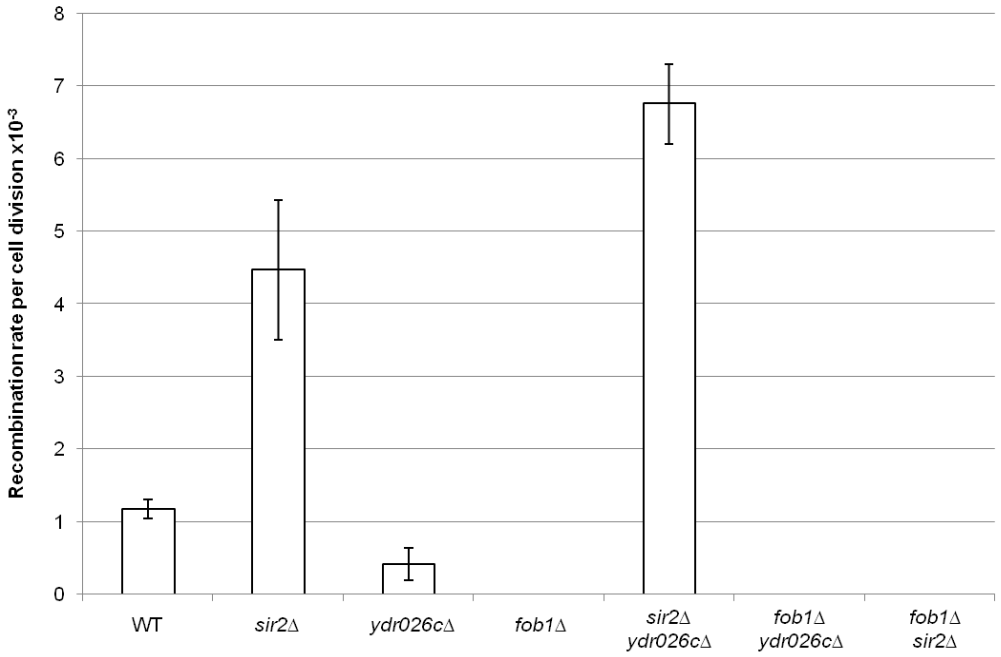

Figure 36. rDNA recombination rates as assayed by integrated *ADE2* marker loss on initial cell divisions in selected putative rDNA maintenance mutants. **(a)** Measured recombination rates for wild-type, *sir2Δ, ydr026cΔ, fob1Δ, sir2Δ ydr026cΔ, fob1Δ ydr026cΔ* and *fob1Δ sir2Δ* mutant strains in the w303 *ade2-1 RDN1-ADE2* background. Cells from logarithmic phase cultures of each strain were diluted and plated onto rich medium and colonies allowed to grow at 30^{O}C. Plates were then stored at 4^{O}C for two days to allow red pigment to accumulate. Number of half-sectored colonies were counted for >9000 total colonies for each strain to determine incidence rate per cell division. Data shown is mean of n=3 biological replicates. A recombination rate very close to that previously reported in the literature was calculated for wild-type cells ($1.1x10^{-3}$ events per division), elevated in *sir2Δ* cells ($4.4x10^{-3}$ events per division). As previously reported, *fob1Δ* cells demonstrate very low levels of recombination. In contrast, a significantly lower rate of recombination was observed in *ydr026cΔ* compared to wild-type ($0.4x10^{-3}$ events per division); but the double mutant *sir2Δ ydr026cΔ* demonstrated a recombination rate even higher than that of *sir2Δ* ($6.7x10^{-3}$ events per division), consistent with poor longevity. Double mutants of *fob1Δ* with *sir2Δ* and *ydr026cΔ* gave undetectably low recombination rates greatly resembling *fob1Δ* alone in both strains.

To investigate whether the replicative longevity phenotypes measured above correlated with differences in recombination rate at the rDNA, null mutants for *sir2Δ*, *fob1Δ*, *ydr026cΔ* and double mutants *ydr026cΔ sir2Δ* and *ydr026cΔ fob1Δ* were constructed in a strain containing a single copy of the *ADE2* marker cassette embedded in the rDNA locus.

Logarithmic phase cultures of these strains were diluted and plated onto rich medium plates, and following colony growth, the number of half-sectored red colonies recorded. Representative plates and measured recombination rates from >9000 colonies for each strain are shown in **Figure 36**. In agreement with previously published results (Kaeberlein et al., 1999; Merker and Klein, 2002), the wild-type strain demonstrated an average recombination rate of 1.1 half-colonies per 10^3 cell divisions. As expected, the *sir2Δ* mutant had a strongly and significantly elevated rate of recombination, recording 4.5 half-colonies per 10^3 cell divisions. Similarly the fork blocking mutant *fob1Δ* exhibited extremely low levels of recombination, with zero identifiable half-colonies recorded. However, the long-lived *ydr026cΔ* mutant exhibited a consistent and significant reduction in half-colony occurrence rate compared to wild-type, with 0.4 half colonies per 10^3 cell divisions measured on average. This suggests a correlation between the reduced observed recombination rate and the enhanced replicative longevity. Corresponding with this, the short-lived double mutant *ydr026cΔ sir2Δ* demonstrated a strongly elevated recombination rate of mean 6.8 half colonies per 10^3 cell divisions. The *ydr026cΔ fob1Δ* double mutant, similar to the *fob1Δ* mutant, demonstrates undetectably low rates of recombination (no colonies detected).

6.4 Extrachromosomal ribosomal circles

Generation of ERCs through recombination events between rDNA spacer regions is associated with reduced replicative longevity in a number of mutants, including the very short lived *sir2Δ* mutant (Kaeberlein et al., 1999). ERCs are generated through unequal recombination events, and persist as extrachromosomal circles containing an independent replication origin (ARS) and one or more rDNA cassettes. Common to plasmids containing an ARS but lacking a centromeric region, ERC plasmids replicate normally but demonstrate strong asymmetric segregation to the mother cells during cell divisions. This leads to their exponential accumulation in mother cells over the course of replicative ageing (**Figure 37a**).

An assay was designed for the measurement of ERC accumulation in the strains above. Whole cell DNA was gently extracted from harvested cells by removal of cell wall using yeast lytic enzyme, followed by phenol-chloroform extraction of DNA, and precipitation and washing in 70% ethanol. DNA was run on low percentage agarose 1x TAE gels for 36 hours at low voltage at $4^{O}C$. Southern blotting and hybridisation using a radiolabelled probe specific for the rDNA cassette revealed both the genomic rDNA array and satellite bands corresponding to supercoiled species of ERCs.

To test the specificity of this assay, ERC accumulation over the course of replicative ageing could be directly observed through purification of replicatively aged cells and identification of ERCs on Southern blots. Budding in *S. cerevisiae* involves completely *de novo* synthesis of new cell wall. Amino groups on the surface of mother cells can be chemically labelled using activated biotin, and this labelling is retained on the mother cell and not passed to any budded off daughters. After several cell divisions, the mother cells can be effectively purified using strepavidin-conjugated magnetic beads.

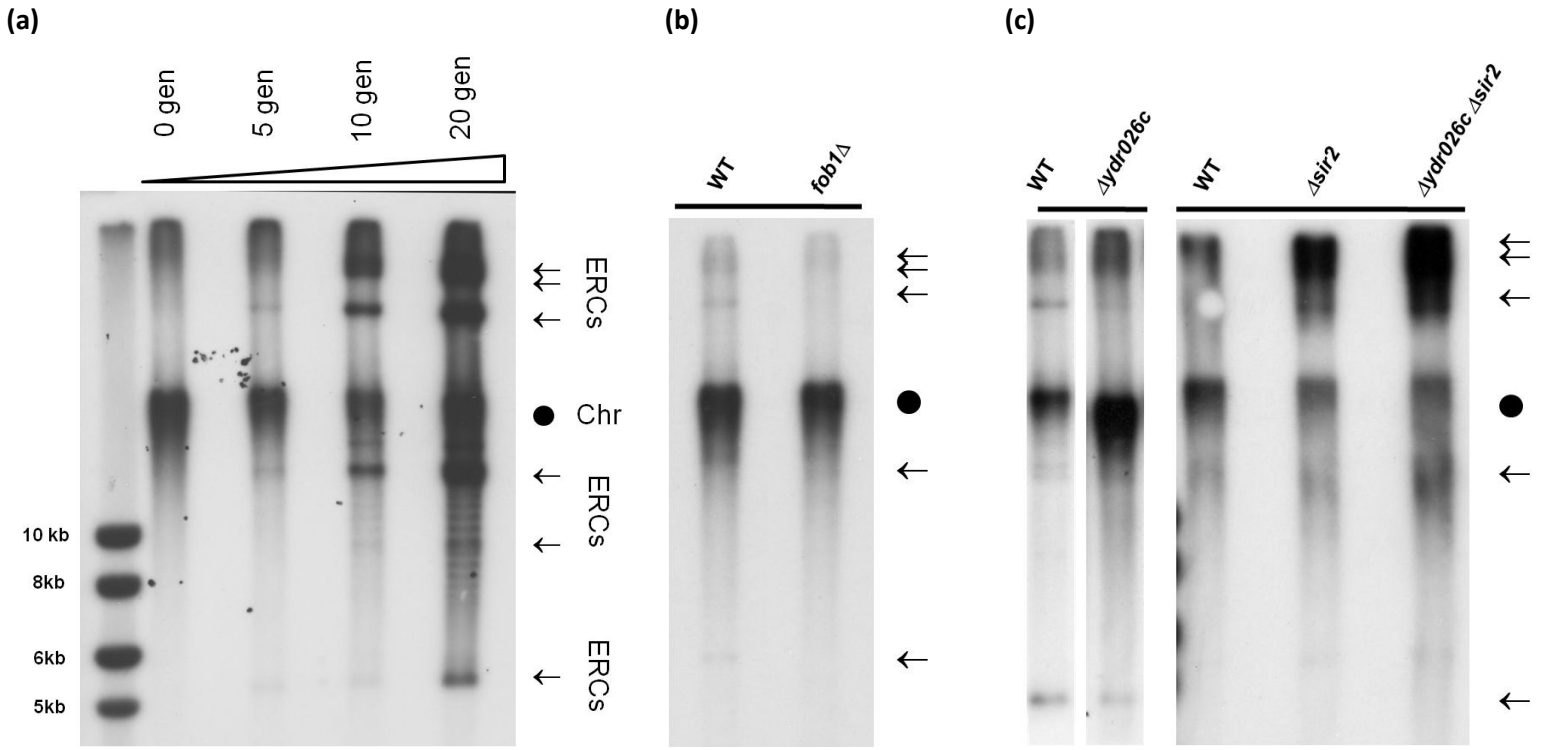

Figure 37. Generation of extrachromosomal ribosomal circles (ERCs) through recombination at the rDNA during replicative ageing. **(a)** Assay for the detection of ERCs in replicatively aged cells. Replicatively aged cells were purified by biotin labelling of mother cell walls, followed by logarithmic growth. Original mother cells could then be recovered by magnetic sorting with strepavidin conjugated iron beads. Mother cells were recovered after 0, 5, 10 and 20 generations had elapsed, the cell walls removed using yeast lytic enzyme, and DNA purified by phenol:chloroform extraction. Cellular DNA was run on low percentage TAE gels for 36 hours and Southern blotted onto neutral nylon membranes, which were hybridised with a radiolabelled probe homologous to the rDNA repeat region. Replicatively young cells (generation 0) demonstrated a broad band corresponding to the chromosomal rDNA array. Supercoiled ERC species emerge progressively over replicative ageing as tight bands above and below the chromosomal array (arrows). **(b)** Assay of ERC production in wild-type and *fob1Δ* strains in log phase culture. *fob1Δ* is well established as having a very low rDNA recombination rate and ERC accumulation. Markedly lower levels of ERCs were assayed in logarithmically growing *fob1Δ* cells than wild-type. **(c)** Assay of ERC production in log phase cultures of wild-type, *ydr026cΔ*, *sir2Δ* and *sir2Δ ydr026cΔ* strains.

A logarithmic phase culture of a wild-type strain was harvested, and the cells' surface labelled using NHS-LC-biotin. The cells were reinoculated into rich medium and incubated, and following sufficient time had elapsed to permit 5, 10 and 15 generations, an aliquot of the culture was harvested and the mother cells recovered by magnetic sorting on streptavidin-coated beads. DNA was extracted from these cells. These ERC species are detectable even in exponentially growing wild-type cultures (generation 0) but become progressively enriched in the mother cells after having undergone an increasing number of cell divisions, while the genomic rDNA array remains intensity remains constant (**Figure 37**b). This supports use of this assay in the detection of ERCs.

The *sir2Δ* and *fob1Δ* mutant strains have previously been identified as demonstrating strong ERC abundance phenotypes: *sir2Δ* strains accumulate greatly elevated levels of ERCs, and *fob1Δ* accumulate greatly reduced, in concordance with their rDNA recombination rates (Kaeberlein et al., 1999). To further test the specificity of this ERC assay, exponentially growing cultures of wild-type, *sir2Δ* and *fob1Δ* strains in rich medium were harvested, DNA extracted, and Southern blots prepared to indicate accumulation of ERC species (**Figure 37b-c**). ERC abundance levels were quantified using phosphorimaging and normalised to the genomic rDNA band. As previously reported, *sir2Δ* strains demonstrated strongly enhanced levels of ERC accumulation compared to wild-type, correlating with their elevated rDNA recombination rate. Conversely, the *fob1Δ* mutant produces a very low incidence of ERCs.

To investigate whether the differing unequal recombination rates measured for the *ydr026cΔ*, *ydr026cΔ sir2Δ*, and *ydr026cΔ fob1Δ* strains also lead to differing levels of ERC generation, the ERC assay was performed on logarithmic phase cultures of these strains (**Figure 37b-c**). Concordant with the low recombination rate observed in the *ydr026cΔ* mutant, reduced levels of ERC accumulation were measured in this strain. Similarly, the

ydr026cΔ sir2Δ strain appears to have a recombination rate comparable or higher than *sir2Δ*, and ERC accumulation is seen to be highly elevated in this strain. As would be expected, the *ydr026cΔ fob1Δ* strain, which lacks rDNA replication fork-blocking activity, demonstrated very low levels of detectable ERCs.

6.5 Discussion

Replicative senescence was the first form of ageing to be discovered in *Saccharomyces cerevisiae* and, as such, for many years constituted the most important use of yeast as a model system to test interventions into ageing (MacLean et al., 2001). The discovery of chronological ageing in this microbial system has lead to a readjustment of research focus, and many of the interventions earlier discovered to modify replicative longevity have similar effects on chronological ageing, suggesting significant crosstalk between regulatory pathways. These include calorie restriction, TOR signalling, and autophagy/damage response (Kaeberlein et al., 2007). Much evidence exists for a strong association between replicative longevity in yeast and genomic stability at the rDNA locus. While some rDNA maintenance mutants with strong replicative longevity phenotypes do not have strong chronological ageing phenotyepes (e.g. *fob1Δ* strains), others – including strains mutant for the lysine deacetylase Sir2 – have effects in both domains of ageing (Fabrizio et al., 2005).

The discovery of the novel chronological ageing phenotype of strains mutant for the largely uncharacterised *YDR026C* gene (**Figure 15**) – combined with the lines of evidence indicating a nucleolar function for the Ydr026c protein, implying a role in rDNA maintenance (**Figure 21**, (Ha et al., 2012)) – suggested an investigation into the replicative longevity of strains mutant for this gene. The consensus binding site of Ydr026c characterised by ChIP-on-chip experiments suggests complete inverted binding sites flank the rDNA cassette; yeast two-hybrid and immunoprecipitation experiments indicate association of Ydr026c and nucleolar factors such as Fob1 and the RENT complex; GFP-tagged Ydr026c localises to the nucleolus; and most recently, direct ChIP evidence of association of Ydr026c to the putative rDNA spacer region binding sites has been obtained (Huh et al., 2003; Harbison et al., 2004; Mohanty and Bastia, 2004; Ha et al., 2012).

Measurement of the replicative survival of wild-type, *sir2Δ*, *ydr026cΔ* and *sir2Δ ydr026cΔ* strains recapitulated the very short replicative lifespan of strains mutant for *SIR2*. The double mutant *sir2Δ ydr026cΔ* was also found to be short lived, statistically indistinguishable from the *sir2Δ* mutant strain. However, contrary to one recent study (Ha et al., 2012), strains missing *YDR026C* in the BY4741 background were found to be consistently, and statistically significantly, longer lived than wild-type throughout the replicative ageing timecourse. The replicative longevity phenotype of the *ydr026cΔ* mutant therefore appears to follow the same epistatic relationship to *sir2Δ* mutants as the chronological longevity phenotype: deletion of *SIR2* being a downstream, or chronologically earlier, modulator of the regulatory pathway.

The recent work of Ha *et al* (Ha et al., 2012) presented a small (but significant) *loss* of replicative lifespan in the *ydr026cΔ* strain compared to wild-type. Interestingly, these experiments were performed in a different background derived from W303. Original W303 backgrounds lack the repair helicase gene *RAD5*, and this may impact the rate of rDNA repeat recombination and possibly replicative longevity (Gangavarapu et al., 2011).

Initial research into the influence of genomic stability at the rDNA over replicative senescence appeared to indicate that the generation, and accumulation, of ERC species in ageing mother cells was the causative pathway of loss of replicative viability (Sinclair and Guarente, 1997). While the correlation between ERC accumulation and replicative lifespan is generally linear, as discussed in the Introduction, several lines of evidence now point to ERCs as diagnostic of genomic instability over replicative ageing, and not the causal agent (Ganley et al., 2009). Genomic instability at the rDNA spacer region is, in some instances, a better indication of maintenance of genomic stability at that locus over the ageing timecourse.

To investigate whether the long replicative lifespan observed in the *ydr026cΔ* mutant would translate to reduced recombination rates at the rDNA spacer region recombination hotspot, and to further test the conflicting results observed in the BY4741 and W303 strain backgrounds, a series of experiments were performed to assay unequal recombination events at the rDNA locus leading to loss of an embedded *ADE2* marker. These results demonstrated that strains mutant for *YDR026C* experience a considerable and significant reduction in the production of half-sectored colony revertants, and hence unequal recombination events at the marked rDNA locus. *sir2Δ* strains demonstrate greatly enhanced rates of recombination, while the rate of recombination in *fob1Δ* mutants is very low, as previously reported (Kaeberlein et al., 1999). To definitively determine the epistasis between *sir2Δ* and *fob1Δ* mutations on the rDNA recombination phenotype, the unequal recombination frequency of a *sir2Δ fob1Δ* double mutant was measured, and found to be very low. As might be expected from this epistasis pattern, double mutants for *fob1Δ ydr026cΔ* demonstrated lower rates of rDNA recombination than in strains mutant for *ydr026cΔ* alone, suggesting functional Fob1 is required for detectable operation of this rDNA recombination hotspot.

rDNA spacer region recombination frequency often correlates with the production of extrachromosomal rDNA circles, even in unaged cells. The abundance of ERCs in wild-type, *fob1Δ, sir2Δ, ydr026cΔ,* and *sir2Δ ydr026cΔ* strains was assayed. As previously reported (Kaeberlein et al., 1999), *sir2Δ* and *fob1Δ* strains contain greatly elevated and reduced accumulations of ERC species respectively. Supporting the observation of a reduced recombination rate in the *ydr026cΔ* strain, low ERC abundance was demonstrated in extracts prepared from this mutant. Following the epistasis with the *sir2Δ* mutant, a *sir2Δ ydr026cΔ* strain contained levels of ERCs comparable with the *sir2Δ* strain alone.

These results suggest that the extended replicative longevity phenotype of mutants lacking *YDR026C* correlates with reduced rDNA hotspot recombination and ERC production, and that this effect is epistatic to the *sir2Δ* mutation. There is some ambiguity in the literature with regards to the epistasis of the *sir2Δ* and *fob1Δ* mutations with respect to the replicative longevity, rDNA recombination, and ERC generation phenotypes. The replicative lifespan of *sir2Δ fob1Δ* strains has previously been determined to be extended compared to wild-type, but significantly shorter than exhibited by strains mutant for *FOB1* alone (Kaeberlein et al., 1999), suggesting a combination of epistasis and additional lifespan-extending pathways dependent upon functional Sir2 but not influenced by Fob1. Sir2 has been demonstrated to participate in other functions controlling replicative age, including asymmetric segregation of damaged material (oxidised proteins) to the ageing mother cell and suppression of the silent mating locus (Kaeberlein et al., 1999; Erjavec et al., 2007). These experiments demonstrate that, at the level of recombination and downstream ERC generation, *FOB1* is completely epistatic to *SIR2* and mutation of *FOB1* is sufficient to repress recombination completely in the *sir2Δ* strain. Traditionally, the role of Fob1 at the rDNA spacer region has been hypothesised to be asymmetric blocking of replication forks to prevent downstream collision with replication forks (or transcription) occurring in the opposite direction. The diminuation of ERC formation and marker loss through rDNA recombination in the *fob1Δ* mutant has undercut this idea, suggesting that Fob1 plays an active role in promoting recombination rather than preventing fork collision. (Mayan-Santos et al., 2008).

These observations in the *ydr026cΔ* strain (**Figure 33**) further supports the extended replicative lifespan observed above. Ha *et al* (Ha et al., 2012) also performed recombination assays upon wild-type and *ydr026cΔ* strains using the same technique, in a background obtained from the same source (Sinclair and Guarente, 1997) but observed a mildly enhanced recombination rate, correlating with the short replicative lifespan in their

system. This discrepancy may be explained by their use of synthetic medium for culture growth and half-sectoring assay rather than rich medium, which is more commonly used (Falcon and Aris, 2003). Observations in our system indicate that the global rDNA recombination rate is somewhat reduced on synthetic medium, and this reduction can make the difference between the already low rate in wild-type strains (~1.0 x 10^{-3} events per cell division) and a reduced rate in strains such as *ydr026cΔ* difficult to detect without large amounts of comparative statistical power.

These data suggest that, in addition to the chronological ageing phenotype observed above, the *ydr026cΔ* mutant strain also demonstrates a novel long-lived replicative ageing phenotype. As has been well established, the *sir2Δ* strain exhibits a markedly shortened replicative longevity; when combined with the first mutation, *sir2Δ* is epistatic to *ydr026cΔ* as for the chronological ageing phenotype. The enhanced survival over replicative ageing in the *ydr026cΔ* mutant correlates with reduced recombination frequency at the rDNA spacer region hotspot and ERC generation, in common with the majority of replicative longevity mutants dissected in yeast. This provides indirect evidence for a role of Ydr026c at the rDNA spacer region: the putative binding site for the protein is in close proximity to the putative binding site of Fob1 and the recombinational hotspot, and it has been shown to interact with Sir2 *in vivo*, so modified recombination frequency at this locus suggests regulation by DNA binding at this position. It is then hypothesised that reduced ERC generation and enhanced replicative longevity is a result of the reduced recombinogenicity of the rDNA hotspot in mutants lacking Ydr026c.

There are several broad mechanisms by which it might be hypothesised that this occurs. Ydr026c may act to recruit, or drive the recruitment, of Fob1, so leading to a partial *fob1Δ*-like phenotype when Ydr026c is missing. Supporting this, co-immunoprecipitation data suggests that Fob1 and Ydr026c physically interact in the nucleolus, and ChIP data

indicates that Ydr026c does bind close to Fob1 *in vivo* (Ha et al., 2012). However, Ha *et al* found that ChIP analysis in deletion mutants suggested that Ydr026c could not bind in the absence of Fob1, and they conclude the opposite order of recruitment to the rDNA spacer locus (Ha et al., 2012). Alternatively, Ydr026c may enhance recombination at the hotspot through local changes to the chromatin environment. Finally, Ydr026c may function in transcription termination of the main rDNA transcript, in analogy to TTF-1 in mammalian cells. Read-through of this transcript into the spacer region may interfere with local chromatin conditions over the fork-blocking region or the production of the non-coding RNA polymerase II-derived transcripts that are suppressed by Sir2.

7 Chromatin at the rDNA

7.1 Introduction

The observation of reduced rates of rDNA recombination, ERC formation, and enhanced replicative and chronological longevity in the *ydr026cΔ* mutant compared to wild-type; and the converse high rates of recombination, ERC formation, and reduced replicative and chronological longevity in the *sir2Δ* and *sir2Δ ydr026cΔ* double mutant; suggest that modified regulatory activity at the rDNA in these mutants may be responsible for the ageing phenotypes. The *sir2Δ* mutant is well characterised (Li et al., 2006) as demonstrating defective silencing of the RNA polymerase II transcriptional activity over the rDNA cassette as a whole as well as upon transcripts originating from the spacer region between the rDNA repeats (Bryk et al., 1997; Houseley et al., 2007). In addition, it has also been demonstrated that strains lacking *FOB1* exhibit defective RNA polymerase II silencing at the rDNA spacer region through interaction with the Sir2-containing RENT complex (Bairwa et al., 2010). *fob1Δ* mutants posses an archetypically extended replicative lifespan and show numerous rDNA locus phenotypes, including virtually undetectable levels of ERC accumulation and rDNA hotspot recombination rates (Kobayashi and Horiuchi, 1996). However, in contrast with *ydr026cΔ* and *sir2Δ* strains analysed above, *fob1Δ* strains do not appear to show any modification in chronological longevity.

Two putative complete inverted consensus binding sites for Ydr026c, established by genome-wide ChIP-on-chip (Harbison et al., 2004), exist flanking each copy of the yeast 9.1 kb rDNA cassette. Ydr026c has been shown to physically interact with both Fob1 and Sir2 *in vivo*, and has been localised to the nucleolus (Huh et al., 2003). More recently, direct ChIP experiments have suggested that Ydr026c does indeed bind to the consensus site nearest the termination region of the 35S rRNA transcript *in vivo*; this study also

suggested that Ydr026c binding was completely abrogated in *fob1Δ* mutants and hence Ydr026c is recruited to the rDNA spacer region by Fob1 (Ha et al., 2012).

It is hence hypothesised that, in analogy with the epistatic *sir2Δ* mutants, the *ydr026cΔ* mutant demonstrates modified silencing at the rDNA spacer locus, and that the *sir2Δ ydr026cΔ* mutant would exhibit silencing behaviour epistatic to the *sir2Δ* mutant. Some recent indirect evidence already exists that position effect silencing in the rDNA spacer region is reduced in *ydr026cΔ* mutants (Ha et al., 2012). Crude lack of silencing in the rDNA spacer region therefore seems to be a phenotype of the *ydr026cΔ*, *sir2Δ* and *fob1Δ* mutants; however, the interacting but highly distinct replicative and chronological ageing phenotypes in the mutants requires more detailed investigation.

Much of the investigation into silencing in the rDNA region has been carried out with RNA-polymerase II-transcribed reporter constructs integrated into the genomic sequence (Smith and Boeke, 1997; Straight et al., 1999; Kaeberlein et al., 2005a). While valuable position effect data can be obtained from these experiments, they have a number of shortcomings, including: imprecision in indicating where desilencing of transcription is occurring; no sense-specificity for detected transcripts; and the incorporation of large expression cassettes, often with intact promoters and terminators, which may cause considerable and uncontrolled for disruption of the native locus *in vivo*. As such, direct detection of transcripts produced from the native locus represents a more sensitive and specific method of assaying silencing phenotypes in this instance. Northern blots hybridised to strand-specific probes can have been used to detect a number of very low-level RNA polymerase II-dependent transcripts originating and terminating in the rDNA spacer region (Li et al., 2006; Houseley et al., 2007).

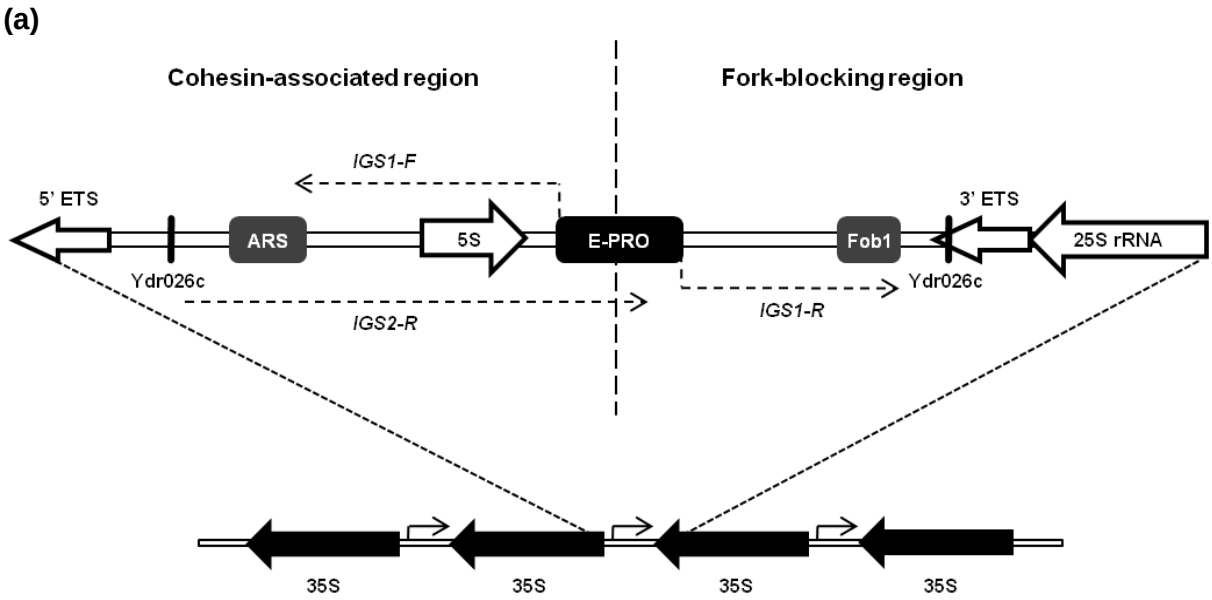

Figure 38. Schematic of the rDNA spacer region NTS2-1 and NTS1-2. The region is 2.2 kbps in length and separates copies of the main RNA polymerase I-transcribed 35S region. Each spacer contains a DNA replication origin (ARS) and the antisense 5S rRNA template, and is flanked by putative Ydr026c binding sites. A putative binding site for the replication fork blocking protein Fob1, established *in vitro*, is present near the most downstream Ydr026c binding site. Previous work has identified a number of low-level RNA polymerase II-derived transcripts subject to silencing by Sir2 at this locus. These transcripts both begin (*IGS1-F, IGS1-R*) or terminate (*IGS2-R*) at a region named the E-promoter (E-PRO) in the centre of the locus. Chromatin immunoprecipitation experiments have demonstrated the association of cohesin with the region between the start of the 5' ETS and the E-promoter, and so this area is termed the *cohesin-association region* (CAR). Because replication fork-blocking and associated recombination occurs downstream of the E-promoter, this region is termed the *fork-blocking region* (FBR).

Each rDNA repeat is flanked by a ~2.2 kb region not transcribed as part of the main 35S transcript (**Figure 38**). This spacer region contains a replication origin (ARS) as well as the small RNA polymerase II-transcribed 5S rRNA transcript, which reads in the opposite sense to the 35S transcript. *sir2Δ* null mutant strains have previously been reported to experience enhanced expression of the RNA polymerase II-generated transcripts in this spacer region running both sense and antisense to the main 35S transcript (Li et al., 2006). These transcripts apparently originate from a central region of the spacer region, termed the

E-promoter, downstream of both the ARS and the 5S transcript. The region upstream of the E-promoter is termed the *cohesin associated region* (CAR) due to the detection of cohesin deposition in over this locus. Based on the consensus binding site for Ydr026c, putative flanking binding sites exists just before the start of the upstream 35S transcript (**Figure 21**). Downstream, between the E-promoter and the end of the 35S transcript, lies another putative flanking Ydr026c binding site, inverted. Fob1 has been shown to bind close to this region *in vitro* by footprinting studies, and it is in this region when fork blocking and the associated recombinogenic hotspot exists, so this locus is termed the *fork-blocking region* (FBR). Transcripts have previously been detected both beginning and terminating at the E-promoter over the CAR locus, and originating at the E-promoter on the FBR side (Li et al., 2006).

In addition to loss of silencing of transcription at this locus, previous investigations have demonstrated changes to chromatin state over the rDNA spacer region. Investigation of chromatin structure by micrococcal nuclease protection assays has revealed that Sir2 is required for maintenance of two closed chromatin regions, in the rDNA spacer region and the 18S rRNA coding region (Fritze et al., 1997). Psoralen crosslinking experiments have shown that active rDNA repeats in yeast are highly nucleosome depleted, while inactive repeats show closed chromatin structure (Dammann et al., 1993). Moreover, RNA polymerase I enhancers in the spacer regions of active repeats contain nucleosome depleted regions, and (unlike the body of the coding regions) this chromatin structure is not dependent upon transcription by RNA polymerase I (Dammann et al., 1995). ChIP experiments have shown that chromatinisation of the rDNA as a whole is reduced in *sir2Δ* mutants (Li et al., 2006). These mutants also exhibit histone H4 hyperacetylation at the rDNA spacer (Hoppe et al., 2002) and hyperacetylation of H3K9 and K14 throughout the rDNA array (Huang and Moazed, 2003) due to loss of the deacetylation function of Sir2, as well as enhanced RNA polymerase II deposition and H3K4me3, a mark of chromatin

active for RNA polymerase II transcription (Li et al., 2006). Evidence exists for association of Fob1 with the RENT complex and subsequent histone deacetylation (Huang and Moazed, 2003). One recent study also suggested an increase in pan-acetylation of histone H3 over the rDNA spacer region in the *ydr026cΔ* mutant compared to wild-type (Ha et al., 2012).

YDR026C is the closest homologue of mammalian rRNA transcription termination factor (TTF-1) in *Saccharomyces cerevisiae*. TTF-1 binds between rDNA repeats at the mammalian rDNA locus and is responsible for RNA polymerase I termination and pre-rRNA processing (Langst et al., 1998). TTF-1 mutants have been shown to be associated with a number of intriguing chromatin modification phenotypes at the mammalian rDNA locus.

Mammalian rRNA genes contain CpG islands at their promoters. By performing ChIP experiments with chromatin digested by restriction enzymes incapable of cutting methylated sequences, it has been determined that mammalian rDNA repeats containing non-methylated promoter CpG islands (Lawrence et al., 2004) correlate with the presence of DNA-binding proteins indicative of active transcription, including UBF and PAF53. By this method, it has subsequently been shown that TTF-1 binds specifically to these non-methylated rDNA repeats, and so is associated with active rDNA regions. Additional H3 and H3K79me2 immunoprecipitation could also be detected in inactive repeats with methylated CpG islands (Németh et al., 2008).

Because of the similarity of factor crosslinking to the promoter and terminator of mammalian rDNA it has been suggested that higher-order chromatin structures may maintain each repeat as a functional domain (Sander and Grummt, 1997). Chromatin conformation capture (3C) technology is a technique that can measure juxtaposition of distant genomic loci *in vivo*, and has been used in the analysis of higher order chromatin

structures regulating active and repressed chromatin (Dekker et al., 2002). Crosslinked chromatin is fragmented with a restriction enzyme before being diluted to high volume. The mixture is then subject to ligation using T4 DNA ligase: the high dilution favours intramolecular religation events, and separate genomic loci crosslinked in close proximity *in vivo* become ligated together. These 3C products are then detected by PCR, or on a genome-wide scale, through deep sequencing. 3C has been used in a variety of systems to investigate both interactions between specific loci and as a genome-wide technique at lower resolutions to attempt to establish a physical model of chromosomal arrangement (Tolhuis et al., 2002; Simonis et al., 2006; Skok et al., 2007). Physical association of enhancer elements and promoters has been studied in mammalian systems (Choi et al., 2007), and association of promoter and terminator elements (*gene loops*) have been demonstrated in *S. cerevisiae* (O'Sullivan et al., 2004; Singh and Hampsey, 2007).

Using 3C, Németh *et al* demonstrated that the promoter and terminator of mammalian rDNA transcript templates are juxtaposed *in vivo* by more than eight-fold above background levels (Németh et al., 2008). By combining 3C with digestion by DNA methylation-sensitive endonucleases, this juxtaposition was found to be associated with unmethylated rDNA repeats, and it was therefore inferred that the active rDNA repeats assumed this higher order chromatin domain formation. Moreover, by overexpression of loss-of-function mutants of *TTF-1*, it was shown that this promoter-terminator juxtaposition – and activation of the rDNA repeats – was dependent upon fully functional TTF-1 protein (Németh et al., 2008).

Ydr026c diverges from this in not being required for activation of RNA polymerase I expression in *S. cerevisiae*; however, Ydr026c may still play a homologous role in organising higher order chromatin structure over the yeast rDNA or acting as a termination factor. Given the evidence for a function for Ydr026c at the yeast rDNA spacer and its homology to TTF-1, chromatin status in the *ydr026cΔ* mutant represents a possible

underlying mechanism for the longevity phenotypes previously observed. Transcript silencing, histone deposition, and higher order chromatin structures were therefore investigated in the *ydr026cΔ*, *sir2Δ* and *fob1Δ* mutants over the rDNA spacer region, in an attempt to dissect the divergent phenotypes observed in these strains.

7.2 rDNA spacer transcription in replicative and chronological longevity mutants

To investigate levels of transcription of around the rDNA spacer region, a series of sense-specific Northern blotting experiments were performed to measure transcript levels over defined regions. RNA was extracted from logarithmic phase rich medium cultures of wild-type and various mutants, subject to electrophoresis on formaldehyde agarose gels, and blotted onto neutral nylon membrane. Strand-specific radiolabelled probes were generated using asymmetric PCR in the presence of ^{32}P-dCTP upon templates produced by PCR of genomic DNA, and hybridised to the membranes under standard conditions. This allowed highly strand-specific and sensitive detection of low-abundance transcripts originating from the spacer region. Two sets of probes were designed to indicate transcripts originating or terminating at the E-promoter over the CAR and FBR regions, in either direction (**Figure 39a**).

Northern hybridisation experiments performed with a probe homologous to the CAR in both senses verified the presence of a transcript of ~700 nt broadly originating in the vicinity of the E-promoter that is repressed by Sir2 (**Figure 39d**). This transcript largely corresponds to previously observed IGS1-F (700-1200 nt long) and exhibits similarly strong repression by Sir2. The transcript was undetectable in the wild-type and *ydr026cΔ* strains, but is sufficiently abundant to be easily detectable in the *sir2Δ* and *sir2Δ ydr026cΔ* double mutant to a similar degree. This transcript is present in both the logarithmic phase of growth as well as following the diauxic shift, when its abundance further increases. The size of this transcript broadly corresponds to that previously reported (Houseley et al., 2007). Probes homologous to the opposite sense (terminating at the E-promoter) could not detect any apparent transcript, both in wild-type strains and the *sir2Δ* null.

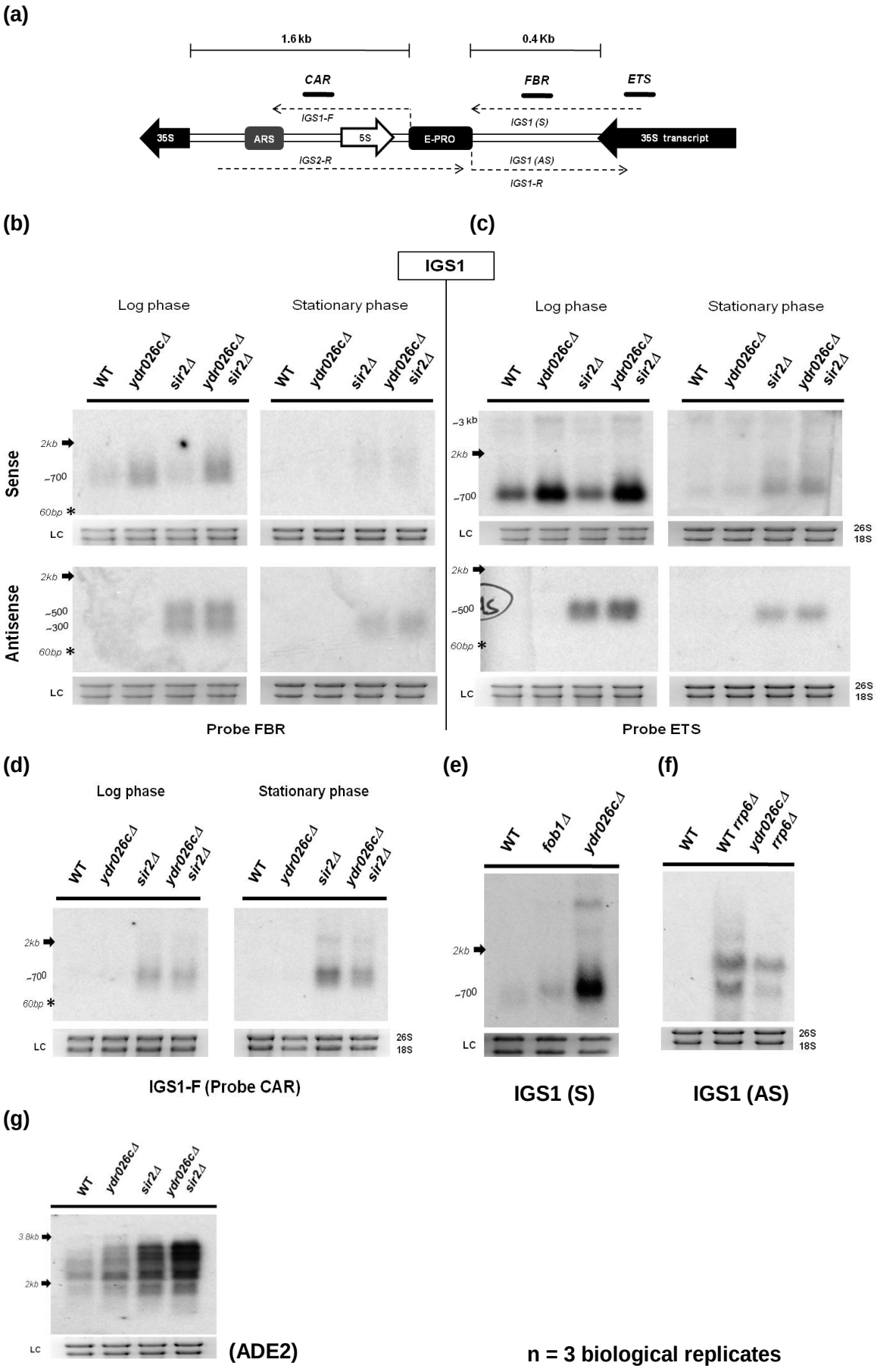
(a)
1.6 kb
0.4 Kb
CAR
FBR
ETS
IGS1-F
IGS1 (S)
35S
ARS
5S
E-PRO
35S transcript
IGS2-R
IGS1 (AS)
IGS1-R
(b)
(c)
IGS1
Log phase
Stationary phase
Log phase
Stationary phase
WT
ydr026cΔ
sir2Δ
ydr026cΔ sir2Δ
Sense
Antisense
2kb
~700
60bp
LC
~3 kb
~500
~300
26S
18S
Probe FBR
Probe ETS
(d)
(e)
(f)
Log phase
Stationary phase
fob1Δ
WT rrp6Δ
ydr026cΔ rrp6Δ
IGS1-F (Probe CAR)
IGS1 (S)
IGS1 (AS)
(g)
3.8kb
(ADE2)
n = 3 biological replicates

Figure 39.

Figure 39. Measuring transcript levels over the rDNA spacer region. **(a)** Probe positions in the rDNA spacer region. Radiolabelled strand-specific probes were produced at each position by single-primer asymmetric PCR in the presence of α-^{23}P-dCTP on pre-prepared probe templates. RNA was extracted from logarithmic and stationary phase (4 hrs and 1 day, respectively) cultures of appropriate strains for each experiment. Sense (S) and antisense (AS) in this context corresponds to the sense of the main rRNA 35S transcript. Blots were exposed to film for 3-7 days to obtain suitable exposures. Equal loading is demonstrated by levels of 26S and 18S rRNA loading controls (LC) stained by ethidium bromide, shown below each blot (colour inverted). Arrow indicates 26S rRNA (2.0 kb) and * tRNA (60 bp). **(b)** Northern blot hybridised to the FBR probe, demonstrating evidence of transcription in both senses over the fork-blocking region. A Ydr026c-repressed sense transcript, as well as the previously detected Sir2-repressed antisense transcripts are detected. **(c)** Northern blot hybridised to the ETS probe in both orientations also detects transcription in both directions. Additionally, very long sense transcripts (>5 kb) are visible near the top of the blot and become more abundant in the *ydr026cΔ* and *sir2Δ ydr026cΔ* strains. These are likely to correspond to the unprocessed 35S RNA-polymerase I-derived transcript. **(d)** Northern blot hybridised to the CAR probe. Previously described Sir2-repressed transcript IGS1-F is detectable. **(e)** Northern blot analysed with a probe homologous to the IGS1 (S) transcript in *fob1Δ* and *ydr026cΔ* mutants. The Ydr026c-repressed transcript, as well as long read-through transcripts, are present only in low abundance in the *fob1Δ* strain. Long read-through transcripts are again visible in the *ydr026cΔ* strain. **(f)** Northern blot analysed with a probe specific for the IGS1 (AS) (IGS1-R) transcript in the *rrp6Δ* background, in which it accumulates. Strikingly, deletion of *YDR026C* and derepression of the sense spacer transcript in the *rrp6Δ* background leads to re-repression of the Sir2-repressed sense transcripts emanating from the E-promoter region. **(g)** Sense transcript levels of an *ADE2* construct embedded within one rDNA repeat.

Further northern blots were performed to investigate transcriptional activity over the FBR locus. Two sets of probes were used in both directions: the first equidistant between the E-promoter and the end of the 35S transcript, near the putative Fob1 binding site (FBR); and the second within the external transcribed spacer (3' ETS) near the putative Ydr026c binding site (**Figure 39b-c**). Probes antisense-specific for transcripts originating from the E-promoter detected Sir2-repressed transcripts of roughly ~300-500 nt emanating from this region. This transcript appears to correspond to the previously observed IGS1-R, which is reported as a similar range of sizes and also shows repression by Sir2, albeit not to the same degree as IGS1-F. Transcript IGS1-R was effectively undetectable under the same conditions in the wild-type and *ydr026cΔ* strains, with marked increases in abundance in the *sir2Δ* and *sir2Δ ydr026cΔ* double mutant. The transcript could be detected, with varying efficiency, by both the FBR and ETS probes.

The same probes specific for IGS1 sense transcripts also indicated evidence of transcription through the FBR region towards the E-pro. Transcripts are weakly detectable in the wild-type background by both sets of probes, with varying efficiency. In the case, however, transcription does not appear to be silenced by Sir2: transcript abundances in the *sir2Δ* mutant are equivalent to that of wild-type, as indicated by both probes. Rather, appearance of transcripts in this direction are repressed by Ydr026c (**Figure 39b-c**). A transcript of approximately 700nt is detectable and of markedly higher abundance in both the *ydr026cΔ* mutant and *sir2Δ ydr026cΔ* double mutants, suggesting a non-epistatic repression of transcript accumulation in this sense by Ydr026c. Both sets of probes produced similar results, with the ETS probe giving greater hybridisation efficiencies. Detection by both probes suggests that the transcript ranges at least from inside the RNA polymerase I-transcribed 35S rRNA region and through into the fork-blocking locus, terminating in region between this and the E-promoter. At least two transcripts are detectable running in this direction. A long transcript (> 3kb), possibly corresponding to the 3' end of the 35S

transcript, is detectable using the ETS probe, and is enhanced in the *ydr026cΔ* and *sir2Δ ydr026cΔ* mutants. This transcript is also detectable when the FBR probe is used (**Figure 39e**). Interestingly, this suggests that strains mutant for *YDR026C* may experience defective termination of the main 35S RNA polymerase I transcript, leading to the accumulation of this transcript and especially short processed products corresponding to regions upstream of the putative Ydr026c binding site.

Previous studies investigating the DNA binding activity of Ydr026c have suggested that recruitment of Ydr026c to the rDNA spacer region *in vivo* is completely dependent upon Fob1 (Ha et al., 2012). This model would predict that the silencing phenotype associated with specific sense transcripts detected in the spacer region in the *ydr026cΔ* mutant should be reconstituted in strains lacking Fob1. Northern analysis of wild-type, *fob1Δ*, and *ydr026cΔ* strains demonstrated that deletion of *FOB1* was not sufficient to reconstitute the transcript phenotype observed in mutants lacking Ydr026c (**Figure 39e**). This suggests that, contrary to previous models, Ydr026c has Fob1-independent functions at the rDNA including silencing of rDNA spacer region transcripts.

The Sir2-repressed transcripts emanating from the E-promoter exist at very low steady state levels in the wild-type background. In order to investigate whether these transcripts may be further repressed when transcription in the opposite sense was desilenced in the *ydr026cΔ* mutants, Northern analysis was performed in a background lacking the RNA-degrading exosome complex component Rrp6, with and without *YDR026C* (**Figure 39f**). The Sir2-repressed antisense transcript is markedly elevated in the *rrp6Δ* background strain, suggesting that Rrp6 does participate in its degradation (or otherwise reduce accumulation). Interestingly, when Ydr026c was deleted in this background, markedly lower levels of steady-state antisense transcript were detected. This suggests that in mutants lacking Ydr026c, sense transcription over the FBR region of the rDNA spacer locus is favoured

over antisense transcription, and the Sir2-repressed transcripts emanating from the E-promoter are repressed.

In addition, silencing outside of the spacer region was determined by use of a probe homologous to an *ADE2* cassette integrated into a single rDNA copy. Deletion mutants strains were constructed in a background containing this cassette and lacking the normal *ADE2* locus (w303 *ade2Δ RDN1::ADE2*). Transcript levels in wild-type, *sir2Δ*, *ydr026cΔ* and *sir2Δ ydr026cΔ* deletion mutants were measured by northern hybridisation to a probe specific for the sense of the ADE2 cassette (**Figure 39g**). Greatly enhanced levels of cassette transcript were observed in the *sir2Δ* and *ydr026cΔ sir2Δ* double mutant, suggesting concomitant loss of silencing in the main body of the rDNA repeats in this mutant.

7.3 Chromatin at the rDNA

To investigate whether the loss of transcriptional silencing phenotypes associated with the *sir2Δ*, *ydr026cΔ* and *sir2Δ ydr026cΔ* mutants had a basis in changes to chromatin state, a series of chromatin immunoprecipitation (ChIP) experiments were performed to investigate chromatin density over the rDNA locus. Crosslinked chromatin was prepared from logarithmically growing cells and fragmented by sonication. Immunoprecipitation was performed using anti-H3 antibody, and recovered DNA quantified using qPCR with primers specific to regions across the rDNA locus normalised to material input (**Figure 40a**).

Despite the 100-200 rDNA repeats present in each cell, only moderate H3 ChIP signals were observed. All ChIP signals were, however, normalised to qPCR signals generated from total chromatin before immunoprecipitation. Hence, high qPCR signals given by the large number of rDNA repeat targets are taken into account by this primer efficiency, and become normalised out of the final result. **Figure 40b** shows the pattern of H3 deposition as determined by ChIP over the rDNA region in chromatin extracted from a wild-type logarithmic phase culture. Two regions depleted of nucleosomes are observed flanking the main 35S rDNA region, corresponding exactly with the edges of the spacer region and the putative inverted Ydr026c binding sites.

The interior of the main RNA polymerase I-transcribed region has higher nucleosome density. A particularly strong H3 peak is however observed between these two binding sites, near to the 5S rDNA template and the E-promoter in the spacer region.

H3 deposition was assayed by chromatin immunoprecipitation in wild-type, *sir2Δ*, *ydr026cΔ* and *sir2Δ ydr026cΔ* cells. Chromatin was extracted from logarithmic phase cultures and H3 deposition determined across the locus using the same primer set (**Figure**

40a-b). A strong H3 signal depletion phenotype was observed in the *sir2Δ* and *sir2Δ ydr026cΔ* mutant. Significantly less H3 could be immunoprecipitated throughout the locus, with particular loss of deposition observed over the putative Ydr026c binding sites in the spacer region, and dramatic loss over the region near the E-promoter and 5S template. Depletion levels were similar in the *sir2Δ* and *sir2Δ ydr026cΔ* mutants, with generally lower signals in the latter. Conversely, the *ydr026cΔ* mutant demonstrates strong and significant enhancement of nucleosome deposition throughout the rDNA locus (**Figure 40c**). Outside of the spacer region an average of two-fold increase of H3 immunoprecipitation signal is given in the *ydr026cΔ* mutant compared to wild-type. Similarly high levels of H3 deposition are recorded over the putative Ydr026c binding sites in the spacer region. Primers over the E-promoter region, however, record levels of H3 deposition similar to wild-type.

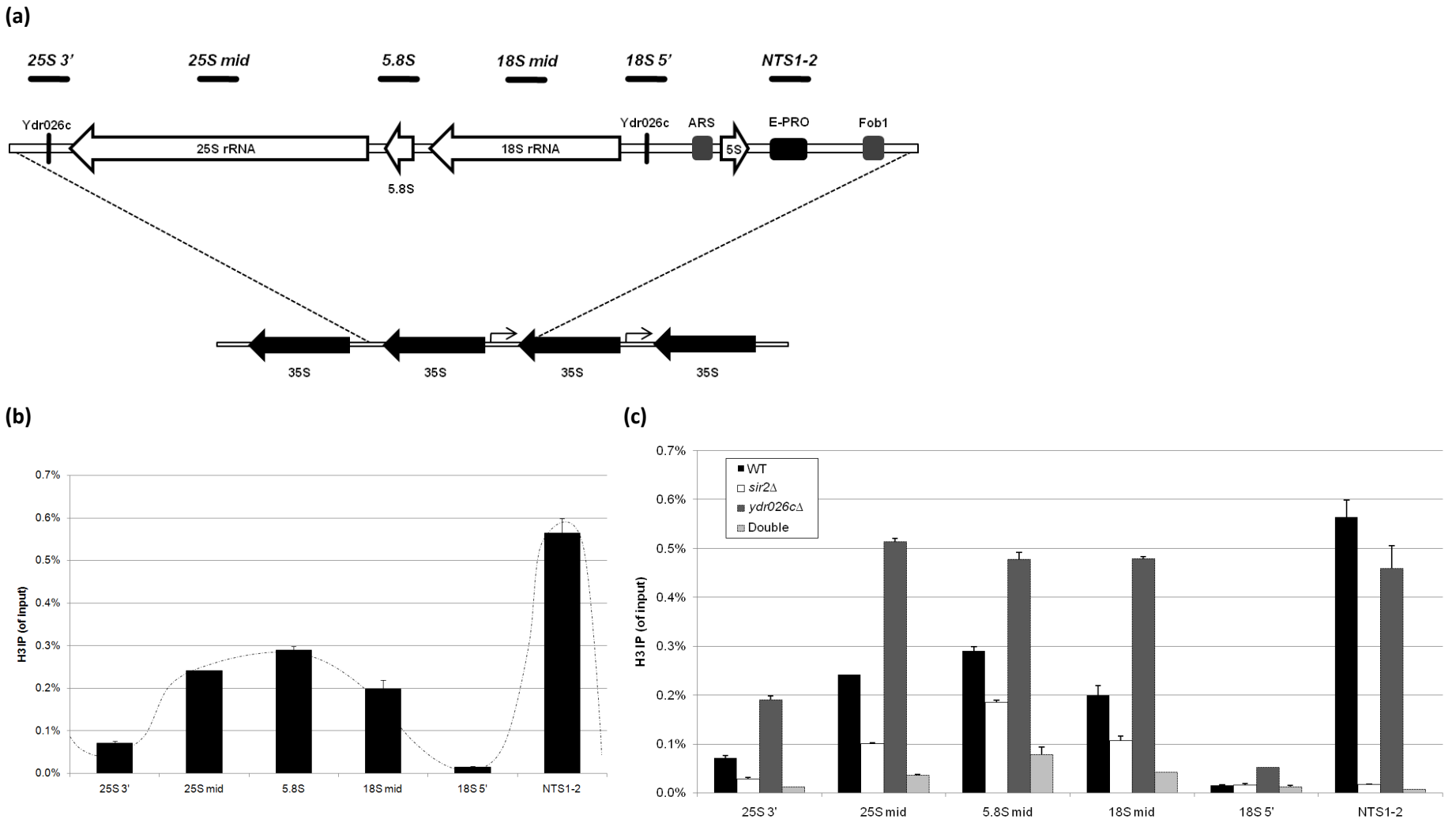

Figure 40. Chromatin immunoprecipitation of histone H3 across the rDNA locus. A series of ChIP experiments were performed in wild-type, *sir2Δ*, *ydr026cΔ* and double mutant *sir2Δ ydr026cΔ*. **(a)** Crosslinked chromatin was extracted, fragmented by sonication, and H3-associated chromatin recovered by immunoprecipitation. Recovered DNA was decrosslinked, purified, and quantified by qPCR using the six primer pairs shown spanning the rDNA locus and spacer region. **(b)** H3 deposition across the rDNA locus determined by ChIP in a logarithmic phase wild-type strain. **(c)** H3 deposition across the rDNA locus comparing wild-type, *sir2Δ*, *ydr026cΔ* and *sir2Δ ydr026cΔ* mutant strains.

7.4 Higher order nucleolar chromatin organisation

Previous work on the mammalian homologue of Ydr026c, TTF-1, suggested that the position of binding sites flanking the human rDNA repeat promoted physical juxtaposition of copies of this locus within the nucleolus. Evidence for this effect was gathered by immunoprecipitation of identical factors and chromatin modifications to loci hypothesised to be in close physical interaction. A more direct method of determining physical juxtaposition of DNA loci is chromosome conformation capture (3C). 3C has been used in a variety of systems to investigate both interactions between specific loci and as a genome-wide technique at lower resolutions to attempt to establish a physical model of chromosomal arrangement (Singh and Hampsey, 2007; Lieberman-Aiden et al., 2009). To investigate whether higher order chromatin structures may be involved in the regulation of the rDNA locus and whether such structures were modified in mutants with silencing phenotypes, a 3C assay was developed for use over the rDNA locus in this system.

The principle of 3C (**Figure 41a**) rests upon genomic fragmentation of cross-linked DNA by restriction enzymes followed by re-ligation to genetic regions maintained physically nearby through the cross-links. This re-ligation step is performed after dilution of the input chromatin to a high degree, making intermolecular ligations as rare an event as possible and promoting intramolecular ligation of DNA ends held together by crosslinks. Following decrosslinking and purification of the DNA, re-ligation products can be detected by PCR using primers specific for each juxtaposed locus to be tested. Primers able to generate PCR products on uncut DNA (convergent) are avoided; rather divergent (opposite directions) or tandem (same direction) primers are used to ensure only religation products are detected. Abundance of PCR product generate gives an assay of juxtaposition frequency of the loci tested. In the absence of specific juxtaposition, loci near to each other on a chromosome are more likely to become ligated together and generate 3C signal, as they are more likely to

physically juxtapose through diffusion before ligation; the likelihood of this juxtaposition falls exponentially with distance. When specific physical association exists, primers homologous for the juxtaposing regions produce a peak 3C signal (PCR product) distinct from this distance-dependent background. This indicates physical juxtaposition *in vivo*.

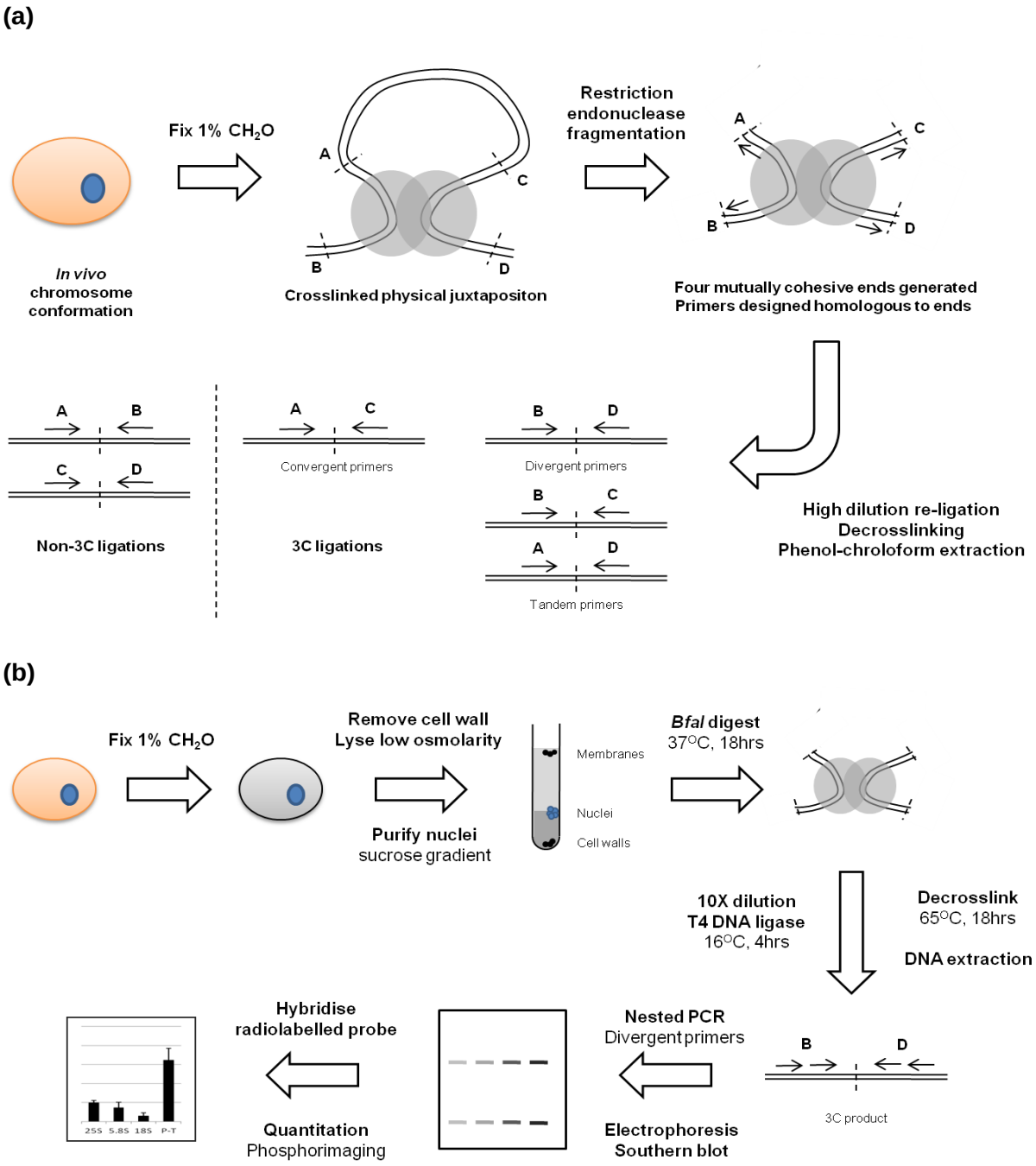

Figure 41. 3C in *S. cerevisiae*. **(a)** Cells are fixed in 1% formaldehyde and nuclei extracted. Upon digestion and ligation at high dilution, genomic loci juxtaposed *in vivo* and crosslinked together are subject to religation together. For two genomic fragments, of the six possible religation products two are generated by locus self-ligation and do not indicate juxtaposition. The remaining four combinations can be detected by PCR using primers which on the unfragmented genome would be convergent, divergent, or tandem respectively. **(b)** Developed protocol for quantified 3C in this system. Cells are fixed, cell walls are removed using yeast lytic enzyme, spheroplasts are lysed and nuclei extracted using a discontinuous sucrose gradient. Restriction enzyme *BfaI* was chosen to digest crosslinked chromatin, and DNA was extracted following ligation at high dilution. Divergent primers were used to perform nested PCR to detect specific 3C religation products, which were then separated on agarose gels, Southern blotted, and hybridised to radiolabelled probes. Signals were quantified by a phosphorimager system.

A 3C assay of this sort was developed for this system (**Figure 41b**). Logarithmic phase cells are harvested, washed, and cross-linked in 1% formaldehyde. The cell walls are removed using yeast lytic enzyme, and the spheroplasts burst in high osmolarity solution. Density equilibrium centrifugation on discontinuous sucrose gradient columns was then used to purify nuclei away from cytoplasm, membrane and cell wall components. Purified nuclei are lysed and genomic DNA digested with a selected restriction enzyme overnight. The restriction enzyme is heat inactivated, the samples diluted 10-fold, and T4 DNA ligase used to religate juxtaposed ends at 16^{O}C. DNA is purified by phenol:chloroform extraction and precipitated and washed in 70% ethanol. Intramolecular ligations are detected by nested PCR reaction using pairs of divergent primers extending over the rDNA locus. Aliquots are removed from the PCR reaction at progressive cycle numbers to allow an extended linear range of comparison, separated on TBE-agarose gels, and Southern blotted onto neutral nylon membranes. These are hybridised with a radiolabelled probe homologous with all 3C products combinations possible in each reaction. PCR products are then visualised by autoradiography, and quantified by phosphorimaging. This protocol was found to allow sensitive, specific and reproducible detection of 3C signals indicating chromatin juxtapositions.

To investigate possible juxtaposition of the promoter and terminator of the 35S RNA polymerase I rDNA transcript a restriction enzyme was selected to conveniently fragment the rDNA locus and a set of divergent nested primers were designed to span the region (**Figure 42a**). While restriction enzymes with 6bp recognition sequences are commonly used in mammalian 3C experiments, the average cutting frequency of these enzymes (4^6 = 4096 bps) leads to insufficiently fine resolution for many 3C experiments in yeast. Restriction enzymes with 4bp recognition sequences give much higher resolution (cutting on average every 4^4 = 256 bps) at the trade-off of the presence of many more recognition sites within the genome and therefore the potential for incomplete digestion if not all of

these sites are targeted. *BfaI* (CTAG) was selected as the optimum enzyme for fragmentation of the rDNA locus while preserving uncut regions against which to design primers. To search for promoter-terminator juxtapositions while accounting for background rate of intramolecular ligations, interactions between the region including the terminator of the 35S transcript to a series of regions spanning the locus up to the promoter region. The putative Ydr026c binding sites are also included in the anchor regions tested for promoter-terminator juxtaposition. Primer nests were designed in the reverse orientation at the terminator anchor, and the forward orientation for the other primer sets. The terminator primer sets were designed homologous to a non-repeated region present on the endmost rDNA repeat to prevent convergent products being formed on unfragmented substrate, which would not be representative of 3C interactions.

Multiple PCR products were generated in some of the primer combinations. A possible cause of this is incomplete restriction enzyme digestion leading to generation of multiple possible ends subject to re-ligation in subsequent steps of the protocol. If this is the case, each PCR product represents a valid 3C product and should be taken into account when the total abundance of 3C products is calculated. To verify that bona-fide 3C products were being amplified in the PCR reaction and that longer products are generated by incomplete digestion, these PCR products were gel-purified and sequenced. Sequence comparison verified that cutting and religation of valid 3C products and incomplete digestion at some *BfaI* sites. Protein complexes crosslinked to the chromatin substrate may protect densely arrayed restriction sites from digestion.

Physical chromatin juxtaposition measured by 3C product formation was tested in cells from a logarithmic phase culture of a wild-type strain (**Figure 42b**). Small amounts of 3C product are detected on autoradiographs of Southern blotted PCR products for interactions between the 35S terminator and the neighbouring locus. This signal falls progressively with greater distance from the 35S terminator anchor, as expected. However, the 35S

terminator-promoter anchor primer combination, produces a strong and reproducible peak of detectable 3C products. Quantification of this effect suggested an approximately 4-fold increase of 3C interaction above that expected at the distance between these two loci, apparently reproducing the promoter-terminator juxtaposition observed in mammalian cells.

Several controls are important to validate 3C experiments performed in this way: quantitative comparison between sets of primer pairs must be controlled for relative primer efficiency, and quantitative comparison between different 3C preparations must be controlled for material input..

Firstly, comparison between different primer sets requires the experiment to be controlled for the efficiency of primer hybridisation and performance in the PCR reaction. By fragmenting the uncrosslinked chromatin using the same restriction enzyme, and performing the re-ligation reaction without high dilution, a library of religated products can be generated unbiased for physical juxtaposition. This randomly ligated library can then be used to test the relative efficiencies of pairs of nested primers under identical conditions used for PCR assay of 3C product formation (**Figure 42c**). Southern blotting, radiolabelled probe hybridisation, and phosphorimager analysis gives a quantitative estimate of each primer pair's efficiency. PCR reactions were performed on randomly ligated chromatin from wild-type cells using the same primer combinations spanning the rDNA locus (**Figure 42d**). Only small variations were observed in the relative primer pair efficiencies, with the promoter-terminator pair being slightly less efficient than average. Quantitation of these efficiencies verified this.

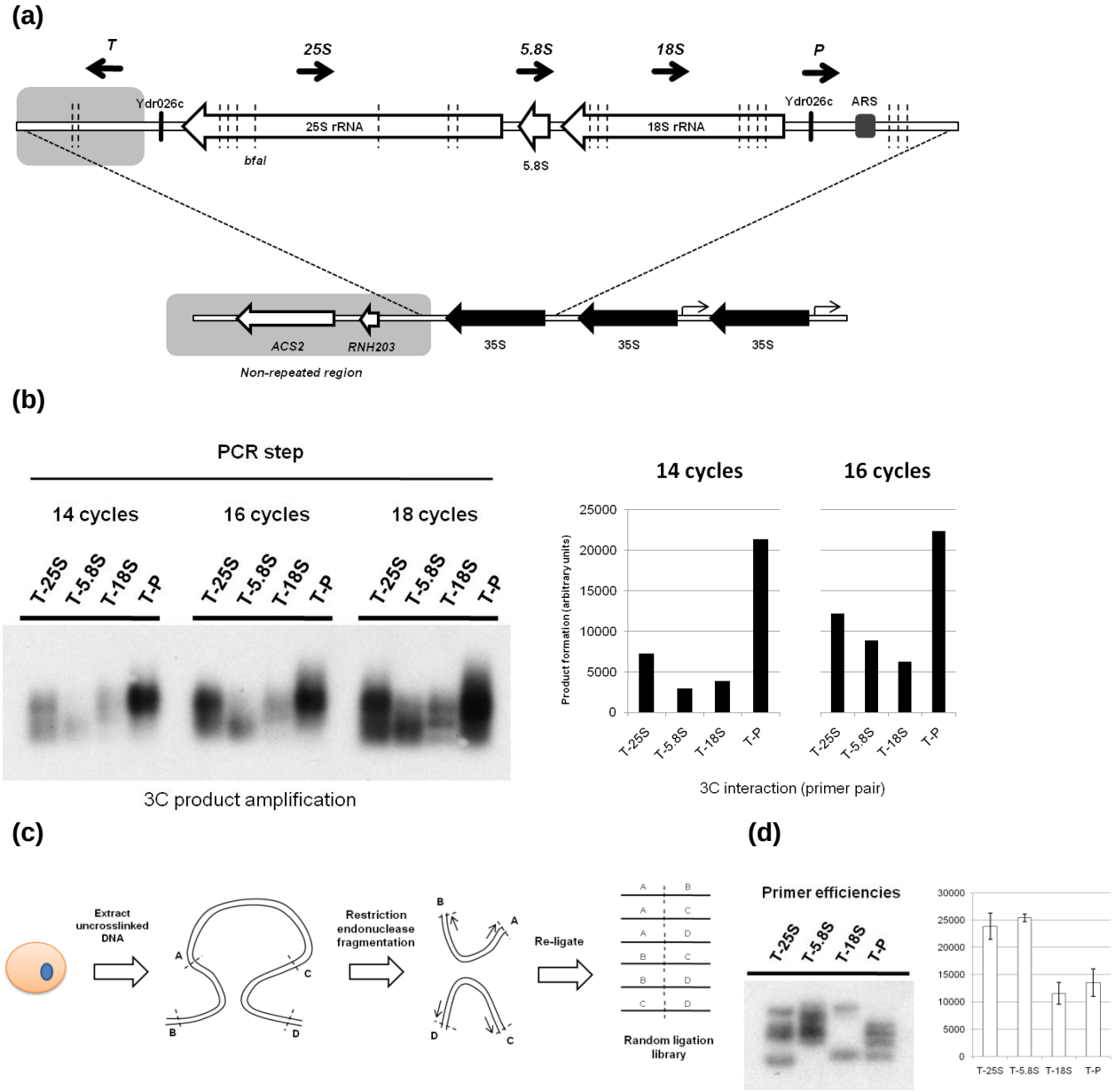

Figure 42. Preliminary 3C analysis of the rDNA locus. **(a)** Anchor primer positions used to establish juxtaposition of the 35S terminator region with loci spanning the rDNA. The T anchor region contained the terminator of the 35S transcript, the putative Ydr026c and Fob1 binding sites. **T** primer used for each interaction was designed homologous to the endmost rDNA repeat, at a region not repeated throughout the rDNA but still contained within the anchor. **(b)** Quantified Southern blot of initial 3C analysis of the wild-type rDNA locus. Samples were taken from 3C-product specific PCR reactions at 14, 16 and 18 cycles of the second nest, Southern blotted, and hybridised to an rDNA specific probe. In some lanes multiple bands are observed, indicative of incomplete digestion of the crosslinked chromatin. Juxtaposition frequency can be determined by signal intensity, dependent upon PCR efficiency for each primer pair. Juxtaposition hence falls away from the terminator over the rDNA locus, before peaking for interactions between the Ter and Pro regions. **(c)** Random ligation generation. Uncrosslinked DNA is digested with the same restriction enzyme (*BfaI*) and religated at high concentration. **(d)** Primer efficiency measured on randomly ligated product. The four primer pair combinations tested were found to be of comparable efficiency, with T-18S and Ter-P somewhat reduced.

Secondly, comparison of re-ligation products in different 3C preparations by PCR must be controlled for material input. By using an additional (non-nested) convergent primer set over a region predicted not to be subject to fragmentation by the chosen restriction enzyme the amount of input material can be assayed using PCR or qPCR. Primers over the gene *HMS2* were used for this purpose.

Chromosome conformation capture experiments were carried out on cross-linked chromatin extracted from logarithmic phase cultures of wild-type, *sir2Δ* and *ydr026cΔ* null mutants and the *sir2Δ ydr026cΔ* double mutant. 3C products were detected by nested PCR and visualised and quantified on Southern blots hybridised with a radiolabelled probe as above (**Figure 43**). The *sir2Δ* mutant demonstrates a wild-type conformation phenotype, with evidence of a decaying physical interactions with the terminator anchor over the region of the 35S transcript, followed by a distinct peak for juxtaposition of the promoter and terminator anchors. Again, an approximately 4-fold significant increase in 3C products is observed between these two primer sets, indicating a specific physical interaction between these two loci.

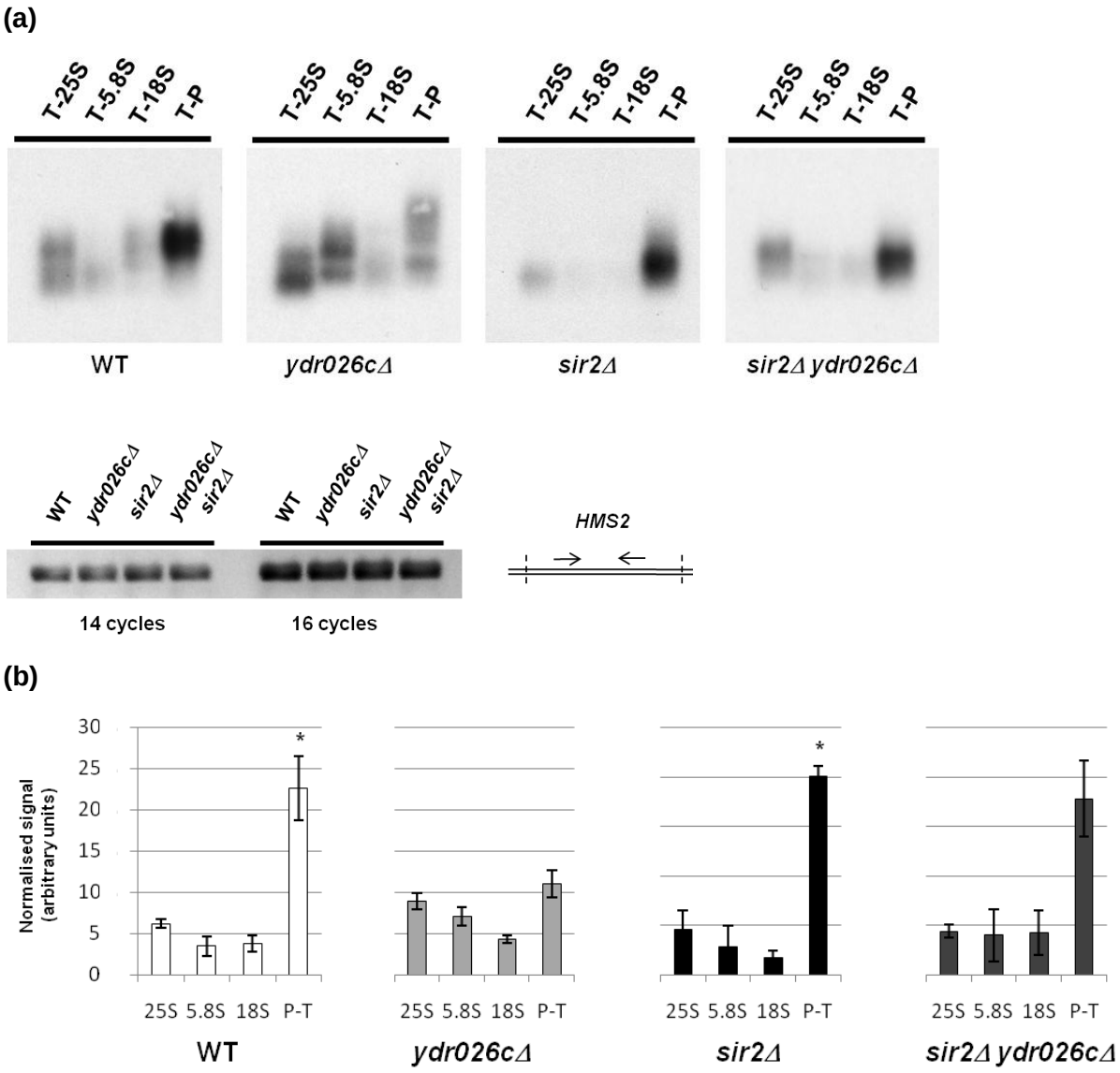

Error bars are standard error. n = 3 biological replicates.

Figure 43. Higher order chromatin interactions assayed by 3C in *ydr026cΔ*, *sir2Δ* and *sir2Δ ydr026cΔ* mutant strains. **(a)** Southern blots of PCR amplified 3C products using primers corresponding to interaction of the terminator anchor region with 25S, 5.8S, 18S and Promoter region as above at cycle 14 of the second nest. Multiple bands are again visible, suggesting incomplete digestion. A strong interaction between the promoter-terminator anchors elevated above background is visible in the WT, *sir2Δ* and *sir2Δ ydr026cΔ* strains but appears abrogated in the *ydr026cΔ* strain. Below is shown an ethidium bromide stained agarose gel of PCR products generated over the uncut *HMS2* locus, demonstrating equal loading of the strains. **(b)** Quantified normalised 3C results of n=3 biological replicates. Phosphorimager quantitation was used to measure signal intensity of all 3C product bands generated at cycle 14 of the second nest. Signal was then normalised for primer efficiency (for each primer) and loading (*HMS2* qPCR for each strain). Signals are arbitrary units normalised to both primer efficiency (**Figure 42d**) and loading.

In contrast, this conformation pattern appears to be entirely disrupted in the *ydr026cΔ* mutant. Slightly more abundant 3C products are obtained for interactions across the rDNA locus in this mutant: however, the normally strong product given using the terminator and promoter primer sets is not demonstrated. Rather, religation between these loci appears to occur at a frequency not significantly higher than background at that distance. This suggests that the physical juxtaposition of the terminator and promoter anchors (and putative Ydr026c binding sites) which predominates in wild-type cells is disrupted in when Ydr026c is not present, and that this protein plays a role in maintenance of that specific chromatin structure.

Interestingly, however, analysis of re-ligation products from the *sir2Δ ydr026cΔ* double mutant demonstrated reconstitution of the wild-type conformation phenotype. 3C product abundance over the rDNA locus gave a profile similar to that of wild-type and the *sir2Δ* single mutant, with approximately a four-fold increase in detected interaction frequency between the promoter and terminator anchors. This reinforces the epistasis of *SIR2* with *YDR026C* observed in replicative longevity and H3 deposition previously observed, and suggests that the physiological effects of Sir2 loss are sufficient to reconstitute the chromatin phenotype that is disrupted when *YDR026C* is deleted.

The *fob1Δ* mutant shares a number of phenotypes with the *ydr026cΔ* mutant. It has extended replicative lifespan and experiments above demonstrate a reduced rate of unequal recombination between rDNA spacer regions and lower ERC accumulation in both strains. In addition, the putative Fob1 binding established in vitro is very close to the putative Ydr026c binding site in the FBR of the rDNA spacer region, and recent work has suggested that Fob1 is required for the binding of Ydr026c. Preliminary 3C experiments were performed to investigate the chromatin conformation over the rDNA array in the *fob1Δ* and *fob1Δ ydr026cΔ* mutants (**Figure 44**). In both the *fob1Δ* and *fob1Δ ydr026cΔ* strains, very

low abundance of religation products was detected for interactions between the terminator anchor across the rDNA locus. In particular, the intense signal given between the terminator and promoter primer sets in the wild-type was not present. In this respect, the *fob1Δ* and *fob1Δ ydr026cΔ* strains have a similar conformation phenotype to the *ydr026cΔ* strain, suggesting epistasis of *FOB1* over *YDR026C* for the conformation phenotype, and disruption of the promoter-terminator juxtaposition interaction when Fob1 is not present.

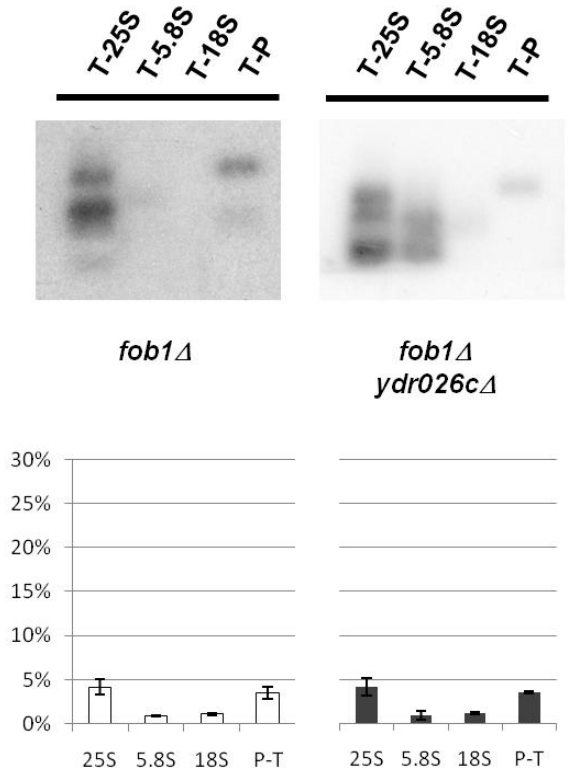

Figure 44. Preliminary 3C analysis of chromatin juxtaposition over the rDNA in the *fob1Δ* and *ydr026cΔ fob1Δ* strains. Little signal is observed for the interaction of the promoter and terminator anchor regions, suggesting this interaction is abrogated in the *fob1Δ* as well as the *ydr026cΔ* strains.

7.5 Discussion

These series of northern blots, chromatin immunoprecipitation (3C), and chromosome conformation capture experiments (ChIP) demonstrate that the recombination and longevity phenotypes previously observed in the *ydr026cΔ* and *sir2Δ* mutant strains (and the epistatic relationship between them) is reflected in the transcriptional activity and chromatin state at the rDNA locus.

Mutants lacking the *SIR2* lysine deacetylase, but not other members of the SIR complex including *SIR3* and *SIR4*, are well established to experience desilencing in the rDNA spacer regions. This has previously been demonstrated both by position effect of embedded reporter constructs (Bryk et al., 1997; Straight et al., 1999) and direct steady-state RNA assay by northern blot (Li et al., 2006; Houseley et al., 2007). Transcripts have been detected emanating from the E-promoter region in both senses. By sense-specific northern blotting analysis, this phenotype of *sir2Δ* mutant strains was reproduced in this study. The transcript emanating in the antisense direction from the E-promoter appears as a doublet, suggesting either staggered transcription initiation or termination sites for this transcript. These Sir2-repressed transcripts were present when Sir2 was missing in several genetic backgrounds, including in the *sir2Δ ydr026cΔ* double mutant strain.

In strains lacking the putative rDNA spacer region binding protein Ydr026c, an additional small non-coding transcript could be detected in the spacer region. This RNA is transcribed in the same sense as the main 35S rRNA transcript, and is detectable immediately following the annotated terminator of this transcript. This transcript was observed in all strains lacking *YDR026C* assayed. Long transcripts of the same sense can also be detected in these strains, suggesting significant read-through from the region corresponding to the 35S transcript is occurring. The RNA-polymerase I-transcribed 35S transcript is subject to

processing to remove the 3'-external transcribed sequence from the mature 25S rRNA near the putative Ydr026c binding site (van Nues et al., 1995). It is therefore possible that these read-through transcripts, and the short transcripts reading into the rDNA spacer region, accumulate in the *ydr026cΔ* strain due to defective termination and/or processing of the pre-mature 35S transcript. In this way, Ydr026c may be operating as a transcription termination factor for the polymerase producing the ribosomal transcript – generally RNA polymerase I, although polymerase II has been shown to participate in productive rRNA transcription under some conditions (Conrad-Webb and Butow, 1995) – in the same way as its mammalian ortholog, TTF-1 (**Figure 21**).

The only previous work on the physiology of the *ydr026cΔ* mutant suggested that Ydr026c recruitment to the rDNA was completely dependent upon Fob1 presence, and hence *ydr026cΔ* mutants should not exhibit additional phenotypes from *fob1Δ* mutants. Ha *et al* found that tagged Ydr026c could not be detected by ChIP at the rDNA spacer region in a *fob1Δ* strain (Ha et al., 2012). However, the *fob1Δ* strain was found not to accumulate the spacer transcript associated with *YDR026C* disruption; moreover, when *ydr026cΔ* is disrupted in the *fob1Δ* background the transcript is easily observed. This suggests at least one additional function of Ydr026c independent from Fob1. Two putative Ydr026c binding sites are present in the rDNA spacer region: while Ha *et al* could not detect binding of Ydr026c to the other putative binding site, it is possible that Ydr026c has a Fob1-indepedent repressive effect upon the FBR transcript by binding at this locus.

Mammalian TTF-1 is associated with actively transcribing rDNA repeats and is necessary for maintenance of an unusual higher-order chromatin structure juxtaposing the promoter and terminator of the rDNA cassette (Németh et al., 2008). Because the physiological function of Ydr026c is almost completely undefined, given this analogous behaviour with TTF-1 a series of 3C experiments were performed to determine whether similar higher

order structures could be detected over the *S. cerevisiae* rDNA cassette, and whether disruption of Ydr026c function could modify the chromatin environment over the locus. From the terminator of the main 35S transcript in the yeast rDNA array, juxtaposition frequency decreases asymptotically with distance as expected where no specific locus-locus interaction exit. Non-specific distance-dependent background juxtaposition occurs because loci tethered closely together are more likely to interact randomly than those more distantly connected. Exceeding this background, a strong, specific juxtaposition interaction is detectable between the promoter and terminator loci, adjoining the rDNA spacer region. Because the ~150 rDNA repeats in the BY4741 yeast background are perfectly homologous, this assay does not determine whether interactions are made between single rDNA repeats (loop formation) or between distant repeats.

This interaction was found to completely disappear in strains lacking Ydr026c. In this way, the higher order chromatin structure detected over the yeast rDNA may behave in some part analogous to the mammalian system studied with TTF-1, although it is unknown whether the active rDNA repeats are responsible for forming the higher order interactions here. Whether such higher order chromatin interactions are observed or not in strains containing only two, permanently active, rDNA repeats may settle this question. Initially it was hypothesised that Ydr026c may be mediating the long-range juxtaposition directly. However, further experiments determined that the promoter-terminator 3C signal was reconstituted in the *ydr026cΔ* background upon deletion of *SIR2*. In this way, unlike the transcription pattern recorded over the spacer region, formation of this specific higher order structure correlates with the recombination and ageing phenotype epistasis previously observed. Wild-type background strains lacking Sir2 do not show a 3C phenotype markedly different from the wild-type interaction.

Interestingly, the promoter-terminator juxtaposition can also be disrupted by deletion of Fob1. The *fob1Δ* strain has a physiological phenotype similar (but stronger) to the

ydr026cΔ strain, in that unequal rDNA hot-spot recombination is reduced and replicative longevity enhanced in these mutants. The disruption, and restoration, of the promoter-terminator juxtaposition is therefore likely to represent a downstream consequence of dysregulation in these mutants, rather than direct consequences of factor loss. In each case, hot-spot recombination frequency as measured in section 6.3 correlates with promoter-terminator locus juxtaposition signal as measured by 3C. Mutation of *SIR2* in the *ydr026cΔ* background rescues both the highly recombinogenic phenotype characteristic of the *sir2Δ* mutant, but also the presence of the higher order interaction. Homologous recombination leading to marker loss in an rDNA repeat must proceed through physical co-localisation of the spacer regions of the marker-containing and a non-marker containing rDNA repeat. Hence, one interpretation of the chromatin juxtaposition peak observed in these 3C experiments is as an indication of inter-rDNA repeat colocalisation caused by more active recombination occurring between the space region hotspot.

ChIP experiments were performed to measure chromatin changes on the nucleosome level over the rDNA. It has previously been reported that deletion of *SIR2* leads to hyperacetylation of histones H3 and H4 and dechromatinisation of the rDNA array (Hoppe et al., 2002; Huang and Moazed, 2003; Li et al., 2006). ChIP experiments measuring DNA immunoprecipitating to crosslinked H3 suggest a pattern of nucleosome deposition leaving two nucleosome depleted regions in the rDNA spacer region, while the rRNA template region (the 35S and 5S transcript template, including the E-promoter region) are relatively chromatinised. The dechromatinisation phenotype in the *sir2Δ* mutant is reproduced here, particularly with dramatically less H3 immunoprecipitation recorded in the middle of the spacer region, proximal to the E-promoter. Conversely, the *ydr026cΔ* mutant strain appears to have enhanced levels of chromatinisation across the rDNA cassette, although the nucleosome depleted regions remain and there is no significant difference in the spacer region. There is some previous evidence that actively transcribed rDNA repeats in

Saccharomyces cerevisiae are subject to nucleosome depletion (Dammann et al., 1993). One interpretation of these assays is therefore higher rDNA transcriptional activity in the *sir2Δ* and *sir2Δ ydr026cΔ* mutant strains, and reduced activity in the *ydr026cΔ* mutant. The chromatinisation phenotypes again correlate with the epistasis of the ageing phenotypes for these two mutants, suggesting an indirect effect.

Both the higher order and nucleosome-scale chromatin phenotypes in the *ydr026cΔ* mutant can be rescued by deletion of *SIR2*, hence suggesting an effect not directly mediated by presence of functional Ydr026c. Conversely, the transcriptional silencing effects observed over the spacer region are not subject to this epistasis, providing the possibility that these are directly regulated by Ydr026c and Sir2 respectively. If this is the case, a mechanistic model whereby these transcripts are responsible for regulating the downstream phenotypes (specifically: chromatin behaviour, rDNA inter-hot-spot recombinogenicity, and physiological longevity) is a potentially fruitful hypothesis.

If such a mechanism exists, a pre-requisite is that the epistatic relationship between Ydr026c and Sir2 must be reflected in the biology of the mechanism. One line of evidence for such an effect is given by the interference of *YDR026C* deletion upon the Sir2-repressed antisense transcript originating from the E-promoter. In the wild-type background, this transcript is of very low abundance and is effectively undetectable. Deletion of the gene encoding exosome component Rrp6 allows low levels of the transcript to be detected under normal conditions. When *YDR026C* is removed in this background, as well as the accumulation of the sense transcript normally observed, considerable suppression of the antisense transcript is seen. Such an effect does not occur in *sir2Δ* background, where very high levels of the antisense transcript are detectable.

Hence, a simple mechanism of epistasis appears to be established in the rDNA spacer region transcripts. Appearance of the sense transcript (or the processed end of the 35S

rRNA transcript) is repressed by Ydr026C. When Ydr026C is missing, this transcript can suppress the antisense E-promoter transcript, potentially through transcriptional interference at the E-promoter. If *SIR2* is deleted, however, strong desilencing of this antisense transcript occurs, and high levels of it accumulate in wild-type of *ydr026cΔ* backgrounds. A natural corollary of this is that the prediction that the physiological phenotypes of the *ydr026cΔ* and *sir2Δ* mutants – modified rates of recombination and ageing – may be downstream consequences of the transcriptional activity at the rDNA spacer region.

8 Overexpression of rDNA spacer transcripts

8.1 Introduction

Strains lacking the lysine deacetylase *SIR2* exhibit several phenotypes indicating profound dysregulation of the rDNA. *sir2Δ* strains exhibit loss of silencing RNA polymerase II over the rDNA array, leading to derepression of short transcripts originating from the spacer region between each repeat (Li et al., 2006). Concomitant with this, *sir2Δ* strains also exhibit greatly elevated levels of unequal recombination at the recombinogenic hotspot proximal to the terminator of the main 35S rRNA transcript, increased accumulation of ERC species and reduced replicative lifespan (Gottlieb and Esposito, 1989; Kaeberlein et al., 1999). This study has also demonstrated strongly and reproducibly reduced chronological lifespans in *sir2Δ* mutants. Activity of the recombination hotspot has long been recognised to be largely dependent upon the replication fork-blocking protein, Fob1.

This study has demonstrated that the largely uncharacterised putative DNA binding protein Ydr026c possesses a consensus binding site proximal to the Fob1 binding region and also promotes recombinogenicity. Recent work has shown that *in vivo* Ydr026c and Fob1 appear to bind in close proximity at this locus (Ha et al., 2012). In the *ydr026cΔ* mutant, evidence has been found for a novel lifespan extension phenotype in both the replicative (chapter 6) and chronological (chapter 4) domains of ageing. Epistasis analysis indicates that *sir2Δ* influences the ageing phenotypes downstream of *ydr026cΔ*, and that (for replicative longevity only) *fob1Δ* is downstream of both of these mutations. Molecular biological phenotypes affecting the rDNA: ERC formation (section 6.4), rDNA spacer hot-spot recombinogenicity (section 6.3), chromatinisation (section 7.3), higher order structures juxtaposing rDNA repeats (section 7.4) and small rDNA spacer transcript accumulation (section 7.2) – have been found to correlate with the physiological ageing phenotypes.

Previous work has associated RNA polymerase II-derived *SIR2*-repressed short non-coding transcripts emanating from the rDNA spacer region in maintenance of copy number and recombination of the rDNA array. The spacer transcripts repressed by Sir2 were found to be associated with several chromatin modifications and disruption of cohesin association at the locus (Li et al., 2006). Kobayashi *et al* demonstrated that bidirectional transcription from the E-promoter repressed by *SIR2* was sufficient for rDNA copy number expansion in yeast. By replacing the E-promoter with a galactose-driven promoter in a strain containing reduced rDNA copy number, it was demonstrated that transcription-dependent expansion of the genomic rDNA array occurred upon induction of expression (Kobayashi and Ganley, 2005a). The transcripts produced emanated from both sides of the E-promoter and resembled the IGS1-R and IGS1-F transcripts observed in *sir2Δ* mutant strains. When transcription from this locus was repressed in non-inducing conditions, *SIR2* deletion did not produce the usual rDNA instability phenotype. In this case, cohesin association with the *Cohesin-associated region* (CAR) was found to negatively correlate with transcription from the E-promoter in strains with actively expanding rDNA repeats. Kobayashi *et al* therefore hypothesised that cohesin recruitment, disrupted by IGS1-F transcription in *sir2Δ* mutants, was responsible for preventing unequal recombination between sister chromatids and variations in rDNA copy number.

Houseley *et al* demonstrated that one of the rDNA spacer region transcripts spanning the fork-blocking region, IGS1-R, was regulated by the yeast TRAMP complex component *TRF4*. Deletion of *TFR4* leads to accumulation of this transcript, but not the transcripts spanning the CAR, IGS1-F and IGS2-R (Houseley et al., 2007). TRAMP activity targets aberrant RNAs to the exosome leading to their immediate degradation within the nucleoplasm (Houseley et al., 2006). Trf4 was found to associate specifically with the IGS1-R locus in an RNA polymerase II-dependent manner, suggesting co-transcriptional recruitment of Trf4 to elongating IGS1-R transcript. *trf4Δ* mutants exhibit sporadic rDNA

repeat length changes, distinct from the hyperrecombinogenic instability observed in *sir2Δ* strains or mutants of the DNA-damage response such as *top1Δ*; and no hyperrecombination phenotype at the rDNA hotspot is observed in the *trf4Δ* mutant strain (Houseley et al., 2007). Interestingly, no change in cohesin deposition was observed in the *trf4Δ* mutant, suggesting a cohesin-independent pathway of rDNA repeat number instability in this case.

Based upon this previous work and the data presenting in chapter 7, a working model for the mechanism of rDNA maintenance dysfunction in the *ydr026cΔ* and *sir2Δ* strains hypothesises regulation by the small RNAs produced in the spacer region can be constructured. Sir2 represses RNA polymerase II-dependent transcript generation in the direction of the recombinogenic hotspot, and this transcript is appears to be responsible for mediating the hyperrecombinogenic phenotype observed in *sir2Δ* mutants. Transcription across the fork-blocking region may promote recombination by enhancing Fob1-association, modifying the local chromatin environment, or changing the balance of cohesin recruitment at the spacer region as suggested by Housely *et al* (Houseley et al., 2007). The transcript repressed by Ydr026c interferes with production of this Sir2 repressed transcript, so antagonising downstream recombinogenicity. The correlative data presented in the previous chapters strongly suggests a functional relationship between the various phenotypes, but establishing underlying cause and effect mechanisms is more difficult, as the regulatory order (if any) of the described molecular events is difficult to establish.

In the case of *cis* acting non-coding RNAs in yeast, dissection of expression regulation has been complicated by the fact that directly engineering the promoter of the non-coding RNA to modulate expression levels generally has undesirable effects on expression of nearby genes, which become difficult to disambiguate from the intervention upon the non-coding RNA. For *trans*-acting non-coding RNAs, evidence of causative regulation is more direct.

Two broad lines of evidence can be demonstrated for *trans*-activity of a non-coding RNA rather than *cis*. Firstly, ectopic overexpression of the RNA (under the correct conditions, given variations in processing, localisation of the RNA to cellular compartments such as the nucleoplasm or cytoplasm, and degradation) should be predicted to modulate the expression of the reporter gene. Secondly, disruption of degradative processes – for example those mediated by the exosome in the nucleus or Xrn1 in the cytoplasm – should raise the steady-state levels of accumulated transcript, which should then regulate expression of the reporter target.

To test whether the small transcripts of the spacer region are responsible for the recombination and other downstream phenotypes – whether through the process of transcription itself, or through steady-state levels of accumulated transcript – a series of interventional experiments were designed to allow controlled transcription of the *SIR2* repressed antisense RNA IGS1-R. If this spacer transcript is responsible for the rDNA recombinogenic phenotype of the *sir2Δ* mutant in yeast and the non-coding RNA can operate in *trans* in addition to *cis*, then the model would predict (other factors, such as compartmentalisation, being equal) that the hyperrecombinogenic phenotype of *sir2Δ* mutants would be reconstituted in wild-type cells expressing the non-coding RNA from this construct: i.e. high levels of *ADE2* marker loss as measured by the half-sectored colony assay; short replicative lifespan as measured by individual cell microdissection; and rescued rDNA array loop phenotype in the *ydr026cΔ* background.

To test the hypothesis, a series of plasmids were constructed expressing a sequence homologous to the fork-blocking region of the rDNA spacer under control of a galactose-inducible promoter *in trans*. The high-copy 2-micron based pYES2 plasmid was chosen as an expression vector as this construct has been shown not to asymmetrically segregate to mother cells (Falcon and Aris, 2003).

A 733 bp stretch of the FBR locus was blunt-end cloned in both antisense (corresponding to *SIR2*-repressed IGS1-R) and sense (corresponding to IGS1-S) directions into vector pYES2 to produce plasmids pYES2-FBR(F) and pYES2-FBR(R) respectively (**Figure 45**). Expression of the insert is under galactose-inducible control of a modified (leaky) *GAL1* promoter, and terminated by the strong *CYC1* terminator. All strains containing expression vectors were maintained on complete synthetic medium without uracil for plasmid maintenance.

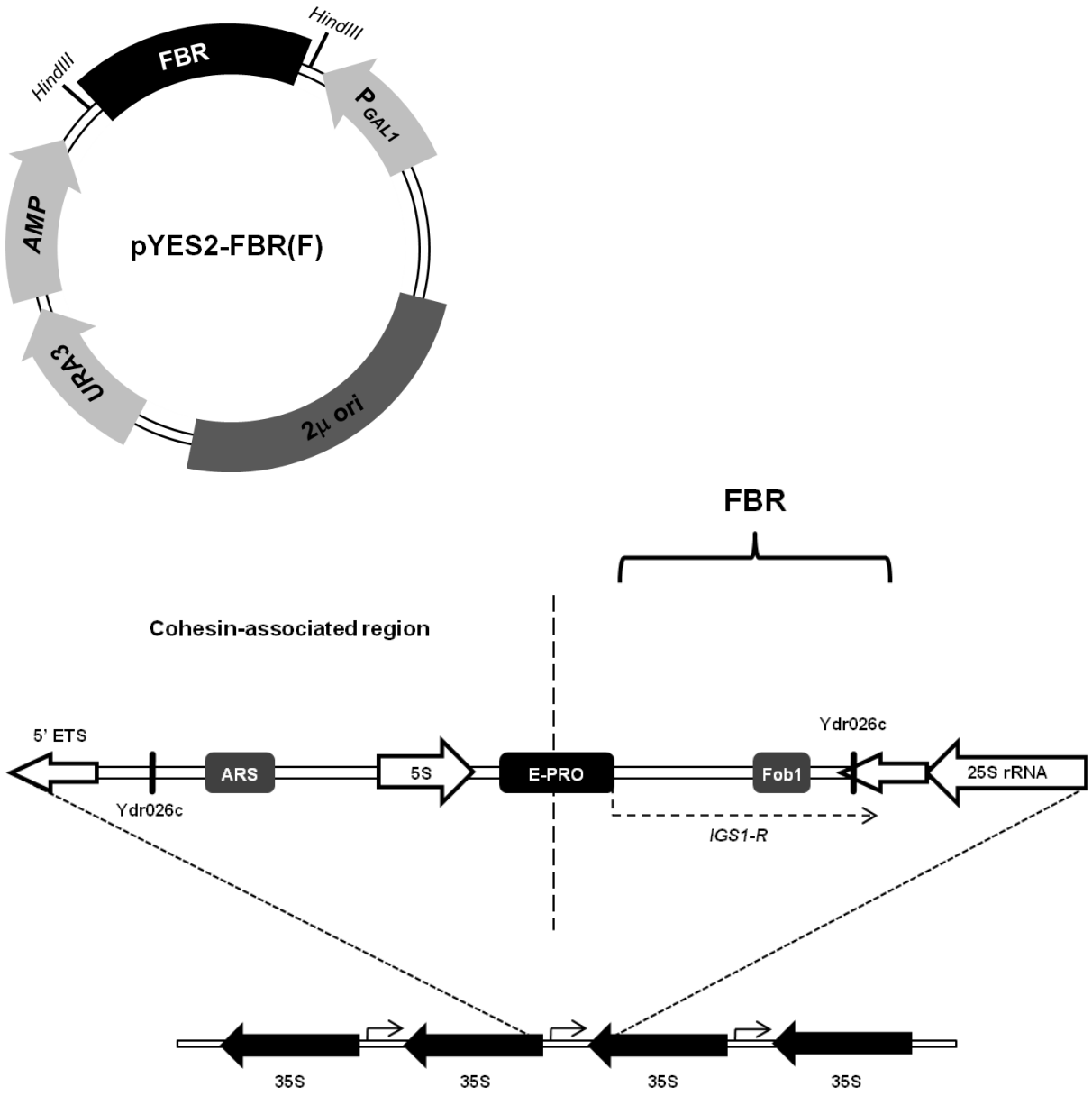

Figure 45. Vector construction for galactose-inducible overexpression of the non-coding rDNA spacer transcript IGS1-R in sense and antisense orientation. Vectors pYES2-FBR(F) and pYES2-FBR(R) were constructed by blunt-end cloning of a 733 bp region corresponding to a region of the rDNA spacer locus stretching from the edge of the E-promoter to 223 bps beyond the putative Ydr026c binding site proximal to the main 35S transcript terminator (the fork-blocking region, or *FBR*) into the empty 2μ-based expression vector pYES2 digested with *HindIII*. Constructs were verified by PCR, restriction digest analysis and sequencing, and *in vivo* induction of transcription validated by northern blot analysis using probes homologous to the respective non-coding transcript incorporated into the expression vector.

8.2 Reconstitution of *sir2Δ* phenotype: recombinogenicity

To test the level of recombinogenicity in wild-type strains overexpressing the IGS1-R non-coding RNA, empty vector pYES2 and pYES2-FBR(F) were transformed into the W303R background carrying the *ADE2* marker embedded within one rDNA repeat on chromosome XII for both wild-type and *sir2Δ* strains. Selective minimal media logarithmic cultures supplemented with 2% galactose of strains carrying were prepared, diluted, and plated onto appropriate minimal medium for the development of red pigment in ade- colonies following incubation. It was determined that supplied csm-uracil medium contained adenine at 40 mg/ml which suppressed the adenine biosynthetic pathways and did not lead to development of red colouration in Ade^- strains; therefore a customised csm-ura medium containing reduced adenine (20 mg/ml) was used for reliable half-sectored colony assay. Colonies were allowed to grow for 3 days at 30^OC, and then left at 4^OC for two days to allow further colour development.

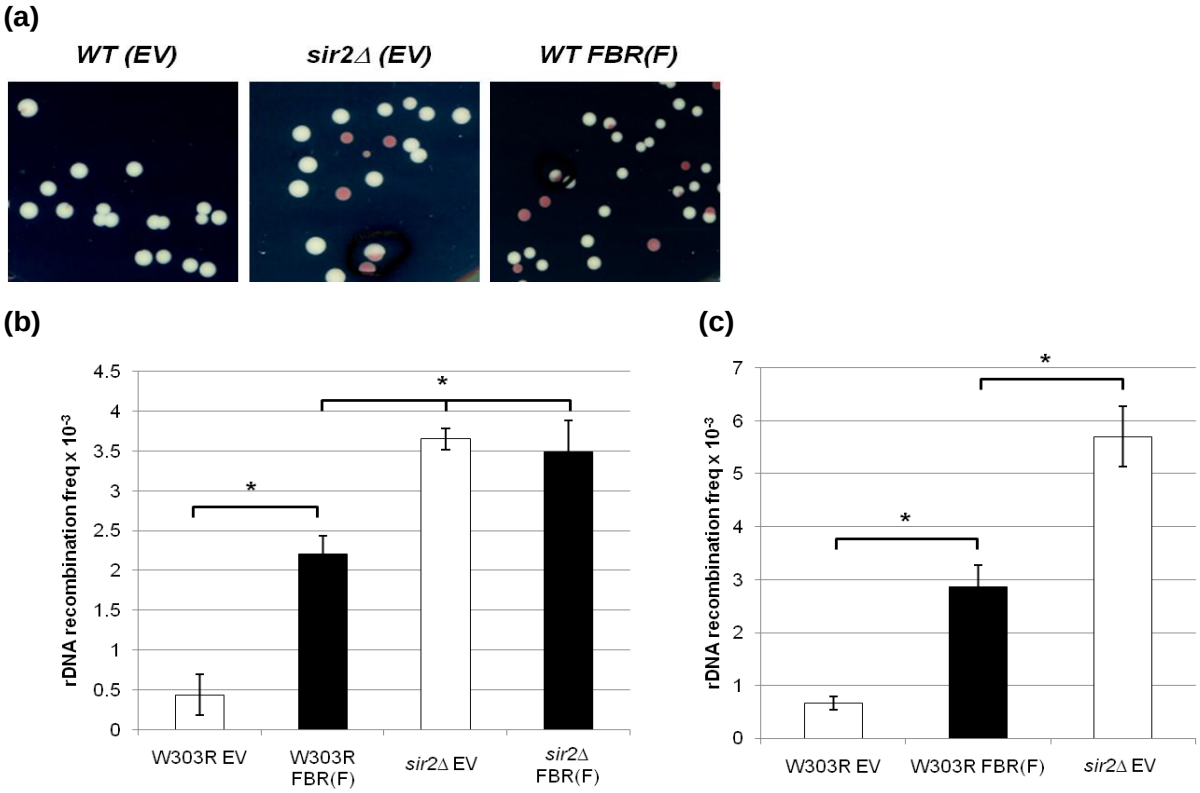

Error bars represent standard error. * p < 0.05. n = 3 biological replicates for >5000 colonies per strain.

Figure 46. rDNA recombination rates as assayed by integrated *ADE2* marker loss on initial cell divisions in wild-type and *sir2Δ* strains containing empty vector pYES2 (*EV*) or constructs expressing the non-coding rDNA spacer transcript IGS1-R in antisense [pYES2-FBR(F)] orientation. **(a)** Representative colonies grown from single *RDN1::ADE2* cells in the wild-type and *sir2Δ* backgrounds containing empty vector or expression constructs. Cells remaining ADE+ appear white; reversion causing loss of the *ADE2* cassette leads to accumulation of red pigment. Very few revertants are visible in the wild-type strain carrying the empty vector. The hyperrecombinogenic mutant *sir2Δ* carrying the empty vector yields a high number of cells already revertant before plating (wholly red colonies) as well as reverting during the first or subsequent cell divisions (sectored colonies). Strikingly, the wild-type strain carrying the forward orientation vector pYES2-FBR(F) demonstrates similarly high levels of reversion. **(b)** Quantification of unequal recombination rates in wild-type and *sir2Δ* strains carrying empty and expression vector constructs induced in galactose-containing medium. Wild-type cells carrying empty vector demonstrate basal recombination rate of ~$0.5x10^{-3}$ reversion events per cells division; the *sir2Δ* strain exhibits elevated rates of >$3.5x10^{-3}$ reversion events per cells division, with no significant difference between constructs. However, wild-type cells carrying the forward (sense) orientation pYES2-FBR(F) vector demonstrated a significantly enhanced recombination rate of $2.2x10^{-3}$ reversion events per cell division, reconstituting >50% of the recombination phenotype of the *sir2Δ* mutant. **(c)** Quantification of unequal recombination rates in non-inducing medium containing glucose as a carbon source. Even under non-inducing conditions, the wild-type strain overexpressing the FBR(F) antisense transcript exhibits significantly enhanced frequency of recombination, reconstituting ~50% of the *sir2Δ* phenotype. Generally higher recombination rates are observed throughout, probably a consequence of differential growth rate using the more favourable carbon source.

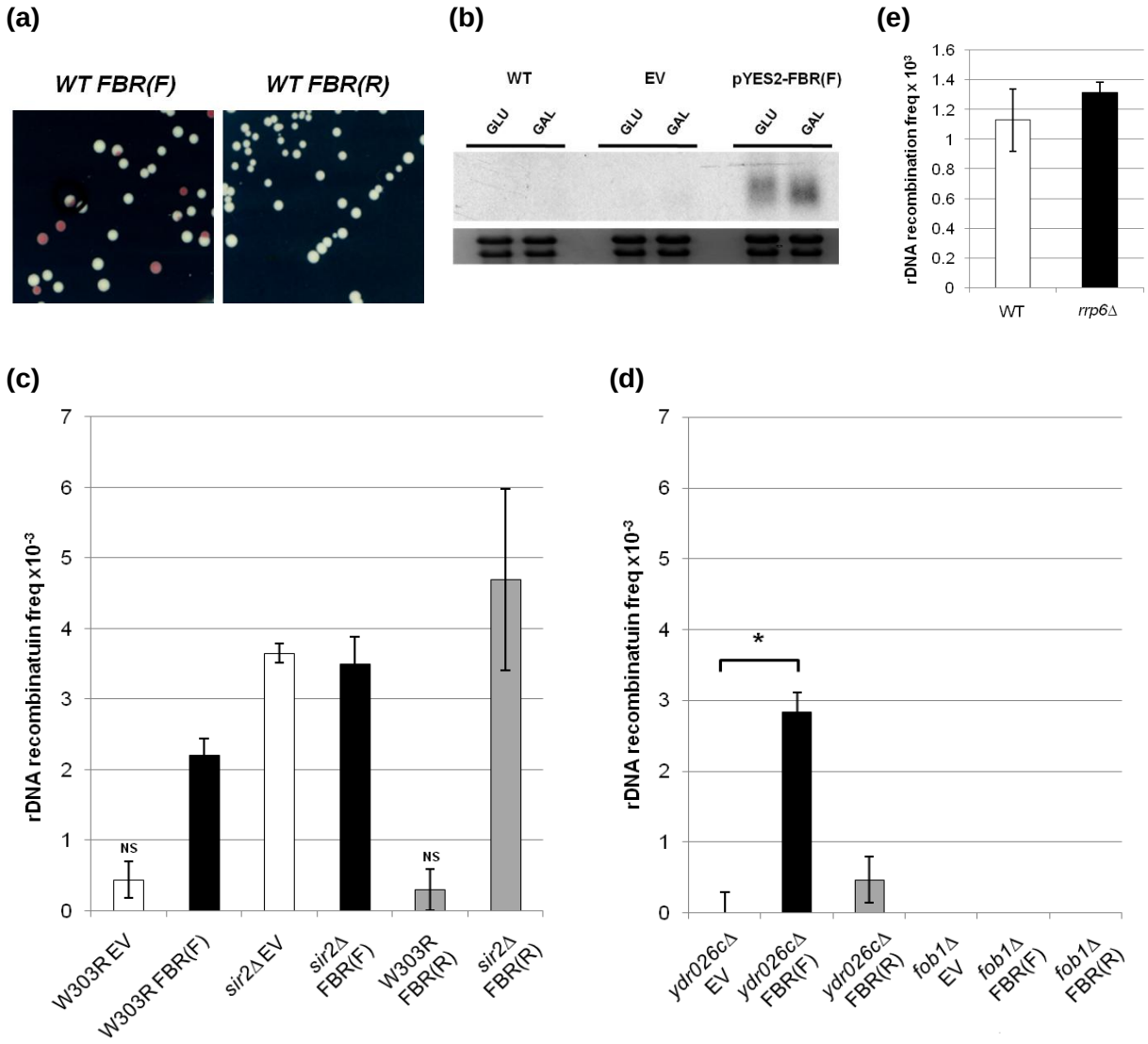

* $p < 0.05$. NS = Not significant compared to EV.

Figure 47. rDNA recombination in wild-type, *sir2Δ*, *ydr026cΔ*, and *fob1Δ* strains containing empty vector or constructs expressing IGS1-R in forward [pYES2-FBR(F)] and reverse [pYES2-FBR(R)] orientations. **(a)** Representative colonies grown from single *RDN1::ADE2* cells in the wild-type backgrounds containing empty vector or expression construct demonstrating lack of recombinogenic phenotype in the strain expressing FBR in the reverse (sense) direction. **(b)** Sense-specific northern blot to determine steady-state transcript presence in strains containing the expression vector FBR(F), empty vector and wild-type controls under both non-inducing (glucose) and inducing (galactose) conditions. Considerable transcript is produced from the vector under non-inducing conditions, verifying leakiness of the construct promoter. **(c)** Quantification of unequal recombination rates in wild-type and *sir2Δ* strains carrying empty and expression vector constructs. Strains expressing the reversed (sense) transcript from the FBR(R) exhibit recombination frequencies not significantly different from empty vector controls, both in the case of wild-type background and the *sir2Δ* mutant. **(d)** Quantification of recombination frequencies in *ydr026cΔ* and *fob1Δ* strains carrying empty and expression vector constructs. *ydr026cΔ* cells expressing the IGS1-R transcript (*FBR(F)*) significant enhancement of rDNA recombination was observed while in the *fob1Δ* background recombination rate remained undetectably low when containing this construct. **(e)** rDNA recombination frequency in a *rrp6Δ* strain demonstrates no significant elevation above WT.

A strong and reproducible rise in both half-colony and pre-reverted red colony incidence was observed in a wild-type strain carrying the pYES2-FBR(F) vector and overexpressing the FBR(F) non-coding RNA compared to an isogenic strain carrying the pYES2 empty vector under inducible conditions (**Figure 46a**). Quantification of half-colony incidence showed that the wild-type strain carrying empty vector demonstrated a baseline of $0.5x10^{-3}$ reversion events per cell division, with the same background carrying pYES2-FBR(F) yielded a significantly higher recombination rate of $2.2x10^{-3}$ events per cell division (**Figure 46b**). Analysis of recombination rate in *sir2Δ* strains carrying the empty vector or pYES2-FBR(F) did not demonstrate any significant difference. This data suggests that the rate of reversion in the wild-type strain carrying the pYES2-FBR(F) vector reconstituted around 60% of the magnitude of the hyperrecombination phenotype in the equivalent *sir2Δ* strain, a significant effect.

As a control, recombination rates were also measured under non-inducing conditions (glucose as medium carbon source). If expression of the transcript from the pYES2-FBR(F) expression vector is responsible for the partial reconstitution of the *sir2Δ* phenotype, then no effect should be seen when expression is not induced. However, a phenotype of similar magnitude could be observed when unequal recombination frequency was assayed in a wild-type strain containing the pYES2-FBR(F) construct under non-induced conditions (**Figure 46c**) with ~50% of the magnitude of the hyperrecombinogenic *sir2Δ* phenotype reconstituted under these conditions. Interestingly, recombination frequencies were generally higher in cells grown in glucose, possibly related to the increased growth rate under this more favourable carbon source.

8.3 Sense specificity and transcript dependency

The previous observation raises (1) the possibility that transcription or transcript accumulation is not responsible for the reconstitution of the *sir2Δ* hyperrecombinogenic phenotype in strains containing this construct, and (2) the potential that presence of the construct itself may drive enhanced recombination frequency. To investigate this question, wild-type and *sir2Δ* mutant strains were transformed with a further pYES2-derived construct containing an inverted version of the FBR(F) insert. This vector was termed pYES2-FBR(R) and overexpresses the sense FBR transcript (IGS1-S).

Wild-type strains containing this expression vector were not found to have a significantly higher unequal recombination phenotype compared to the empty vector control (**Figure 47a, c**). Similarly, no significant difference was observed in rDNA recombinogenicity in *sir2Δ* mutant strains containing empty vector or pYES2-FBR(R). This implies that the sense of the insert relative to the promoter – i.e. the direction of transcription – is responsible for the reconstitution of recombinogenicity observed in pYES2-FBR(F) containing wild-type strains. To further investigate the occurrence of high recombination in non-induced strains, northern analysis with sense-specific radiolabelled probes homologous to the FBR region was performed on RNA extracted from wild-type strains containing pYES2 empty vector, FBR(F), or FBR(R) (**Figure 47b**). While higher levels of transcript were detected under induced conditions, considerable transcript remained detectable under completely non-induced conditions, suggesting that not inconsiderable transcription was taking place, and that this may underlie the residual hyperrecombinogenic phenotype in this state.

To further investigate the introduction of hyperrecombination in strains carrying the FBR(F) vector, empty vector, pYES2-FBR(F), and pYES2-FBR(R) was transformed into

W303R strains null mutant for Ydr026c and Fob1, both of which demonstrate hyporecombination phenotypes. Recombination rate was assayed by half-sectored colony assay under the medium conditions described above. Quantified rate was extremely low in the *fob1Δ* mutant carrying the empty vector, as expected (**Figure 47d**). *fob1Δ* mutants carrying the pYES2-FBR(F) and pYES2-FBR(R) vectors did not exhibit any elevation in recombination rate, similar to the phenotype observed in the double *sir2Δ fob1Δ* mutant in chapter 3. As demonstrated above, in the case of strains mutant for *YDR026C* recombination rate is reduced, but deletion of *sir2Δ* reconstitutes the hyperrecombination phenotype observed in the *sir2Δ* mutant alone. This epistasis could be reconstituted using strains carrying the FBR expression vectors. *ydr026cΔ* strains carrying the empty vector or pYES2-FBR(R) exhibited reduced recombination rates; while *ydr026cΔ* strains carrying pYES2-FBR(F) demonstrated recombination rate enhanced to close to the levels observed in the wild-type strain carrying the same expression vector (**Figure 47d**).

8.4 Transcript action in *cis*

The possibility remains that highly active transcription of the expression construct, in the correct (forward) sense, leads to hyperrecombination through participation of the vector itself as a recombinogenic hotspot. To investigate whether the FBR(F) transcript can also partially reconstitute the *sir2Δ* hyperrecombinogenic phenotype in *trans*, frequencies of unequal recombination were measured in the W303R strain mutant for the exosome component Rrp6 responsible for the degradation of many nuclear non-coding RNAs. In section 7.2 it was demonstrated that steady-state levels of the FBR(F) transcript accumulate several-fold in strains containing the *rrp6Δ* mutant. If transcript levels, rather than transcription, is responsible for the phenotype, enhanced recombination rates should be observed in this strain. In fact, no enhancement of rDNA recombination frequency above wild-type is observed (**Figure 47e**). This suggests that the FBR(F) overexpressed transcript is not operating in *trans* in activating higher levels of inter-rDNA hotspot recombination, but rather transcription in *cis* over the fork-blocking region in the expression vector activates the vector for recombination with the genomic rDNA array.

8.5 Replicative longevity

rDNA chromosomal instability and shortened replicative lifespan in *sir2Δ* mutants has been partially attributed to hyperrecombination at the rDNA. To determine whether the reconstituted hyperrecombinogenic phenotype observed in wild-type strains containing pYES2-FBR(F) would lead to reduced replicative longevity, a series of microdissection experiments were performed on strains carrying the expression vectors above. n>25 Individual cells were plated out as above, virgin mother cells prepared, and daughters produced recorded. Minimal medium for plasmid maintenance was used supplemented with 2% galactose carbon source to induce expression. Under these conditions replicative lifespans were found to be somewhat shorter than on rich medium: a wild-type strain containing the empty vector demonstrated a median replicative lifespan of 11.7 generations. Wild-type strain containing the pYES2-FBR(R) vector did not exhibit any significant change in replicative longevity (median lifespan 12.5 generations), as might be expected from its equivalent recombination rate (**Figure 48**). However, the wild-type strain expressing the FBR(F) region demonstrated a strong and significant increase in the rate of replicative senescence (median RLS 8.6 generations). The *sir2Δ* mutant, carrying the empty vector, exhibited a dramatically shortened replicative lifespan of median 4.4 generation. Hence, the introduction of an overexpression FBR(F) non-coding RNA could again reconstitute around 50% of the phenotype observed in a mutant lacking SIR2.

(a)

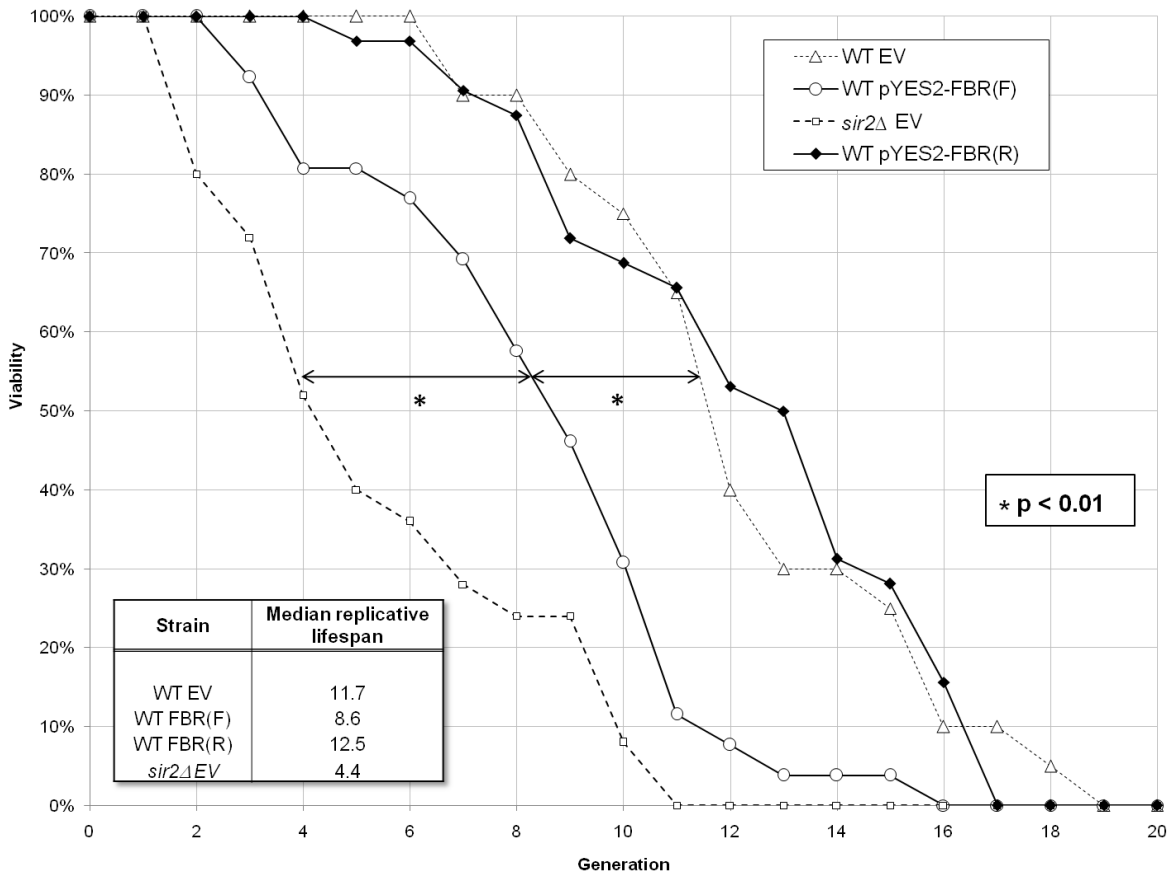

Figure 48. Replicative lifespans of wild-type strains carrying empty pYES2 vector *(EV)*, pYES2 expressing the IGS1-R non-coding spacer transcript in forward [pYES2-FBR(F)] and reverse [pYES2-FBR(R)] orientations, and a *sir2Δ* mutant strain carrying the empty pYES2 vector, measured by microdissection. **(a)** n > 25 individual virgin mother cells of each strain were plated onto complete synthetic medium without uracil and supplemented with 2% galactose carbon source to induce construct expression using a micromanipulator. Cells were inspected every 90 minutes and new daughters removed by microdissection. Cells which had failed to produce any daughters for three contiguous inspections were deemed to have succumbed to replicative senescence and were censored. Growth on minimal medium was found to lead to a marked drop in replicative viability compared to rich medium. Wild-type cells carrying the empty vector and pYES2-FBR(R) construct demonstrated a median replicative lifespan of 11.7 and 12.5 generations respectively, with no significant difference between the viability loss rate in each strain. However, wild-type cells carrying the pYES2-FBR(F) plasmid were found to demonstrate a strong and significant reduction in replicative longevity, exhibiting a median replicative lifespan of 8.6 generations. In comparison, the short-lived *sir2Δ* mutant strain showed a shortened median replicative lifespan of only 4.4 generations, significantly shorter than all wild-type constructs. Overexpression of the IGS1-R non-coding transcript in the wild-type strain carrying pYES2-FBR(F) was again sufficient to reconstitute ~50% of the phenotype of the *sir2Δ* strain. Statistical comparisons were made using the log-rank test for mortality; median replicative lifespans were calculated by using linear interpolation of mean-smoothed viability curve data at 50% replicative viability.

8.6 Higher order chromatin structure

An additional phenotype observed in the *sir2Δ* strain earlier in this study is the rescuing of the whole-locus long-distance chromatin organisation over repeats of the rDNA cassette in the *ydr026cΔ* mutant as measured by chromosome conformation capture (3C). The wild-type locus exhibits a strong and specific interaction between the promoter and terminator of the main rDNA 35S transcript. This interaction is abrogated in the *ydr026cΔ* mutant, but appears to be rescued in strains additionally lacking *SIR2*. To test whether this phenotype could be reconstituted by the pYES2 vector expressing the FBR(F) region, cross-linked chromatin was extracted from wild-type, *ydr026cΔ* and *sir2Δ ydr026cΔ* strains carrying the pYES2 empty vector, pYES2-FBR(F), and pYES2-FBR(R). Chromatin was subject to 3C analysis as above: restriction enzyme *BfaI* was used to digest, 3C products were subject to PCR and separated on agarose gels, and product signals quantified by phosphorimager analysis of Southern blots hybridised to radiolabelled probes homologous to a region contained in all 3C products derived from this locus (**Figure 49**). The strong promoter-terminator chromatin juxtaposition signal was again observed in the wild-type strain carrying the empty pYES2 vector, and this signal could be seen to be abrogated in the *ydr026cΔ* mutant strain carrying the pYES2 empty vector and rescued in the *sir2Δ ydr026cΔ* double mutant with pYES2 empty vector. However, when chromatin from *ydr026cΔ* strain carrying the pYES2-FBR(F) expression vector was analysed, the promoter-terminator 3C interaction appeared to be strongly reconstituted. Quantification and combination of biological repeats verified that the promoter-terminator juxtaposition was significantly elevated above the baseline expected signal at that distance. This similarly suggests that this aspect of the *sir2Δ* phenotype can also be reconstituted by overexpression of this transcript.

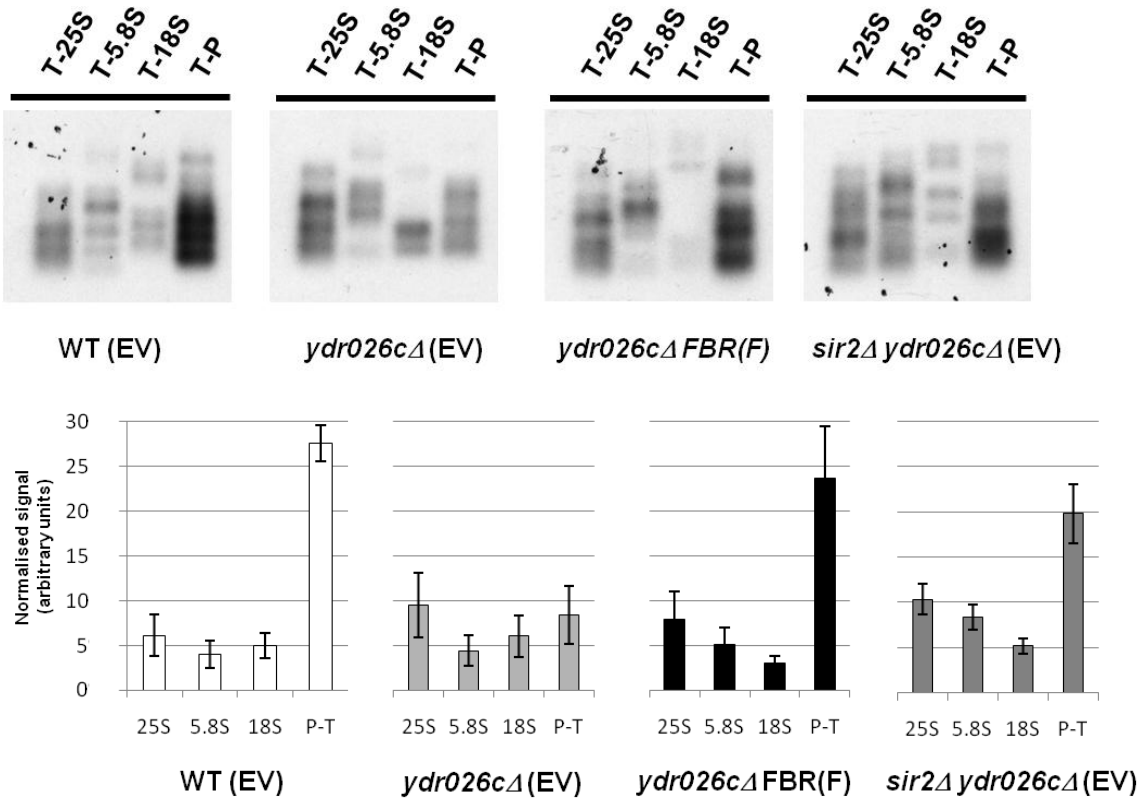

n = 2 biological replicates. Error bars represent standard error.

Figure 49. Higher order chromatin organisation over the rDNA locus in wild-type, *ydr026cΔ*, and *sir2Δ ydr026cΔ* cells containing pYES2 empty vector (*EV*) or the construct overexpressing the non-coding rDNA spacer transcript IGS1-R *FBR(F)* determined by chromosome conformation capture (3C). **(a)** Quantified southern blots of 3C PCR products for wild-type, *ydr026cΔ*, and *sir2Δ ydr026cΔ* strains carrying empty vector and *ydr026cΔ* carrying pYES2-FBR(F). Logarithmic phase cultures in minimal medium supplemented with 2% galactose to induce construct expression were harvested, crosslinked, and chromatin digested with enzyme *BfaI*. Samples were religated at low concentration and 3C products detected by nested PCR with primers shown in **Figure 42**a. PCR products were Southern blotted, hybridised to a radiolabelled universal probe, and quantified using a phosphorimager system. The wild-type strain recapitulates the strong juxtaposition peak of the promoter and terminator (P-T) of the 35S rRNA reading frame significantly above background. This interaction is abrogated in the *ydr026cΔ* mutant containing empty vector, but as before can be rescued by the deletion of *SIR2* in the *sir2Δ ydr026cΔ* strain containing empty vector. This phenotype of the *sir2Δ* mutant could be recapitulated by overexpression of the IGS1-R transcript from the pYES2-FBR(F) vector in the *ydr026cΔ* background.

8.7 Discussion

A series of experiments were carried out to assay the various rDNA misregulation phenotypes exhibited by strains mutant in *SIR2*: rDNA hotspot hyperrecombination, short replicative longevity, and rescue of higher order chromatin structure in the *ydr026cΔ* background, in a wild-type strain overexpressing an rDNA spacer transcript derepressed when *SIR2* is not present. Initial results demonstrated that the characteristic *sir2Δ* phenotypes could indeed be partially (50-60%) reconstituted when this region was overexpressed from a high-copy 2μ-based expression vector induced by galactose. These phenotypes were robust, reproducible and statistically significant, suggesting a functional role for this transcript as it spans the recombinational hotspot near the Fob1 and putative Ydr026c binding sites.

The observation that the phenotype remains, at comparable strength, in the same strains under non-inducing conditions was initially puzzling. Because the pYES2-FBR(F) construct itself contains the recombination hotspot, Fob1 and Ydr026c binding sites, the possibility remained that the presence of high copy numbers of this vector would promote recombination between the vector and the genomic rDNA array (containing the marker used to assay inter-rDNA recombination), leading to artificially enhanced recombination rates and downstream phenotypes (reduced replicative longevity, restitution of higher order chromatin structure). Alternatively, residual leaky expression from the modified *GAL1* promoter present in pYES2 could be sufficient to drive the phenotype: expression has previously been reported from pYES2-derived expression vectors under non-inducing conditions (Kristoffersen et al., 2000).

To distinguish between these two possibilities, two lines of evidence were pursued. Firstly, northern analysis indicated that considerable expression of the insert was indeed occurring

from the expression construct under non-inducing conditions. Secondly, an additional expression vector was constructed containing an inverted FBR insert. No hyperrecombination (or reduced longevity) phenotype was observed in strains containing this expression vector under induced or non-induced conditions, and these strains were more generally indistinguishable from strains carrying the pYES2 empty vector. This result suggests that the hyperrecombination phenotype observed in strains containing the pYES2-FBR expression constructs is dependent upon the orientation of the insert relative to the promoter and terminator of the vector, and hence upon the sense of the transcript produced. Together, these data strongly suggests a transcript- or transcription-dependent partial reconstitution of the *sir2Δ* hyperrecombinogenic phenotype mediated by the antisense FBR(F) transcript.

In terms of rDNA hotspot recombination, the *sir2Δ* mutation is epistatic to the *ydr026cΔ* mutation, which is reduced from wild-type. It would therefore be predicted that overexpression of the FBR(F) transcript should also reconstitute the hyperrecombination phenotype in the *ydr026cΔ* background, and yield an rDNA recombination frequency significantly higher than wild-type. *ydr026cΔ* mutant strains containing the pYES2-FBR(F) indeed exhibit rDNA hotspot recombination markedly higher than the same background containing the empty vector pYES2, or the reversed insert pYES2-FBR(R). Similarly, in previous assays rDNA hotspot recombination was always dependent upon Fob1: *fob1Δ* backgrounds exhibit extremely low (almost undetectable) frequencies of rDNA recombination even when *SIR2* is deleted. Accordingly, *fob1Δ* strains containing the pYES2-FBR(F) expression vector did not demonstrate any enhancement of recombination frequency, and the same background containing pYES empty vector or the pYES2-FBR(R) reversed construct did not show a significantly different phenotype. Hence, elevation of inter-rDNA spacer hotspot recombination by the overexpressed FBR transcript appears to

be Fob1-dependent, and operate epistatically to deletion of *YDR026C*, in analogy with the phenotype of the *sir2Δ* mutant.

The above observations suggest that sense-specific transcription of the FBR portion of the rDNA spacer region in a high-copy expression vector is sufficient to reconstitute these identified phenotypes of the *sir2Δ* strain, and so suggest regulation of FBR transcript production from the E-promoter mediate the recombinogenic phenotype seen in strains lacking *SIR2*. However, the mechanism of action remains unclear in these experiments as to whether it is the act of transcription, or the transcript accumulation itself, that is responsible for the phenotype. Houseley *et al* also observed an rDNA array maintenance phenotype in a strain accumulating the IGS1-R transcript. *trf4Δ* mutant strains disrupt degradation of this specific transcript in the rDNA spacer region, and exhibit sporadic rDNA copy length changes. However, basal recombination frequency at the fork-blocking region was not found to be elevated in this strain, in contrast to mutants which demonstrate rDNA instability and repeat length heterogenization such as *sir2Δ* (Houseley et al., 2007). In *tr4Δ* strains, several mechanisms were proposed to explain the rDNA maintenance phenotype: interference with the balance of transcription occurring over the cohesin-associated region, activity of the TRAMP complex in suppressing unequal recombination, or action of the accumulated transcript itself. Because no rise in recombination frequency was observed when elevated levels of the IGS1-R transcript were present; in contrast to the clear enhancement observed when FBR(F) is overexpressed from the pYES2 construct and accumulates; this suggests that the hyperrecombinogenic phenotype in strains containing pYES2-FBR(F) does not occur in *trans*. The observation that when degradation of IGS1-R is slowed by deletion of the exosome component (Chlebowski et al., 2013) Rrp6 in a wild-type background, no such elevation of basal recombination rate is recorded, further implies that steady-state levels of IGS1-R or FBR(F) are not responsible for the hyperrecombinogenic phenotype. Maintenance of rDNA copy number has yet to be

measured in strains overexpressing FBR(F) – it would be predicted that due to hyperrecombination at the spacer hot-spot heterogenization of rDNA repeat lengths would be observed. Previous studies measuring reincorporation into the genomic array by recombination of minichromosomes containing entire rDNA repeats have demonstrated that this only occurs in *sir2Δ* strains (Benguria et al., 2003); recombinogenic disruption of the genomic rDNA array occurs here in the wild-type background carrying the pYES2-FBR(F) construct.

While the action of a transcript overexpressed from an ectopic vector is suggestive of a *trans*-acting effect, they do not rule out conceivable *cis*-acting mechanisms. Transfection of the high-copy vector effectively introduces large numbers of copies of the rDNA spacer region, containing the recombinogenic hotspot, into the cell. While it is clear that transcription of this region, in the correct sense, is required to activate it, it is possible that when this occurs these extra copies artificially elevate inter-spacer recombination with the genomic rDNA array and measured recombination frequencies. Because the 2μ origin of replication on the pYES2 vector lies close to the site of insertion of the FBR sequence; and the replication fork-blocking activity associated with Fob1 action at the FBR operates in a unidirectional manner (Kobayashi and Horiuchi, 1996); the contingency remains that blocking of plasmid replication fork occurs when the FBR sequence is inserted in the sense direction (FBR[F]) and not the antisense (FBR[R]). Fork stalling in this situation would then lead to recruitment of homologous recombination machinery and promoter recombination between the vector and the genomic rDNA array. In this model, transcription would be required to establish the correct chromatin state over the FBR region for fork-blocking and/or recombination to proceed effectively.

While many questions remain with regard to the mechanism leading to elevated recombination rates in strains overexpressing FBR(F), the strain represents a useful model to study the effects of interventional rDNA hyper-recombination upon the physiological

phenotypes predicted to occur downstream. While large amounts of correlative data suggest that rDNA instability leads to curtailed replicative lifespan, fewer studies have attempted to directly modify recombination frequency to find downstream physiological effects. Hyperrecombination has been induced by DNA damaging agents, which leads to shortened replicative longevity; more directly, studies on strains containing reduced rDNA arrays which exhibit enhanced rates of recombination also shows correlation with reduced lifespan (Wilson et al., 2008). The *sir2Δ* mutant accumulates greatly elevated levels of ERCs through rDNA spacer recombination, even in unaged cells. It was initially hypothesised that this ERC load became rapidly toxic to replicating mother cells, and that this lead to the greatly curtailed replicative lifespan of *sir2Δ* strains. More recent studies (see section 6.1) have cast doubt upon ERC operating as the primary driver of replicative senescence – rather they appear to be symptomatic of genomic instability at the rDNA in the *sir2Δ* strain, and it is this instability that leads to replicative ageing. To investigate whether the correlating short replicative lifespan phenotype observed in the *sir2Δ* could also be reconstituted by enhanced rDNA hotspot recombinogenicity as a result of FBR(F) overexpression, replicative longevity was measured in wild-type and *sir2Δ* backgrounds containing the pYES2-FBR(F) overexpression vector, control empty vector or the pYES2-FBR(R) vector containing the reversed insert. As has been previously reported, generally shorter replicative lifespans were measured on the restrictive, galactose-containing medium (Jarolim et al., 2004), but the *sir2Δ* mutant still exhibited strongly shortened replicative longevity. The concomitant short replicative lifespan associated with a partial reconstitution of the *sir2Δ* phenotype was observed in the wild-type strain containing the pYES2-FBR(F) vector, but not the control vectors. Interestingly, approximately 50% reconstitution of the *sir2Δ* phenotype was again observed.

A novel phenotype of *sir2Δ* mutants demonstrated in section 7.4 is the reconstitution of an rDNA-spanning higher-order chromatin structure observed in wild-type strains but disrupted in *ydr026cΔ* and *fob1Δ* backgrounds. This interaction is hypothesised to be a consequence of the resumption of inter-rDNA recombination in the *sir2Δ ydr026cΔ* strain, and so it would be predicted that the enhanced recombination in *ydr026cΔ* mutant strains containing the pYES2-FBR(F) expression construct would show resumption of the distinctive higher order juxtaposition as detected by 3C. As above, sufficient reconstitution of the phenotype does indeed occur to allow the promoter-terminator interaction to be reliably re-detected in the *ydr026cΔ* strain overexpressing FBR(F), but not the empty vector or reversed controls.

Together, these results suggest that modification of Fob1-dependent rDNA spacer hotspot recombination frequency and rDNA array stability is sufficient to change the physiological replicative longevity, ERC generation, and higher-order chromatin structure phenotypes – as observed in the *sir2Δ* and *ydr026cΔ.* In addition, that transcriptional activity over the fork-blocking region of the rDNA spacer region correlates with this recombination frequency in these strains. Finally, a construct containing a model rDNA spacer complete with transcription driven from a *GAL1* promoter and recombinational hotspot, suggests that transcription of IGS1-R from the spacer region is responsible for potentiating recombination at the hotspot.

9 Discussion

The results presented above provide evidence for a novel regulator of chronological and replicative longevity in *S. cerevisiae*: the poorly characterised putative DNA-binding product of *YDR026C* – and suggests that maintenance and regulation of the rDNA array constitutes an important part of the mechanism of its action and epistatic relationship with *SIR2*.

An initial screen of mutants extending chronological lifespan in yeast using a high-throughput screening methodology and novel analysis and identification algorithm identified the strain *ydr026cΔ*. The extended longevity in *ydr026cΔ* strains was found to be dependent upon function *SIR2*, *sir2Δ* mutations being epistatic to *ydr026cΔ*. Previous studies have reported both positive and negative effects on chronological longevity in *sir2Δ* strains (Fabrizio et al., 2005). High precision measurements from many replicates in the high-throughput system established the *sir2Δ* strain as being dramatically short-lived in the BY4741 background. *ydr026cΔ* appeared synergistic with mutations of the TOR pathway, well established to extend chronological longevity in numerous model systems including yeast (Bonawitz et al., 2007). The lifespan extending phenotype of *ydr026cΔ* was also found to be dependent upon acetic acid medium accumulation, suggesting Ydr026c plays a role in the caloric restriction response in yeast, but clearly genetically distinct from the established role of TOR pathway disruption in life extension.

Ydr026c is indentified as a putative Myb-like DNA-binding protein. Sequence comparison determined *YDR026C* to show considerable homology to the yeast transcription factor *REB1*, and be the closest paralog to the rRNA transcription termination factor 1 in mammals. This study also identified consensus Ydr026c binding sites, as determined by ChIP-on-chip data, flanking each copy of the yeast rDNA repeat (**Figure 21**). Previous

work suggested Ydr026c interacts *in vivo* with Fob1: a nucleolar protein implicated in unidirectional fork-blocking of rDNA replication; and Sir2, which plays a major role in RNA polymerase II-silencing over the rDNA; and that Ydr026c localises to the nucleolus. More recent work has determined that Ydr026c binds to the rDNA spacer region *in vivo*, and appears to regulate transcriptional silencing over the spacer region in concert with Fob1 and Sir2.

Several lines of evidence suggest that apoptotic and necrotic cell death as a result of failure of quiescence maintenance play an important role in establishing survival under conditions of chronological ageing in yeast (Gray et al., 2004). Isolation of quiescent and non-quiescent cell populations in ageing culture of a strongly short-lived strain *snf1Δ* allowed the development of a flow cytometry assay to determine genomic fragmentation. Apoptosis-like DNA fragmentation was strongly associated with non-quiescent subpopulations of cells, and in turn enriched in strains such as *snf1Δ* that fail to enter quiescence. Using this system to investigate the novel short-lived phenotype of the *sir2Δ* strain, early failure of quiescence, non-quiescent cell morphology; and enhanced apoptosis-like genome fragmentation could be observed. Some evidence was also present that the *ydr026cΔ* strain demonstrates enhanced quiescence maintenance, particularly in cell morphology.

Numerous parallels exist between interventions into chronological and replicative longevity in yeast (Longo et al., 2012). Sir2, in particular, has long been recognised as a regulator of replicative longevity. *ydr026cΔ* mutants were also found to demonstrate extended replicative longevity and show an equivalent epistasis with *sir2Δ*. It has been hypothesised that replicative longevity is largely determined by genomic stability of the rDNA locus in mother cells. *ydr026cΔ* strains show reduced levels of rDNA hotspot recombination frequency, while *sir2Δ ydr026cΔ* strains have enhanced recombination.

Fob1 is required for high recombination hotspot activity in each case. Extrachromosomal ribosomal circle generation – while controversial as a cause of replicative ageing – correlated with the recombination frequencies observed in these strains.

Production of non-coding RNA polymerase-II derived transcripts in the rDNA spacer region have been shown to be repressed by Sir2, and there is some evidence that activation of transcription of this locus in *sir2Δ* strains leads to disruption of cohesin association over the *cohesin association region* and a greater rate of unequal recombination, leading to rDNA copy number instability (Kobayashi and Ganley, 2005b). Sir2 also represses non-coding transcription over the fork-blocking region (Houseley et al., 2007). Recent evidence suggests that Ydr026c also represses transcription in this spacer region (Ha et al., 2012). A series of northern blots determined that Ydr026c suppresses transcription through the fork-blocking region, apparently as a continuation of the main rRNA transcript. In strains lacking *RRP6* and accumulating the Sir2-repressed transcript, deletion of *YDR026C* and derepression of the IGS1 (S) transcript appeared to lead to an inverse repression of the IGS1 (AS) transcript regulated by Sir2.

The latter data suggest a mechanism for the influence of *YDR026C* and *SIR2* upon the physiological phenotypes of rDNA hyperrecombination and replicative longevity – a possible model is depicted in **Figure 50a**. Sir2, as has been well documented, represses RNA polymerase II-driven transcription from the E-pro in the rDNA spacer region. This transcript spans the fork-blocking region, the putative binding sites of Ydr026c and Fob1, and the spacer region recombinational hotspot (Li et al., 2006). Our model predicts that the act of transcription over this region in *cis* leads to establishment of a chromatin environment in the fork-blocking region that potentiates hyperrecombination in a Fob1-dependent manner. The spacer transcripts IGS1-F and IGS2-R have previously been implicated in disruption of cohesin association with the rDNA spacer region, as a consequence leading to rDNA copy length heterogeneity (Kobayashi and Ganley, 2005a;

Huang et al., 2006). Disruption of degradation of the IGS1-R transcript specifically through *TRF4* mutation, has been also been shown to regulate rDNA copy number instability through a cohesin-independent mechanism (Houseley et al., 2007). Here, we show that overexpression of the IGS1-R transcript on a plasmid construct model of the rDNA spacer region is sufficient to drive hyperrecombination at the genomic rDNA locus. Predicted in these strains is high rDNA copy length, although this remains to be tested.

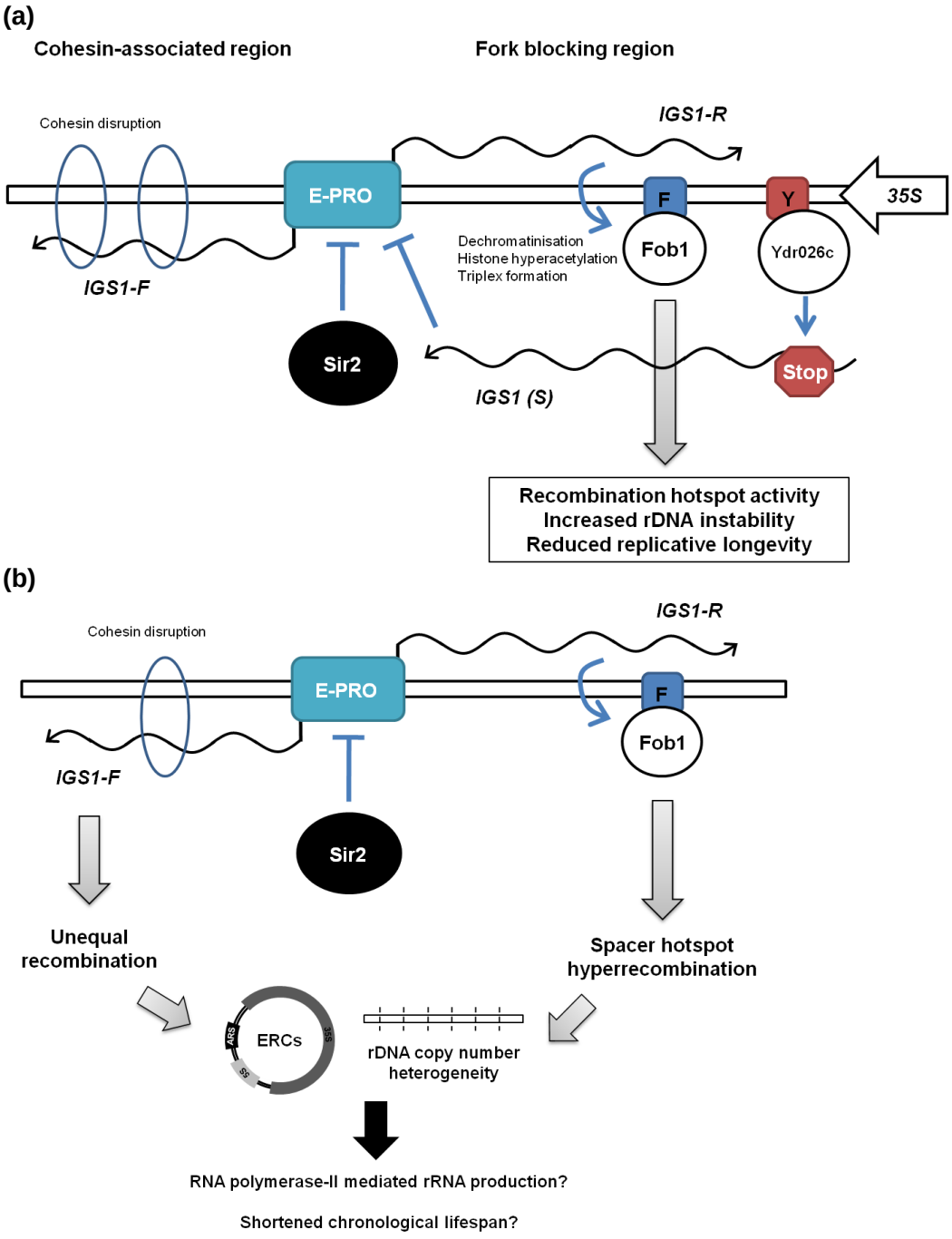

Figure 50. Mechanistic models. **F** and **Y** represent putative Fob1 and Ydr026c binding sites respectively.

The nature of the environment established by IGS-R transcription at the fork-blocking site remains speculative. Section 7.3 presents some evidence of high levels of dechromatinisation over the spacer region in the *sir2Δ* strain, although whether this is a causal or correlative effect remains to be established. *sir2Δ* strains also are recognised to lead to several chromatin modification at this locus, including hyperacetylation of H3K9 and H3K14 at the rDNA spacer, higher levels of H3K4me3, and dechromatinisation of the rDNA as a whole and loss of a closed chromatin region in the rDNA spacer. One model is that establishment of this chromatin environment promotes association of Fob1, which is absolutely required for the hyperrecombination phenotypes observed both in the *sir2Δ* mutant and wild-type strains containing the IGS-1R overexpression construct pYES2-FBR(F). An intriguing possibility is suggested by the recent observation in the Mellor lab that the IGS1-R transcript can form DNA:DNA:RNA triplex structures at points proximal to the putative Fob1 binding site. If so, formation of these structures cotranscriptionally in the production of IGS1-R may drive association of Fob1 at the fork-blocking locus, leading to high levels of recombination.

While the details of the mechanism or mechanisms of action of IGS1-R remain tantalizing, the results above also present data which strengthens the suggested causal link between rDNA recombination frequency and the physiological phenotype of replicative longevity. This has some significance as another example of a non-coding RNA with a well defined physiological role.

If the non-coding RNA IGS1-R is responsible, at least in part, for the phenotype of *sir2Δ* mutants at the rDNA spacer, then its behaviour in the *ydr026cΔ* mutant also allows explanation of the *ydr026cΔ* phenotype (reduced recombination, extended replicative longevity) within this model. Evidence presented in section 7.2 demonstrates that in *rrp6Δ* background strains, deletion of Ydr026c leads to reduction in the transcript abundance of

IGS1-R, as well as allowing transcription in the other direction through the fork-blocking region. While changes in IGS1-R degradation rates cannot be ruled out, if this depletion of steady-state RNA levels is due to reduced transcription of IGS1-R, then this may explain why reduced levels of rDNA hotspot recombination, and as a downstream consequence, extended longevity is observed in the *ydr026cΔ* strain.

A phenotype observed in the *ydr026cΔ* strain is the abrogation of a novel spacer-spacer higher-order chromatin interaction detected in wild-type cells. Disruption of this interaction also occurs in *fob1Δ* mutants; but can be restored in the *ydr026cΔ* strain upon deletion of *SIR2*. The appearance of this interaction hence correlates with Fob1-dependent recombinogenic activity at the rDNA spacer hotspot. The interaction can be restored in strain carrying the IGS1-R overexpression construct. An intriguing hypothesis is that this chromatin juxtaposition represents recombination precursors or intermediates in the process of homologous repeat recombination.

Replicative longevity was the first form of senescence to be investigated in the *S. cerevisiae* model. As attention turned to chronological ageing, many of the interventions found to influence replicative longevity were also found to modify chronological survival, such as calorie restriction and TOR signalling. Many questions remains as to whether a concerted pathway in each case underlies the longevity phenotypes in both domains of ageing. This study has found that the rDNA maintenance mutants *ydr026cΔ* and *sir2Δ* – but not *fob1Δ* – also exhibit chronological ageing phenotypes. In analogy, it is unclear whether the mechanisms driving replicative longevity: rDNA instability and ERC generation; are also operating to modulate chronological longevity. Ydr026c has been identified as a transcription factor binding to diverse sites across the genome, and hence regulation of additional gene expression may be the underlying cause of chronological life-extension. However, the clear role Ydr026c plays at the rDNA spacer region, and its

genetic and biochemical interactions with Sir2 in the regulation of chronological lifespan, suggest that action at the rDNA may well be at least partially responsible for the phenotypes in this domain of ageing. Moreover, evidence of dysregulation of other genetic pathways – such as metabolic genes induced before, during and following the diauxic shift – present in the case of TOR pathway disruption or caloric restriction – is not manifest in strains mutant for *YDR026C* and *SIR2*.

The results of chapter 5 suggest that the ability to maintain a non-dividing, stable quiescent state – the failure of which leads to apoptotic-like cell death – underlies the chronological ageing phenotypes observed in the *sir2Δ* and *ydr026cΔ* strains. In other examples of this mode of death over chronological ageing, the maintenance of a stable quiescent state is determined by the ability to suppress expression of metabolic and regulatory genes responsible for high levels of metabolism, particularly of carbohydrates (Gray et al., 2004). Reinduction of carbohydrate catabolism in ageing quiescent cells leads to depletion of the stored carbohydrate reserves of trehalose and glycogen, leading to the reduction of density observed in these cells as they exit the quiescent phase. Exit of quiescence leads to re-entry to the cell cycle, and cell budding reappears (Allen et al., 2006). Finally, the lack of nutrient availability leads to oxidative and other stresses and apoptotic-like death of the non-quiescent population of cells (Aragon et al., 2008). There is some evidence that nutrients released by the lysis of the non-quiescent subfraction of the culture population leads to re-feeding of the quiescent, stable, population, and this may help clonal yeast cultures survive in nutrient-stressed natural environments (Murakami and Kaeberlein, 2009).

Since repression of active metabolism (carbohydrate catabolism and protein synthesis) are important for maintenance of the quiescent state, it might be expected that strains which exhibit changes in quiescence maintenance may demonstrate dysregulation of genes controlling these processes. *snf1Δ* strains, for example, fail to activate genes normally

subject to glucose repression, and so do not express the post-diauxic genes required for oxidative metabolism and quiescence. Mutants disrupting the TOR pathway reduce the expression of ribosomal proteins, so downregulating global translation levels, and reducing metabolism and energy expenditure generally (Powers and Walter, 1999). Hence, a possible working model of the action of *YDR026C* and *SIR2* in ageing cells is the regulation of the rate of production of ribosomes through the synthesis of pre-rRNA.

The yeast rDNA locus is usually transcribed by RNA polymerase I, but recent studies have shown that in strains lacking components of this polymerase, strains can survive by transcription of the 35S rRNA using RNA polymerase II to produce functional ribosomes (Vu et al., 1999). Evidence exists that the substrate for RNA polymerase II in this case is episomal circles (ERCs) produced by recombination from the genomic rDNA array (Conrad-Webb and Butow, 1995). Further studies found that polymerase switching could be induced by mutation of the transcription factor UAF which normally drives RNA polymerase I transcription. Mutation of UAF lead to both productive transcription of the rRNA transcripts by RNA polymerase II, and also a 7-fold expansion of the rDNA array repeat length (Oakes et al., 1999). Expansion of the rDNA array was required for the RNA polymerase switch, and was influenced positively and negatively by the deletion of *SIR2* and *FOB1* respectively. This suggests that rDNA instability promotes either rDNA repeat expansion, or generation of episomal circles (or both), and that this allows RNA polymerase-II driven expression of the rRNA. In this case, this could provide a link between rDNA instability as mediated by *YDR026C, SIR2,* and *FOB1* through expression of the rDNA spacer transcripts, and bulk ribosomal RNA expression by RNA polymerase II. In this model (**Figure 50b**), high levels of rDNA instability and ERC generation in the *sir2Δ* mutant would allow expression of additional rRNA by RNA polymerase II, leading to global overactivity of translation and early failure of quiescence as nutrient reserves are more quickly depleted: and hence shorter chronological lifespan. Conversely, the

suppression of recombination in the *ydr026cΔ* strain would reduce this occurrence during the stressful extent of chronological ageing, extending longevity.

The question remains in this model why the *fob1Δ* strain, which shows near abrogation of recombination, does not appear to possess a chronological longevity phenotype. While rDNA spacer hotspot recombination is largely dependent upon Fob1, the action of Sir2 in repressing RNA polymerase II mediated transcription across the rDNA locus appears to be independent of Fob1. Hence, Sir2 remains active at the rDNA in *fob1Δ* in this model, and hence may still drive RNA polymerase II-mediated transcription of the main rRNA transcript in genomic rDNA repeats or episomal ERCs. This may maintain the basal level of quiescence failure and chronological senescence observed in the wild-type.

This study presents evidence for regulation of the physiological phenotypes of replicative longevity through the mechanism of epigenetic control of rDNA spacer hotspot recombinogenicity. The data above represent another line of evidence for the role of maintenance of rDNA genomic stability in replicative ageing in *S. cerevisiae*, and suggests an underlying role for transcription of the non-coding spacer region in regulating this maintenance. Two prominent unknowns remain in this model described above, however. Firstly, the mechanism of regulation by the non-coding spacer transcripts remains unknown. Secondly, the role rDNA maintenance plays in chronological ageing remains uncharacterised.

Future work will address these questions. One hypothesis on the underlying mechanism of action of *cis* transcription over the fork-blocking region is suggested by preliminary work in the Mellor lab, which has demonstrated that RNAs corresponding to IGS1-R can form triplexes over the putative Fob1 binding site *in vitro*. Demonstration that these complexes specifically recruit Fob1 – *in vitro* and *in vivo* – would provide a compelling mechanism for the promotion of recombination upon transcription over this region. Additionally,

evidence of modified chromatin state over the fork-blocking region in *sir2Δ* strains will be investigated as a causative mechanism through the use of histone mutants in the *sir2Δ* strains and wild-type strains carrying the pYES2-FBR(F) construct. Another factor that may play a role in the function of this transcript, or the IGS1-(S) transcript repressed by Ydr026c, is deposition of cohesin in the CAR region of the rDNA spacer. Both expression of IGS1-R and IGS1-S may upset the balance of the IGS1-F/IGS2-R transcripts which span the CAR region and are suggested to disturb chromatin deposition. ChIP experiments will be performed to measure cohesin levels in the *ydr026cΔ* background, and at the levels of transcripts of IGS1-F and IGS2-R will be studied in the *rrp6Δ* background when *YDR026C* is deleted, to determine whether the IGS1-(S) transcript repressed by Ydr026c also interferes with transcription from the E-PRO in the sense direction. Finally, while the rates of rDNA hotspot recombination have been precisely measured in these mutants, the effect this has upon rDNA copy number has not been established. Hence, rDNA copy number analysis using pulsed field gel electrophoresis will be performed on DNA from these strains.

Knowledge of rDNA copy number variation will provide a method of testing the model in **Figure 50b**. Chronological longevity assays will be performed to determined whether the reconstitution of the *sir2Δ* phenotype in the wild-type strain containing the pYES2-FBR(F) construct extends to curtailed chronological lifespan. If these two aspects of the model can be established, then physiological overproduction of functional ribosomes in the *sir2Δ* strain – and the inverse in the *ydr026cΔ* mutant – will be investigated using ^{35}S-incorporation based translation assays.

Agrelo, R., Cheng, W.H., Setien, F., Ropero, S., Espada, J., Fraga, M.F., Herranz, M., Paz, M.F., Sanchez-Cespedes, M., Artiga, M.J., Guerrero, D., Castells, A., von Kobbe, C., Bohr, V.A. and Esteller, M., 2006. Epigenetic inactivation of the premature aging Werner syndrome gene in human cancer. Proc Natl Acad Sci U S A 103, 8822-7.

Allen, C., Buttner, S., Aragon, A.D., Thomas, J.A., Meirelles, O., Jaetao, J.E., Benn, D., Ruby, S.W., Veenhuis, M., Madeo, F. and Werner-Washburne, M., 2006. Isolation of quiescent and nonquiescent cells from yeast stationary-phase cultures. J Cell Biol 174, 89-100.

Alvers, A.L., Fishwick, L.K., Wood, M.S., Hu, D., Chung, H.S., Dunn, W.A., Jr. and Aris, J.P., 2009a. Autophagy and amino acid homeostasis are required for chronological longevity in Saccharomyces cerevisiae. Aging Cell 8, 353-69.

Alvers, A.L., Wood, M.S., Hu, D., Kaywell, A.C., Dunn, W.A., Jr. and Aris, J.P., 2009b. Autophagy is required for extension of yeast chronological life span by rapamycin. Autophagy 5, 847-9.

Andersen, S.L., Sebastiani, P., Dworkis, D.A., Feldman, L. and Perls, T.T., 2012. Health span approximates life span among many supercentenarians: compression of morbidity at the approximate limit of life span. J Gerontol A Biol Sci Med Sci 67, 395-405.

Aragon, A.D., Rodriguez, A.L., Meirelles, O., Roy, S., Davidson, G.S., Tapia, P.H., Allen, C., Joe, R., Benn, D. and Werner-Washburne, M., 2008. Characterization of differentiated quiescent and nonquiescent cells in yeast stationary-phase cultures. Molecular biology of the cell 19, 1271-80.

Arking, R., 1988. Genetic analyses of aging processes in Drosophila. Exp Aging Res 14, 125-35.

Artandi, S.E. and Attardi, L.D., 2005. Pathways connecting telomeres and p53 in senescence, apoptosis, and cancer. Biochem Biophys Res Commun 331, 881-90.

Ashrafi, K., Sinclair, D., Gordon, J.I. and Guarente, L., 1999. Passage through stationary phase advances replicative aging in Saccharomyces cerevisiae. Proceedings of the National Academy of Sciences of the United States of America 96, 9100-5.

Austad, S.N., 1993. Retarded senescence in an insular population of Virginia opossums (Didelphis virginiana). Journal of Zoology 229, 695-708.

Bairwa, N.K., Zzaman, S., Mohanty, B.K. and Bastia, D., 2010. Replication fork arrest and rDNA silencing are two independent and separable functions of the replication terminator protein Fob1 of Saccharomyces cerevisiae. J Biol Chem 285, 12612-9.

Balaban, R.S., Nemoto, S. and Finkel, T., 2005. Mitochondria, oxidants, and aging. Cell 120, 483-95.

Bandyopadhyay, D. and Medrano, E.E., 2003. The emerging role of epigenetics in cellular and organismal aging. Exp Gerontol 38, 1299-307.

Bandyopadhyay, D., Okan, N.A., Bales, E., Nascimento, L., Cole, P.A. and Medrano, E.E., 2002. Down-regulation of p300/CBP histone acetyltransferase activates a senescence checkpoint in human melanocytes. Cancer Res 62, 6231-9.

Barker, M.G. and Walmsley, R.M., 1999. Replicative ageing in the fission yeast Schizosaccharomyces pombe. Yeast 15, 1511-8.

Barton, A.A., 1950. Some Aspects of Cell Division in Saccharomyces cerevisiae. Journal of General Microbiology 4, 84-86.

Baur, J.A., Pearson, K.J., Price, N.L., Jamieson, H.A., Lerin, C., Kalra, A., Prabhu, V.V., Allard, J.S., Lopez-Lluch, G., Lewis, K., Pistell, P.J., Poosala, S., Becker, K.G., Boss, O., Gwinn, D., Wang, M., Ramaswamy, S., Fishbein, K.W., Spencer, R.G., Lakatta, E.G., Le Couteur, D., Shaw, R.J., Navas, P., Puigserver, P., Ingram, D.K., de Cabo, R. and Sinclair, D.A., 2006. Resveratrol improves health and survival of mice on a high-calorie diet. Nature 444, 337-42.

Benguria, A., Hernandez, P., Krimer, D.B. and Schvartzman, J.B., 2003. Sir2p suppresses recombination of replication forks stalled at the replication fork barrier of ribosomal DNA in Saccharomyces cerevisiae. Nucleic Acids Res 31, 893-8.

Berger, A.B., Decourty, L., Badis, G., Nehrbass, U., Jacquier, A. and Gadal, O., 2007. Hmo1 is required for TOR-dependent regulation of ribosomal protein gene transcription. Mol Cell Biol 27, 8015-26.

Berretta, J., Pinskaya, M. and Morillon, A., 2008. A cryptic unstable transcript mediates transcriptional trans-silencing of the Ty1 retrotransposon in S. cerevisiae. Genes Dev 22, 615-26.

Berry, R.J. and Bronson, F.H., 1992. Life history and bioeconomy of the house mouse. Biological Reviews of the Cambridge Philosophical Society 67, 519-50.

Bird, A.J., Gordon, M., Eide, D.J. and Winge, D.R., 2006. Repression of ADH1 and ADH3 during zinc deficiency by Zap1-induced intergenic RNA transcripts. Embo J 25, 5726-34.

Bitterman, K.J., Medvedik, O. and Sinclair, D.A., 2003. Longevity regulation in Saccharomyces cerevisiae: linking metabolism, genome stability, and heterochromatin. Microbiol Mol Biol Rev 67, 376-99, table of contents.

Bjedov, I., Toivonen, J.M., Kerr, F., Slack, C., Jacobson, J., Foley, A. and Partridge, L., 2010. Mechanisms of life span extension by rapamycin in the fruit fly Drosophila melanogaster. Cell Metab 11, 35-46.

Blagosklonny, M.V., 2007a. Paradoxes of aging. Cell Cycle 6, 2997-3003.

Blagosklonny, M.V., 2007b. Program-like aging and mitochondria: instead of random damage by free radicals. Journal of Cellular Biochemistry 102, 1389-99.

Blagosklonny, M.V., 2008. Aging: ROS or TOR. Cell Cycle 7, 3344-54.

Bland, J.M. and Altman, D.G., 2004. The logrank test. Bmj 328, 1073.

Blander, G. and Guarente, L., 2004. The Sir2 family of protein deacetylases. Annu Rev Biochem 73, 417-35.

Blomen, V.A. and Boonstra, J., 2007. Cell fate determination during G1 phase progression. Cell Mol Life Sci 64, 3084-104.

Bodkin, N.L., Alexander, T.M., Ortmeyer, H.K., Johnson, E. and Hansen, B.C., 2003. Mortality and morbidity in laboratory-maintained Rhesus monkeys and effects of long-term dietary restriction. J Gerontol A Biol Sci Med Sci 58, 212-9.

Bonawitz, N.D., Chatenay-Lapointe, M., Pan, Y. and Shadel, G.S., 2007. Reduced TOR signaling extends chronological life span via increased respiration and upregulation of mitochondrial gene expression. Cell Metabolism 5, 265-77.

Boucherie, H., 1985. Protein synthesis during transition and stationary phases under glucose limitation in Saccharomyces cerevisiae. Journal of bacteriology 161, 385-92.

Bracken, A.P., Kleine-Kohlbrecher, D., Dietrich, N., Pasini, D., Gargiulo, G., Beekman, C., Theilgaard-Monch, K., Minucci, S., Porse, B.T., Marine, J.C., Hansen, K.H. and Helin, K., 2007. The Polycomb group proteins bind throughout the INK4A-ARF locus and are disassociated in senescent cells. Genes Dev 21, 525-30.

Brauer, M.J., Saldanha, A.J., Dolinski, K. and Botstein, D., 2005. Homeostatic adjustment and metabolic remodeling in glucose-limited yeast cultures. Mol Biol Cell 16, 2503-17.

Brockdorff, N., Ashworth, A., Kay, G.F., McCabe, V.M., Norris, D.P., Cooper, P.J., Swift, S. and Rastan, S., 1992. The product of the mouse Xist gene is a 15 kb inactive X-specific transcript containing no conserved ORF and located in the nucleus. Cell 71, 515-26.

Brody, J.A. and Schneider, E.L., 1986. Diseases and disorders of aging: an hypothesis. J Chronic Dis 39, 871-6.

Bryk, M., Banerjee, M., Murphy, M., Knudsen, K.E., Garfinkel, D.J. and Curcio, M.J., 1997. Transcriptional silencing of Ty1 elements in the RDN1 locus of yeast. Genes Dev 11, 255-69.

Burnett, C., Valentini, S., Cabreiro, F., Goss, M., Somogyvari, M., Piper, M.D., Hoddinott, M., Sutphin, G.L., Leko, V., McElwee, J.J., Vazquez-Manrique, R.P., Orfila, A.M., Ackerman, D., Au, C., Vinti, G., Riesen, M., Howard, K., Neri, C., Bedalov, A., Kaeberlein, M., Soti, C., Partridge, L. and Gems, D., 2011. Absence of effects of Sir2 overexpression on lifespan in C. elegans and Drosophila. Nature 477, 482-5.

Burtner, C. and Kaeberlein, M., 2009. A molecular mechanism of chronological aging in yeast. Cell Cycle 8, 1256-1270.

Busuttil, R.A., Dolle, M., Campisi, J. and Vijga, J., 2004. Genomic instability, aging, and cellular senescence. Ann N Y Acad Sci 1019, 245-55.

Buttner, S., Eisenberg, T., Herker, E., Carmona-Gutierrez, D., Kroemer, G. and Madeo, F., 2006. Why yeast cells can undergo apoptosis: death in times of peace, love, and war. The Journal of cell biology 175, 521-5.

Cailliet, G.M., Andrews, A.H., Burton, E.J., Watters, D.L., Kline, D.E. and Ferry-Graham, L.A., 2001. Age determination and validation studies of marine fishes: do deep-dwellers live longer? Exp Gerontol 36, 739-64.

Camblong, J., Beyrouthy, N., Guffanti, E., Schlaepfer, G., Steinmetz, L.M. and Stutz, F., 2009. Trans-acting antisense RNAs mediate transcriptional gene cosuppression in S. cerevisiae. Genes Dev 23, 1534-45.

Camblong, J., Iglesias, N., Fickentscher, C., Dieppois, G. and Stutz, F., 2007. Antisense RNA stabilization induces transcriptional gene silencing via histone deacetylation in S. cerevisiae. Cell 131, 706-17.

Campisi, J., 1997. The biology of replicative senescence. Eur J Cancer 33, 703-9.

Campisi, J., 2000. Cancer, aging and cellular senescence. In Vivo 14, 183-8.

Carmona-Gutierrez, D., Eisenberg, T., Buttner, S., Meisinger, C., Kroemer, G. and Madeo, F., 2010. Apoptosis in yeast: triggers, pathways, subroutines. Cell Death Differ 17, 763-73.

Carré, V. and Guilloton, M., 1997. DNA fragmentation attested by TUNEL in Saccharomyces cerevisiae subjected to photodynamic treatment. Journal of Microbiological Methods 29, 185-190.

CDC, 2006. United States Life Tables, 2003, 14 ed. Centers for Disease Control, Hyattsville, MD.

Chaumeil, J., Waters, P.D., Koina, E., Gilbert, C., Robinson, T.J. and Graves, J.A., 2011. Evolution from XIST-independent to XIST-controlled X-chromosome inactivation: epigenetic modifications in distantly related mammals. PLoS One 6, e19040.

Chen, B.R. and Runge, K.W., 2009. A new Schizosaccharomyces pombe chronological lifespan assay reveals that caloric restriction promotes efficient cell cycle exit and extends longevity. Exp Gerontol 44, 493-502.

Chen, Q., Ding, Q. and Keller, J.N., 2005. The stationary phase model of aging in yeast for the study of oxidative stress and age-related neurodegeneration. Biogerontology 6, 1-13.

Chlebowski, A., Lubas, M., Jensen, T.H. and Dziembowski, A., 2013. RNA decay machines: The exosome. Biochim Biophys Acta.

Choder, M., 1991. A general topoisomerase I-dependent transcriptional repression in the stationary phase in yeast. Genes & development 5, 2315-26.

Choi, Y.S., Hur, J. and Jeong, S., 2007. Beta-catenin binds to the downstream region and regulates the expression C-reactive protein gene. Nucleic Acids Res 35, 5511-9.

Churchman, L.S. and Weissman, J.S., 2011. Nascent transcript sequencing visualizes transcription at nucleotide resolution. Nature 469, 368-73.

Cioci, F., Vu, L., Eliason, K., Oakes, M., Siddiqi, I.N. and Nomura, M., 2003. Silencing in yeast rDNA chromatin: reciprocal relationship in gene expression between RNA polymerase I and II. Mol Cell 12, 135-45.

Clarke, A.S., Lowell, J.E., Jacobson, S.J. and Pillus, L., 1999. Esa1p is an essential histone acetyltransferase required for cell cycle progression. Mol Cell Biol 19, 2515-2526.

Claypool, J.A., French, S.L., Johzuka, K., Eliason, K., Vu, L., Dodd, J.A., Beyer, A.L. and Nomura, M., 2004. Tor pathway regulates Rrn3p-dependent recruitment of yeast RNA polymerase I to the promoter but does not participate in alteration of the number of active genes. Molecular biology of the cell 15, 946-56.

Cohen, S., Agmon, N., Sobol, O. and Segal, D., 2010. Extrachromosomal circles of satellite repeats and 5S ribosomal DNA in human cells. Mob DNA 1, 11.

Colman, R.J., Anderson, R.M., Johnson, S.C., Kastman, E.K., Kosmatka, K.J., Beasley, T.M., Allison, D.B., Cruzen, C., Simmons, H.A., Kemnitz, J.W. and Weindruch, R., 2009. Caloric restriction delays disease onset and mortality in rhesus monkeys. Science 325, 201-4.

Colmenares, S.U., Buker, S.M., Buhler, M., Dlakic, M. and Moazed, D., 2007. Coupling of double-stranded RNA synthesis and siRNA generation in fission yeast RNAi. Mol Cell 27, 449-61.

Conrad-Webb, H. and Butow, R.A., 1995. A polymerase switch in the synthesis of rRNA in Saccharomyces cerevisiae. Mol Cell Biol 15, 2420-8.

Counter, C.M., Avilion, A.A., LeFeuvre, C.E., Stewart, N.G., Greider, C.W., Harley, C.B. and Bacchetti, S., 1992. Telomere shortening associated with chromosome instability is arrested in immortal cells which express telomerase activity. Embo J 11, 1921-9.

Cournil, A. and Kirkwood, T.B., 2001. If you would live long, choose your parents well. Trends Genet 17, 233-5.

Cox, L.S. and Faragher, R.G.A., 2007. From old organisms to new molecules: integrative biology and therapeutic targets in accelerated human ageing. Cell Mol Life Sci 64, 2620-41.
Cuervo, A.M., Bergamini, E., Brunk, U.T., Droge, W., Ffrench, M. and Terman, A., 2005. Autophagy and aging: the importance of maintaining "clean" cells. Autophagy 1, 131-40.
Dammann, R., Lucchini, R., Koller, T. and Sogo, J.M., 1993. Chromatin structures and transcription of rDNA in yeast Saccharomyces cerevisiae. Nucleic Acids Res 21, 2331-8.
Dammann, R., Lucchini, R., Koller, T. and Sogo, J.M., 1995. Transcription in the yeast rRNA gene locus: distribution of the active gene copies and chromatin structure of their flanking regulatory sequences. Mol Cell Biol 15, 5294-303.
Dasgupta, P., Padmanabhan, J. and Chellappan, S., 2006. Rb function in the apoptosis and senescence of non-neuronal and neuronal cells: role in oncogenesis. Curr Mol Med 6, 719-29.
David, L., Huber, W., Granovskaia, M., Toedling, J., Palm, C.J., Bofkin, L., Jones, T., Davis, R.W. and Steinmetz, L.M., 2006. A high-resolution map of transcription in the yeast genome. Proc Natl Acad Sci U S A 103, 5320-5.
Davidson, G.S., Joe, R.M., Roy, S., Meirelles, O., Allen, C.P., Wilson, M.R., Tapia, P.H., Manzanilla, E.E., Dodson, A.E., Chakraborty, S., Carter, M., Young, S., Edwards, B., Sklar, L. and Werner-Washburne, M., 2011. The proteomics of quiescent and nonquiescent cell differentiation in yeast stationary-phase cultures. Molecular biology of the cell 22, 988-98.
de Magalhaes, J.P., 2005. Open-minded scepticism: inferring the causal mechanisms of human ageing from genetic perturbations. Ageing Res Rev 4, 1-22.
De Virgilio, C., 2012. The essence of yeast quiescence. FEMS Microbiol Rev 36, 306-39.
Defossez, P.A., Park, P.U. and Guarente, L., 1998. Vicious circles: a mechanism for yeast aging. Current Opinion in Microbiology 1, 707-11.
Defossez, P.A., Prusty, R., Kaeberlein, M., Lin, S.J., Ferrigno, P., Silver, P.A., Keil, R.L. and Guarente, L., 1999. Elimination of replication block protein Fob1 extends the life span of yeast mother cells. Mol Cell 3, 447-55.
Dekker, J., Rippe, K., Dekker, M. and Kleckner, N., 2002. Capturing chromosome conformation. Science 295, 1306-11.
DeRisi, J.L., Iyer, V.R. and Brown, P.O., 1997. Exploring the metabolic and genetic control of gene expression on a genomic scale. Science (New York, N.Y 278, 680-6.
Dickinson, J.R. and Schweizer, M., 1999. The Metabolism and Molecular Physiology of Saccharomyces cerevisiae, Taylor & Francis, Philadelphia.
Driver, J.A., Djousse, L., Logroscino, G., Gaziano, J.M. and Kurth, T., 2008. Incidence of cardiovascular disease and cancer in advanced age: prospective cohort study. Bmj 337, a2467.
Ebert, T.A. and Southon, J.R., 2003. Red sea urchins (Strongylocentrotus franciscanus) can live over 100 years: Confirmation with A-bomb 14carbon. Fishery Bulletin 101, 915-922.
Economos, A.C., 1981. Beyond rate of living. Gerontology 27, 258-65.
Eisenberg, T., Knauer, H., Schauer, A., Buttner, S., Ruckenstuhl, C., Carmona-Gutierrez, D., Ring, J., Schroeder, S., Magnes, C., Antonacci, L., Fussi, H., Deszcz, L., Hartl, R., Schraml, E., Criollo, A., Megalou, E., Weiskopf, D., Laun, P., Heeren, G., Breitenbach, M., Grubeck-Loebenstein, B., Herker, E., Fahrenkrog, B., Frohlich, K.U., Sinner, F., Tavernarakis, N., Minois, N., Kroemer, G. and Madeo, F., 2009. Induction of autophagy by spermidine promotes longevity. Nat Cell Biol 11, 1305-14.
Entian, K.D. and Barnett, J.A., 1992. Regulation of sugar utilization by Saccharomyces cerevisiae. Trends Biochem Sci 17, 506-10.
Erjavec, N., Larsson, L., Grantham, J. and Nystrom, T., 2007. Accelerated aging and failure to segregate damaged proteins in Sir2 mutants can be suppressed by overproducing the protein aggregation-remodeling factor Hsp104p. Genes Dev 21, 2410-21.
Esquela-Kerscher, A. and Slack, F.J., 2006. Oncomirs - microRNAs with a role in cancer. Nat Rev Cancer 6, 259-69.
Evans, D.S., Kapahi, P., Hsueh, W.C. and Kockel, L., 2011. TOR signaling never gets old: aging, longevity and TORC1 activity. Ageing Res Rev 10, 225-37.
Fabrizio, P., Gattazzo, C., Battistella, L., Wei, M., Cheng, C., McGrew, K. and Longo, V.D., 2005. Sir2 blocks extreme life-span extension. Cell 123, 655-67.

Fabrizio, P., Liou, L.L., Moy, V.N., Diaspro, A., Valentine, J.S., Gralla, E.B. and Longo, V.D., 2003. SOD2 functions downstream of Sch9 to extend longevity in yeast. Genetics 163, 35-46.

Fabrizio, P. and Longo, V.D., 2003. The chronological life span of Saccharomyces cerevisiae. Aging Cell 2, 73-81.

Fabrizio, P., Pozza, F., Pletcher, S.D., Gendron, C.M. and Longo, V.D., 2001. Regulation of longevity and stress resistance by Sch9 in yeast. Science (New York, N.Y 292, 288-90.

Falcon, A.A. and Aris, J.P., 2003. Plasmid accumulation reduces life span in Saccharomyces cerevisiae. J Biol Chem 278, 41607-17.

Finch, C.E., 2009. Update on slow aging and negligible senescence--a mini-review. Gerontology 55, 307-13.

Finch, C.E. and Austad, S.N., 2001. History and prospects: symposium on organisms with slow aging. Exp Gerontol 36, 593-7.

Fire, A., Xu, S., Montgomery, M.K., Kostas, S.A., Driver, S.E. and Mello, C.C., 1998. Potent and specific genetic interference by double-stranded RNA in Caenorhabditis elegans. Nature 391, 806-11.

Fraga, M.F. and Esteller, M., 2007. Epigenetics and aging: the targets and the marks. Trends Genet 23, 413-8.

Fritze, C.E., Verschueren, K., Strich, R. and Easton Esposito, R., 1997. Direct evidence for SIR2 modulation of chromatin structure in yeast rDNA. Embo J 16, 6495-509.

Fuke, C., Shimabukuro, M., Petronis, A., Sugimoto, J., Oda, T., Miura, K., Miyazaki, T., Ogura, C., Okazaki, Y. and Jinno, Y., 2004. Age related changes in 5-methylcytosine content in human peripheral leukocytes and placentas: an HPLC-based study. Ann Hum Genet 68, 196-204.

Funk, W.C., Tyburczy, J.A., Knudsen, K.L., Lindner, K.R. and Allendorf, F.W., 2005. Genetic basis of variation in morphological and life-history traits of a wild population of pink salmon. J Hered 96, 24-31.

Galdieri, L., Mehrotra, S., Yu, S. and Vancura, A., 2010. Transcriptional regulation in yeast during diauxic shift and stationary phase. Omics 14, 629-38.

Gangavarapu, V., Santa Maria, S.R., Prakash, S. and Prakash, L., 2011. Requirement of replication checkpoint protein kinases Mec1/Rad53 for postreplication repair in yeast. MBio 2, e00079-11.

Ganley, A.R., Ide, S., Saka, K. and Kobayashi, T., 2009. The effect of replication initiation on gene amplification in the rDNA and its relationship to aging. Mol Cell 35, 683-93.

Garcia-Cao, I., Garcia-Cao, M., Martin-Caballero, J., Criado, L.M., Klatt, P., Flores, J.M., Weill, J.C., Blasco, M.A. and Serrano, M., 2002. "Super p53" mice exhibit enhanced DNA damage response, are tumor resistant and age normally. Embo J 21, 6225-35.

Gasch, A.P., Spellman, P.T., Kao, C.M., Carmel-Harel, O., Eisen, M.B., Storz, G., Botstein, D. and Brown, P.O., 2000. Genomic expression programs in the response of yeast cells to environmental changes. Molecular biology of the cell 11, 4241-57.

Gelfand, B., Mead, J., Bruning, A., Apostolopoulos, N., Tadigotla, V., Nagaraj, V., Sengupta, A.M. and Vershon, A.K., 2011. Regulated antisense transcription controls expression of cell-type-specific genes in yeast. Mol Cell Biol 31, 1701-9.

Gershon, H. and Gershon, D., 2000. The budding yeast, Saccharomyces cerevisiae, as a model for aging research: A critical review. Mechanisms of Ageing and Development 120, 1-22.

Gertz, M., Nguyen, G.T., Fischer, F., Suenkel, B., Schlicker, C., Franzel, B., Tomaschewski, J., Aladini, F., Becker, C., Wolters, D. and Steegborn, C., 2012. A molecular mechanism for direct sirtuin activation by resveratrol. PLoS One 7, e49761.

Gesellchen, V. and Boutros, M., 2004. Managing the genome: microRNAs in Drosophila. Differentiation 72, 74-80.

Gheorghe, C.P., Goyal, R., Mittal, A. and Longo, L.D., 2010. Gene expression in the placenta: maternal stress and epigenetic responses. Int J Dev Biol 54, 507-23.

Giaimo, S. and d'Adda di Fagagna, F., 2012. Is cellular senescence an example of antagonistic pleiotropy? Aging Cell 11, 378-83.

Goldmark, J.P., Fazzio, T.G., Estep, P.W., Church, G.M. and Tsukiyama, T., 2000. The Isw2 chromatin remodeling complex represses early meiotic genes upon recruitment by Ume6p. Cell 103, 423-33.

Gompertz, B., 1825. On the Nature of the Function Expressive of the Law of Human Mortality, and on a New Mode of Determining the Value of Life Contingencies. Philosophical Transactions of the Royal Society of London 115, 513-583.
Gottlieb, S. and Esposito, R.E., 1989. A new role for a yeast transcriptional silencer gene, SIR2, in regulation of recombination in ribosomal DNA. Cell 56, 771-6.
Gray, J.V., Petsko, G.A., Johnston, G.C., Ringe, D., Singer, R.A. and Werner-Washburne, M., 2004. "Sleeping beauty": quiescence in Saccharomyces cerevisiae. Microbiol Mol Biol Rev 68, 187-206.
Greenwood, M.T. and Ludovico, P., 2010. Expressing and functional analysis of mammalian apoptotic regulators in yeast. Cell Death Differ 17, 737-45.
Gregory, P.D., Schmid, A., Zavari, M., Munsterkotter, M. and Horz, W., 1999. Chromatin remodelling at the PHO8 promoter requires SWI-SNF and SAGA at a step subsequent to activator binding. Embo J 18, 6407-14.
Grune, T., Jung, T., Merker, K. and Davies, K.J., 2004. Decreased proteolysis caused by protein aggregates, inclusion bodies, plaques, lipofuscin, ceroid, and 'aggresomes' during oxidative stress, aging, and disease. Int J Biochem Cell Biol 36, 2519-30.
Guarente, L., 2000. Sir2 links chromatin silencing, metabolism, and aging. Genes Dev 14, 1021-6.
Ha, C.W. and Huh, W.K., 2011. Rapamycin increases rDNA stability by enhancing association of Sir2 with rDNA in Saccharomyces cerevisiae. Nucleic Acids Res 39, 1336-50.
Ha, C.W., Sung, M.K. and Huh, W.K., 2012. Nsi1 plays a significant role in the silencing of ribosomal DNA in Saccharomyces cerevisiae. Nucleic Acids Res.
Hammond, S.M., Bernstein, E., Beach, D. and Hannon, G.J., 2000. An RNA-directed nuclease mediates post-transcriptional gene silencing in Drosophila cells. Nature 404, 293-6.
Harbison, C.T., Gordon, D.B., Lee, T.I., Rinaldi, N.J., Macisaac, K.D., Danford, T.W., Hannett, N.M., Tagne, J.B., Reynolds, D.B., Yoo, J., Jennings, E.G., Zeitlinger, J., Pokholok, D.K., Kellis, M., Rolfe, P.A., Takusagawa, K.T., Lander, E.S., Gifford, D.K., Fraenkel, E. and Young, R.A., 2004. Transcriptional regulatory code of a eukaryotic genome. Nature 431, 99-104.
Hardie, D.G., Carling, D. and Carlson, M., 1998. The AMP-activated/SNF1 protein kinase subfamily: metabolic sensors of the eukaryotic cell? Annual review of biochemistry 67, 821-55.
Hardwick, J.S., Kuruvilla, F.G., Tong, J.K., Shamji, A.F. and Schreiber, S.L., 1999. Rapamycin-modulated transcription defines the subset of nutrient-sensitive signaling pathways directly controlled by the Tor proteins. Proc Natl Acad Sci U S A 96, 14866-70.
Harley, C.B. and Villeponteau, B., 1995. Telomeres and telomerase in aging and cancer. Curr Opin Genet Dev 5, 249-55.
Harrison, D.E., Strong, R., Sharp, Z.D., Nelson, J.F., Astle, C.M., Flurkey, K., Nadon, N.L., Wilkinson, J.E., Frenkel, K., Carter, C.S., Pahor, M., Javors, M.A., Fernandez, E. and Miller, R.A., 2009. Rapamycin fed late in life extends lifespan in genetically heterogeneous mice. Nature 460, 392-5.
Haurie, V., Perrot, M., Mini, T., Jeno, P., Sagliocco, F. and Boucherie, H., 2001. The transcriptional activator Cat8p provides a major contribution to the reprogramming of carbon metabolism during the diauxic shift in Saccharomyces cerevisiae. The Journal of biological chemistry 276, 76-85.
Hayflick, L., 1974. The longevity of cultured human cells. J Am Geriatr Soc 22, 1-12.
Hayflick, L. and Moorhead, P.S., 1961. The serial cultivation of human diploid cell strains. Exp Cell Res 25, 585-621.
Heard, E., 2004. Recent advances in X-chromosome inactivation. Curr Opin Cell Biol 16, 247-55.
Heeren, G., Rinnerthaler, M., Laun, P., von Seyerl, P., Kossler, S., Klinger, H., Hager, M., Bogengruber, E., Jarolim, S., Simon-Nobbe, B., Schuller, C., Carmona-Gutierrez, D., Breitenbach-Koller, L., Muck, C., Jansen-Durr, P., Criollo, A., Kroemer, G., Madeo, F. and Breitenbach, M., 2009. The mitochondrial ribosomal protein of the large subunit, Afo1p, determines cellular longevity through mitochondrial back-signaling via TOR1. Aging (Albany NY) 1, 622-36.
Heilbronn, L.K. and Ravussin, E., 2003. Calorie restriction and aging: review of the literature and implications for studies in humans. Am J Clin Nutr 78, 361-9.

Henderson, K.A. and Gottschling, D.E., 2008. A mother's sacrifice: what is she keeping for herself? Curr Opin Cell Biol 20, 723-8.
Heo, S.J., Tatebayashi, K., Ohsugi, I., Shimamoto, A., Furuichi, Y. and Ikeda, H., 1999. Bloom's syndrome gene suppresses premature ageing caused by Sgs1 deficiency in yeast. Genes Cells 4, 619-25.
Herker, E., Jungwirth, H., Lehmann, K.A., Maldener, C., Frohlich, K.U., Wissing, S., Buttner, S., Fehr, M., Sigrist, S. and Madeo, F., 2004. Chronological aging leads to apoptosis in yeast. The Journal of cell biology 164, 501-7.
Holloszy, J.O. and Fontana, L., 2007. Caloric restriction in humans. Exp Gerontol 42, 709-12.
Hongay, C.F., Grisafi, P.L., Galitski, T. and Fink, G.R., 2006. Antisense transcription controls cell fate in Saccharomyces cerevisiae. Cell 127, 735-45.
Hoopes, L.L., Budd, M., Choe, W., Weitao, T. and Campbell, J.L., 2002. Mutations in DNA replication genes reduce yeast life span. Mol Cell Biol 22, 4136-46.
Hoppe, G.J., Tanny, J.C., Rudner, A.D., Gerber, S.A., Danaie, S., Gygi, S.P. and Moazed, D., 2002. Steps in assembly of silent chromatin in yeast: Sir3-independent binding of a Sir2/Sir4 complex to silencers and role for Sir2-dependent deacetylation. Mol Cell Biol 22, 4167-80.
Horowitz, H. and Haber, J.E., 1985. Identification of autonomously replicating circular subtelomeric Y' elements in Saccharomyces cerevisiae. Mol Cell Biol 5, 2369-80.
Houseley, J., Kotovic, K., El Hage, A. and Tollervey, D., 2007. Trf4 targets ncRNAs from telomeric and rDNA spacer regions and functions in rDNA copy number control. Embo J 26, 4996-5006.
Houseley, J., LaCava, J. and Tollervey, D., 2006. RNA-quality control by the exosome. Nat Rev Mol Cell Biol 7, 529-39.
Houseley, J., Rubbi, L., Grunstein, M., Tollervey, D. and Vogelauer, M., 2008. A ncRNA modulates histone modification and mRNA induction in the yeast GAL gene cluster. Mol Cell 32, 685-95.
Howes, R.M., 2006. The free radical fantasy: a panoply of paradoxes. Ann N Y Acad Sci 1067, 22-6.
Huang, J., Brito, I.L., Villen, J., Gygi, S.P., Amon, A. and Moazed, D., 2006. Inhibition of homologous recombination by a cohesin-associated clamp complex recruited to the rDNA recombination enhancer. Genes Dev 20, 2887-901.
Huang, J. and Moazed, D., 2003. Association of the RENT complex with nontranscribed and coding regions of rDNA and a regional requirement for the replication fork block protein Fob1 in rDNA silencing. Genes Dev 17, 2162-76.
Huarte, M., Guttman, M., Feldser, D., Garber, M., Koziol, M.J., Kenzelmann-Broz, D., Khalil, A.M., Zuk, O., Amit, I., Rabani, M., Attardi, L.D., Regev, A., Lander, E.S., Jacks, T. and Rinn, J.L., 2010. A large intergenic noncoding RNA induced by p53 mediates global gene repression in the p53 response. Cell 142, 409-19.
Hughes, L.A., van den Brandt, P.A., de Bruine, A.P., Wouters, K.A., Hulsmans, S., Spiertz, A., Goldbohm, R.A., de Goeij, A.F., Herman, J.G., Weijenberg, M.P. and van Engeland, M., 2009. Early life exposure to famine and colorectal cancer risk: a role for epigenetic mechanisms. PLoS One 4, e7951.
Huh, W.K., Falvo, J.V., Gerke, L.C., Carroll, A.S., Howson, R.W., Weissman, J.S. and O'Shea, E.K., 2003. Global analysis of protein localization in budding yeast. Nature 425, 686-91.
Iakova, P., Awad, S.S. and Timchenko, N.A., 2003. Aging reduces proliferative capacities of liver by switching pathways of C/EBPalpha growth arrest. Cell 113, 495-506.
Ikeda, K., Steger, D.J., Eberharter, A. and Workman, J.L., 1999. Activation domain-specific and general transcription stimulation by native histone acetyltransferase complexes. Mol Cell Biol 19, 855-63.
Ingram, D.K., Weindruch, R., Spangler, E.L., Freeman, J.R. and Walford, R.L., 1987. Dietary restriction benefits learning and motor performance of aged mice. J Gerontol 42, 78-81.
Ito, H., Fukuda, Y., Murata, K. and Kimura, A., 1983. Transformation of intact yeast cells treated with alkali cations. Journal of Bacteriology 153, 163-8.
Jarolim, S., Millen, J., Heeren, G., Laun, P., Goldfarb, D.S. and Breitenbach, M., 2004. A novel assay for replicative lifespan in Saccharomyces cerevisiae. FEMS Yeast Res 5, 169-77.
Jazwinski, S.M., 2005. The retrograde response links metabolism with stress responses, chromatin-dependent gene activation, and genome stability in yeast aging. Gene 354, 22-7.

Jazwinski, S.M., Egilmez, N.K. and Chen, J.B., 1989. Replication control and cellular life span. Exp Gerontol 24, 423-36.
Johnson, T.E. and Lithgow, G.J., 1992. The search for the genetic basis of aging: the identification of gerontogenes in the nematode Caenorhabditis elegans. J Am Geriatr Soc 40, 936-45.
Jones-Rhoades, M.W., Bartel, D.P. and Bartel, B., 2006. MicroRNAS and their regulatory roles in plants. Annu Rev Plant Biol 57, 19-53.
Jones, P.A. and Baylin, S.B., 2002. The fundamental role of epigenetic events in cancer. Nat Rev Genet 3, 415-28.
Kadosh, D. and Struhl, K., 1998. Targeted recruitment of the Sin3-Rpd3 histone deacetylase complex generates a highly localized domain of repressed chromatin in vivo. Mol Cell Biol 18, 5121-7.
Kaeberlein, M., 2010. Lessons on longevity from budding yeast. Nature 464, 513-9.
Kaeberlein, M., Burtner, C.R. and Kennedy, B.K., 2007. Recent developments in yeast aging. PLoS Genet 3, e84.
Kaeberlein, M., McDonagh, T., Heltweg, B., Hixon, J., Westman, E.A., Caldwell, S.D., Napper, A., Curtis, R., DiStefano, P.S., Fields, S., Bedalov, A. and Kennedy, B.K., 2005a. Substrate-specific activation of sirtuins by resveratrol. J Biol Chem 280, 17038-45.
Kaeberlein, M., McVey, M. and Guarente, L., 1999. The SIR2/3/4 complex and SIR2 alone promote longevity in Saccharomyces cerevisiae by two different mechanisms. Genes and Development 13, 2570-2580.
Kaeberlein, M., Powers, R.W., 3rd, Steffen, K.K., Westman, E.A., Hu, D., Dang, N., Kerr, E.O., Kirkland, K.T., Fields, S. and Kennedy, B.K., 2005b. Regulation of yeast replicative life span by TOR and Sch9 in response to nutrients. Science 310, 1193-6.
Kamada, Y., Sekito, T. and Ohsumi, Y., 2004. Autophagy in yeast: a TOR-mediated response to nutrient starvation. Curr Top Microbiol Immunol 279, 73-84.
Kanfi, Y., Naiman, S., Amir, G., Peshti, V., Zinman, G., Nahum, L., Bar-Joseph, Z. and Cohen, H.Y., 2012. The sirtuin SIRT6 regulates lifespan in male mice. Nature 483, 218-21.
Kang, H.L., Benzer, S. and Min, K.T., 2002. Life extension in Drosophila by feeding a drug. Proc Natl Acad Sci U S A 99, 838-43.
Kang, J.J., Schaber, M.D., Srinivasula, S.M., Alnemri, E.S., Litwack, G., Hall, D.J. and Bjornsti, M.A., 1999. Cascades of mammalian caspase activation in the yeast Saccharomyces cerevisiae. J Biol Chem 274, 3189-98.
Kapahi, P., Zid, B.M., Harper, T., Koslover, D., Sapin, V. and Benzer, S., 2004. Regulation of lifespan in Drosophila by modulation of genes in the TOR signaling pathway. Curr Biol 14, 885-90.
Kapranov, P., Cheng, J., Dike, S., Nix, D.A., Duttagupta, R., Willingham, A.T., Stadler, P.F., Hertel, J., Hackermuller, J., Hofacker, I.L., Bell, I., Cheung, E., Drenkow, J., Dumais, E., Patel, S., Helt, G., Ganesh, M., Ghosh, S., Piccolboni, A., Sementchenko, V., Tammana, H. and Gingeras, T.R., 2007. RNA maps reveal new RNA classes and a possible function for pervasive transcription. Science 316, 1484-8.
Katayama, S., Tomaru, Y., Kasukawa, T., Waki, K., Nakanishi, M., Nakamura, M., Nishida, H., Yap, C.C., Suzuki, M., Kawai, J., Suzuki, H., Carninci, P., Hayashizaki, Y., Wells, C., Frith, M., Ravasi, T., Pang, K.C., Hallinan, J., Mattick, J., Hume, D.A., Lipovich, L., Batalov, S., Engstrom, P.G., Mizuno, Y., Faghihi, M.A., Sandelin, A., Chalk, A.M., Mottagui-Tabar, S., Liang, Z., Lenhard, B. and Wahlestedt, C., 2005. Antisense transcription in the mammalian transcriptome. Science 309, 1564-6.
Kato, M. and Slack, F.J., 2008. microRNAs: small molecules with big roles - C. elegans to human cancer. Biol Cell 100, 71-81.
Kawahara, T.L., Michishita, E., Adler, A.S., Damian, M., Berber, E., Lin, M., McCord, R.A., Ongaigui, K.C., Boxer, L.D., Chang, H.Y. and Chua, K.F., 2009. SIRT6 links histone H3 lysine 9 deacetylation to NF-kappaB-dependent gene expression and organismal life span. Cell 136, 62-74.
Keller, L. and Genoud, M., 1997. Extraordinary lifespans in ants: A test of evolutionary theories of ageing. Nature 389, 958-960.
Kennedy, B.K., Austriaco, N.R., Jr. and Guarente, L., 1994. Daughter cells of Saccharomyces cerevisiae from old mothers display a reduced life span. J Cell Biol 127, 1985-93.

Kennedy, B.K., Gotta, M., Sinclair, D.A., Mills, K., McNabb, D.S., Murthy, M., Pak, S.M., Laroche, T., Gasser, S.M. and Guarente, L., 1997. Redistribution of silencing proteins from telomeres to the nucleolus is associated with extension of life span in S. cerevisiae. Cell 89, 381-91.

Kenyon, C.J., 2010. The genetics of ageing. Nature 464, 504-12.

Khan, M.A., Chock, P.B. and Stadtman, E.R., 2005. Knockout of caspase-like gene, YCA1, abrogates apoptosis and elevates oxidized proteins in Saccharomyces cerevisiae. Proc Natl Acad Sci U S A 102, 17326-31.

Kim, E.B., Fang, X., Fushan, A.A., Huang, Z., Lobanov, A.V., Han, L., Marino, S.M., Sun, X., Turanov, A.A., Yang, P., Yim, S.H., Zhao, X., Kasaikina, M.V., Stoletzki, N., Peng, C., Polak, P., Xiong, Z., Kiezun, A., Zhu, Y., Chen, Y., Kryukov, G.V., Zhang, Q., Peshkin, L., Yang, L., Bronson, R.T., Buffenstein, R., Wang, B., Han, C., Li, Q., Chen, L., Zhao, W., Sunyaev, S.R., Park, T.J., Zhang, G., Wang, J. and Gladyshev, V.N., 2011. Genome sequencing reveals insights into physiology and longevity of the naked mole rat. Nature 479, 223-7.

Kirkwood, T.B., 1977. Evolution of ageing. Nature 270, 301-4.

Kirkwood, T.B., 2005. Understanding the odd science of aging. Cell 120, 437-47.

Kirkwood, T.B. and Austad, S.N., 2000. Why do we age? Nature 408, 233-8.

Kirkwood, T.B. and Shanley, D.P., 2005. Food restriction, evolution and ageing. Mech Ageing Dev 126, 1011-6.

Kobayashi, T. and Ganley, A.R., 2005a. Recombination regulation by transcription-induced cohesin dissociation in rDNA repeats. Science 309, 1581-4.

Kobayashi, T. and Ganley, A.R.D., 2005b. Recombination regulation by transcription-induced cohesin dissociation in rDNA repeats. Science (New York, N Y) 309, 1581-4.

Kobayashi, T., Heck, D.J., Nomura, M. and Horiuchi, T., 1998. Expansion and contraction of ribosomal DNA repeats in Saccharomyces cerevisiae: requirement of replication fork blocking (Fob1) protein and the role of RNA polymerase I. Genes Dev 12, 3821-30.

Kobayashi, T. and Horiuchi, T., 1996. A yeast gene product, Fob1 protein, required for both replication fork blocking and recombinational hotspot activities. Genes Cells 1, 465-74.

Kobayashi, T., Horiuchi, T., Tongaonkar, P., Vu, L. and Nomura, M., 2004. SIR2 regulates recombination between different rDNA repeats, but not recombination within individual rRNA genes in yeast. Cell 117, 441-53.

Krebs, J.E., Fry, C.J., Samuels, M.L. and Peterson, C.L., 2000. Global role for chromatin remodeling enzymes in mitotic gene expression. Cell 102, 587-98.

Kristoffersen, P., Jensen, G.B., Gerdes, K. and Piskur, J., 2000. Bacterial toxin-antitoxin gene system as containment control in yeast cells. Appl Environ Microbiol 66, 5524-6.

Kuilman, T., Michaloglou, C., Mooi, W.J. and Peeper, D.S., 2010. The essence of senescence. Genes Dev 24, 2463-79.

Langst, G., Becker, P.B. and Grummt, I., 1998. TTF-I determines the chromatin architecture of the active rDNA promoter. Embo J 17, 3135-45.

Lapointe, J., Stepanyan, Z., Bigras, E. and Hekimi, S., 2009. Reversal of the mitochondrial phenotype and slow development of oxidative biomarkers of aging in long-lived Mclk1+/- mice. J Biol Chem 284, 20364-74.

Lau, J.C., Hanel, M.L. and Wevrick, R., 2004. Tissue-specific and imprinted epigenetic modifications of the human NDN gene. Nucleic Acids Res 32, 3376-82.

Laun, P., Bruschi, C.V., Dickinson, J.R., Rinnerthaler, M., Heeren, G., Schwimbersky, R., Rid, R. and Breitenbach, M., 2007. Yeast mother cell-specific ageing, genetic (in)stability, and the somatic mutation theory of ageing. Nucleic Acids Res 35, 7514-26.

Lawrence, R.J., Earley, K., Pontes, O., Silva, M., Chen, Z.J., Neves, N., Viegas, W. and Pikaard, C.S., 2004. A concerted DNA methylation/histone methylation switch regulates rRNA gene dosage control and nucleolar dominance. Mol Cell 13, 599-609.

Lengauer, C., 2003. Cancer. An unstable liaison. Science 300, 442-3.

Lengeler, K.B., Davidson, R.C., D'Souza, C., Harashima, T., Shen, W.C., Wang, P., Pan, X., Waugh, M. and Heitman, J., 2000. Signal transduction cascades regulating fungal development and virulence. Microbiology and molecular biology reviews : MMBR 64, 746-85.

Lewis, D.L. and Gattie, D.K., 1991. The ecology of quiescent microbes. ASM news 57, 27-32.

Li, C., Mueller, J.E. and Bryk, M., 2006. Sir2 represses endogenous polymerase II transcription units in the ribosomal DNA nontranscribed spacer. Mol Biol Cell 17, 3848-59.
Li, L., Lu, Y., Qin, L.X., Bar-Joseph, Z., Werner-Washburne, M. and Breeden, L.L., 2009. Budding yeast SSD1-V regulates transcript levels of many longevity genes and extends chronological life span in purified quiescent cells. Molecular biology of the cell 20, 3851-64.
Li, Q., Xiao, H. and Isobe, K., 2002. Histone acetyltransferase activities of cAMP-regulated enhancer-binding protein and p300 in tissues of fetal, young, and old mice. J Gerontol A Biol Sci Med Sci 57, B93-8.
Li, W. and Vijg, J., 2012. Measuring genome instability in aging - a mini-review. Gerontology 58, 129-38.
Lieberman-Aiden, E., van Berkum, N.L., Williams, L., Imakaev, M., Ragoczy, T., Telling, A., Amit, I., Lajoie, B.R., Sabo, P.J., Dorschner, M.O., Sandstrom, R., Bernstein, B., Bender, M.A., Groudine, M., Gnirke, A., Stamatoyannopoulos, J., Mirny, L.A., Lander, E.S. and Dekker, J., 2009. Comprehensive mapping of long-range interactions reveals folding principles of the human genome. Science 326, 289-93.
Liko, D., Slattery, M.G. and Heideman, W., 2007. Stb3 binds to ribosomal RNA processing element motifs that control transcriptional responses to growth in Saccharomyces cerevisiae. The Journal of biological chemistry 282, 26623-8.
Lillie, S.H. and Pringle, J.R., 1980. Reserve carbohydrate metabolism in Saccharomyces cerevisiae: responses to nutrient limitation. Journal of bacteriology 143, 1384-94.
Lin, S.J., Defossez, P.A. and Guarente, L., 2000. Requirement of NAD and SIR2 for life-span extension by calorie restriction in Saccharomyces cerevisiae. Science 289, 2126-8.
Lindsay, J., Laurin, D., Verreault, R., Hebert, R., Helliwell, B., Hill, G.B. and McDowell, I., 2002. Risk factors for Alzheimer's disease: a prospective analysis from the Canadian Study of Health and Aging. Am J Epidemiol 156, 445-53.
Livas, D., Almering, M.J., Daran, J.M., Pronk, J.T. and Gancedo, J.M., 2011. Transcriptional responses to glucose in Saccharomyces cerevisiae strains lacking a functional protein kinase A. BMC Genomics 12, 405.
Lloyd-Jones, D.M., Larson, M.G., Beiser, A. and Levy, D., 1999. Lifetime risk of developing coronary heart disease. Lancet 353, 89-92.
Loeb, L.A., Loeb, K.R. and Anderson, J.P., 2003. Multiple mutations and cancer. Proc Natl Acad Sci U S A 100, 776-81.
Longo, V.D., 2003. The Ras and Sch9 pathways regulate stress resistance and longevity. Exp Gerontol 38, 807-11.
Longo, V.D., Gralla, E.B. and Valentine, J.S., 1996. Superoxide dismutase activity is essential for stationary phase survival in Saccharomyces cerevisiae. Mitochondrial production of toxic oxygen species in vivo. The Journal of biological chemistry 271, 12275-80.
Longo, V.D., Shadel, G.S., Kaeberlein, M. and Kennedy, B., 2012. Replicative and chronological aging in Saccharomyces cerevisiae. Cell Metab 16, 18-31.
Longtine, M.S., McKenzie, A., 3rd, Demarini, D.J., Shah, N.G., Wach, A., Brachat, A., Philippsen, P. and Pringle, J.R., 1998. Additional modules for versatile and economical PCR-based gene deletion and modification in Saccharomyces cerevisiae. Yeast 14, 953-61.
Lorenz, D.R., Cantor, C.R. and Collins, J.J., 2009. A network biology approach to aging in yeast. Proc Natl Acad Sci U S A 106, 1145-50.
Luckinbill, L.S., Arking, R., Clare, M.J., Cirocco, W.C. and Buck, S.A., 1984. Selection for Delayed Senescence in Drosophila melanogaster. Evolution 38, 996-1003.
Ludovico, P., Rodrigues, F., Almeida, A., Silva, M.T., Barrientos, A. and Corte-Real, M., 2002. Cytochrome c release and mitochondria involvement in programmed cell death induced by acetic acid in Saccharomyces cerevisiae. Molecular biology of the cell 13, 2598-606.
Ludovico, P., Sousa, M.J., Silva, M.T., Leao, C. and Corte-Real, M., 2001. Saccharomyces cerevisiae commits to a programmed cell death process in response to acetic acid. Microbiology 147, 2409-15.
Lynch, M.D., 2005. Replicative Aging in E. coli. Rejuvenation Res 8, 79-81.
Macieira-Coelho, A., 1980. Implications of the reorganization of the cell genome for aging or immortalization of dividing cells in vitro. Gerontology 26, 276-82.

MacLean, M., Harris, N. and Piper, P.W., 2001. Chronological lifespan of stationary phase yeast cells; a model for investigating the factors that might influence the ageing of postmitotic tissues in higher organisms. Yeast 18, 499-509.
MacLellan, W.R. and Schneider, M.D., 1997. Death by design. Programmed cell death in cardiovascular biology and disease. Circ Res 81, 137-44.
Madeo, F., Frohlich, E. and Frohlich, K.U., 1997. A yeast mutant showing diagnostic markers of early and late apoptosis. The Journal of cell biology 139, 729-34.
Madeo, F., Herker, E., Maldener, C., Wissing, S., Lachelt, S., Herlan, M., Fehr, M., Lauber, K., Sigrist, S.J., Wesselborg, S. and Frohlich, K.U., 2002. A caspase-related protease regulates apoptosis in yeast. Molecular cell 9, 911-7.
Madia, F., Wei, M., Yuan, V., Hu, J., Gattazzo, C., Pham, P., Goodman, M.F. and Longo, V.D., 2009. Oncogene homologue Sch9 promotes age-dependent mutations by a superoxide and Rev1/Polzeta-dependent mechanism. The Journal of cell biology 186, 509-23.
Maniatis, T., Fritsch, E.F. and Sambrook, J., 1982. Molecular cloning : a laboratory manual, Cold Spring Harbour Laboratory, New York.
Markus, M.A. and Morris, B.J., 2008. Resveratrol in prevention and treatment of common clinical conditions of aging. Clin Interv Aging 3, 331-9.
Martens, J.A., Laprade, L. and Winston, F., 2004. Intergenic transcription is required to repress the Saccharomyces cerevisiae SER3 gene. Nature 429, 571-4.
Martianov, I., Ramadass, A., Serra Barros, A., Chow, N. and Akoulitchev, A., 2007. Repression of the human dihydrofolate reductase gene by a non-coding interfering transcript. Nature 445, 666-70.
Masanovic, M., Sogoric, S., Kolcic, I., Curic, I., Smoljanovic, A., Ramic, S., Cala, M. and Polasek, O., 2009. The geographic patterns of the exceptional longevity in Croatia. Coll Antropol 33 Suppl 1, 147-52.
Masoro, E.J., 1988. Food restriction in rodents: an evaluation of its role in the study of aging. J Gerontol 43, B59-64.
Masoro, E.J., 2005. Overview of caloric restriction and ageing. Mech Ageing Dev 126, 913-22.
Matheu, A., Maraver, A., Klatt, P., Flores, I., Garcia-Cao, I., Borras, C., Flores, J.M., Vina, J., Blasco, M.A. and Serrano, M., 2007. Delayed ageing through damage protection by the Arf/p53 pathway. Nature 448, 375-9.
Mattison, J.A., Roth, G.S., Beasley, T.M., Tilmont, E.M., Handy, A.M., Herbert, R.L., Longo, D.L., Allison, D.B., Young, J.E., Bryant, M., Barnard, D., Ward, W.F., Qi, W., Ingram, D.K. and de Cabo, R., 2012. Impact of caloric restriction on health and survival in rhesus monkeys from the NIA study. Nature 489, 318-21.
Mayan-Santos, M.D., Martinez-Robles, M.L., Hernandez, P., Schvartzman, J.B. and Krimer, D.B., 2008. A redundancy of processes that cause replication fork stalling enhances recombination at two distinct sites in yeast rDNA. Mol Microbiol 69, 361-75.
Mayordomo, I., Estruch, F. and Sanz, P., 2002. Convergence of the target of rapamycin and the Snf1 protein kinase pathways in the regulation of the subcellular localization of Msn2, a transcriptional activator of STRE (Stress Response Element)-regulated genes. The Journal of biological chemistry 277, 35650-6.
McCay, C.M., Crowell, M.F. and Maynard, L.A., 1935. The effect of retarded growth upon the length of life span and upon the ultimate body size. Nutrition 10, 63-79.
McMurray, M.A. and Gottschling, D.E., 2003. An age-induced switch to a hyper-recombinational state. Science 301, 1908-11.
McMurray, M.A. and Gottschling, D.E., 2004. Aging and genetic instability in yeast. Current Opinion in Microbiology 7, 673-9.
McVey, M., Kaeberlein, M., Tissenbaum, H.A. and Guarente, L., 2001. The short life span of Saccharomyces cerevisiae sgs1 and srs2 mutants is a composite of normal aging processes and mitotic arrest due to defective recombination. Genetics 157, 1531-42.
Medawar, P.B., 1952. An Unsolved Problem of Biology, Lewis, London.
Medvedev, Z.A., 1990. An attempt at a rational classification of theories of ageing. Biological Reviews of the Cambridge Philosophical Society 65, 375-98.
Mellor, J., 2010. Epigenetics and aging. Biochemist 32, 14-17.

Mendrysa, S.M., O'Leary, K.A., McElwee, M.K., Michalowski, J., Eisenman, R.N., Powell, D.A. and Perry, M.E., 2006. Tumor suppression and normal aging in mice with constitutively high p53 activity. Genes Dev 20, 16-21.

Merker, R.J. and Klein, H.L., 2002. hpr1Delta affects ribosomal DNA recombination and cell life span in Saccharomyces cerevisiae. Mol Cell Biol 22, 421-9.

Mohanty, B.K. and Bastia, D., 2004. Binding of the replication terminator protein Fob1p to the Ter sites of yeast causes polar fork arrest. J Biol Chem 279, 1932-41.

Morbey, Y.E., Brassil, C.E. and Hendry, A.P., 2005. Rapid senescence in pacific salmon. Am Nat 166, 556-68.

Morillon, A., Karabetsou, N., O'Sullivan, J., Kent, N., Proudfoot, N. and Mellor, J., 2003. Isw1 chromatin remodeling ATPase coordinates transcription elongation and termination by RNA polymerase II. Cell 115, 425-35.

Morley, A., 1998. Somatic mutation and aging. Ann N Y Acad Sci 854, 20-2.

Morselli, E., Galluzzi, L., Kepp, O., Criollo, A., Maiuri, M.C., Tavernarakis, N., Madeo, F. and Kroemer, G., 2009. Autophagy mediates pharmacological lifespan extension by spermidine and resveratrol. Aging (Albany NY) 1, 961-70.

Mortimer, R.K. and Johnston, J.R., 1959. Life span of individual yeast cells. Nature 183, 1751-2.

Moser, M.J., Oshima, J. and Monnat, R.J., Jr., 1999. WRN mutations in Werner syndrome. Hum Mutat 13, 271-9.

Muller, I., Zimmermann, M., Becker, D. and Flomer, M., 1980. Calendar life span versus budding life span of Saccharomyces cerevisiae. Mech Ageing Dev 12, 47-52.

Murakami, C. and Kaeberlein, M., 2009. Quantifying yeast chronological life span by outgrowth of aged cells. J Vis Exp.

Murakami, C.J., Burtner, C.R., Kennedy, B.K. and Kaeberlein, M., 2008. A method for high-throughput quantitative analysis of yeast chronological life span. J Gerontol A Biol Sci Med Sci 63, 113-21.

Myers, D.D., 1978. Review of disease patterns and life span in aging mice: genetic and environmental interactions. Birth Defects Orig Artic Ser 14, 41-53.

Nagano, T., Mitchell, J.A., Sanz, L.A., Pauler, F.M., Ferguson-Smith, A.C., Feil, R. and Fraser, P., 2008. The Air noncoding RNA epigenetically silences transcription by targeting G9a to chromatin. Science 322, 1717-20.

Nakayashiki, H., Kadotani, N. and Mayama, S., 2006. Evolution and diversification of RNA silencing proteins in fungi. J Mol Evol 63, 127-35.

Narita, M., Nunez, S., Heard, E., Lin, A.W., Hearn, S.A., Spector, D.L., Hannon, G.J. and Lowe, S.W., 2003. Rb-mediated heterochromatin formation and silencing of E2F target genes during cellular senescence. Cell 113, 703-16.

Németh, A., Guibert, S., Tiwari, V.K., Ohlsson, R. and Langst, G., 2008. Epigenetic regulation of TTF-I-mediated promoter-terminator interactions of rRNA genes. Embo J 27, 1255-65.

O'Sullivan, J.M., Tan-Wong, S.M., Morillon, A., Lee, B., Coles, J., Mellor, J. and Proudfoot, N.J., 2004. Gene loops juxtapose promoters and terminators in yeast. Nat Genet 36, 1014-8.

Oakes, C.C., Smiraglia, D.J., Plass, C., Trasler, J.M. and Robaire, B., 2003. Aging results in hypermethylation of ribosomal DNA in sperm and liver of male rats. Proc Natl Acad Sci U S A 100, 1775-80.

Oakes, M., Siddiqi, I., Vu, L., Aris, J. and Nomura, M., 1999. Transcription factor UAF, expansion and contraction of ribosomal DNA (rDNA) repeats, and RNA polymerase switch in transcription of yeast rDNA. Mol Cell Biol 19, 8559-69.

Ogryzko, V.V., Hirai, T.H., Russanova, V.R., Barbie, D.A. and Howard, B.H., 1996. Human fibroblast commitment to a senescence-like state in response to histone deacetylase inhibitors is cell cycle dependent. Mol Cell Biol 16, 5210-8.

Olshansky, S.J., Hayflick, L. and Perls, T.T., 2004. Anti-aging medicine: The hype and the reality - Part I. Introduction. Journals of Gerontology - Series A Biological Sciences and Medical Sciences 59, 513-514.

Pearl, R., 1928. The rate of living, Knopf, New York.

Penny, G.D., Kay, G.F., Sheardown, S.A., Rastan, S. and Brockdorff, N., 1996. Requirement for Xist in X chromosome inactivation. Nature 379, 131-7.

Perocchi, F., Xu, Z., Clauder-Munster, S. and Steinmetz, L.M., 2007. Antisense artifacts in transcriptome microarray experiments are resolved by actinomycin D. Nucleic Acids Res 35, e128.

Peters, A., Morrison, J.H., Rosene, D.L. and Hyman, B.T., 1998. Feature article: are neurons lost from the primate cerebral cortex during normal aging? Cereb Cortex 8, 295-300.

Pfeiffer, T., Schuster, S. and Bonhoeffer, S., 2001. Cooperation and competition in the evolution of ATP-producing pathways. Science 292, 504-7.

Phelan, J.P. and Austad, S.N., 1989. Natural selection, dietary restriction, and extended longevity. Growth Dev Aging 53, 4-6.

Pinton, P., Rimessi, A., Marchi, S., Orsini, F., Migliaccio, E., Giorgio, M., Contursi, C., Minucci, S., Mantovani, F., Wieckowski, M.R., Del Sal, G., Pelicci, P.G. and Rizzuto, R., 2007. Protein kinase C beta and prolyl isomerase 1 regulate mitochondrial effects of the life-span determinant p66Shc. Science 315, 659-63.

Piper, P., Calderon, C.O., Hatzixanthis, K. and Mollapour, M., 2001. Weak acid adaptation: the stress response that confers yeasts with resistance to organic acid food preservatives. Microbiology 147, 2635-42.

Piper, P.W., Jones, G.W., Bringloe, D., Harris, N., MacLean, M. and Mollapour, M., 2002. The shortened replicative life span of prohibitin mutants of yeast appears to be due to defective mitochondrial segregation in old mother cells. Aging Cell 1, 149-57.

Postma, E., Verduyn, C., Scheffers, W.A. and Van Dijken, J.P., 1989. Enzymic analysis of the crabtree effect in glucose-limited chemostat cultures of Saccharomyces cerevisiae. Appl Environ Microbiol 55, 468-77.

Powers, R.W., 3rd, Kaeberlein, M., Caldwell, S.D., Kennedy, B.K. and Fields, S., 2006. Extension of chronological life span in yeast by decreased TOR pathway signaling. Genes & Development 20, 174-84.

Powers, T. and Walter, P., 1999. Regulation of ribosome biogenesis by the rapamycin-sensitive TOR-signaling pathway in Saccharomyces cerevisiae. Mol Biol Cell 10, 987-1000.

Pozniakovsky, A.I., Knorre, D.A., Markova, O.V., Hyman, A.A., Skulachev, V.P. and Severin, F.F., 2005. Role of mitochondria in the pheromone- and amiodarone-induced programmed death of yeast. The Journal of cell biology 168, 257-69.

Prokesch, S., 1991. Small British Brewers Make a Dent, The New York Times. New York.

Pruneski, J.A., Hainer, S.J., Petrov, K.O. and Martens, J.A., 2011. The Paf1 complex represses SER3 transcription in Saccharomyces cerevisiae by facilitating intergenic transcription-dependent nucleosome occupancy of the SER3 promoter. Eukaryot Cell 10, 1283-94.

Querol, A., Fernandez-Espinar, M.T., del Olmo, M. and Barrio, E., 2003. Adaptive evolution of wine yeast. Int J Food Microbiol 86, 3-10.

Radonjic, M., Andrau, J.C., Lijnzaad, P., Kemmeren, P., Kockelkorn, T.T., van Leenen, D., van Berkum, N.L. and Holstege, F.C., 2005. Genome-wide analyses reveal RNA polymerase II located upstream of genes poised for rapid response upon S. cerevisiae stationary phase exit. Molecular cell 18, 171-83.

Reid, J.L., Iyer, V.R., Brown, P.O. and Struhl, K., 2000. Coordinate regulation of yeast ribosomal protein genes is associated with targeted recruitment of Esa1 histone acetylase. Mol Cell 6, 1297-307.

Reik, W., Dean, W. and Walter, J., 2001. Epigenetic reprogramming in mammalian development. Science 293, 1089-93.

Reinke, H. and Gatfield, D., 2006. Genome-wide oscillation of transcription in yeast. Trends Biochem Sci 31, 189-91.

Replansky, T., Koufopanou, V., Greig, D. and Bell, G., 2008. Saccharomyces sensu stricto as a model system for evolution and ecology. Trends Ecol Evol 23, 494-501.

Reverter-Branchat, G., Cabiscol, E., Tamarit, J. and Ros, J., 2004. Oxidative damage to specific proteins in replicative and chronological-aged Saccharomyces cerevisiae: common targets and prevention by calorie restriction. J Biol Chem 279, 31983-9.

Ribeiro, G.F., Corte-Real, M. and Johansson, B., 2006. Characterization of DNA damage in yeast apoptosis induced by hydrogen peroxide, acetic acid, and hyperosmotic shock. Molecular biology of the cell 17, 4584-91.

Ricklefs, R.E., 1998. Evolutionary theories of aging: confirmation of a fundamental prediction, with implications for the genetic basis and evolution of life span. Am Nat 152, 24-44.

Ridgway, I.D. and Richardson, C.A., 2011. Arctica islandica: The longest lived non colonial animal known to science. Reviews in Fish Biology and Fisheries 21, 297-310.
Robida-Stubbs, S., Glover-Cutter, K., Lamming, D.W., Mizunuma, M., Narasimhan, S.D., Neumann-Haefelin, E., Sabatini, D.M. and Blackwell, T.K., 2012. TOR Signaling and Rapamycin Influence Longevity by Regulating SKN-1/Nrf and DAF-16/FoxO. Cell Metab 15, 713-24.
Rockenfeller, P. and Madeo, F., 2008. Apoptotic death of ageing yeast. Exp. Gerontol. 43, 876-81.
Rogina, B. and Helfand, S.L., 2004. Sir2 mediates longevity in the fly through a pathway related to calorie restriction. Proc Natl Acad Sci U S A 101, 15998-6003.
Rogina, B., Helfand, S.L. and Frankel, S., 2002. Longevity regulation by Drosophila Rpd3 deacetylase and caloric restriction. Science 298, 1745.
Ronne, H., 1995. Glucose repression in fungi. Trends Genet 11, 12-7.
Rose, M. and Charlesworth, B., 1980. A test of evolutionary theories of senescence. Nature 287, 141-2.
Ross, P.D., 1996. Osteoporosis. Frequency, consequences, and risk factors. Arch Intern Med 156, 1399-411.
Sander, E.E. and Grummt, I., 1997. Oligomerization of the transcription termination factor TTF-I: implications for the structural organization of ribosomal transcription units. Nucleic Acids Res 25, 1142-7.
Sanz, A., Pamplona, R. and Barja, G., 2006. Is the mitochondrial free radical theory of aging intact? Antioxid Redox Signal 8, 582-99.
Sasieni, P.D., Shelton, J., Ormiston-Smith, N., Thomson, C.S. and Silcocks, P.B., 2011. What is the lifetime risk of developing cancer?: the effect of adjusting for multiple primaries. Br J Cancer 105, 460-5.
Saxton, J.A. and Kimball, G.C., 1941. Relation to nephrosis and other diseases of albino rat to age and to modifications of diet. Archives of Pathology 32, 951-965.
Scheckhuber, C.Q., Wanger, R.A., Mignat, C.A. and Osiewacz, H.D., 2011. Unopposed mitochondrial fission leads to severe lifespan shortening. Cell Cycle 10, 3105-10.
Schoneich, C., 1999. Reactive oxygen species and biological aging: a mechanistic approach. Exp Gerontol 34, 19-34.
Severin, F.F., Meer, M.V., Smirnova, E.A., Knorre, D.A. and Skulachev, V.P., 2008. Natural causes of programmed death of yeast Saccharomyces cerevisiae. Biochim Biophys Acta 1783, 1350-3.
Sgro, C.M. and Partridge, L., 1999. A delayed wave of death from reproduction in Drosophila. Science 286, 2521-4.
Shanahan, F., Seghezzi, W., Parry, D., Mahony, D. and Lees, E., 1999. Cyclin E associates with BAF155 and BRG1, components of the mammalian SWI-SNF complex, and alters the ability of BRG1 to induce growth arrest. Mol Cell Biol 19, 1460-9.
Shanley, D.P. and Kirkwood, T.B., 2006. Caloric restriction does not enhance longevity in all species and is unlikely to do so in humans. Biogerontology 7, 165-8.
Sharp, Z.D. and Bartke, A., 2005. Evidence for down-regulation of phosphoinositide 3-kinase/Akt/mammalian target of rapamycin (PI3K/Akt/mTOR)-dependent translation regulatory signaling pathways in Ames dwarf mice. J Gerontol A Biol Sci Med Sci 60, 293-300.
Shattuck, M.R. and Williams, S.A., 2010. Arboreality has allowed for the evolution of increased longevity in mammals. Proc Natl Acad Sci U S A 107, 4635-9.
Shi, L., Sutter, B.M., Ye, X. and Tu, B.P. Trehalose is a key determinant of the quiescent metabolic state that fuels cell cycle progression upon return to growth. Molecular biology of the cell 21, 1982-90.
Shigenaga, M.K., Hagen, T.M. and Ames, B.N., 1994. Oxidative damage and mitochondrial decay in aging. Proc Natl Acad Sci U S A 91, 10771-8.
Shirogane, T., Fukada, T., Muller, J.M., Shima, D.T., Hibi, M. and Hirano, T., 1999. Synergistic roles for Pim-1 and c-Myc in STAT3-mediated cell cycle progression and antiapoptosis. Immunity 11, 709-19.
Simonis, M., Klous, P., Splinter, E., Moshkin, Y., Willemsen, R., de Wit, E., van Steensel, B. and de Laat, W., 2006. Nuclear organization of active and inactive chromatin domains uncovered by chromosome conformation capture-on-chip (4C). Nat Genet 38, 1348-54.

Sinclair, D.A. and Guarente, L., 1997. Extrachromosomal rDNA circles--a cause of aging in yeast. Cell 91, 1033-42.
Sinclair, D.A., Mills, K. and Guarente, L., 1997. Accelerated aging and nucleolar fragmentation in yeast sgs1 mutants. Science 277, 1313-6.
Singh, B.N. and Hampsey, M., 2007. A transcription-independent role for TFIIB in gene looping. Mol Cell 27, 806-16.
Singh, J. and Tyers, M., 2009. A Rab escort protein integrates the secretion system with TOR signaling and ribosome biogenesis. Genes & development 23, 1944-58.
Skok, J.A., Gisler, R., Novatchkova, M., Farmer, D., de Laat, W. and Busslinger, M., 2007. Reversible contraction by looping of the Tcra and Tcrb loci in rearranging thymocytes. Nat Immunol 8, 378-87.
Skutches, C.L., Holroyde, C.P., Myers, R.N., Paul, P. and Reichard, G.A., 1979. Plasma acetate turnover and oxidation. J Clin Invest 64, 708-13.
Slator, A., 1913. The Rate of Fermentation by Growing Yeast Cells. The Biochemical journal 7, 197-203.
Smets, B., Ghillebert, R., De Snijder, P., Binda, M., Swinnen, E., De Virgilio, C. and Winderickx, J. Life in the midst of scarcity: adaptations to nutrient availability in Saccharomyces cerevisiae. Current genetics 56, 1-32.
Smith, D.L., Jr., McClure, J.M., Matecic, M. and Smith, J.S., 2007. Calorie restriction extends the chronological lifespan of Saccharomyces cerevisiae independently of the Sirtuins. Aging Cell 6, 649-62.
Smith, J.S. and Boeke, J.D., 1997. An unusual form of transcriptional silencing in yeast ribosomal DNA. Genes Dev 11, 241-54.
Smith, J.S., Brachmann, C.B., Pillus, L. and Boeke, J.D., 1998. Distribution of a limited Sir2 protein pool regulates the strength of yeast rDNA silencing and is modulated by Sir4p. Genetics 149, 1205-19.
Sohal, R.S., 2002. Role of oxidative stress and protein oxidation in the aging process. Free Radic Biol Med 33, 37-44.
Sommer, M., Poliak, N., Upadhyay, S., Ratovitski, E., Nelkin, B.D., Donehower, L.A. and Sidransky, D., 2006. DeltaNp63alpha overexpression induces downregulation of Sirt1 and an accelerated aging phenotype in the mouse. Cell Cycle 5, 2005-11.
Speakman, J.R. and Hambly, C., 2007. Starving for life: what animal studies can and cannot tell us about the use of caloric restriction to prolong human lifespan. J Nutr 137, 1078-86.
Stadtman, E.R. and Berlett, B.S., 1997. Reactive oxygen-mediated protein oxidation in aging and disease. Chem Res Toxicol 10, 485-94.
Straight, A.F., Shou, W., Dowd, G.J., Turck, C.W., Deshaies, R.J., Johnson, A.D. and Moazed, D., 1999. Net1, a Sir2-associated nucleolar protein required for rDNA silencing and nucleolar integrity. Cell 97, 245-56.
Thebault, P., Boutin, G., Bhat, W., Rufiange, A., Martens, J. and Nourani, A., 2011. Transcription regulation by the noncoding RNA SRG1 requires Spt2-dependent chromatin deposition in the wake of RNA polymerase II. Mol Cell Biol 31, 1288-300.
Thevelein, J.M., Cauwenberg, L., Colombo, S., De Winde, J.H., Donation, M., Dumortier, F., Kraakman, L., Lemaire, K., Ma, P., Nauwelaers, D., Rolland, F., Teunissen, A., Van Dijck, P., Versele, M., Wera, S. and Winderickx, J., 2000. Nutrient-induced signal transduction through the protein kinase A pathway and its role in the control of metabolism, stress resistance, and growth in yeast. Enzyme Microb Technol 26, 819-825.
Tian, D., Sun, S. and Lee, J.T., 2010. The long noncoding RNA, Jpx, is a molecular switch for X chromosome inactivation. Cell 143, 390-403.
Tolhuis, B., Palstra, R.J., Splinter, E., Grosveld, F. and de Laat, W., 2002. Looping and interaction between hypersensitive sites in the active beta-globin locus. Mol Cell 10, 1453-65.
Tsai, M.C., Manor, O., Wan, Y., Mosammaparast, N., Wang, J.K., Lan, F., Shi, Y., Segal, E. and Chang, H.Y., 2010. Long noncoding RNA as modular scaffold of histone modification complexes. Science 329, 689-93.
Tyner, S.D., Venkatachalam, S., Choi, J., Jones, S., Ghebranious, N., Igelmann, H., Lu, X., Soron, G., Cooper, B., Brayton, C., Park, S.H., Thompson, T., Karsenty, G., Bradley, A. and Donehower, L.A., 2002. p53 mutant mice that display early ageing-associated phenotypes. Nature 415, 45-53.

Urban, J., Soulard, A., Huber, A., Lippman, S., Mukhopadhyay, D., Deloche, O., Wanke, V., Anrather, D., Ammerer, G., Riezman, H., Broach, J.R., De Virgilio, C., Hall, M.N. and Loewith, R., 2007. Sch9 is a major target of TORC1 in Saccharomyces cerevisiae. Mol Cell 26, 663-74.

Vaissiere, T., Sawan, C. and Herceg, Z., 2008. Epigenetic interplay between histone modifications and DNA methylation in gene silencing. Mutat Res 659, 40-8.

Valcourt, J.R., Lemons, J.M., Haley, E.M., Kojima, M., Demuren, O.O. and Coller, H.A., 2012. Staying alive: Metabolic adaptations to quiescence. Cell Cycle 11, 1680-96.

van Dijk, E.L., Chen, C.L., d'Aubenton-Carafa, Y., Gourvennec, S., Kwapisz, M., Roche, V., Bertrand, C., Silvain, M., Legoix-Ne, P., Loeillet, S., Nicolas, A., Thermes, C. and Morillon, A., 2011. XUTs are a class of Xrn1-sensitive antisense regulatory non-coding RNA in yeast. Nature 475, 114-7.

van Nues, R.W., Venema, J., Rientjes, J.M., Dirks-Mulder, A. and Raue, H.A., 1995. Processing of eukaryotic pre-rRNA: the role of the transcribed spacers. Biochem Cell Biol 73, 789-801.

Vanrobays, E., Leplus, A., Osheim, Y.N., Beyer, A.L., Wacheul, L. and Lafontaine, D.L., 2008. TOR regulates the subcellular distribution of DIM2, a KH domain protein required for cotranscriptional ribosome assembly and pre-40S ribosome export. Rna 14, 2061-73.

Vaupel, J.W., Baudisch, A., Dolling, M., Roach, D.A. and Gampe, J., 2004. The case for negative senescence. Theor Popul Biol 65, 339-51.

Vellai, T., Takacs-Vellai, K., Zhang, Y., Kovacs, A.L., Orosz, L. and Muller, F., 2003. Genetics: influence of TOR kinase on lifespan in C. elegans. Nature 426, 620.

Venters, B.J. and Pugh, B.F., 2009. A canonical promoter organization of the transcription machinery and its regulators in the Saccharomyces genome. Genome Res 19, 360-71.

Verdel, A., Jia, S., Gerber, S., Sugiyama, T., Gygi, S., Grewal, S.I. and Moazed, D., 2004. RNAi-mediated targeting of heterochromatin by the RITS complex. Science 303, 672-6.

Verduyn, C., Postma, E., Scheffers, W.A. and van Dijken, J.P., 1990. Physiology of Saccharomyces cerevisiae in anaerobic glucose-limited chemostat cultures. J Gen Microbiol 136, 395-403.

Vermulst, M., Bielas, J.H., Kujoth, G.C., Ladiges, W.C., Rabinovitch, P.S., Prolla, T.A. and Loeb, L.A., 2007. Mitochondrial point mutations do not limit the natural lifespan of mice. Nat Genet 39, 540-3.

Vignali, M., Steger, D.J., Neely, K.E. and Workman, J.L., 2000. Distribution of acetylated histones resulting from Gal4-VP16 recruitment of SAGA and NuA4 complexes. Embo J 19, 2629-40.

Vijg, J. and Dolle, M.E., 2002. Large genome rearrangements as a primary cause of aging. Mech Ageing Dev 123, 907-15.

Vu, L., Siddiqi, I., Lee, B.S., Josaitis, C.A. and Nomura, M., 1999. RNA polymerase switch in transcription of yeast rDNA: role of transcription factor UAF (upstream activation factor) in silencing rDNA transcription by RNA polymerase II. Proc Natl Acad Sci U S A 96, 4390-5.

Walker, D.W., McColl, G., Jenkins, N.L., Harris, J. and Lithgow, G.J., 2000. Evolution of lifespan in C. elegans. Nature 405, 296-7.

Wallace, D.C., 2005. A mitochondrial paradigm of metabolic and degenerative diseases, aging, and cancer: a dawn for evolutionary medicine. Annu Rev Genet 39, 359-407.

Wang, C., Skinner, C., Easlon, E. and Lin, S.J., 2009. Deleting the 14-3-3 protein Bmh1 extends life span in Saccharomyces cerevisiae by increasing stress response. Genetics 183, 1373-84.

Wang, K.C. and Chang, H.Y., 2011. Molecular mechanisms of long noncoding RNAs. Mol Cell 43, 904-14.

Wang, Y. and Tissenbaum, H.A., 2006. Overlapping and distinct functions for a Caenorhabditis elegans SIR2 and DAF-16/FOXO. Mech Ageing Dev 127, 48-56.

Wei, Y.H., 1998. Oxidative stress and mitochondrial DNA mutations in human aging. Proc Soc Exp Biol Med 217, 53-63.

Weinberger, M., Mesquita, A., Caroll, T., Marks, L., Yang, H., Zhang, Z., Ludovico, P. and Burhans, W.C., 2010. Growth signaling promotes chronological aging in budding yeast by inducing superoxide anions that inhibit quiescence. Aging (Albany NY) 2, 709-26.

Weindruch, R. and Walford, R.L., 1982. Dietary restriction in mice beginning at 1 year of age: effect on life-span and spontaneous cancer incidence. Science 215, 1415-8.

Weismann, A., 1889. Essays upon Heredity and Kindred Biological Problems, Clarendon Press, Oxford.
Weitao, T., Budd, M., Hoopes, L.L. and Campbell, J.L., 2003. Dna2 helicase/nuclease causes replicative fork stalling and double-strand breaks in the ribosomal DNA of Saccharomyces cerevisiae. J Biol Chem 278, 22513-22.
Werner-Washburne, M., Braun, E., Johnston, G.C. and Singer, R.A., 1993. Stationary phase in the yeast Saccharomyces cerevisiae. Microbiol Rev 57, 383-401.
WHO, 2007. The top ten causes of death, WHO, Geneva.
Williams, G.C., 1957. Pleiotropy, natural selection, and the evolution of senescence. Evolution 11, 398-411.
Wilson, D.M., 3rd, Bohr, V.A. and McKinnon, P.J., 2008. DNA damage, DNA repair, ageing and age-related disease. Mech Ageing Dev 129, 349-52.
Wilson, V.L. and Jones, P.A., 1983. DNA methylation decreases in aging but not in immortal cells. Science 220, 1055-7.
Wilson, V.L., Smith, R.A., Ma, S. and Cutler, R.G., 1987. Genomic 5-methyldeoxycytidine decreases with age. J Biol Chem 262, 9948-51.
Wissing, S., Ludovico, P., Herker, E., Buttner, S., Engelhardt, S.M., Decker, T., Link, A., Proksch, A., Rodrigues, F., Corte-Real, M., Frohlich, K.U., Manns, J., Cande, C., Sigrist, S.J., Kroemer, G. and Madeo, F., 2004. An AIF orthologue regulates apoptosis in yeast. The Journal of cell biology 166, 969-74.
Wood, J.G., Rogina, B., Lavu, S., Howitz, K., Helfand, S.L., Tatar, M. and Sinclair, D., 2004. Sirtuin activators mimic caloric restriction and delay ageing in metazoans. Nature 430, 686-9.
Wu, P.Y. and Winston, F., 2002. Analysis of Spt7 function in the Saccharomyces cerevisiae SAGA coactivator complex. Mol Cell Biol 22, 5367-79.
Wyers, F., Rougemaille, M., Badis, G., Rousselle, J.C., Dufour, M.E., Boulay, J., Regnault, B., Devaux, F., Namane, A., Seraphin, B., Libri, D. and Jacquier, A., 2005. Cryptic pol II transcripts are degraded by a nuclear quality control pathway involving a new poly(A) polymerase. Cell 121, 725-37.
Xu, Z., Wei, W., Gagneur, J., Perocchi, F., Clauder-Munster, S., Camblong, J., Guffanti, E., Stutz, F., Huber, W. and Steinmetz, L.M., 2009. Bidirectional promoters generate pervasive transcription in yeast. Nature 457, 1033-7.
Yao, T.P., Oh, S.P., Fuchs, M., Zhou, N.D., Ch'ng, L.E., Newsome, D., Bronson, R.T., Li, E., Livingston, D.M. and Eckner, R., 1998. Gene dosage-dependent embryonic development and proliferation defects in mice lacking the transcriptional integrator p300. Cell 93, 361-72.
Young, E.T., Dombek, K.M., Tachibana, C. and Ideker, T., 2003. Multiple pathways are co-regulated by the protein kinase Snf1 and the transcription factors Adr1 and Cat8. The Journal of biological chemistry 278, 26146-58.
Young, J.I. and Smith, J.R., 2001. DNA methyltransferase inhibition in normal human fibroblasts induces a p21-dependent cell cycle withdrawal. J Biol Chem 276, 19610-6.
Yuan, J. and Yankner, B.A., 2000. Apoptosis in the nervous system. Nature 407, 802-9.
Zhang, H., Pan, K.H. and Cohen, S.N., 2003. Senescence-specific gene expression fingerprints reveal cell-type-dependent physical clustering of up-regulated chromosomal loci. Proc Natl Acad Sci U S A 100, 3251-6.
Zong, W.X. and Thompson, C.B., 2006. Necrotic death as a cell fate. Genes & development 20, 1-15.